



TECHNISCHE
UNIVERSITÄT
DARMSTADT

Generation of a Host Cell line containing a MAR-rich landing pad for site specific integration and expression of transgenes

From the Department of Chemistry
at the Technischen Universität Darmstadt

Submitted in fulfillment of the requirements for the degree of
Doctor rerum naturalium
(Dr. rer. nat.)

Dissertation
from

M. Sc. Claudia Oliviero

First reviewer: Prof. Dr. Harald Kolmar

Second reviewer: Prof. Dr. Gerrit Hagens

Darmstadt 2023

Oliviero, Claudia: Generation of a Host Cell line containing a MAR-rich landing pad for site specific integration and expression of transgenes

Darmstadt, Technische Universität Darmstadt,

Year thesis published in TUprints 2023

Date of the viva voce: 27 November 2023

Published under CC BY-SA 4.0 International

<https://creativecommons.org/licenses/>

Publications derived from this work

The project resulted in the following scientific publication (submitted to "Biotechnology progress" on 11/01/2022 and accepted on 03/31/2022):

"Oliviero C, Hinz SC, Bogen JP, Kornmann H, Hock B, Kolmar H, Hagens G. **Generation of a host cell line containing a MAR-rich landing pad for site-specific integration and expression of transgenes.** Biotechnol Prog. 2022 Jul;38(4):e3254. doi: 10.1002/btpr.3254. Epub 2022 Apr 25. PMID: 35396920; PMCID: PMC9539524."

In addition, the following article is being submitted to Methods in Molecular Biology:

"Oliviero C, Hinz SC, Grzeschik J, Hock B, Kolmar R, Hagens G. **Cell line development using targeted gene integration into MAR-rich landing pads for stable expression of transgenes.**"

Table of Content

| | | |
|-------------------------------------|---|-----------|
| Publications derived from this work | iii | |
| Table of Content | iv | |
| Zusammenfassung | 1 | |
| Abstract | 3 | |
| 1 | Introduction | 5 |
| 1.1 | Biologics: definition and global market | 5 |
| 1.2 | Antibodies | 6 |
| 1.2.1 | Structure and function | 6 |
| 1.2.2 | Monoclonal antibodies | 8 |
| 1.2.3 | Bispecific antibody format and their applications | 9 |
| 1.3 | Antibody production and process development | 12 |
| 1.4 | Expression host | 13 |
| 1.4.1 | CHO cells | 13 |
| 1.5 | Cell line development (CLD) for antibody production | 14 |
| 1.5.1 | Common selection methods and clone isolation strategies for CHO cell CLD | 15 |
| 1.5.2 | Emerging trends in CHO cell line development | 16 |
| 1.6 | Epigenetic regulatory elements: a focus on MAR sequences | 17 |
| 1.7 | TI using Site-specific recombinases | 18 |
| 1.7.1 | Overview on recombinases | 19 |
| 1.7.2 | The use of site-specific recombinases for recombinant protein production in mammalian hosts | 21 |
| 2 | Objective | 24 |
| 3 | Materials | 26 |
| 3.1 | Bacterial Strains | 26 |
| 3.2 | Mammalian cell lines | 26 |
| 3.3 | Vectors | 26 |
| 3.4 | Oligonucleotides | 34 |
| 3.4.1 | Cloning primers | 34 |
| 3.4.2 | Genomic PCR primers | 34 |
| 3.4.3 | qPCR - qRT-PCR primers | 34 |
| 3.4.4 | Primers for the generation of FISH probes | 35 |
| 3.5 | Molecular biology enzymes and kits | 35 |
| 3.6 | Mammalian cell cultures media, feeds and reagents | 36 |
| 3.7 | Consumables and reagents | 36 |
| 3.8 | Solutions | 37 |
| 3.9 | Chemicals | 38 |
| 3.10 | Instruments | 38 |
| 4 | Methods | 40 |
| 4.1 | Microbiological Methods | 40 |

| | | |
|--------|---|----|
| 4.2 | Molecular Biology Methods | 40 |
| 4.2.1 | Polymerase Chain Reaction (PCR) | 40 |
| 4.2.2 | Restriction digestion | 40 |
| 4.2.3 | Ethanol precipitation of DNA | 41 |
| 4.2.4 | DNA ligation reaction | 41 |
| 4.2.5 | Agarose gel electrophoresis | 41 |
| 4.3 | Vector generation | 41 |
| 4.3.1 | Generation of chicken 5' Lysozyme MAR LP vectors | 41 |
| 4.3.2 | Generation of human 1-68 MAR LP vectors | 42 |
| 4.3.3 | Generation of w/o-MAR LP vectors | 42 |
| 4.3.4 | Generation of msAb/bsAb donor vectors | 42 |
| 4.3.5 | Generation of DGV (msAb) lonza vector | 43 |
| 4.3.6 | Generation of TGV (bsAb) lonza vector | 43 |
| 4.4 | Mammalian Cell Culture | 43 |
| 4.4.1 | Routine culture | 43 |
| 4.4.2 | Cell cryopreservation and cell recover from cryopreservation | 43 |
| 4.4.3 | Transfection using Neon electroporator system | 44 |
| 4.4.4 | Clonal selection in semi-solid medium | 44 |
| 4.4.5 | Flow cytometry and single cell-cloning | 45 |
| 4.5 | Generation of host cell line containing 5' chicken lysozyme MAR-rich landing pads | 45 |
| 4.6 | Generation of control host cell line containing landing pads without MAR | 45 |
| 4.7 | Generation of host cell line containing h1-68 MAR-rich landing pads | 46 |
| 4.8 | Generation of stable msAb clones using the LP system | 46 |
| 4.9 | Generation of stable msAb clones using the GS system | 47 |
| 4.10 | Generation of stable bsAb clones using the LP system | 47 |
| 4.11 | Generation of stable bsAb clones using the GS system | 48 |
| 4.12 | Cell adaptation to different media | 48 |
| 4.13 | Fed-batch cultures | 48 |
| 4.14 | Culture expansion for shake flask scale up and bioreactor inoculum | 49 |
| 4.15 | SB 10-X bioreactor set-up and run | 50 |
| 4.16 | BioFlo320 Eppendorf bioreactor set-up and run | 51 |
| 4.17 | Stability studies | 52 |
| 4.18 | Transcript level analysis | 52 |
| 4.19 | Determination of gene copy number | 53 |
| 4.20 | Genomic PCR amplification of targeted regions | 53 |
| 4.21 | Fluorescence in situ hybridization analyses | 53 |
| 4.22 | Analytical Methods | 54 |
| 4.22.1 | Protein purification and buffer exchange | 54 |
| 4.22.2 | SDS-PAGE and immunoblotting | 55 |
| 4.22.3 | BLI antibody quantitation analysis | 55 |
| 4.22.4 | Size exclusion chromatography | 55 |
| 4.22.5 | HPLC quantification of Glucose and Lactate in sample supernatant | 56 |

| | | |
|-------|--|-----|
| 5 | Results and discussion | 57 |
| 5.1 | Generation of host cell line containing landing pads | 57 |
| 5.1.1 | Generation of chicken 5' lysozyme MAR (cMAR)-rich landing pad clones | 57 |
| 5.1.1 | Generation of human 1-68 MAR (h1-68_MAR)-rich landing pad clones | 62 |
| 5.1.2 | Generation of control (w/o_MAR) landing pad clones | 63 |
| 5.2 | Generation, selection, and characterization of LP-derived anti-CCR9-expressing clones | 65 |
| 5.3 | Generation and selection of CHO-K1 SV GS ⁻ (Lonza)anti-CCR9-expressing clones | 72 |
| 5.4 | Generation, selection and characterization of LP-derived bsAb-Fer-expressing clones | 73 |
| 5.5 | Generation and selection of CHO-K1 SV GS ⁻ (Lonza) bsAb-Fer-expressing clones | 80 |
| 5.6 | Fed-batch cultures and media test for msAb and bsAb | 83 |
| 5.7 | System scale-up to 5L using LP-derived bsAb-expressing clone | 86 |
| 6 | Conclusion and Outlook | 90 |
| 7 | Literature | 95 |
| 8 | Appendix | 111 |
| 8.1 | Supplementary figures | 111 |
| 8.2 | Supplementary tables | 113 |
| 8.3 | Protein sequence | 114 |
| 8.4 | MAR sequences | 115 |
| 8.5 | List of figures | 117 |
| 8.6 | List of tables | 118 |
| 8.7 | Aknowledgments | 119 |
| 8.8 | Affirmations | 121 |

Zusammenfassung

In den letzten Jahren wurde die gezielte Genintegration (*targeted integration*; TI) als Strategie zur Herstellung rekombinanter Säugetierzelllinien für die Produktion von Biotherapeutika eingeführt. Neben der Verringerung der potenziell immensen Heterogenität innerhalb eines Pools rekombinanter Transfektanten zielt die TI auch darauf ab, die Dauer des Zelllinienentwicklungsprozesses zu verkürzen.

Ziel dieser Arbeit war es, eine Wirtszelllinie zu generieren, die mehrere Kopien einer *Matrix Attachment Region* (MAR) enthält, die als Zielregion für die ortsspezifische Integration von Transgenen dient. Das entwickelte System basiert auf der Integration von zwei Landstellen, die dieselbe MAR, zwei orthogonale Rekombinationsstellen für die Serin-Integrase BxB1 (AttB Wildtyp und AttB mit GA-Mutation) und zwei verschiedene Fluoreszenzreportergene (EGFP und DsRed) enthalten.

Der erste Teil der Arbeit konzentrierte sich auf die Herstellung von Landstellen-Wirtszelllinien. Es wurden drei verschiedene Typen von dualen Landstellen entwickelt und in das CHO-S-Genom integriert: solche, die die 5'-MAR von Hühnerlysozym enthalten, solche, die die menschliche 1-68-MAR enthalten, und eine Kontrollzelllinie ohne eine MAR-Sequenz. Klone, die beide Landstellen integrieren, können durch antibiotische Selektion und durch parallele Erfassung der Expression der beiden Reportergenen ausgewählt werden. Die Landstellen-Klone wurden ausgewählt und charakterisiert, um die Auswirkungen der MAR-Sequenz auf die Anzahl der in das Genom integrierten LP-Kopien, die Expression der Reportergene und die Stabilität der Klone zu bewerten.

Der zweite Teil der Arbeit konzentrierte sich auf die ortsspezifische Integration von GOI in die ausgewählten Wirtszelllinien unter Verwendung der BxB1-Integrase. Die Sequenz eines monospezifischen menschlichen Antikörpers (msAb-Fer) wurde für diesen Konzeptnachweis verwendet. Um das System weiter zu validieren und seine Vielseitigkeit zu demonstrieren, wurde auch ein bispezifischer Antikörper (bsAb-Fer) mit Hilfe des Landstellensystems exprimiert. Es wurden Klone ausgewählt und analysiert, um die erfolgreiche Integration der *Donor*-Vektoren und ihre korrekte Expression zu überprüfen. Diese Experimente verdeutlichten die Möglichkeit, das entwickelte Landstellen-System als "*Chassis*" für die Expression verschiedener Gene zu nutzen. Darüber hinaus wurden verschiedene Erkenntnisse über Punkte gewonnen, die optimiert werden müssen, um eine robustere Expressionsplattform zu erhalten.

Der letzte Teil dieser Arbeit konzentrierte sich auf die Verbesserung der Kulturbedingungen im Fed-Batch-Verfahren und einen Scale-up der Kultur. Es wurden verschiedene kommerzielle Basalmedien in Kombination mit unterschiedlichen Fütterungsstrategien getestet, um die Auswirkungen auf die Zellwachstumskurven und den Antikörpertiter zu untersuchen. Durch die Verbesserung der Kulturbedingungen konnten die Kulturdauer und der Antikörpertiter im Vergleich zu den ursprünglich getesteten Bedingungen deutlich erhöht werden. Die besten

Bedingungen wurden beim Scale-up des Systems verwendet, das sich in einem Schüttelbioreaktor von bis zu 5 Liter bewährt hatte.

Zusammenfassend lässt sich sagen, dass durch diese Arbeit Methoden für die Umsetzung und Entwicklung einer Plattform für die Simultanexpression mehrerer Zielgene entwickelt werden konnten. Das duale Landstellen-System, das aus verschiedenen Reportergenen und einer MAR-Sequenz besteht, ermöglicht die effiziente Auswahl stabiler Wirtszelllinien. Das Landstellen-Design in Verbindung mit der *Promotor-Trap*-Strategie ermöglicht eine effiziente und schnelle Selektion von produktiven Klonen, sobald die Rekombination und Integration der GOI stattgefunden hat. Dieses System hat sich sowohl für die Expression von einem monospezifischen und einem bispezifischen Antikörper bewährt, hat aber auch das Potenzial für eine schnelle und effiziente Expression anderer Moleküle. Daher könnte dieses System nach seiner Optimierung in Zukunft für die Erzeugung stabiler Zelllinien für die Produktion, aber auch für die schnelle Expression verschiedener Biologika verwendet werden, ohne dass transiente Transfektionsschritte oder lange Selektionsprozesse erforderlich sind.

Abstract

In recent years, targeted gene integration (TI) has been introduced as a strategy for the generation of recombinant mammalian cell lines for the production of biotherapeutics. Besides reducing the immense heterogeneity within a pool of recombinant transfectants, TI also aims at shortening the duration of the current cell line development process.

The aim of this work was to generate a host cell line containing several copies of a Matrix Attachment Region (MAR) rich landing pad for site-specific integration of Gene Of Interests (GOIs). The developed system is based on the integration of dual landing pads containing the same MAR, two different orthogonal recombination sites for the serine integrase BxB1 (AttB wild type, and AttB with GA mutation) and two different reporter genes (EGFP and DsRed).

The first part of the work focused on the generation of landing pad host cell lines. Three different typologies of dual landing pads were developed and integrated into the CHO-S genome: ones containing the chicken lysozyme 5' MAR, ones containing the human 1-68 MAR and a control ones without the MAR sequence. Clones integrating both landing pads can be selected by antibiotic selection and by following the dual reporter gene expression. Landing pad clones were selected and characterized to evaluate the effect of MAR sequence on the number of copies of LPs integrated into the genome, the expression of reporter genes, and the stability of the clones.

The second part of the work focused on the site-specific integration of GOIs into the selected host cell lines, using BxB1 integrase. The sequence of a monospecific human antibody (msAb-Fer) was used for this proof of concept. To further validate the system and demonstrate its versatility, a bispecific antibody (bsAb-Fer) was also expressed using the landing pad system. Clones were selected and analyzed in order to verify the successful integration of donor vectors and their correct expression. These experiments highlighted the possibility of using the developed landing pads system as a "chassis" for the expression of different genes. In addition, various insights were obtained regarding points to be optimized to achieve a more robust expression platform.

The last part of this work focused on improving culture conditions in fed batch and a culture scale up. Different commercial basal media were tested in combination with different feeding strategies to evaluate the impact in cell growth curves and antibody titer. Improvements in culture conditions allowed to increase culture duration and antibody titer significantly compared to the initial tested conditions. The best conditions found were used during the scale-up of the system, which was proven up to 5L in a shaking bioreactor.

In summary, this work provides methods for the implementation and development of a platform for the expression of several genes of interest at the same time. The dual landing pad system, associated with different reporter genes and a MAR sequence allows the efficient selection of stable host cell lines. The landing pad design, coupled with the promoter trap strategy, allows efficient and rapid selection of producing clones once recombination and integration of GOIs has occurred. This system has been proven for expression of both

monospecific and bispecific antibodies but has the potential for rapid and efficient expression of other molecules as well. Therefore upon optimization, this system could be used in the future for generating stable cell lines for production but also for rapid expression of different biologics without having to go through transient transfection steps or long selection processes.

1 Introduction

Since the approval of the first biological in 1982, the recombinant human insulin (Humulin)¹, biopharmaceutical drugs revolutionized the treatment for an ample spectra of diseases² and deeply changed the entire pharmaceutical industry and market³. The development of these class of molecules is linked to the progresses in biochemistry and molecular biology done during the 20th century⁴. The discovery of the DNA structure as well as the advances in genetic and protein engineering formed the basis for the development of recombinant DNA technologies. Nowadays, improvements in production of biopharmaceutical molecules has become the center of attention, in order to reduce cost and to develop fine-tuned systems for complex biologics production.

1.1 Biologics: definition and global market

Biopharmaceuticals or simply “biologics” included a heterogeneous group of substances such as vaccine, blood and blood components, allergenics, somatic cells, gene therapy, tissues and recombinant therapeutic proteins⁵. In contrast with chemically-synthesized drugs, these classes of molecules contain active substances that are made by a living system or may be represented by a living entities⁶. Most biologics are produced by biotechnology methods^{5,7} and this results in structurally complex, large molecules reaching 100 to 1000 times the small molecules drug size. The complex structure of biologics, which is frequently at least partially unknown, is a mixture of sugars, proteins, or nucleic acids, or a combination of them and makes these molecules hard to characterize⁸. In addition, due to their biological origin, biologics are sensitive to changing conditions during the manufacturing process and starting materials⁶ resulting in a certain degree of batch-to-batch variability⁹ which makes the process of characterization even harder. Other major differences between small molecules and biologics are represented by reduced stability¹⁰, sensitivity to light and heat¹¹, risk of process-related impurities^{12,13} and potential immunogenicity^{14,15} of biopharmaceuticals. For these reasons, not only the production process, but also steps of product purification and storage are crucial for the quality¹⁶ of the final product and contribute to the high cost of these drugs⁶. Despite the fact that small molecules still predominate the pharmaceutical market, the market value for biologics has been estimated to be \$285.5 billion in 2020 and it is expected to reach \$421.8 billion by 2025¹⁷. To date, more than 300 biopharmaceutical with current active licenses are on the market in Europe and/or USA¹⁸, and 19 new biologics have been approved by FDA in 2020¹⁹ showing a constant approval trend for these molecules (approximately 50-60 approvals every five years)¹⁸. Among the different classes of biologics, antibodies and derivatives predominate the biopharmaceutical approvals and market²⁰, becoming the main treatment for several different diseases over the past 25 years²¹.

1.2 Antibodies

1.2.1 Structure and function

Antibody molecules are glycoproteins, related to the family of *immunoglobulins*, produced and secreted by differentiated B-cells (plasma cells) in response to infection or immunization²². Their function, based on the recognition and binding to a specific molecule called *antigen*, is correlated to their structure. The monomeric immunoglobulin (Ig) structure is composed by two heavy chains (50kDa each) and two light chains (25kDa each), connected by disulphide bonds, forming a flexible Y-shaped structure of molecular weight of 150kDa. Each light chain contains one variable domain (V_L) and one constant domain (C_L). Heavy chains contain one variable domain (V_H) and up to three constant domains (C_{H1} C_{H2} C_{H3}) with an additional “hinge region” between C_{H1} and C_{H2} (Figure 1). The constant domain of both heavy and light chains makes up the constant (C) region, whereas the variable domains of both heavy and light chains make up the variable (V) region. Located within the variable regions, each antigen binding site contains six complementarity-determining regions (CDR), three for each variable domain. These loops also known as “hypervariable loops” are strongly involved in antigen recognition, creating a single hypervariable site at the tip of each arm of the molecule²².

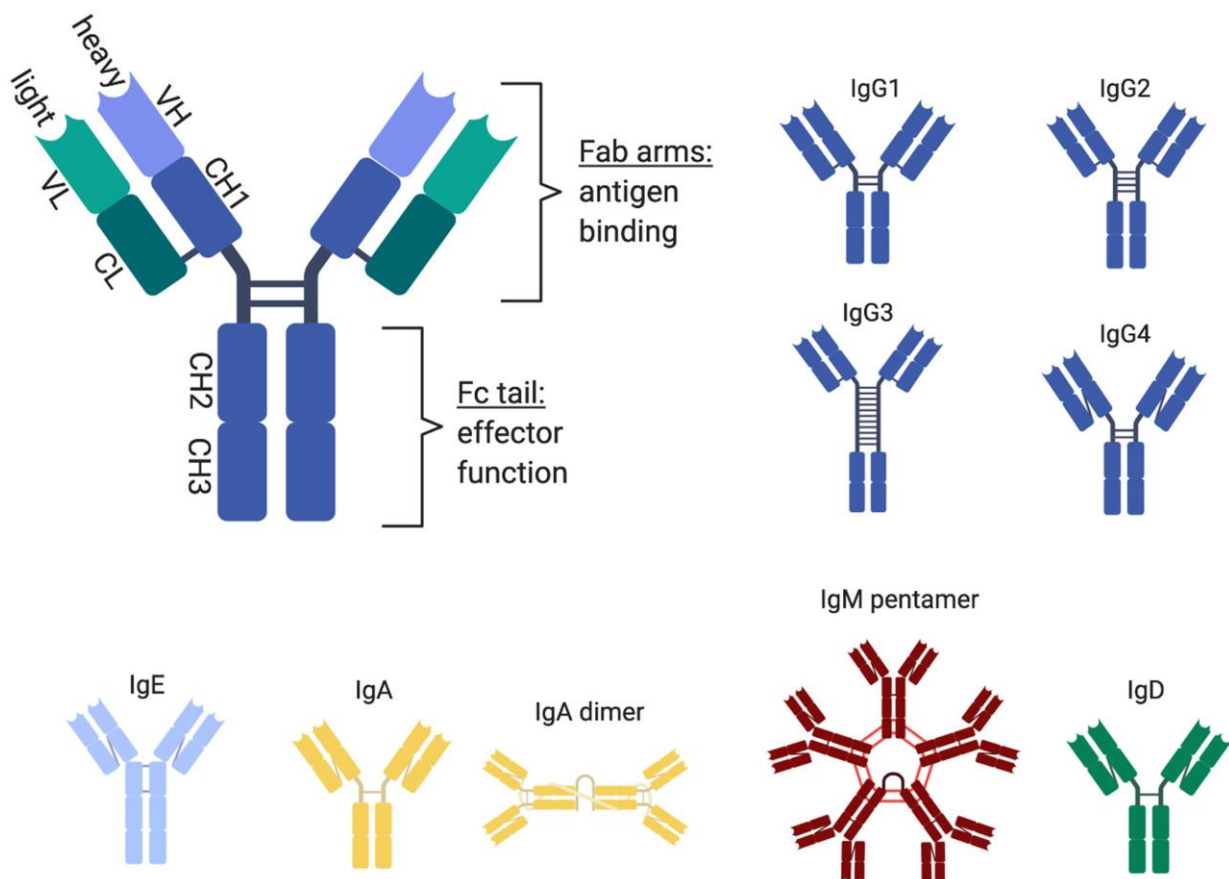


Figure 1. Antibody structure and immunoglobulin classes.

From: Vukovic, N., van Elsas, A., Verbeek, J. S. & Zaiss, D. M. W. Isotype selection for antibody-based cancer therapy. *Clin. Exp. Immunol.* **203**, 351–365 (2021). © 2020 British Society for Immunology

Using the proteolytic enzyme *Papain*, it is possible to dissect the antibody structure and identify the parts of the molecule that are responsible for the antibody functions. Three fragments are obtained from the cleavage: two Fab fragments (for Fragment Antigen Binding), that contain the antigen-binding site (paratope) and the Fc fragment (for Fragment Crystallisable) that mediates the antibody's effector functions²³.

Two different light chain variants, called κ and λ , are encoded by human genes which are located in two different chromosomal loci, IGK and IGL respectively²⁴. Heavy chain genes are found within a single gene locus (IGH) and five heavy chain classes or isotype exist, and they are denoted by five Greek letters: α , γ , δ , ϵ and μ ^{25,26}. These heavy chains characterize, respectively, the five major classes of human immunoglobulin: IgA, IgG, IgD, IgE, and IgM (Figure 1)²⁷.

The different classes of antibodies differ in their biological function, half-life and serum concentration and valency as a result of different numbers of monomers that join to form a complete antibody molecule²⁸. IgG is the most abundant immunoglobulin (serum concentration of ≈ 9 mg/mL), it has several subclasses (IgG1, 2, 3 and 4 in humans, numbered in reference to serum level) which exhibit different functional activities, and it is involved in long-term immunity²⁹. IgM antibodies are usually found as pentameric structures and are associated with the primary immune response. Monomeric forms of IgM and IgD are expressed in B cells and used as receptors (BCR)³⁰. However, IgD is mostly expressed on mature naïve B cells³¹. IgD is found at very low levels in the serum, show a low half-life and can participate in immune surveillance and regulation³². IgA is mostly found in secretions (e.g., breast milk) and mucosal membranes and appear generally as dimer. This antibody isotype is involved in the protection of mucosal surfaces from toxins, viruses and bacteria³³. IgE is present at the lowest serum concentration (≈ 0.00005 mg/mL), has the shortest half-life and mediates hypersensitivity and allergic reactions³⁴. The different antibody classes differ also for the glycosylation pattern which influence the antibody effector function, secretion efficiency, the Fc stability and hinge flexibility^{35,36}.

The effector function of antibodies is triggered when these molecules recognize and bind a specific antigen. Most of these effector functions are induced by the constant region (Fc) of the antibody, which can interact with complement proteins and specialized Fc receptors³⁷. These receptors are expressed by different immune cells including B-cells, natural killer cells, macrophages, neutrophils, basophils, mast cells, monocyte which contribute to the defensive control against pathogens³⁸. The binding between the Fc receptor and the Fc part of the antibody results in the activation of the cell or its inhibition³⁹. The activated effector cell can release cytokines or other molecules that leads to target lysis or, if the effector cell is a phagocytic cell, it can lead to the target phagocytosis. These effects are called, respectively, ADCC, antibody-dependent cell-mediated cytotoxicity and ADCP, antibody-dependent cellular phagocytosis⁴⁰. On the other side, Fc portion of antigen:antibody complex can activate the complement cascade through the binding to the C1q complement protein (CDC, complement-dependent cytotoxicity)⁴¹. A specific Fc receptor, the neonatal Fc receptor for IgG (FcRn), is responsible for the transfer of passive humoral immunity from the mother to the newborn in rodents and humans. Throughout life, FcRn contributes to effective humoral immunity by recycling IgG and extending its half-life in the circulation^{42,43}.

In addition to these functions, antibodies can act via direct neutralization of a given pathogen or toxin, in a mechanism that does not directly seem to involve the Fc portion⁴⁴.

1.2.2 Monoclonal antibodies

Monoclonal antibodies are antibodies produced by a single B-cell clone and are able to recognize and bind the same epitope. On the other hand, antibodies produced by a population of B-cells, directed against different epitopes of the same antigens, are defined as “polyclonal”. Both type of antibodies found a large variety of applications, from diagnostic to therapy. The first licenced monoclonal antibody was Orthoclone OKT3 (also known as “muromonab-CD3”) which was approved in 1986 for kidney transplant rejection application⁴⁵. Its production was based on the Nobel price-winning work of Kohler and Milstein (1975) which developed the hybridoma technology^{46,47}. However, since OKT3 antibody was a murine antibody, its therapeutic application was limited due to immunogenicity risks (human anti-mouse antibody response)⁴⁸. To overcome this severe problem, researcher developed techniques to modify rodent antibodies into structures more similar to human antibodies, maintaining the original binding properties. Chimeric monoclonal antibodies were engineered by retaining the murine binding region and by replacing the constant regions of the murine heavy and light chain by human fragments (Figure 2)⁴⁹. The first chimeric antibody, anti-GPIIb/IIIa (abciximab)⁵⁰, was approved in 1994 by the FDA for treatment of cardiovascular diseases, followed by the approval in 1997, of the first chimeric

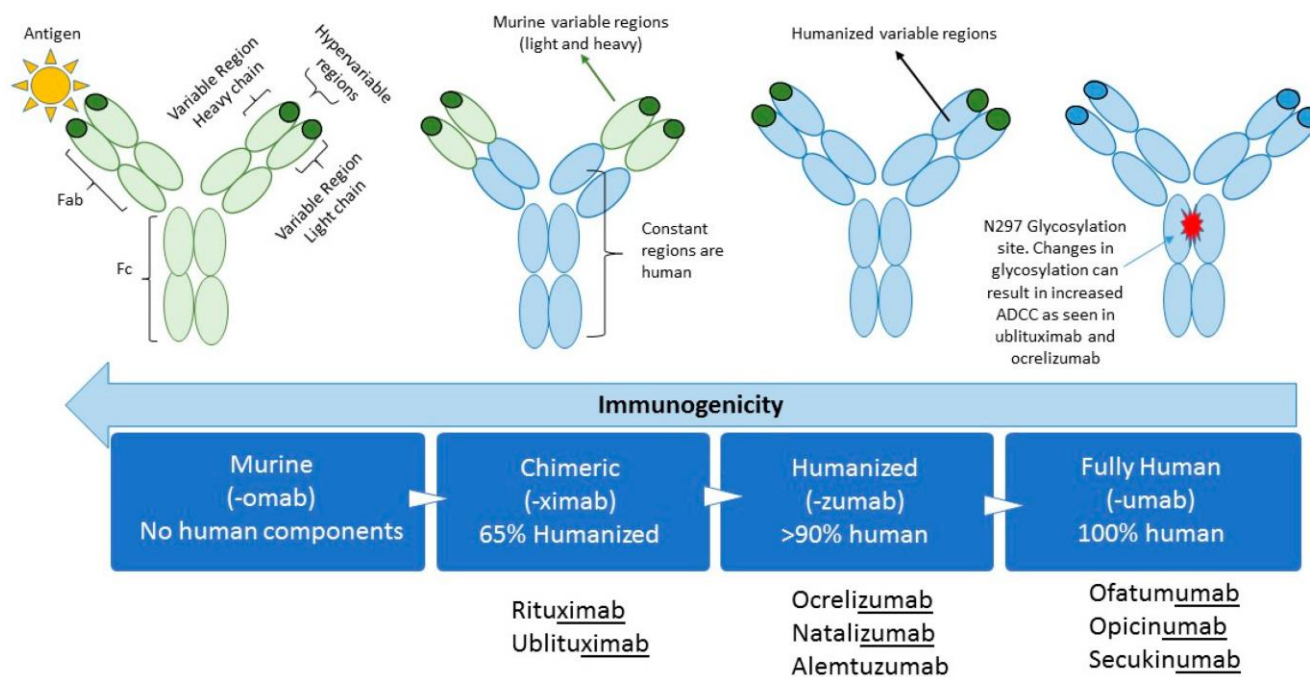


Figure 2 From murine to fully human antibodies

From: Voge, N.V.; Alvarez, E. Monoclonal Antibodies in Multiple Sclerosis: Present and Future. Biomedicines 2019, 7, 20. <https://doi.org/10.3390/biomedicines7010020>

monoclonal antibody intended for oncological applications, anti-CD20 IgG1 (rituximab) for non-Hodgkin's lymphoma⁵¹.

Humanized antibodies were generated by grafting a non-human complementarity determining regions (CDRs) onto a human antibody framework^{52,53}. The first approved humanized mAb was daclizumab in 1997, an anti-IL-2 receptor for the prevention of transplant rejection⁵⁴. The development of humanized antibodies opened the possibility of applications of these biologics in long-term treatments. However, humanized antibodies often have a poorer affinity than the parental murine mAb and require further optimization, e.g. by introducing mutation in the CDRs to increase the affinity and specificity against the target^{55,56}. The first fully human monoclonal antibody was developed in 1990 by using a novel technique, the phage display technology, based on the introduction of exogenous genes into filamentous bacteriophages to create a library of antibody genes (>10¹⁰ genes)⁵⁷. Proteins are presented on the phage surface as fusion with a coat protein and can be screened for binding, affinity against a specific target or other properties^{58,59}. The first fully-human monoclonal antibody, Humira (anti-TNF α), was approved by FDA in 2002, for rheumatoid arthritis and today is still one of the best-selling drugs worldwide⁶⁰. Other display technologies have been developed for antibody discovery, such as yeast surface display, bacterial display or mammalian surface display⁶¹. In addition to in-vitro display technologies, fully-human mAb can be obtained by using transgenic animals (e.g., HuMabMouse and XenoMouse in 1994)⁶². This technology is based on the replacement of the endogenous immunoglobulin genes by human immunoglobulin genes which make the transgenic animals capable of synthesized fully-human antibodies upon immunization^{63,64}. The first fully-human mAb generated in transgenic mouse, an anti-EGFR (panitumumab) was approved by the FDA in 2006⁶⁵.

Today some of the world's blockbuster drugs are monoclonal antibodies⁶⁶. Their principal medical applications are oncology, immunology and haematology, and most of mAb have even multi-disease applications. In addition, few mAb have been already approved for application against infectious disease or are in late clinical trial stage such as ibalizumab (to treat drug-resistant HIV), raxibacumab (ABthrax) for prophylaxis and treatment of anthrax or Ansuvimab against Ebola. In addition to therapeutic applications, antibodies are extensively used in diagnostic and for analytical purpose. In fact, due to their high specificity and sensitivity, antibodies are extensively use in research for western blotting, immunohistochemistry, flow cytometry, immunofluorescence analyses, immunoprecipitation assays and in vivo applications⁶⁷.

1.2.3 Bispecific antibody format and their applications

Over the past decades, the so-called bispecific antibodies (bsAb) have become increasingly of interest for diagnostic and therapeutic applications. Under the definition of "bispecific antibodies", more than 100 different antibody formats can be found, all sharing the ability to recognize two different epitopes either on the same antigen or on different antigens⁶⁸ (Figure 3). Bispecific molecules can be classified based on the presence or

absence of an Fc region. The number of binding sites and symmetrical/asymmetrical architecture are additional discriminating features for bispecific formats. Fc-less bsAbs are composed of single-chain variable fragment (scFv), variable domain of heavy chain (VHH) of Fab fragment of two different antibodies without the Fc region⁶⁹.

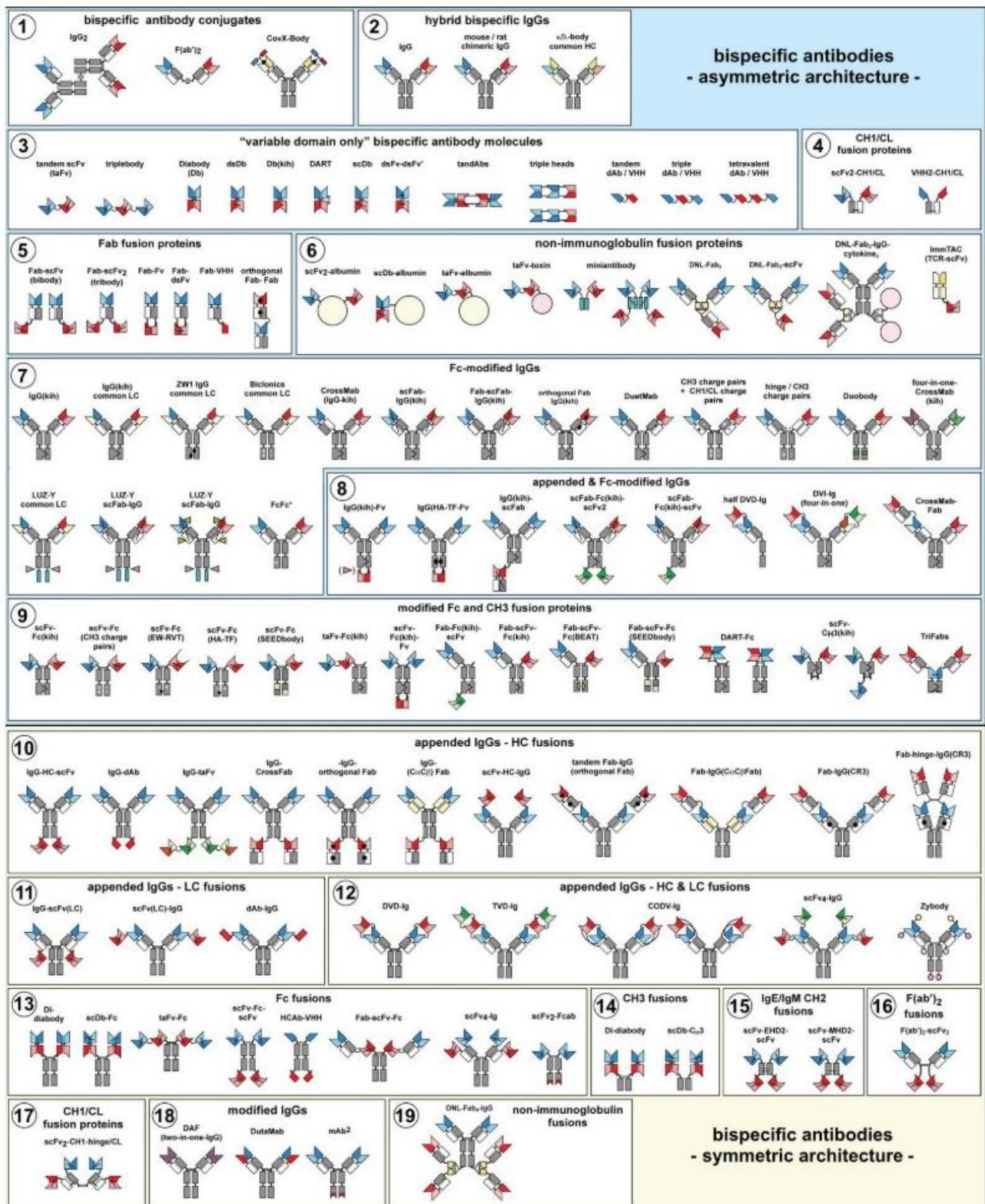


Figure 3 Overview of bispecific format.

From: Brinkmann U, Kontermann RE. The making of bispecific antibodies. *Mabs*. 2017 Feb/Mar;9(2):182-212. DOI: 10.1080/19420862.2016.1268307. PMID: 28071970; PMCID: PMC5297537, © 2017 published with license by Taylor & Francis Group, LLC .

Examples of Fc-less bsAb are the bispecific T-cell engagers (BiTEs), which use linker to connect two scFvs, the DART (dual affinity retargeting) platform in which the Fv is formed by the association of a VL on one chain and a VH on the second chain⁷⁰. Other platforms involve tetravalent antiparallel structures (TandAbs) and VH only (Bi-Nanobody)⁷¹. In the absence of the Fc region, these bsAbs result smaller in size leading to a better tissue-penetrating capacity, short in vivo half life, decreased stability and higher probability of aggregate formation⁶⁹. Bispecific antibodies that include the Fc region can be further divided into IgG-like molecules and those with a modified IgG-like structure (e.g., containing additional binding sites)^{68,72}. Those IgG-like molecules require normally four chains, two different heavy chains and two different light chains. Simultaneous expression of four chains leads to 16 different combinations of chain arrangement (10 different molecules) among which only two represent the desirable heterodimeric bispecific antibody (12.5% of the statistical probability)⁷³. Heavy chain heterodimerization and correct assembly of binding sites represent the main problems in bsAb production and the greatest challenge for IgG-like bsAb manufacturing⁶⁸. For this reason, over the past two decades, several techniques have been developed to help the right chains match and pair. First approaches for bsAb production were based on quadroma technologies expressing two different heavy/light chain, based on the fusion of two hybridoma cells⁷⁴. In addition, the use of co-cultures of cells expressing half-antibody and subsequent chemical crosslink, was also applied to obtain bsAb molecules⁷⁵. However, these methods showed low yields, poor product quality and required complex purification strategies. Most recent techniques are based on antibody chain engineering to ensure heavy chain heterodimerization and specific light chain pairing⁷⁶. The knob-into-hole technology, developed by Carter et al. in 1996⁷⁷, represent steric mutation-based strategies which involve engineering of CH3 domains. The knob is represented by a bulky amino acid residue (tryptophan) which matches an “hole” in the CH3 domain on the other heavy chain, created by smaller amino acid residues such as threonine and alanine⁷⁸. Electrostatic steering of two complementary charged heavy chain, strand-exchange engineered domain (SEED) heterodimerization⁷⁹, which employed alternating segment of IgG and IgA, or artificial leucine zipper, are additional techniques that have been employed for heavy chain dimerization⁸⁰.

Different approaches have been established to ensure cognate heavy-light chain pairing (non-covalently linked chains) in combination with Fc-modified heavy chains. In 2011, Roche presented the CrossMAb technology, based on the crossover of different domains within the Fab fragment of a bispecific IgG antibody⁸¹. Further attempts to direct light chain pairing with its cognate heavy chain involved the substitution of the CH1 and CL domain of one Fab arm with C α and C β domains from the T-cell receptor⁸². Other strategies rely on steric complementary and electrostatic steering at Fab-interface⁸³ or the use of common light chain or common heavy chains ($\kappa\lambda$ -bodies)⁸⁴. Currently, 110 bsAb have been tested in clinical trials for several applications and three have been approved and are commercially available: catumaxomab, blinatumomab and emicizumab⁷¹. Catumaxomab (Fresenius Biotech) has been approved in 2009 for malignant ascites treatment, and it targets EpCAM on tumor cells and CD3 on T cells⁸⁵. Blinatumomab (Amgen) was approved in 2014 to treat relapsed or

refractory precursor B-cell acute lymphoblastic leukemia, acting on CD3/CD19 dual target⁸⁵. Elicizumab (Roche) was approved in 2017, for hemophilia A indication, acting as a bridge by connecting factors FIXa/FX and creating a hemostatic effect⁸⁶.

1.3 Antibody production and process development

Therapeutical and commercial interest in antibody molecules raised the need of developing efficient production systems for recombinant proteins both on a small scale, for research purposes, and on a large scale, for manufacturing. The manufacturing technology for antibodies is traditionally divided in two main step: upstream processing (USP) and downstream processing (DSP). The USP involves cell culture process and the production of the target protein. During cell line development the selection of host cells, the expression vectors, transfection and selection methods, clone screening and isolation are crucial steps for getting high productivity and product quality⁸⁷. After the selection of the productive cell line, a specific customized process is developed for each produced antibody. Process development in USP includes media and feed development, bioprocess development and scale up, and several parameters can be addressed to obtain a robust process leading to high product titer, high productivity and defined quality⁸⁸⁻⁹⁰ (Figure 4). Downstream processing (DSP), which focuses on the purification and formulation of the protein into a drug substance or drug product⁹¹. Screening investigation for a new process or its optimization are often conducted at milliliter scale and recent DoE and high throughput approaches improved significantly process development⁹².

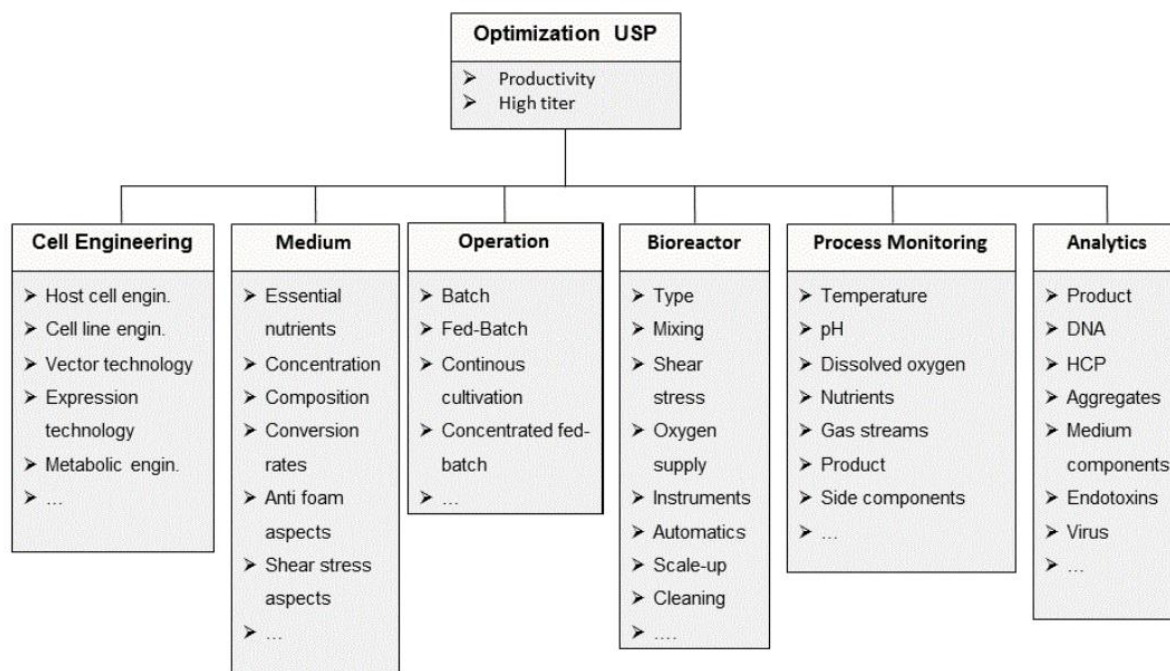


Figure 4 Optimization areas and parameters in upstream processing.

From: Gronemeyer, P., Ditz, R. & Strube, J. Trends in upstream and downstream process development for antibody manufacturing. *Bioengineering* 1, 188–212 (2014).

1.4 Expression host

Cellular system represent the principal expression system for the production of monoclonal antibodies or other recombinant glycoproteins. These expression systems include mammalian⁹³, insect, yeast, bacterial, plant⁹⁴ and algal cells⁹⁵. However, since post-translational modification impact considerably the efficacy and the safety of therapeutic protein, not all listed host cells are equally utilizable⁹³. Non-mammalian expression systems are mainly limited to the expression of simple, non-glycosylated proteins¹⁸ due to the absence of the appropriate chaperones system⁹⁶ or due to the potential immunogenicity of the glycan structure they produce as post translation modifications (PTMs)^{95,97,98}. On the other hand, mammalian expression systems have become dominant for therapeutic recombinant protein production^{18,99} due to their capacity to express and fold large and complex recombinant proteins harboring human-like PMTs⁹⁸. However, mammalian hosts have higher risk of viral contamination, lead to high cultivation cost and achieving high product yield in large scale remains challenging¹⁰⁰. To overcome these limitations many strategies have been applied, such as optimization of expression vector⁹⁹ and selection strategies⁹⁵, cell line engineering¹⁰¹, media and feed formulation¹⁰² and bioprocess development through improvement in batch/fed-batch/perfusion culture¹⁰³. The most common mammalian host for recombinant mAb expression are CHO, NS0, Sp2/0, HEK293 and PER.C6 cells. However, mAb approved for human therapy are only produced in CHO, NS0 and Sp2/0 cells¹⁰¹.

1.4.1 CHO cells

Since the approval of the human tissue plasminogen activator (Genentech) in 1986, Chinese Hamster Ovary (CHO) cells have become the industry's workhorse for biopharmaceutical production and are used for manufacturing about 70% of all biopharmaceuticals proteins and all mAb approved since 2016^{104,105}.

Many aspects make CHO cells so important and predominant in biopharmaceuticals industry such as the efficient post-translation modification of expressed proteins, reduced biosafety risk due to low susceptibility to human viruses¹⁰⁶, tolerance to genetic manipulation, adaptation to growth in serum-free suspension conditions¹⁰⁷ and to manufacturing process scale¹⁰⁸. In addition, since CHO cells have been extensively used in industry for over three decades and are well-characterized as safe host for recombinant protein production, regulatory approval can be rapid^{104,109,110}. Besides low production yield and high manufacturing costs when using mammalian cells, the advances done over the past 30 years of biopharmaceutical development have led to the establishment of CHO cell culture process reaching antibody titers of 13 g/L in fed-batch processes^{105,108}. CHO cells comprise a variety of cell lines such as CHO-S, CHO-K1, CHO-DXB11, CHO-DG44 and CHO-K1SV that share a common ancestor. The immortal primary CHO cell culture (CHO-ori cell line) was isolated in 1957 by Theodor Puck^{100,111}. Extensive mutagenesis and clonal selection allowed the isolation of a variety of lineages which resulted in a genetic¹¹² and phenotypic heterogeneity¹¹³ among them. CHO-K1 cell line was derived by subcloning of the original cell line in 1957. From this lineage, in 1980, the CHO-DXB11¹¹⁴ lineage was generated through chemical

mutagenesis, which lacked DHFR activity due to the loss of one allele and a missense mutation in the other active allele¹¹⁵. This metabolic modification of the original strain can be used as a selection method in cell line development. The CHO-DXB11 cell line was historically the first one used for large scale production of recombinant protein¹¹⁵. Full deletion of both DHFR alleles was realized later, by gamma radiation mutagenesis to generate CHO-DG44 cell line¹¹⁶. A similar approach was adopted by Lonza Biologics, who developed the CHO K1SV (suspension variant) cell line and then CHO K1SV GS^{-/-}, to be used in the GS expression system¹⁰⁷. Today CHO-DG44 and CHO K1SV GS^{-/-} cell line are two of the most prevalent antibody expression systems for therapeutics production in the biopharmaceutical industry¹⁰⁰. The origin of CHO-S cells is not well outlined and documented. However, CHO-S were first described by Thompsons and coworkers which recognized the ability of some CHO cells to grow in single-cell suspension culture^{117,118}. After the sequencing of CHO K1 cell line in 2011¹¹⁹, many advances have been done in terms of cell engineering and process optimization to improve CHO cell lines in regards to cell growth and therapeutic protein production.

1.5 Cell line development (CLD) for antibody production

Recombinant protein can be produced by mammalian host transiently or by stable expression. In transient gene expression (TGE) the expression vectors do not integrate into the host genome, remaining as episomes, and are lost over time and with cell divisions. Protein production is usually limited to 7-14 days post transfection making it possible to obtain a few milligram to gram of protein within 2-4 weeks. This strategy is mostly used for research purposes in low scale production and product quality is generally strongly subjected to batch-to-batch variability^{120,121}. Large scale production and manufacturing require the development of stable cell lines which have integrated the expression construct into their genome and therefore they provide large amounts of proteins with consistent quality⁹³. Stable cell line generation is a critical and time-limiting step in the production of biopharmaceuticals¹⁰⁹ which could take up to 12 months and requires labour-intensive clonal selection processes and expansive laboratory equipment⁹³. The classical cell line development process (CLD, Figure 5) consists of: (a) transfection of selected host with the expression vector containing the GOI cassette and its integration into the host genome; (b) selection of stable pool expressing the GOI via metabolic or antibiotic selection; (c) selection of single-cell clones and screening of high-producing clones; (d) clone characterization and (e) scale-up of promising clones¹²². Early improvements in CLD aimed to increase volumetric productivity and were focused on optimizing expression vectors¹²³⁻¹²⁵, transfection procedures, selection strategies, methods for screening high-producing clones, and by metabolic engineering the host cell line^{126,127}.

Since, the aim of CHO CLD is the generation of a stable, high-producing, single cell-derived clone that can be scaled-up for manufacturing purpose, one of the most critical steps in CLD remain the clonal screening¹²⁸. Classically the GOI is randomly integrated into the host genome, and after the selection step, the obtained stable pool is composed by a phenotypic and genotypic heterogeneous population. Thus, screening of a large number of clones is required to isolate a high producing clone and, in addition, multiple rounds of serial subcloning steps

are necessary to ensure monoclonality^{107,129}. This makes the entire process of clonal screening long and laborious. Recent advances in genome editing technologies and -omics approaches^{100,104} supported the shortening of CLD timeline making the clonal selection steps easier and less time consuming.

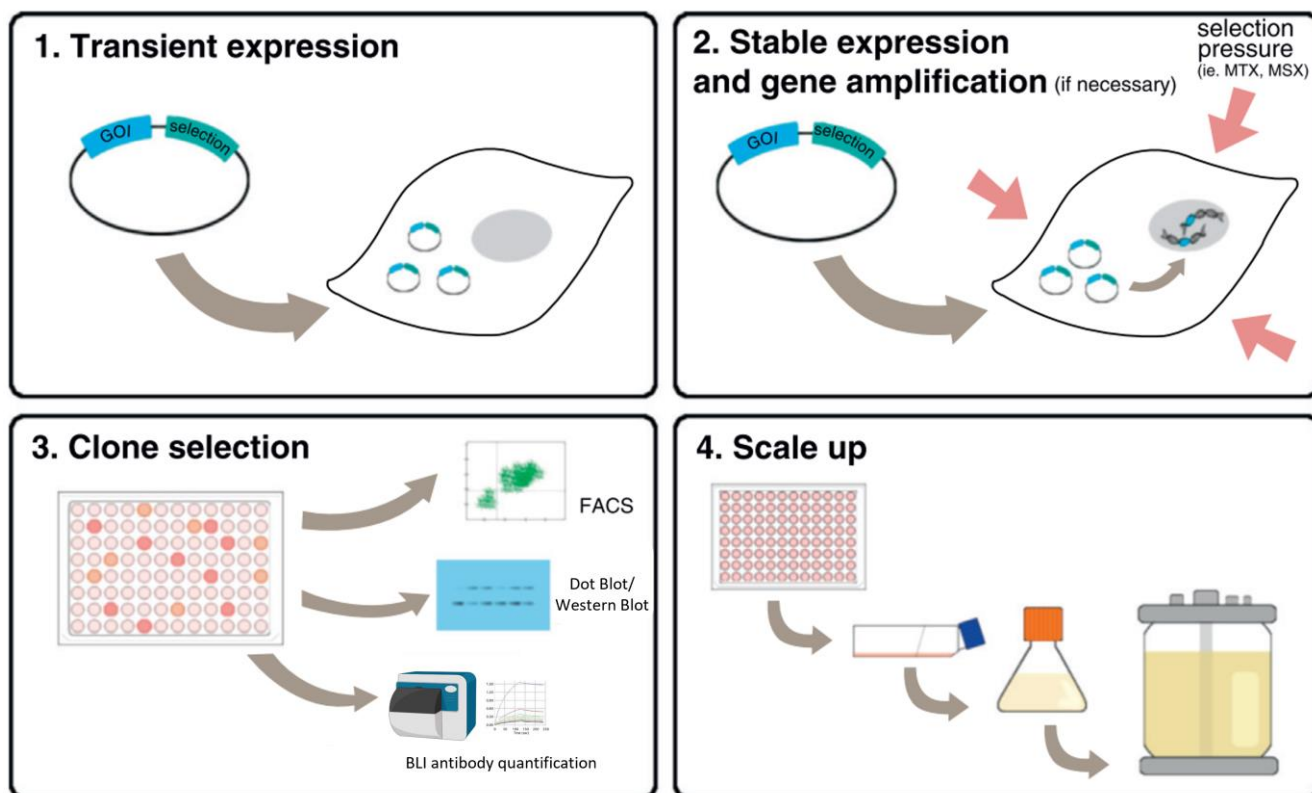


Figure 5 Cell line development scheme. The GOI is expressed transiently to evaluate its efficacy and manufacturability before stable cell line development. Then the GOI is stably integrated into the host cell line for stable expression. Several methods for stable cell selection and gene amplification have been developed to generate and select high producing clones. Single cell clones need to be selected and screened to obtain a good stable producer which fits the requirements for stability, product quality and titer. The last step is then the scale up of the selected cell line, to be used in industrial production.

From: Noh, S. M., Sathyamurthy, M. & Lee, G. M. Development of recombinant Chinese hamster ovary cell lines for therapeutic protein production. *Curr. Opin. Chem. Eng.* 2, 391–397 (2013), ©2013 Elsevier Ltd. All rights reserved.

1.5.1 Common selection methods and clone isolation strategies for CHO cell CLD

For stable cell line development, a selection marker gene is usually inserted into the expression vector with the gene of interest conferring a selective advantage to the transfected cell¹²⁶. Many selection systems have been developed over the years and the most common are the GS systems, the DHFR system and those based on antibiotic resistance⁹⁵. In the GS system, CHO K1SV GS⁻ cell lines lack the glutamine synthase (GS) gene and they need to be continuously supplemented with glutamine. The DHFR expression system is based on the use of DHFR-deficient cell lines which cannot grow unless transfected with a functional copy of DHFR gene or in

media supplemented with thymidine. Cells were transfected with an expression vector containing both the GOI and the DHFR gene and then grown in medium lacking hypoxanthine, thymidine, and glycine. In these culture condition and with the addition of methotrexate (MTX), only cells which are efficiently transfected will survive the selection¹³⁰. Since methotrexate is a DHFR inhibitor, the use of increasing concentration of MTX push cells to produce more DHFR and then more recombinant protein in a mechanism known as gene amplification^{100,114}. In a similar way, the GS system use CHO-K1SV cell line in combination with the GS vector for the expression of GOIs and containing an active copy of the GS gene. In presence of methionine sulfoximine (glutamine synthetase-inhibitor) and glutamine-free medium, CHO K1SV cell line cannot grow unless efficiently transfected with the GS vector^{131,132}. The use of MSX (in a range of 250-500 μ M) helps the inhibition of endogenous glutamine synthetase activity allowing as well the amplification of the transgene¹³³. CHO-K1SV GS knock-out cell line was recently developed enhancing selection stringency⁹⁵. Compared to the DHFR system, the GS system can reach sufficient expression level with a single round of selection and amplification, shortening the timeline for cell line generation¹³⁴.

In antibiotic resistance-based selection, transfected cells are maintained in medium supplemented with the appropriate antibiotic concentration until the population without integration events is eliminated. Commonly used antibiotic resistance genes include neomycin phosphotransferase (Neo), hygromycin resistance gene (Hyg) and puromycin N-acetyl-transferase (Puro)¹³⁵. The described selection strategies are used in combination with methods to isolate and select high-producing single cell clones in order to obtain a productive clonal cell line¹⁰⁷. Classical strategies for clonal selection involved limiting dilution in 96-well plates or single cell-derived colony picking in semi-solid medium¹³⁶. However these techniques are labour-intensive and have low throughput. High-throughput single cell clone selection technologies are based on fluorescence-activated cell sorting (FACS), ClonePix™ system or the more advanced Beacon optofluidic system¹⁰⁹. These techniques require often labelling methods to screen productive clones and due to the high cost are mostly limited to industrial settings. Therefore, there is an increasing demand for new clonal selection strategies, allowing easy visualization of stable integrants and productive clones.

1.5.2 Emerging trends in CHO cell line development

In order to meet the increasing demand of biotherapeutic production, product quality and cost reduction, CHO cells have been continuously optimized to improve cellular productivity, increase product quality and ensuring cell line stability. Different approaches were tested over the years such as host cell engineering, expression vector engineering, optimized non-targeted transgene integration strategies as well as targeted integration techniques¹³⁷. CHO cell hosts have been directly engineered to improve per-cell yields and product quality by modifying cellular metabolism, secretory pathway and inhibiting apoptosis¹³⁸. In addition, continuous improvements in the expression vector design and clone screening strategy significantly increased production yields. Expression vectors have been engineered by using natural or synthetic promoters combined with

enhancer elements or adding epigenetic regulatory elements, such as ubiquitous chromatin opening element (UCOE), scaffold/matrix attachment region (MAR) or stabilizing anti-repressor element (STAR) which increase the number of producing clones and transgene expression^{139,140}. Cell line stability and transgene expression were further improved by using lentiviral vectors¹⁴¹ which tends to integrate in actively transcribed genes or by using transposon/transposase systems^{142,143} which helps the transgene integration into the host genome through a cut-paste system. During the last decade, advances in genome editing tools and deep knowledge of CHO genomic sequence opened new approaches for transgene integration based on targeted integration systems. Developed techniques include the use of artificial nucleases like zinc finger nucleases (ZNFs), CRISPR/Cas system, transcription-activator like effector nucleases (TALENs) or the use of site-specific recombinases in landing pad systems^{122,144}.

1.6 Epigenetic regulatory elements: a focus on MAR sequences

In the nucleus of high eukaryotes, DNA is associated with histones forming a well-compacted and packed structure defined as chromatin. The latter is organized as independent loops and topological associated domains (TADs)¹⁴⁵. The formation of each loop is dependent on specific sequence, called Matrix Attachment Region (MAR) or SAR (Scaffold Attachment Region), which serve as link to the nuclear matrix¹⁴⁶⁻¹⁴⁸. Due to their ability to modulate chromatinic landscape and their involvement on the regulation of gene expression, these sequences are classified as epigenetic regulatory elements^{140,149}. MARs have been identified in several defined gene loci¹⁵⁰⁻¹⁵³ and seem to be involved *in vivo* in the control of chromosomal activity, acting as boundary element and helping transgene expression¹⁵⁴. Despite the nuclear-anchor function of the MAR is conserved from plants to vertebrates¹⁵⁵⁻¹⁵⁷, their sequence is polymorphic and their function is strongly related to their structural properties. The MAR secondary structure forms a specific curvature, with a deep DNA major curvature and a wide minor groove¹⁵⁸, which naturally promotes double-helix denaturation. In addition, although no consensus sequences can be found within the MAR sequences, these regulatory elements show some common features. MAR sequences are 300-3000 bp-long, contain an AT-rich core region which supports DNA unwinding, base unpairing^{159,160} and DNA bending¹⁶¹, and 3'/5' flanking regions containing putative binding sites several proteins such as transcriptional factors¹⁶²⁻¹⁶⁴, protein involved in chromatin rearrangement¹⁶⁵⁻¹⁶⁷ and enhancer/blocking elements¹⁶⁸. The combination of these features and the structural properties of the MAR make these sequences strong "anti-silencing" elements which could prevent heterochromatin spreading and augment expression of those genes contained into their delimited chromatinic loop^{158,169,170}. For these reasons, MARs have been extensively used in expression vectors for a stable expression of transgenes in mammalian expression host¹⁷¹. The inclusion of the MAR into vectors has several effects on the generation of stable cell population. These elements could enhance and stabilize transgene expression in long term culture, increase the number of cells which integrate and express the transgene, reduce the variability in gene expression in a polyclonal population and augment the number of transgenes integrated per cell. The latter seems to be due to an increase in plasmid

concatamerization in the cell nucleus and recombination mechanism which favor transgene integration into permissive chromatin loci¹⁷². Synthesis dependent microhomology-mediated end joining (SD-MMEJ) was identified as the primary mechanism driving plasmid integration into CHO cells¹⁷³ and MAR may promote SD-MMEJ-mediated recombination through the AT-rich region and their potential for double helix denaturing or topoisomerase II cleavage site^{149,173}.

In 1988, the matrix attachment region flanking the chicken lysozyme domain were studied and the chicken lysozyme 5' MAR was identified as one of the most active epigenetic element^{151,174}. The use of this element in expression vector enhances transgene expression¹⁷⁵ and helps the establishment of high-producing stable cell lines reducing clonal screening¹⁷⁶.

The human genome was estimated to contain between 30,000-100,000 MAR sequences and in 2007, P.A. Girod *et al.* developed a genome-scale computational method, a MAR-prediction program, to identify elements that increase gene expression and share structural features with the already-known MAR sequences¹⁵⁸. This tool allowed the finding of most powerful MAR elements into the human genome, such as MAR 1-68, MAR 3-5 and MAR X-29, which are currently used in expression vectors for cell line development^{177,178}. These elements showed an elevated activity in comparison with the chicken lysozyme 5' MAR mediating higher and consistent gene expression^{158,172}. However, due to their potential when included in expression vector, most of these elements have been patented^{179,180} and, as a consequence they are not free to be used as tools in cell line development for improving protein expression for commercial use. Many studies have been done to find the "active" part of the MAR¹⁷⁸, to evaluate which position or combination of MAR elements and promoters result in effective protein expression¹⁸¹⁻¹⁸⁴. However, experiment outcomes were not always clear, suggesting that the MAR function could be MAR specific, cell-specific and influenced by vector components¹⁴⁰.

1.7 TI using Site-specific recombinases

Site-specific recombinases are enzymes which are specialized in recombination processes that involve the reciprocal exchange between DNA strands¹⁸⁵. Through DNA sequence recognition, binding, DNA break and strand inversion, these enzymes are able to mediate integration, excision, or inversion of DNA regions. Recombinases recognize specific DNA sites defined as "recombination sites" and the outcome of the recombination process depends on the initial arrangement of the recombination sites¹⁸⁶. The high specificity, ease of use, and level of conservation, make site-specific recombinases a powerful tool for targeted manipulation of DNA. The ability to modify DNA has been used by scientists as a tool for cell line development¹⁸⁷, using recombination site as landing pad for site specific integration of the gene of interest, and for creation of synthetic gene networks for cell programming^{188,189}.

1.7.1 Overview on recombinases

Site specific recombinases were discovered in the bacteriophage λ system for their involvement in integration and excision of viral chromosome from the chromosome of its *E. coli* host¹⁹⁰. Subsequently, several different site-specific recombination systems were discovered in bacteria and lower eukaryotes¹⁸⁵. Despite the distinct biological role or host in which they act, recombinases can be sorted into two evolutionarily families: serine recombinases (e.g., ϕ C31, R4, BxB1) and tyrosine recombinases (e.g., λ , Cre, Flp).^{191,192} The two groups differ for the amino acid residue present at the catalytic site, for the mechanism of recombination and for the recognized recombination sites (Figure 6). However, some similarities can be found regarding site recognition, synapsis formation and strand turnover. Recombination events start by the binding of the recombinase enzyme and two similar or identical DNA sequences, the target recombination sites. For both recombinase families, recombination is a conservative process and DNA break and rejoining occurs with conservation of phosphodiester bond energy^{193,194}. After DNA binding, the central nucleophilic amino acid residue of the recombinase attacks the phosphodiester bond on DNA molecule and transiently binds the phosphate by covalent bond through the hydroxyl group of the catalytic tyrosine or serine residue. This transient linkage between DNA and recombinase conserves the bond energy avoiding the need of high-energy intermediates¹⁸⁷. Tyrosine-recombinases support reversible reactions (Figure 6 B), mediating integration, resolution or excision and inversion of DNA regions. Recombination sites for tyrosine recombinases are identical and contain 8 bp long asymmetric cross-over spacer region flanked by identical inverted repeats^{186,195}.

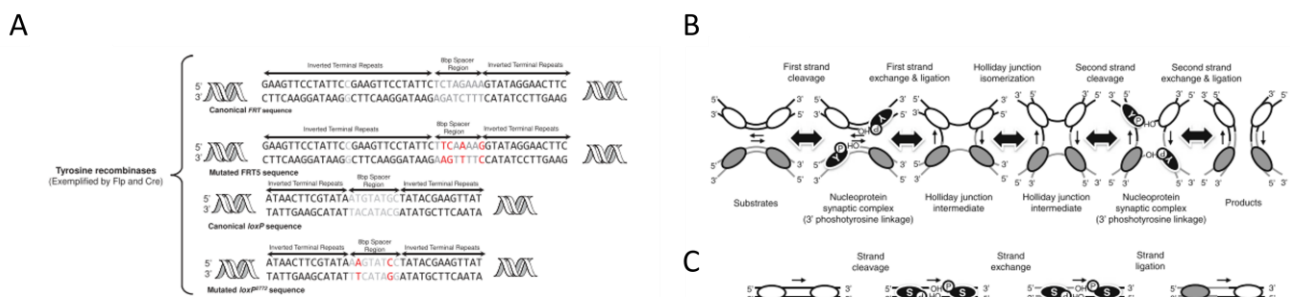


Figure 6 Site-specific recombinases. (A) Architecture of target recombination sites for both tyrosine and serine recombinase. **(B)** Recombination mechanism of tyrosine-type recombinases. **(C)** Recombination mechanism of serine-type recombinases. Serine-type recombinase-catalyzed recombination. Each hydroxyl group of catalytic serine residue in all four recombinase molecules acts as a nucleophile, attacks the substrate DNAs, and forms a 5' phosphoserine linkage. Then, two of four recombinase molecules that are covalently linked to different substrate DNAs rotate with respect to the other pair of recombinases and religate their attached 5' phosphates to the 3'-OH of the unrotated DNAs.

From:

Srirangan K, Loignon M, Durocher Y. The use of site-specific recombination and cassette exchange technologies for monoclonal antibody production in Chinese Hamster ovary cells: retrospective analysis and future directions. *Crit Rev Biotechnol.* 2020 Sep;40(6):833-851. doi: 10.1080/07388551.2020.1768043. Epub 2020 May 26. PMID: 32456474. ©2020 Copyright of the Crown in Canada. National Research Council Canada.

Hirano, N., Muroi, T., Takahashi, H. & Haruki, M. Site-specific recombinases as tools for heterologous gene integration. *Appl Microbiol Biotechnol.* 227–239 (2011) doi:10.1007/s00253-011-3519-5. © 2011 Springer-Verlag.

The recombination mechanism for these recombinases is a multistep process: first strand cleavage, first strand exchange and ligation, Holliday junction isomerization, second strand cleavage, second strand exchange and ligation. Tyrosine-type recombinases bind each recombination site as dimer forming a nucleoprotein synaptic complex¹⁹⁶. The hydroxyl group of the tyrosine residue in the catalytic domain of the two recombinases acts as a nucleophile, attacking the DNA molecule in cis, and forming a 3' phospho-tyrosine linkage. The 5'-OH of each cleaved DNA strand subsequently attacks the 3' phospho-tyrosine linkage of the opposite nucleoprotein complex, and the resulting strand exchange forms a Holliday junction intermediate¹⁹⁷. After isomerization of the Holliday junction intermediate, the other pair of recombinases catalyze the second strand exchange which resolves the Holliday junction intermediate and generates the recombination product¹⁹⁶. Therefore, tyrosine recombinases cut only one strand of each identical recombination site at the time, allowing the formation of a cross-strand intermediate and after recombination the original sequence of the recombination site is reconstituted. Serine recombinases support irreversible recombination (Figure 6 C), unless in the presence of RDFs (recombinase directionality factor), mediating a function of "integrases". Recombination sites for serine integrases, AttP and AttB (phage and bacterial attachment sites) share multiple features but are not identical. Attachment sites show a 3 bp cross-over region flanked by flanking arms which are similar but not identical (P-O-P' and B-O-B', for AttP and AttB site respectively¹⁹¹). After recombination, two "new" sites are generated: Attachment site right (AttR, POB') and Attachment site left (AttL, B'OP). AttL and AttR sites show distinct structures compared with AttP/AttB sites and cannot interact with the recombinase and reverse the recombination reaction^{187,191}. The recombination process for serine recombinases consists of cleavage, clockwise rotation and ligation of DNA strands¹⁹⁸. Unlike tyrosine recombinases, serine recombinases generate double stranded breaks at the crossover sites, without the formation of Holliday junction. Serine recombinases form dimers that link the substrate DNA forming a synaptic complex with two crossover sites and four recombinase subunits. Each hydroxyl group of the catalytic serine residue in all four recombinase molecules acts as nucleophile, attacking the dsDNA at the 3' phosphodiester bonds of the central dinucleotide and generating 2 bp sticky ends with a 5' phosphate end. Then, the free phosphate binds covalently the hydroxyl group of the serine residue in the catalytic domain via a phosphoserine linkage.¹⁹⁹ Two of the four recombinase-DNA complexes in the generated nucleoprotein synaptic complex, rotate 180° with respect to the other pair of recombinase-DNA complexes (subunit rotation) and religate the covalently attached 5' phosphate to the free 3' hydroxyl group of unrotated substrate DNAs¹⁹⁶.

The mechanism of recombination mediated by both serine and tyrosine recombinases has three main outcomes depending on target site orientation: integration, excision (tyrosine recombinase only) and inversion. These structural outcomes are involved in a variety of biological function such as phage integration/excision, DNA transposition, reduction of replicons and regulation of gene activation¹⁸⁵.

1.7.2 The use of site-specific recombinases for recombinant protein production in mammalian hosts

In addition to their biological activity, recombinases can be used together with their matching recombination sites for site-specific integration of gene of interest in mammalian cells. The first attempt to develop cell lines using this genetic tool can be reconducted to the work of Geoffrey Wahl using FLP-recombinases²⁰⁰. For both serine and tyrosine recombinases, additional mutated orthogonal/heterospecific sites have been found which are recognized from the same recombinase but cannot cross-react with the wild-type site^{201–203}. These new orthogonal sites can be used to generate single or several sites for recombinase-mediated DNA insertion (RMDI), or to create a tag-cassette that can be exchanged in recombinase-mediated cassette exchange (RMCE)¹⁸⁶. The RMDI strategy mediates the integration of the entire transgene-bearing plasmid (donor vector) into a specific spot of the host genome. On the other hand, in RMCE only the DNA sequence between two recombination sites of the transgene bearing vector can recombine into the target site¹³⁷. In both cases, the generation of a stable master host cell line which is able to integrate single or multiple recombination sites for DNA insertion or tag-cassettes for RMCE, is necessary¹⁸⁹. The so-called “landing pad”, representing the recombination site or the entire recombination cassette, need to be stably integrated into the host genome (Figure 7 A). This step can be achieved by random integration of the landing pad²⁰⁴ or using genomic tools such as retroviruses²⁰⁵ or nucleases²⁰⁵. The use of the latter, generally allow the integration of the landing pad into a specific site of the genome which should support high and stable transgene expression. These genomic spots are labeled “hot spots” and some of them have been already characterized in the human and CHO genome^{125,205–208}. In order to facilitate the selection of the cells which have integrated the landing pad, the landing pad or the recombination cassette can contain reporter genes and selection markers. After having selected a stable cell line harbouring the landing pad, this host cell line can be used for the recombinase-mediated site-specific integration of the gene of interest. Integration can be achieved by cotransfection of donor vectors and a helper vector expressing the recombinase.

After integration of the donor vector or the GOI-harboured cassette, a stable productive cell line can be selected (Figure 7 A). The use of serine integrases with couple of orthogonal sites in RMCE allow stable and irreversible integration of the target DNA into the landing pad. Several strategies such as promoter-trap or poly-A trap have been developed to help the selection of the productive cell lines^{191,209,210}. These techniques are based on a specific design of the landing pad and the donor vector. The recombination site in the landing pad is often placed between a strong promoter and the reporter gene or between the reporter gene and the poly-A tail. On the other hand, the donor vector contains not only the GOI cassette but also a promoter-less or poly-A tail-less selection marker. Then, only cells which have integrated the donor vector/cassette into the landing pad will correctly express the selection marker, as well as the GOI, and they can be selected. In addition, integration of the donor vector into the landing pad increases the distance between the reporter gene and the promoter/poly-A tail leading to a loss of fluorescence^{186,204}.

Screening and identification of a host cell line with good growth and a preferable production profile is still difficult, however, once generated, this host cell line could serve as customized “chassis” for GOI integration²⁰⁵, reducing the timelines for clones generation compared to the classical methods (Figure 7 B).

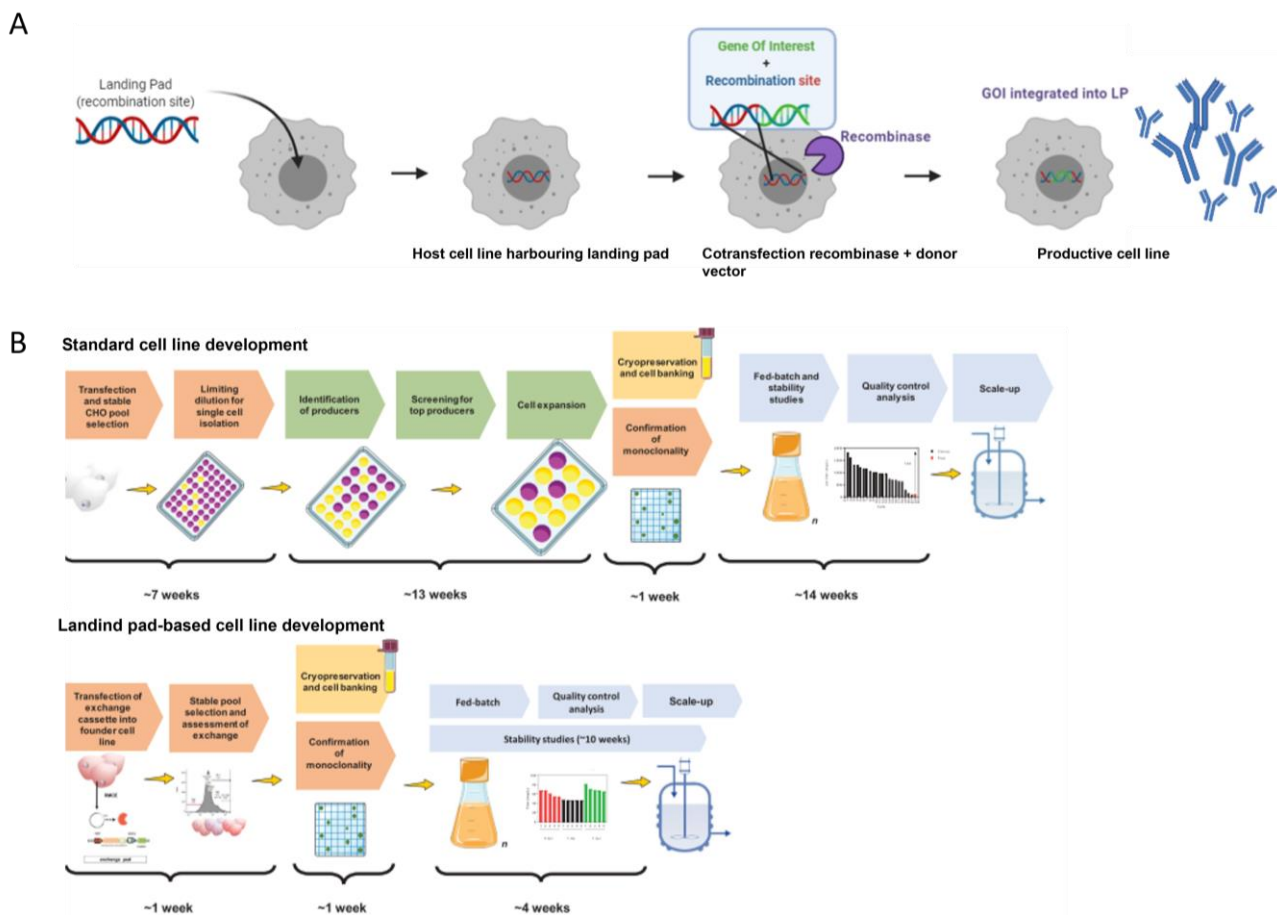


Figure 7 Landing pad-based cell line development. (A) Schematic representation of landing pad cell line development. First, a stable host cell line have to be generated, by integrating the landing pad harbouring the recombination site for a specific recombinase into the cell genome. Then, the host cell line can be used as “chassis” for the integration of a GOI by construct a donor vector, harbouring the GOI and the matching recombination site for the landing pad itself. To induce the integration of the GOI into the landing pad, the correinsponding recombinase enzyme should be expressed into the host cell line. Therefore, an helper vector expressing the recombinase and donor vector containing the GOI and the recombination site have to be cotransfected into the host cell line. After GOI integration via recombination at the landing pad site, productive cell line can be selected with common methods. **(B)** Timeline comparison between a standard cell line development (upper panel) and landing pad-based cell line development (lower panel). The latter results in a significant shortage in development time, starting from the generated host cell line.

Modified from: Srirangan K, Loignon M, Durocher Y. The use of site-specific recombination and cassette exchange technologies for monoclonal antibody production in Chinese Hamster ovary cells: retrospective analysis and future directions. *Crit Rev Biotechnol.* 2020 Sep;40(6):833-851. doi: 10.1080/07388551.2020.1768043. Epub 2020 May 26. PMID: 32456474. ©2020 Copyright of the Crown in Canada. National Research Council Canada.

During the last ten years, many different cell lines have been developed using landing pad techniques for the production of recombinant proteins with a focus on monoclonal antibodies. Developed systems differ for the recombinase used, for the number of integrated landing pads into the host genome, for the landing pad design,

as well as for the trap and selection strategy^{186,201,211–213}. Among the different recombinases tested, serine recombinase BxB1, derived from *Mycobacterium smegmatis*, resulted in high efficiency of plasmid integration and no off-target integration sites in the mammalian genome. For this reason BxB1 integrases have been selected as one of the most efficient site-specific recombinase system in mammalian cells^{214–216}.

First attempts to create cell lines for antibody production using a landing pad system and recombinase-mediated site-specific recombination resulted in low-productivity TI-clones (1-10 pg/cell/day)^{215,217,218} not comparable with industrial standard (>50 pg/cell/day)¹⁰¹. In addition to the landing pad integration into strong genomic hot spot, strategies used to increase TI-clones productivity rely on increasing the copies of integrated GOI or by using multi-copies landing pad cell lines^{205,219,220} or using donor vector harbouring several cassettes of the GOI²⁰⁵. However, the use of large donor vectors carrying multiple copies of the GOI reduces the efficiency of integration into the LP. On the other hand, the integration of multiple copies of a landing pad into the host genome using common genomic tools remains still difficult and needs a pre-screening of suitable genomic hot spots. In this context, the inclusion of epigenetic regulatory elements into the landing pad could open new possibilities for generating master host cell lines, helping the integration of several copies of the landing into the host genome, protecting the landing pad from silencing and potentially increasing the expression of the transgene.

2 Objective

The growth of the biologics market over the past 40 years has increased the need to develop stable and robust production systems in line with market demands. The production of complex molecules, such as antibodies, occurs mainly in mammalian cells of which the chinese hamster ovary cells (CHO cells) are the current workhorse for recombinant protein expression. Although several techniques have been developed to generate stable, highly productive and easy-to-cultivate cell lines, this process of generating and selecting cell lines still remains complex, time and money consuming.

The aim of this work is to develop a novel landing pad system to be used in CHO cells for rapid generation of stable cell lines expressing the antibody of interest.

The landing pad system should be designed as a dual system for simultaneous integration of, at least, two different genes. For this reason, two orthogonal recombination sites of BxB1 integrase should be used to avoid cross-recombination events. To monitor the stable integration of the landing pads into the host genome, a different gene reporter should be included in each landing pad as well as a MAR sequence to improve the stable integration of landing pads and create a synthetic hot-spot in the host genome. For this purpose, two different landing pad vectors were generated for this dual system; one containing the MAR, a strong CMV promoter, the AttB wild type site for BxB1 and the EGFP gene reporter; the other containing the MAR, a strong CMV promoter, the AttB site for BxB1 with the central GA mutation and the DsRed gene reporter. 5' chicken lysozyme MAR and human 1-68 MAR were selected as MAR sequences to be tested in the system and to be compared to a control.

To obtain dual landing pad host cell lines CHO-S cells should be transfected with both landing pad vectors. Transfection parameters and ratio between landing pad vectors should be tested in order to obtain stable pools expressing both reporter genes. Stable host cell lines should be selected testing combinations of selection methods, based on antibiotic selection, semi-solid selection and fluorescence activated cell sorting, selecting EGFP+/DsRed+ clones. Clones containing different MAR sequences should be compared to the control landing pad cell line in terms of fluorescence intensity, landing pad copy number and genomic integration. Clonal stability up to 90 generation should be also evaluated to select the best system for subsequent expression of the genes of interest.

After the selection of promising host cell lines, the latter can be used to generate antibody-producing clones *via* cotransfection with donor vectors and helper vector expressing the BxB1 integrase. The donor vector design should include one light chain cassette and the puromycin promoter-less selection gene preceded by the BxB1 AttP-GA site; the other containing the heavy chain cassette and the hygromycin promoter-less selection gene preceded by the BxB1 AttP-WT site. Due to the landing pad and donor vector designs, after integration, stable integrants could be selected by double antibiotic selection and monitoring the loss of fluorescence. The loss of EGFP fluorescence should correlate with the stable integration of the heavy chain while the loss of DsRed

fluorescence will correlate with the integration of the light chain gene. Clone should be obtained from EGFP-/DsRed- stable pool by FACS or semi-solid colony picking. Then selected clones should be characterized in terms of residual fluorescence, gene copy number analysis, mRNA level, GOI off target integration and GOI expression. In addition, clonal stability should be investigated to evaluate eventual drop in antibody production.

To investigate if the generated platform could be used with other antibody sequences than the one tested, other donor vectors expressing for complex molecules should be generated. For this purpose, three different donor vectors should be created for the expression of a bispecific antibody molecule (bsAb-Fer): one containing the common light chain, one the knob heavy chain and the other one the hole heavy chain. Similarly to the design of the msAb donor, the common light chain cassette should be integrated into the donor vector containing the promoterless puromycin selection marker preceded by the AttB-GA site. The knob and the hole heavy chain should be integrated into the donor vector containing the promoterless hygromycin selection marker generating two different donor vectors for the two heavy chain sequences. After pool generation and clonal selection, selected clones should be characterized, tested for the bsAb production and their production stability over 90 generations will be monitored.

The best selected msAb and bsAb producing clones should be further tested for adaptation in several basal media and in fed batch mode, testing different combinations of media and feed strategies, to ameliorate the culture condition and antibody final titer. Best fed batch conditions obtained should be used to perform a scale up from 20 mL to 5 L, testing shake flask cultures and two different bioreactor setups, a stirred tank and orbital shake bioreactor. Cell growth curves, culture duration and antibody final titer should be analysed to evaluate the scalability of the selected cell line.

In summary, the presented work aimed at developing a new platform for the production of complex molecules such as monospecific and bispecific antibodies. The advantage of this new technology is the establishment of host cell lines that make the generation and selection of productive clones faster and easier. We believe that could result in a significant reduction of time and resources for cell line generation. This represents a further step towards a more efficient and more rapid cell line development process.

3 Materials

3.1 Bacterial Strains

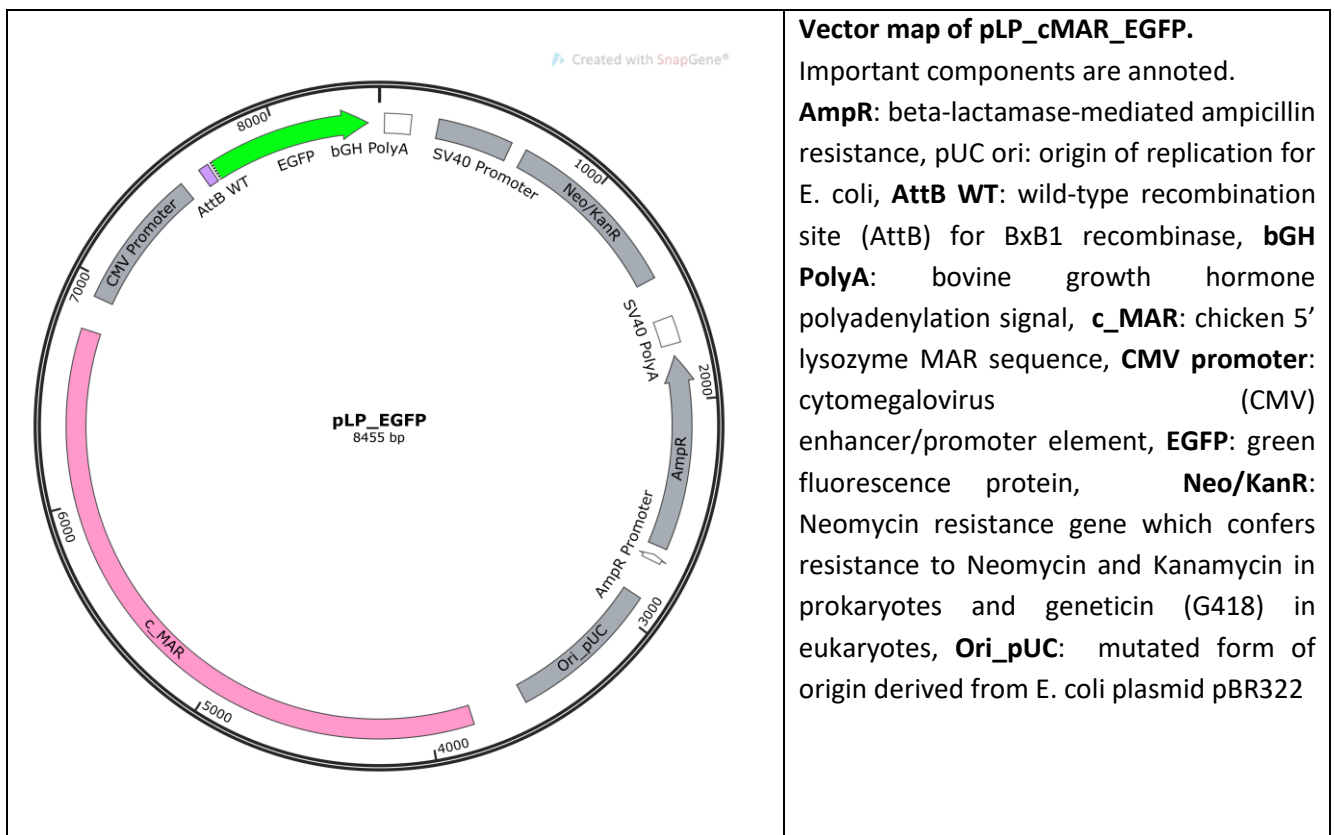
One Shot™ Stbl3™ *E. coli* strand (genotype: *F-mcrB mrrhsdS20*(r_B⁻, m_B⁻) *recA13 supE44 ara-14 galK2 lacY1 proA2 rpsL20*(Str^R) *xyf-5 λ-leumtl-1*; ThermoFisher Scientific) was used for vector transformation and preparation (mini and maxi prep).

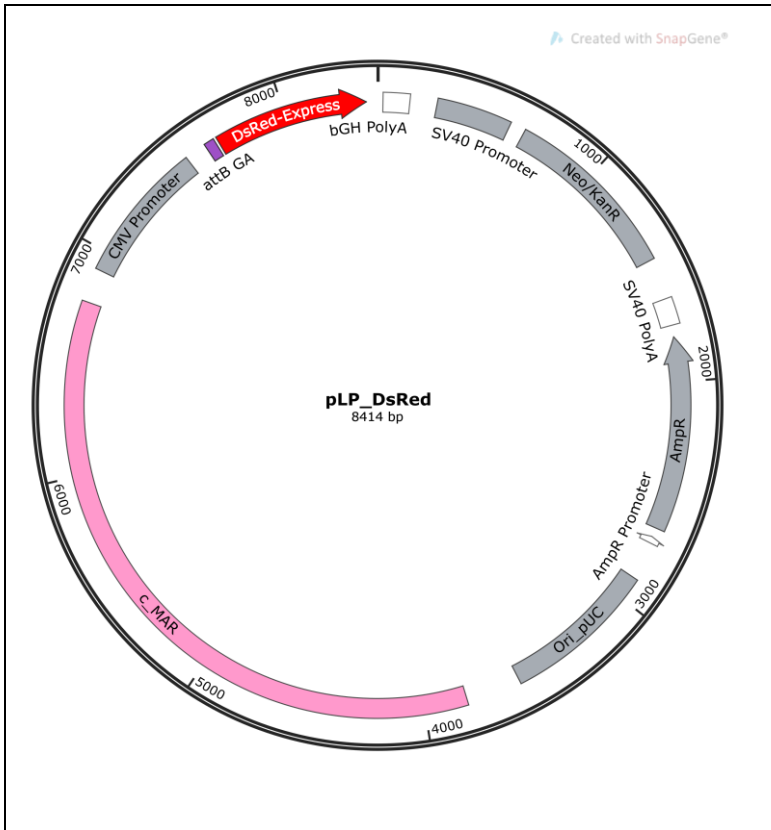
3.2 Mammalian cell lines

In-house CHO-S cells adapted to cultivation in serum-free suspension were used during the entire duration of this project. Due to high clumps formation after cell thawing, cells were adapted to single cell suspension by several cycles of suspension cell selection.

3.3 Vectors

All the vector maps have been generated and visualized using SnapGene® software (SnapGene viewer).

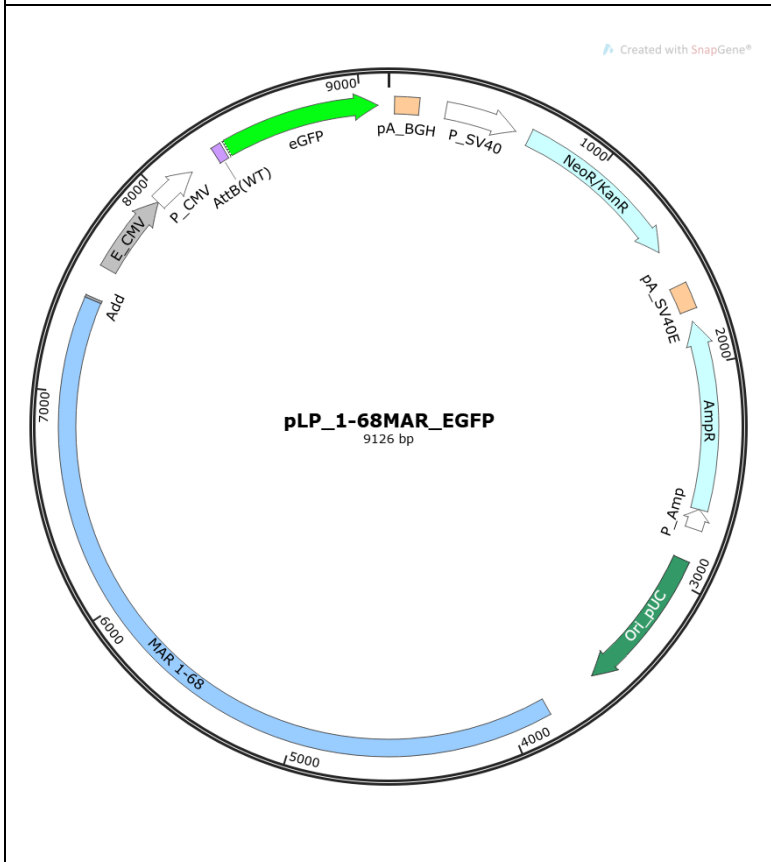




Vector map of pLP_cMAR_DsRed.

Important components are annotated.

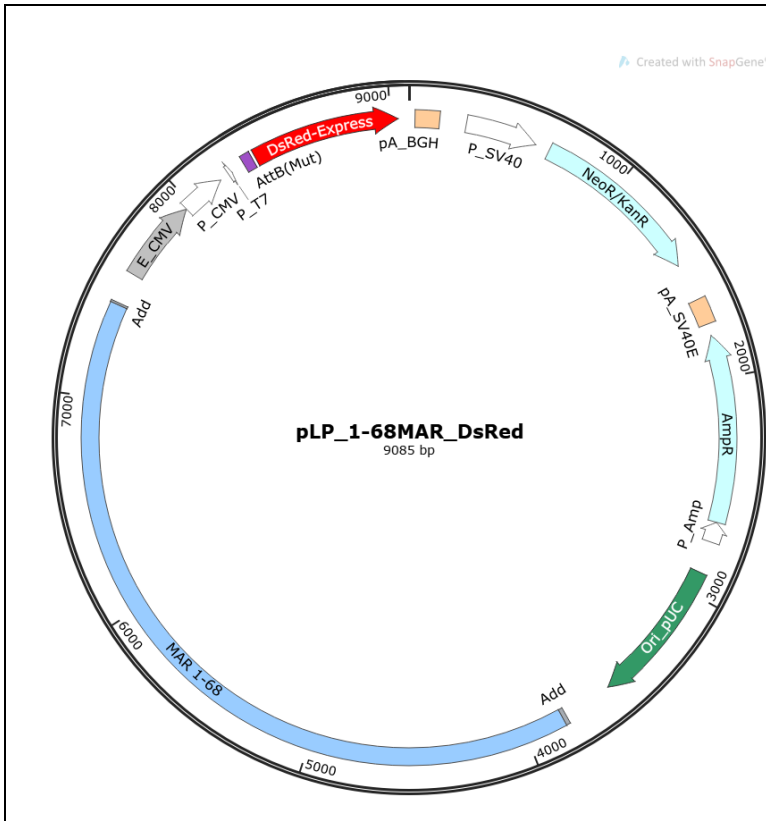
AmpR: beta-lactamase-mediated ampicillin resistance, **pUC ori**: origin of replication for *E. coli*, **AttB GA**: recombination site (AttB) for BxB1 recombinase with GA mutation in central dinucleotide, **bGH PolyA**: bovine growth hormone polyadenylation signal, **c_MAR**: chicken 5' lysozyme MAR sequence, **CMV promoter**: cytomegalovirus (CMV) enhancer/promoter element, **DsRed Express 1**: red fluorescence protein, **Neo/KanR**: Neomycin resistance gene which confers resistance to Neomycin and Kanamycin in prokaryotes and geneticin (G418) in eukaryotes, **Ori_pUC**: mutated form of origin derived from *E. coli* plasmid pBR322,



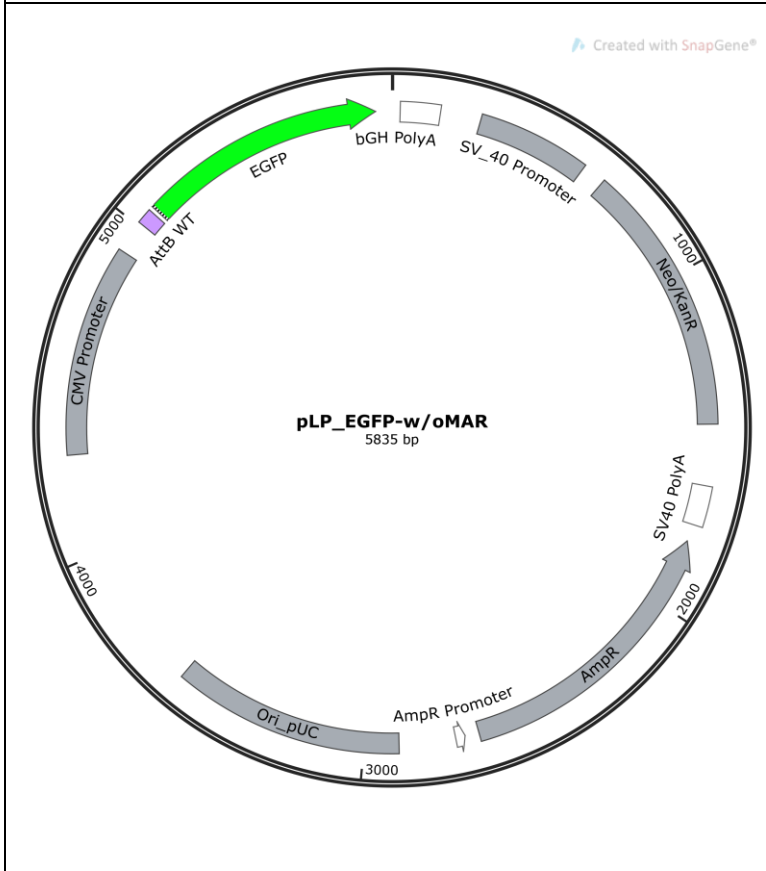
Vector map of pLP_1-68MAR_EGFP.

Important components are annotated.

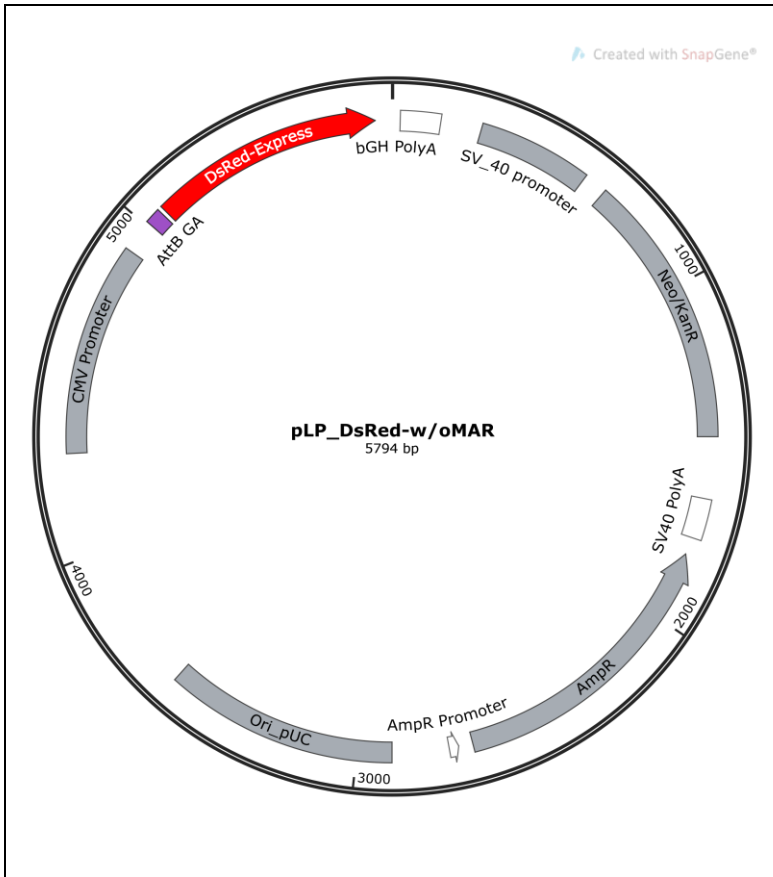
AmpR: beta-lactamase-mediated ampicillin resistance, **pUC ori**: origin of replication for *E. coli*, **AttB WT**: wild-type recombination site (AttB) for BxB1 recombinase, **bGH PolyA**: bovine growth hormone polyadenylation signal, **CMV promoter**: cytomegalovirus (CMV) enhancer/promoter element, **EGFP**: green fluorescence protein, **MAR 1-68**: human MAR 1-68 sequence **Neo/KanR**: Neomycin resistance gene which confers resistance to Neomycin and Kanamycin in prokaryotes and geneticin (G418) in eukaryotes, **Ori_pUC**: mutated form of origin derived from *E. coli* plasmid pBR322,



Vector map of pLP_1-68MAR_DsRed.
 Important components are annotated.
AmpR: beta-lactamase-mediated ampicillin resistance, pUC ori: origin of replication for E. coli, **AttB (Mut):** recombination site (AttB) for BxB1 recombinase with GA mutation in central dinucleotide, **bGH PolyA:** bovine growth hormone polyadenylation signal, **CMV promoter:** cytomegalovirus (CMV) enhancer/promoter element, **DsRed Express 1:** red fluorescence protein, **MAR 1-68:** human MAR 1-68 sequence, **Neo/KanR:** Neomycin resistance gene which confers resistance to Neomycin and Kanamycin in prokaryotes and geneticin (G418) in eukaryotes, **Ori_pUC:** mutated form of origin derived from E. coli plasmid pBR322



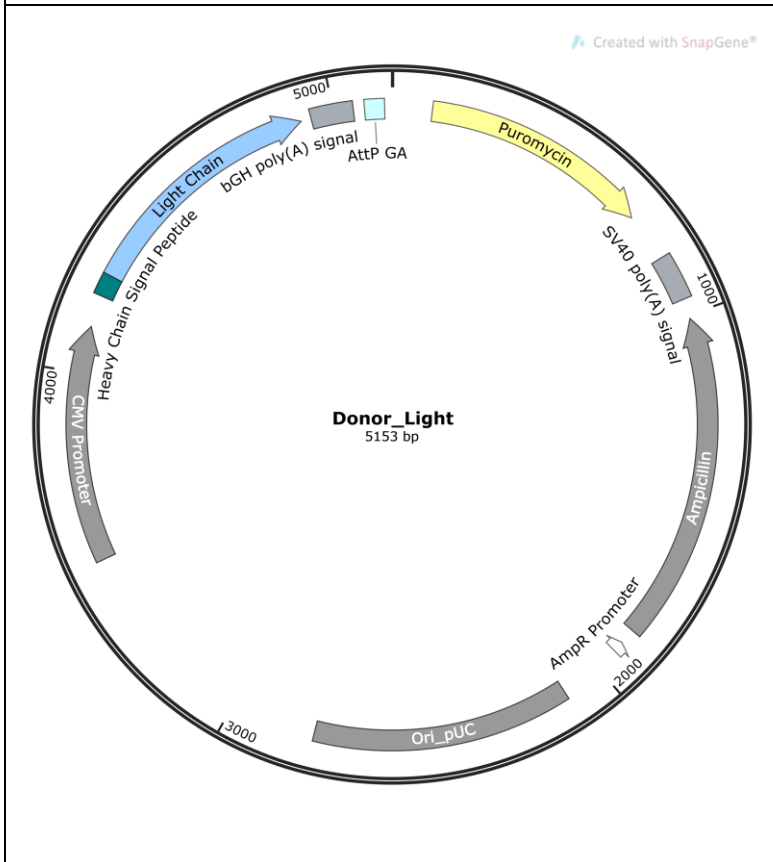
Vector map of pLP_EGFP-w/oMAR.
 Important components are annotated.
AmpR: beta-lactamase-mediated ampicillin resistance, pUC ori: origin of replication for E. coli, **AttB WT:** wild-type recombination site (AttB) for BxB1 recombinase, **bGH PolyA:** bovine growth hormone polyadenylation signal, **CMV promoter:** cytomegalovirus (CMV) enhancer/promoter element, **EGFP:** green fluorescence protein, **Ori_pUC:** mutated form of origin derived from E. coli plasmid pBR322, **Neo/KanR:** Neomycin resistance gene which confers resistance to Neomycin and Kanamycin in prokaryotes and geneticin (G418) in eukaryotes.



Vector map of pLP_DsRed-w/oMAR.

Important components are annotated.

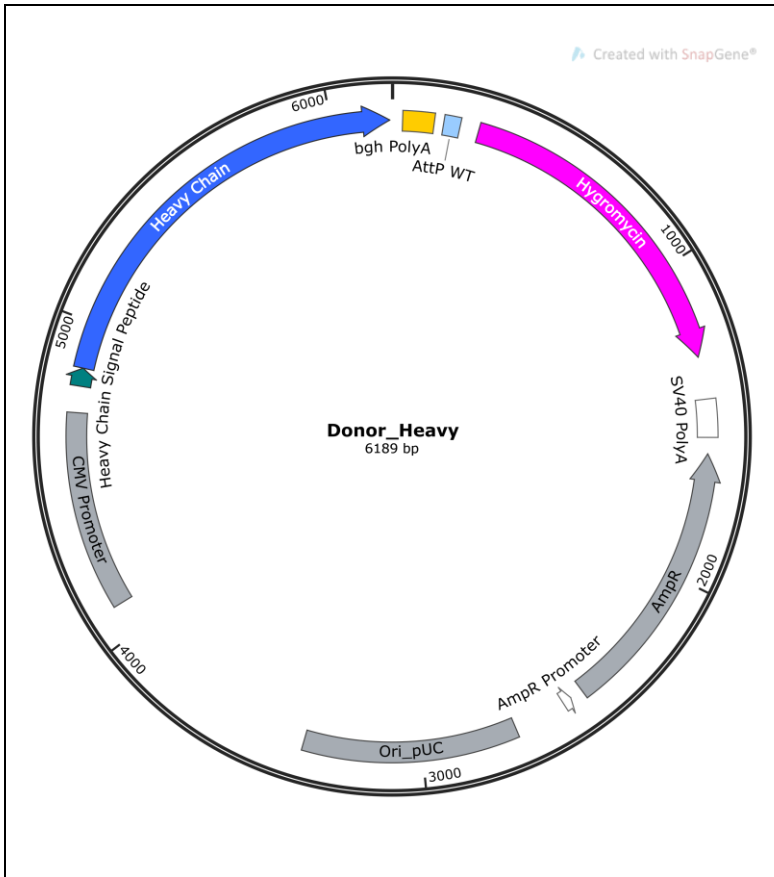
AmpR: beta-lactamase-mediated ampicillin resistance, pUC ori: origin of replication for E. coli, **AttB GA:** recombination site (AttB) for BxB1 recombinase with GA mutation in central dinucleotide, **bGH PolyA:** bovine growth hormone polyadenylation signal, **CMV promoter:** cytomegalovirus (CMV) enhancer/promoter element, **DsRed Express 1:** red fluorescence protein, **Neo/KanR:** Neomycin resistance gene which confers resistance to Neomycin and Kanamycin in prokaryotes and geneticin (G418) in eukaryotes, **Ori_pUC:** mutated form of origin derived from E. coli plasmid pBR322



Vector map of Donor_Light.

Important components are annotated.

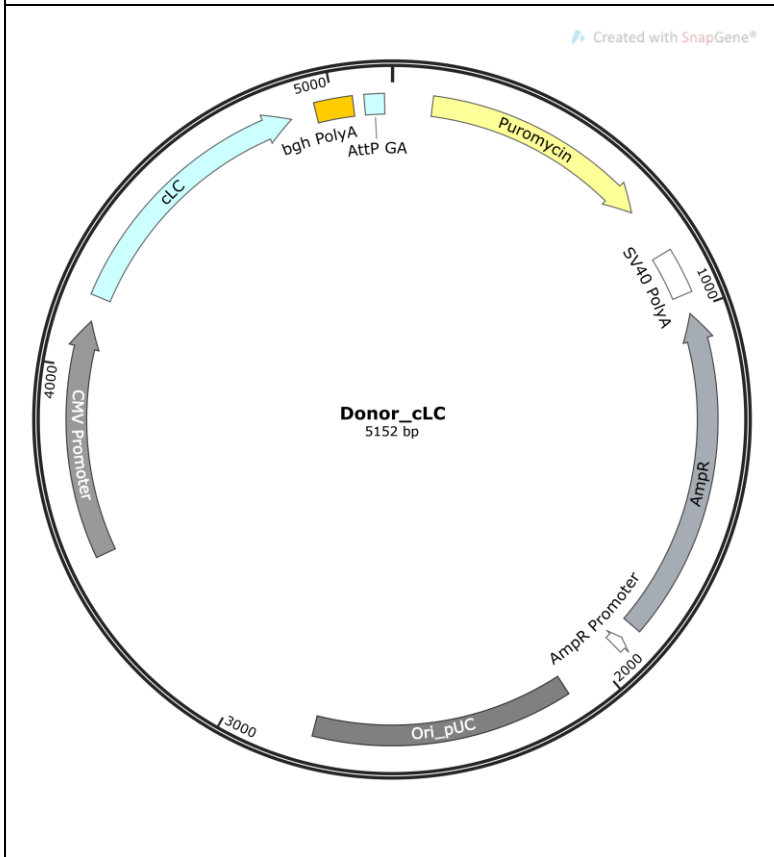
AmpR: beta-lactamase-mediated ampicillin resistance, pUC ori: origin of replication for E. coli, **AttP GA:** recombination site (AttP) for BxB1 recombinase with GA mutation in central dinucleotide, **bGH PolyA:** bovine growth hormone polyadenylation signal, **CMV promoter:** cytomegalovirus (CMV) enhancer/promoter element, **Light Chain:** gene coding for msAb-Fer light chain preceded by signal peptide²²¹, **Puromycin (promotor-less gene):** resistance to puromycin is conferred by the Pac gene encoding a puromycin N-acetyl-transferase (PAC), **Ori_pUC:** mutated form of origin derived from E. coli plasmid pBR322



Vector map of Donor_Heavy.

Important components are annotated.

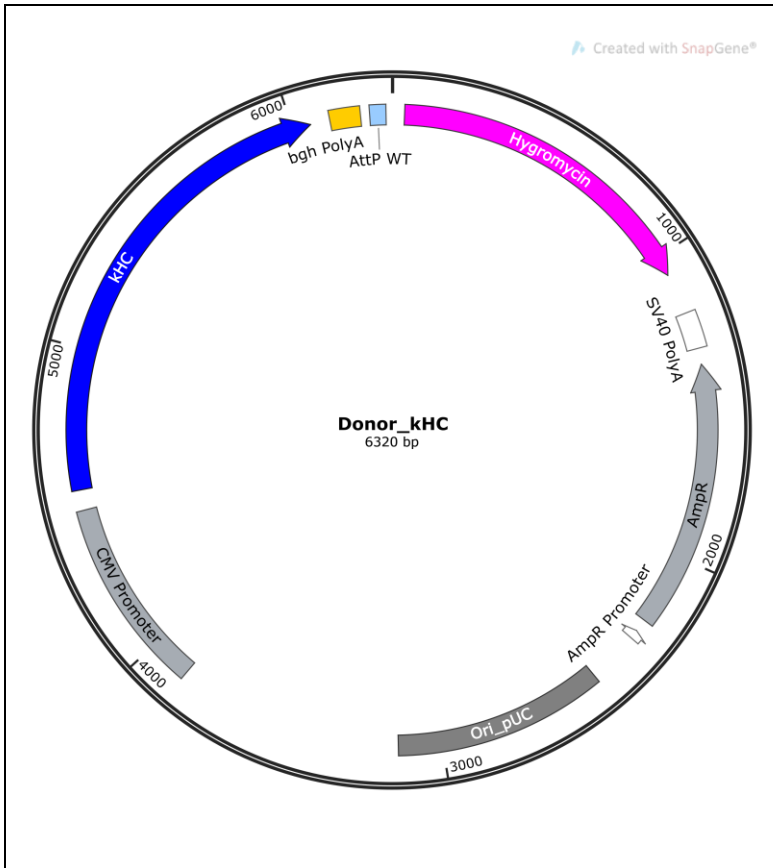
AmpR: beta-lactamase-mediated ampicillin resistance, pUC ori: origin of replication for E. coli, **AttP GA:** recombination site (AttP) for BxB1 recombinase with GA mutation in central dinucleotide, **bGH PolyA:** bovine growth hormone polyadenylation signal, **CMV promoter:** cytomegalovirus (CMV) enhancer/promoter element, **Heavy Chain:** gene coding for msAb-Fer heavy chain preceded by signal peptide²²¹, **Hygromycin (promotor-less gene):** resistance to hygromycin is conferred by hph gene from E.col, **Ori_pUC:** mutated form of origin derived from E. coli plasmid pBR322



Vector map of Donor_cLC.

Important components are annotated.

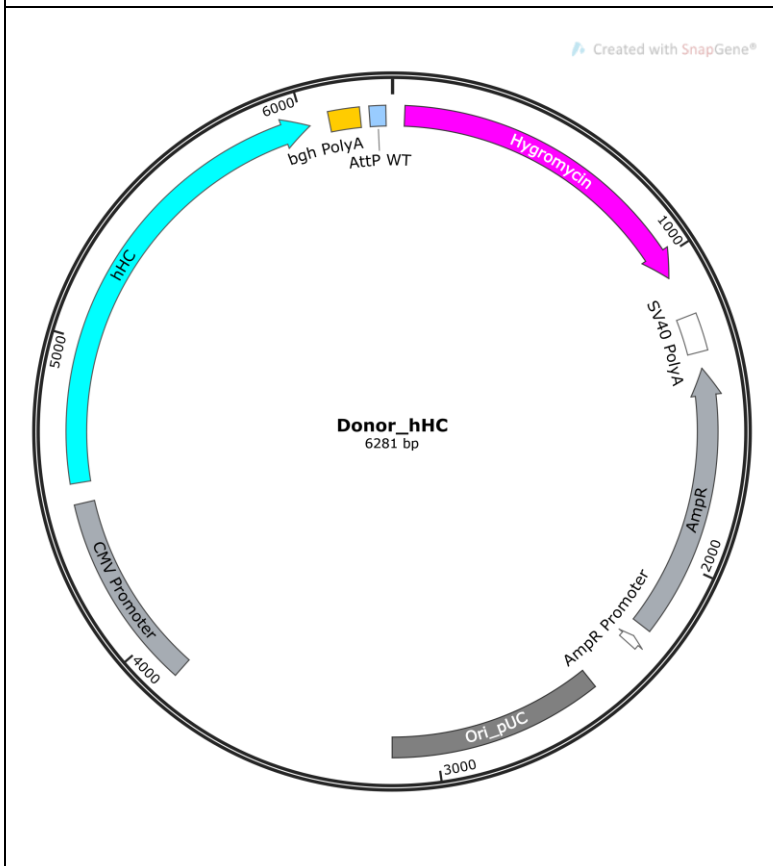
AmpR: beta-lactamase-mediated ampicillin resistance, pUC ori: origin of replication for E. coli, **AttP GA:** recombination site (AttP) for BxB1 recombinase with GA mutation in central dinucleotide, **bGH PolyA:** bovine growth hormone polyadenylation signal, **CMV promoter:** cytomegalovirus (CMV) enhancer/promoter element, **cLC:** gene coding for bsAb-Fer common light chain preceded by signal peptide²²¹, **Puromycin (promotor-less gene):** resistance to puromycin is conferred by the Pac gene encoding a puromycin N-acetyl-transferase (PAC), **Ori_pUC:** mutated form of origin derived from E. coli plasmid pBR322



Vector map of Donor_kHC.

Important components are annotated.

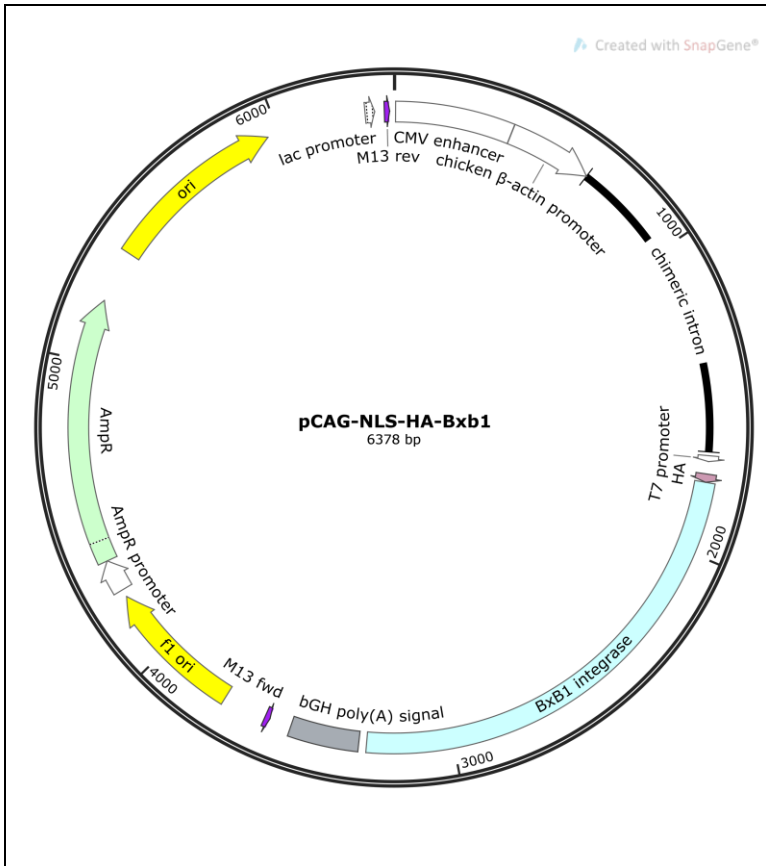
AmpR: beta-lactamase-mediated ampicillin resistance, pUC ori: origin of replication for E. coli, **AttP GA**: recombination site (AttP) for BxB1 recombinase with GA mutation in central dinucleotide, **bGH PolyA**: bovine growth hormone polyadenylation signal, **CMV promoter**: cytomegalovirus (CMV) enhancer/promoter element, **kHC**: gene coding for bsAb-Fer knob heavy chain preceded by signal peptide²²¹, **Hygromycin (promotor-less gene)**: resistance to hygromycin is conferred by hph gene from E.col, **Ori_pUC**: mutated form of origin derived from E. coli plasmid pBR322



Vector map of Donor_hHC.

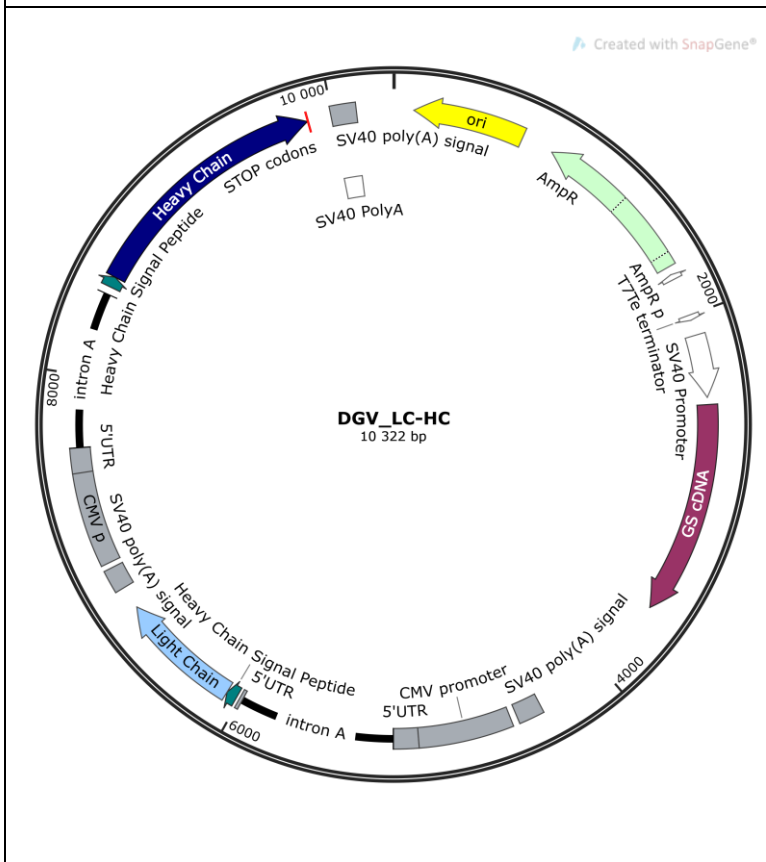
Important components are annotated.

AmpR: beta-lactamase-mediated ampicillin resistance, pUC ori: origin of replication for E. coli, **AttP GA**: recombination site (AttP) for BxB1 recombinase with GA mutation in central dinucleotide, **bGH PolyA**: bovine growth hormone polyadenylation signal, **CMV promoter**: cytomegalovirus (CMV) enhancer/promoter element, **hHC**: gene coding for bsAb-Fer hole heavy chain preceded by signal peptide²²¹, **Hygromycin (promotor-less gene)**: resistance to hygromycin is conferred by hph gene from E.col, **Ori_pUC**: mutated form of origin derived from E. coli plasmid pBR322



Vector map of pCAG-NLS-HA-Bxb1.

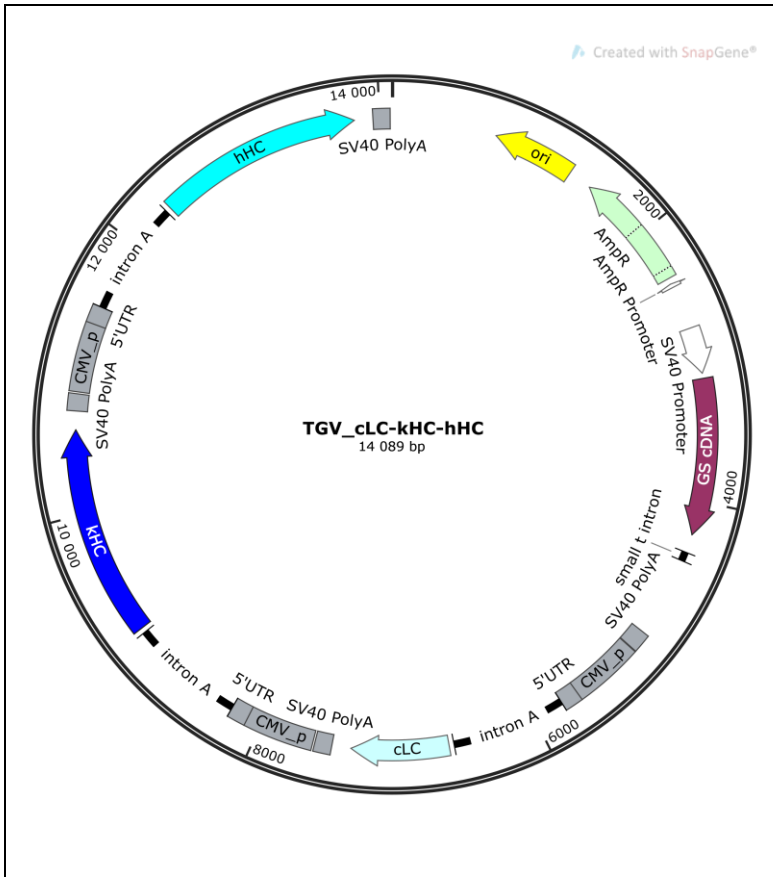
pCAG-NLS-HA-Bxb1 was a gift from Pawel Pelczar (Addgene plasmid # 51271 ; <http://n2t.net/addgene:51271> ; RRID:Addgene_51271).



Vector map of DGV_LC-HC.

Important components are annotated.

GS cDNA transcription unit: consisting of the SV40 early (SV40E) promoter and replication origin, the GS cDNA and SV40 splicing and polyadenylation signals, **Heavy Chain:** gene coding for msAb-Fer heavy chain preceded by signal peptide²²¹, **intron A:** first intron of the human cytomegalovirus major intermediate early gene, **Light Chain:** gene coding for msAb-Fer light chain preceded by signal peptide²²¹, **mCMV:** murine cytomegalovirus (mCMV) promoter, **5' UTR:** 5' untranslated sequences from both the mCMV and human cytomegalovirus major intermediate early genes.



Vector map of TGV_cLC-kHC-hHC.

Important components are annotated.

cLC: gene coding for bsAb-Fer common light chain preceded by signal peptide²²¹, **GS cDNA transcription unit:** consisting of the SV40 early (SV40E) promoter and replication origin, the GS cDNA and SV40 splicing and polyadenylation signals, **hHC:** gene coding for bsAb-Fer hole heavy chain preceded by signal peptide²²¹, **intron A:** first intron of the human cytomegalovirus major intermediate early gene, **kHC:** gene coding for bsAb-Fer knob heavy chain preceded by signal peptide²²¹, **mCMV:** murine cytomegalovirus (mCMV) promoter, **5' UTR:** 5' untranslated sequences from both the mCMV and human cytomegalovirus major intermediate early genes.

3.4 Oligonucleotides

All the oligonucleotides, primers and probes used in this study were purchased at Microsynth AG (CH).

3.4.1 Cloning primers

| <i>Name</i> | <i>Sequence (5 →3')</i> |
|----------------------|--|
| C_MAR Forward primer | TAACGCCTTAAGCTAGTTATTCTACAAAACAA |
| C_MAR reverse primer | TAAGCAGATATCGGATCGATAATATAACTGTA |
| MCS Forward | CTAGAGGCTCTTCAGGATCCACAGATCTGAATTCAAAGCTTACTCGAGCCTATCAGAAGAGC |
| MCS Reverse | ACCGCTCTTCTGATAGGCTCGAGTAAGCTTTGAATTCAGATCTGTGGATCCTGAAGAGCCT |

3.4.2 Genomic PCR primers

| <i>Name</i> | <i>Sequence (5 →3')</i> |
|--------------------|-----------------------------------|
| CMV forward (P1) | CAAATGGGCGGTAGGCGGTACGG |
| EGFP reverse (P2) | TGCGCTCCTGGACGTAGCCTTC |
| DsRed reverse (P3) | TCACGCCGATGAACTTCACCTTGATAGATGAAG |
| Heavy Forward (P4) | CGAGCTGCTTGGCGGCC |
| Light Forward (P5) | GCAATCCAACAACAAGTATGCTGCCTCC |

3.4.3 qPCR - qRT-PCR primers

| <i>Name</i> | <i>Sequence (5 →3')</i> |
|----------------------------|---|
| B2M forward | GTGACATGGGGCATGGTGTA |
| B2M reverse | TTGCACTTGTGGGGGACCTA |
| B2M probe | [HEX]CCCCAGCAAGTTGTCATTTGCTTTCCCCGT[BHQ-1] |
| eEF1A1 forward | TCCACTGGGTCGTTTTGCT |
| eEF1A1 reverse | AGCTTTCTGGGCCGACTT |
| eEF1A1 probe | [HEX]TGCTGGAGCGGGCAAAGTCA[BHQ-1] |
| EGFP forward | AGCAAAGACCCCAACGAGAA |
| EGFP reverse | TCGTCCATGCCGAGAGTGAT |
| EGFP probe | [FAM(Fluorescein)]CCTGCTGGAGTTCGTGACCGCCGC[BHQ-1] |
| DsRed forward | AGCTGCCCGCTACTACTAC |
| DsRed reverse | GCTCGTACTGCTCCACGATG |
| DsRed probe | [ROX]CCAAGCTGGACATCACCTCCCACAACG[BHQ-2] |
| Heavy chain (msAb) forward | CCAGCGGCTTTACTTTTCAGC |
| Heavy chain (msAb) reverse | GGCGTAGTATGTTGACCCCC |
| Heavy chain (msAb) probe | [FAM(Fluorescein)]GGTCCGCCAGGCACCCGGCAA[BHQ-1] |

| | |
|-----------------------------------|---|
| Light chain (msAb) forward | TGAAAGCCGGGGTAGAGACT |
| Light chain (msAb) reverse | TGGCAGGAGTATGACCGATG |
| Light chain (msAb) probe | [ROX]GCTGCCTCCAGTTACCTCAGTCTGACACC[BHQ-2] |
| Knob heavy chain (bsAb) forward | CAGAAGTCCCTGTCTCTG |
| Knob heavy chain (bsAb) reverse | CAAAGTGGGATGGCTCCA |
| Knob heavy chain (bsAb) probe | [FAM(Fluorescein)]CGGATCTTGGTCCCACCC[C[BHQ-1] |
| Hole heavy chain (bsAb) forward | CTTCTTCTGGTGTCCAAGC |
| Hole heavy chain (bsAb) reverse | AATGGTGATGGTGGTGGTG |
| Hole heavy chain (bsAb) probe | [FAM(Fluorescein)]TCCAGATGGCAGCAGGGCAA[BHQ-1] |
| Common light chain (bsAb) forward | CCTCCATCTTCCGAGGAACT |
| Common light chain (bsAb) reverse | TTGTTGTTGGACTGCTTGA |
| Common light chain (bsAb) probe | [ROX]GCGCTGTGACTGTCGCCTGG[BHQ-2] |

3.4.4 Primers for the generation of FISH probes

| <i>Name</i> | <i>Sequence (5 →3')</i> |
|---------------------------------|-------------------------|
| FISH EGFP Forward | AGATCCGCCACAACATCGAG |
| FISH EGFP Reverse | TCGTCCATGCCGAGAGTGAT |
| FISH DsRed Forward | TCCAAGGTGTACGTGAAGCA |
| FISH DsRed Reverse | CTTCTTCTGCATTACGGGGC |
| FISH Light chain (msAb) Forward | ACAGCAGTAACCCAGTGGTC |
| FISH Light chain (msAb) Reverse | TTCCAGGCTACGGTAACAGC |
| FISH Heavy chain (msAb) Forward | TGGTATGTGGATGGGGTGGG |
| FISH Heavy chain (msAb) Reverse | TGCCCTTGGCTTTGCTTAT |

3.5 Molecular biology enzymes and kits

| <i>Product</i> | <i>Supplier</i> |
|---|-----------------------------------|
| DNeasy Blood & Tissue Kit | Qiagen AG, Hombrechtikon, CH |
| EndoFree Plasmid Maxi Kit | Qiagen AG, Hombrechtikon, CH |
| HighFidelity Fluorescein PCR Labeling kit | Jena Bioscience, Germany |
| HighFidelity Orange PCR Labeling kit | Jena Bioscience, Germany |
| Q5® High-Fidelity 2X Master Mix | New England Biolabs Inc., Germany |
| QIAprep Spin Miniprep Kit | Qiagen AG, Hombrechtikon, CH |
| QIAquick Gel Extraction Kit | Qiagen AG, Hombrechtikon, CH |
| QIAquick PCR Purification Kit | Qiagen AG, Hombrechtikon, CH |
| QuantiTect Multiplex PCR Kit | Qiagen AG, Hombrechtikon, CH |
| RNeasy mini kit | Qiagen AG, Hombrechtikon, CH |

| | |
|---------------------------------|-----------------------------------|
| Rotor-Gene Multiplex Rt-PCR kit | Qiagen AG, Hombrechtikon, CH |
| T4 DNA ligase | New England Biolabs Inc., Germany |
| BamHI-HF | New England Biolabs Inc., Germany |
| HindIII-HF | New England Biolabs Inc., Germany |
| SmaI-HF | New England Biolabs Inc., Germany |
| EcoRI-HF | New England Biolabs Inc., Germany |
| NruI-HF | New England Biolabs Inc., Germany |
| NotI-HF | New England Biolabs Inc., Germany |
| PvuI-HF | New England Biolabs Inc., Germany |
| EcoRV-HF | New England Biolabs Inc., Germany |
| ApaI | New England Biolabs Inc., Germany |
| AflII | New England Biolabs Inc., Germany |
| BstZ17I-HF | New England Biolabs Inc., Germany |

3.6 Mammalian cell cultures media, feeds and reagents

| <i>Solution</i> | <i>Composition</i> |
|--------------------------|--|
| CD CHO medium | Gibco, Thermo Fisher scientific, USA |
| Hygromycin B Gold | Invivogen Europe, Toulouse, France |
| L-Methionine Sulfoximine | Sigma-Aldrich, St. Louis, USA |
| Geneticin (G418) | Gibco, Thermo Fisher scientific, USA |
| Puromycin | Thermo Fisher Scientific Inc., Waltham, USA |
| L-Glutamine 200mM | Corning Switzerland GmbH |
| BalanCD growth A medium | Fujifilm Irvine Scientific, Santa Ana, CA, USA |
| CD OptiCHO medium | Gibco, Thermo Fisher scientific, USA |
| Hyclone ActiPro medium | Cytiva LifeSciences Europe GmbH |
| Hyclone Feed 7a | Cytiva LifeSciences Europe GmbH |
| Hyclone Feed 7b | Cytiva LifeSciences Europe GmbH |

3.7 Consumables and reagents

| <i>Product</i> | <i>Supplier</i> |
|--|-------------------------------------|
| 10X Tris Buffered Saline (TBS) | Bio-Rad Laboratories, Hercules, USA |
| 10X Tris/Glycine/SDS (running buffer) | Bio-Rad Laboratories, Hercules, USA |
| 125/250/500/1000 ml Erlenmeyer flask with Vent Cap | Corning Switzerland GmbH |
| 15/50 mL Centrifuge tubes | Corning Switzerland GmbH |
| 4–20% Mini-PROTEAN® TGX Stain-Free™ Protein Gels, 15 well, 15 µl | Bio-Rad Laboratories, Hercules, USA |

| | |
|--|---|
| 4x Laemmli Sample Buffer | Bio-Rad Laboratories, Hercules, USA |
| 5-/10-/25-/50-/100- serological pipettes | Sarstedt AG, Nümbrecht, Germany |
| 96-/24-/12-/6-well plates, suspension | Sarstedt AG, Nümbrecht, Germany |
| Amersham™ Protran® Premium 0.45 µm nitrocellulose blocking membrane | GE Healthcare, Little Chalfont, UK |
| Pierce™ Protein Concentrator PES, 30K MWCO | Thermo Fisher Scientific Inc., Waltham, USA |
| Clarity™ Western ECL Substrate, 200 ml | Bio-Rad Laboratories, Hercules, USA |
| His60 Ni Gravity Columns | Takara Bio Europe SAS, Saint-Germain-en Laye, France |
| HRP-conjugated His-Tag monoclonal antibody | |
| Neon Transfection system 10 µL Kit | Invitrogen, Thermo Fisher Scientific Inc., Waltham, USA |
| Peroxidase-AffiniPure Donkey Anti-Human IgG (H+L) | Jackson ImmunoResearch Europe Ltd, Cambridgeshire, UK |
| Strep-Tactin®XT Spin Column | Iba Lifescience, Göttingen, Germany |
| Strep-Tag Classic:HRP detection antibody | Bio-Rad Laboratories, Hercules, USA |
| Trans-Blot Turbo RTA Mini 0.2 µm Nitrocellulose Transfer Kit, for 40 blots | Bio-Rad Laboratories, Hercules, USA |
| Peq Green, DNA/RNA dye | Peqlab, VWR Life Science AG, Dietikon, Switzerland |
| NAb™ Protein A Plus Spin Columns | Thermo Fisher Scientific Inc., Waltham, USA |
| Yarra SEC-3000 | Phenomenex Inc., Basel, Switzerland |
| Aminex HPX-87H Column | Bio-Rad Laboratories, Hercules, USA |

3.8 Solutions

| <i>Solution</i> | <i>Composition</i> |
|--|---|
| Fixative solution | 3:1 ice cold Metanol/ acetic acid |
| Ampicillin stock solution | 100 mg/mL ampicillin |
| MSX stock solution | 50mM MSX |
| LB medium | 10 g/L Tryptone 5 g/L Yeast extract 10 g/L NaCl |
| SSC 20X solution | 3 M NaCl 0.3 M sodium citrate pH 7 |
| Binding solution (for Nab protein A Spin Columns) | 0.1 M NaH ₂ PO ₄ 0.15 M NaCl pH 7.2 |
| Elution solution (for Nab protein A Spin Columns) | 0.1 M Glycine pH 2-3 |
| Neutralization solution (for Nab protein A Spin Columns) | 1 M Tris |

| | |
|---|--|
| | pH 8-9 |
| Mobile phase for Yarra SEC-3000 | 0.1 M NaH ₂ PO ₄ pH 6.8 |
| Elution phase for Aminex HPX-87H Column | 5mM H ₂ SO ₄ |

3.9 Chemicals

| <i>Product</i> | <i>Supplier</i> |
|---|---|
| 2-Mercaptoethanol | Sigma-Aldrich, St. Louis, USA |
| Agarose | Carl Roth, Karlsruhe, Germany |
| Ammonium persulfate (APS) | Sigma-Aldrich, St. Louis, USA |
| Ampicillin, sodium salt | Sigma-Aldrich, St. Louis, USA |
| DAPI | Invitrogen, Thermo Fisher Scientific Inc., Waltham, USA |
| Hybri-Max, Dimethyl Sulfoxide (DMSO) | Sigma-Aldrich, St. Louis, USA |
| KaryoMAX™ Colcemid™ solution in PBS | Thermo Fisher Scientific Inc., Waltham, USA |
| Nonfat dried milk powder | PanReac AppliChem, Darmstadt, Germany |
| PBS (10x) | PanReac AppliChem, Darmstadt, Germany |
| Sodium Chloride | PanReac AppliChem, Darmstadt, Germany |
| Tryptone/Peptone | Biolife |
| Yeast extract | Biolife |

3.10 Instruments

| <i>Instrument</i> | <i>Supplier</i> |
|--|---|
| MACSQuant® Analyzer 16 Flow Cytometer | Miltenyi Biotec Swiss AG, Solothurn, CH |
| Neon transfection system | Invitrogen, Thermo Fisher Scientific Inc., Waltham, USA |
| Incubator LT-XC | Adolf Kühner AG, Basel CH |
| OrbShake SB10-X bioreactor | Adolf Kühner AG, Basel CH |
| Mini-PROTEAN Tetra Vertical Electrophoresis Cell | Bio-Rad Laboratories, Hercules, USA |
| Trans-Blot® Turbo™ Transfer System | Bio-Rad Laboratories, Hercules, USA |
| Cytation 5 imager reader | BioTek Instruments Inc., Winooski, USA |
| GlucCell | Cesco Bioengineering |
| ChemiDoc Imaging System | Bio-Rad Laboratories, Hercules, USA |
| Nanodrop | DeNovix Inc., Wilmington, USA |
| Mr. Frosty™ isopropanol freezing container | Thermo Fisher Scientific Inc., Waltham, USA |
| Qiacube | Qiagen AG, Hombrechtikon, CH |
| RotorGene Q | Qiagen AG, Hombrechtikon, CH |
| PeqSTAR 2X | PEQLAB, Erlangen, Germany |

| | |
|--|-----------------------------|
| Vi-Cell BLU cell viability analyzer | Beckman Coulter, USA |
| BioFlo 320 process control System | Eppendorf, Hamburg, Germany |
| Vessel Bundle, for BioFlo® 320, stainless-steel dished-bottom, direct-drive, 3 L | Eppendorf, Hamburg, Germany |

4 Methods

4.1 Microbiological Methods

Stbl3 *E. coli* strain was cultivated in LB medium as liquid culture and incubated at 37°C and 200 rpm shaking, or in LB agar plates and incubated at 37°C in static mode. Competent cells were generated in order to be transformed with plasmids using heat-shock procedure. For this purpose, 100 mL of LB medium were inoculated with non-competent Stbl3 *E. coli* at an OD₆₀₀ of 0.1. When culture reached an OD₆₀₀ between 0.6-0.8, cells were incubated 15 min on ice then pelleted for 10 min at 4500 x g at 4°C. After having been resuspended in 32mL of ice cold RF1 solution, cells were incubated 15 min in ice, aliquoted at 100 µL into 1.5 mL tubes and stored at -80°C.

Heat-shock transformation was conducted by mixing 100 µL of competent cells to 10 µL of plasmid DNA (20-200ng) and incubate the mix on ice for 20 min. After that, cells were incubated 45 sec at 42°C, transferred on ice for 2 min, resuspended in 900 µL of preheated LB medium and recovered for 1h at 37°C. Transformed cells were plated into LB agar plates containing the selective antibiotic (e.g., ampicillin 100 µL/mL).

Plasmid extraction from Stbl3 *E. coli* was performed using QIAprep Spin Miniprep Kit or EndoFree Plasmid Maxi Kit (for transfection grade plasmids), according to manufacturer's protocols. Plasmid yield and purity was determined by absorbance at 230 nm, 260 nm and 280 nm, using DeNovix DS-11 Nanodrop system.

4.2 Molecular Biology Methods

4.2.1 Polymerase Chain Reaction (PCR)

PCR reactions were conducted to amplify chicken 5' lysozyme MAR sequence from an in-house vector, to screen colony of transformed bacterial cells, and to test site specific integration of the gene of interest into the landing pad in genomic PCR analyses. Q5 high-fidelity 2X Master Mix was used in all the PCR applications following supplier' indications. Primer annealing temperature was calculated using NEB Tm calculator.

4.2.2 Restriction digestion

Restriction digestion of vector and fragment was performed prior to cloning as well as control digestion after vector generation and bacterial cell transformation. Digestion was performed using NEB restriction enzymes in High-Fidelity (HF) version (when available) and following supplier' protocols. After digestion, fragments were resolved by agarose gel electrophoresis and gel purified using QIAquick gel extraction kit.

4.2.3 Ethanol precipitation of DNA

When needed, digested DNA was purified by ethanol precipitation. For this purpose, Sodium acetate (0.1 volumes) and ice cold 100% Ethanol (2.5 volumes) were mixed to the DNA in a 1.5 mL Eppendorf tube and transferred 1h at -80°C for DNA precipitation. The DNA was then pelleted at full speed (13000 rpm), at 4°C for 30 min and washed twice in 0.5 mL of ice cold 70% Ethanol, spinning at 4°C each time. Ethanol was carefully aspirated being sure to not disturb DNA pellet. The latter was air dried for 10 min and then resuspended in an appropriate volume of Nuclease-free water.

4.2.4 DNA ligation reaction

Ligation reactions were performed using T4 DNA ligase by mixing digested plasmid backbone and fragment, T4 DNA ligase buffer and T4 DNA ligase. Ratio between backbone plasmid and fragment was 1:3 unless specified otherwise. NEBbio Calculator was used to evaluate the amount of backbone and fragment to mix in nanograms. Ligation reaction was run for 1h at room temperature or overnight at 16 °C, for fragment containing sticky ends or blunt ends, accordingly. Ligation solution (10 µL) was used to transform competent *E. coli*.

4.2.5 Agarose gel electrophoresis

DNA fragments from restriction digestion, undigested plasmid, PCR amplicons were resolved and controlled by 1% (w/v) agarose gel electrophoresis. ROTIGarose (agarose standard, Carl Roth) was dissolved in TAE buffer 1X and then mixed with PeqGreen DNA staining (5 µL per 100 mL agarose solution). Electrophoresis was performed at 120V in TAE buffer, for ≈30 min into horizontal electrophoresis chamber. Results were visualized using ChemiDoc imager.

4.3 Vector generation

4.3.1 Generation of chicken 5' Lysozyme MAR LP vectors

Landing pad vectors used in this study were derived from a modified pD603 vector (ATUM) containing a MAR sequence, the AttB site for BxB1 recombination and a reporter gene (EGFP or DsRed, respectively).

A multiple cloning site (MCS) containing SapI-BamHI-BglII-EcoRI-HindIII-XbaI-SapI sites has been integrated into the pD603 vector to generate pD603_MCS. The MCS has been designed as single-strand DNA oligos and, after annealing in a double strand oligo, it was cloned into pD603 linear vector. chicken lysozyme 5' MAR sequence²²² have been synthesized into pUC18 vector (GenScript) and subcloned into pD603_MCS using EcoRV/AflIII restriction sites. Fragment containing AttB wild type (GT central dinucleotide), EGFP reporter gene²²³ and bgh poly A tail was synthesized into pUC57 vector (GeneScript) and subcloned into pD603_cMAR using BamHI and HindIII restriction sites to obtain pLP_cMAR_EGFP. Fragment containing AttB mutated site (GA central dinucleotide), DsRed express 1 reporter gene²²³ and bgh poly A tail was synthesized into pUC57 vector

(GeneScript) and subcloned into pD603_cMAR using BamHI and HindIII restriction sites to obtain pLP_cMAR_DsRed.

4.3.2 Generation of human 1-68 MAR LP vectors

Landing pad vectors containing human MAR 1-68 were constructed starting by pD603_MCS vector. Two single nucleotide mutations were made in the human MAR 1-68 nucleotide sequence (GenBank EF694965.1) in order to suppress *EcoRV* and *AflIII* cleavage sites (thymines were replaced with adenines in position 759 and 3435). Restriction sites *AflIII* and *NheI* were added on the 5' side and *NotI* and *EcoRV* on the 3' side. The modified sequence of 3654 bp length was synthesized artificially and ordered in the pUC57 vector (GeneScript). 1-68 MAR sequence was subcloned into pD603_MCS vector using *AflIII* and *EcoRV* restriction sites. Fragment containing AttB wild type site, EGFP reporter gene and bgh poly A tail was synthesized into pUC57 vector (GeneScript) and subcloned into pD603_1-68MAR using *BamHI* and *HindIII* restriction sites to obtain pLP_1-68MAR_EGFP. Fragment containing AttB mutated site (GA central dinucleotide), DsRed express 1 reporter gene²²³ and bgh poly A tail was synthesized into pUC57 vector (GeneScript) and subcloned into pD603_1-68MAR using *BamHI* and *HindIII* restriction sites to obtain pLP_1-68MAR_DsRed.

4.3.3 Generation of w/o-MAR LP vectors

Control landing pad vectors non-containing MAR sequence were constructed starting by pD603_MCS vector. Fragment containing AttB wild type site, EGFP reporter gene and bgh poly A tail was synthesized into pUC57 vector (GeneScript) and subcloned into pD603_1-68MAR using *BamHI* and *HindIII* restriction sites to obtain pLP_EGFP-w/oMAR. Fragment containing AttB mutated site (GA central dinucleotide), DsRed express 1 reporter gene²²³ and bgh poly A tail was synthesized into pUC57 vector (GeneScript) and subcloned into pD603_1-68MAR using *BamHI* and *HindIII* restriction sites to obtain pLP_DsRed-w/oMAR.

4.3.4 Generation of msAb/bsAb donor vectors

Donor vectors containing AttP recombination sites for BxB1 and light/heavy chains were generated from pD607 and pD609 (ATUM). These vectors have been modified by adding an MCS as previously described, removing the SV40 promoter and subcloning the AttP sites upstream of the resistance gene using *HindIII* and *SmaI* restriction sites. Genetic constructs encoding for the light/ heavy chain of a human monoclonal antibody (msAb-Fer, Ferring) have been synthesized by Genscript into pUC19 vectors and then subcloned into pD609_MCS and pD607_MCS, respectively, using *BamHI* and *HindIII* restriction sites. For the generation of donor vectors for bispecific antibody integration (bsAb-Fer, Ferring), common light chain, knob heavy chain and hole heavy chain genes were optimized for the CHO codon usage with GenSmart™ Codon Optimization from GeneScript. Sequences were synthesized into an empty pUC18 vector (GeneScript) and cloned into pD607_MCS and pD609_MCS using *XbaI* and *SapI* restriction sites. The common light chain sequence was cloned into pD609_MCS and knob and hole heavy chain were cloned into pD607_MCS.

4.3.5 Generation of DGV (msAb) lonza vector

DGV vector for the expression of bispecific antibody (msAb-Fer, Ferring) was generated following the supplier indications (Lonza). First, light chain and heavy chain sequences, synthesized in pUC19 vector (GenScript) were subcloned into pXC-17.4 and pXC-18.4 (Lonza) vector, respectively, using *NruI* and *EcoRI* restriction sites. Then, pXC-17.4-Light and pXC-18.4-Heavy were digested with *NotI* and *PvuI* and the larger fragment from both vectors were ligated to obtain DGV vector.

4.3.6 Generation of TGV (bsAb) lonza vector

TGV vector for the expression of bispecific antibody (bsAb-Fer, Ferring) was generated following the supplier indications (Lonza). First, common light chain, knob heavy chain and hole heavy chain sequences, synthesized in pUC18 vector (GenScript) were subcloned into pXC-Part A, B and C (Lonza) vector, respectively, using *HindIII* and *BamHI* restriction sites. Then, TGV vector was generated by Golden Gate assembly ligation using *BsmBI* restriction sites and following conditions: 42°C for 15 min and 16°C for 5min for 30 cycles then incubation at 55°C for 15min.

4.4 Mammalian Cell Culture

4.4.1 Routine culture

Suspension-adapted CHO-S cells (gift from HES-SO Valais Wallis) were maintained in CD CHO medium supplemented with 8 mM L-glutamine. Routine cultures were inoculated at a cell concentration of 1×10^5 cells/mL in 125 mL Erlenmeyer shake flasks in a working volume of 20 mL and cultivated at 37°C, 10% CO₂, 120 rpm (25 mm shaking diameter) and 85% relative humidity. Cells were passed every 3-4 days. Cell viability and cell density were assessed using ViCell Blue counter.

CHO-K1SV GS KO cells were used to set-up a commercial baseline to be compare with the developed antibody production platform. Cells were maintained in CD CHO medium supplemented with 6 mM L-glutamine and routine cultures were inoculated at a cell concentration of 1×10^5 cells/mL in 125 mL Erlenmeyer shake flasks in a working volume of 20 mL and cultivated at 37°C, 10% CO₂, 120 rpm (25 mm shaking diameter) and 85% relative humidity. Cells were passed every 3-4 days. Cell viability and cell density were assessed using ViCell Blue counter.

4.4.2 Cell cryopreservation and cell recover from cryopreservation

For cryopreservation, 3-4 days old CHO-S culture in exponential growth phase and viability greater than 90% was used to prepare cell banks. Cells were pelleted at 200xg for 5 min and resuspended in cryopreservation medium consisting in 45% CD CHO supplemented with 8 mM L-glutamine, 45% of conditioned medium and 10% DMSO. Aliquot of 1 mL at a concentration of 10^7 cells/mL were prepared into cryogenic vials and stored for 24h at -80°C in *Mister Frosty™* container . For long term storage, vials were transferred into liquid nitrogen.

CHO-K1SV GS KO cells were cryopreserved as described above using 92.5% CD CHO supplemented with 6 mM L-glutamine and 7.5% of DMSO as cryopreservation medium. For transfectant CHO-K1SV GS KO cells (pools or clones) using GS system, 92.5% CD CHO without L-glutamine and 7.5% of DMSO was used as cryopreservation medium. Cryovial of CHO-S cells or CHO-K1SV GS KO were thawed in a water bath at 37° until ice was totally dissolved, then 1 mL of cell suspension was transferred in 125 mL shake flask in 19 mL of pre-warmed culture medium. Cell were incubated at 37°C, 10% CO₂, 120 rpm (25 mm shaking diameter) and 85% relative humidity and passed after 3 days.

4.4.3 Transfection using Neon electroporator system

For stable cell line generation, cells were electroporated using Neon electroporator system and Neon™ Transfection System 10 µL Kit. One/two days before transfection, cells were inoculated at 0.7×10^6 cells/mL in 15 mL of fresh medium. On the day of transfection cells were pelleted at 200xg for 5 minutes, wash in PBS and resuspended in 10 µL in Buffer R at a concentration of 2.0×10^7 cells/mL. For transfection, sterile DNA purified using EndoFree plasmid maxi kit, at a concentration of 0.5-3 µg/mL, was added to the cell suspension and gently mixed. DNA-cells mixture was aspirated using sterile Neon tips and transfected into Neon tubes installed into the Neon station. Both CHO-S and CHO-K1SV GS KO cells were electroporated using 1130 V, 20 ms, 3 pulses as pulse condition. After pulse delivery cells were transferred into 12 well plates in 1 mL pre-warmed culture medium and incubated for 24h at 37°C, 120 rpm (25 mm shaking diameter) and 85% relative humidity in static mode.

4.4.4 Clonal selection in semi-solid medium

To select single clone derived colonies, stable cell pools obtained after antibiotic selection were transferred into semi-solid medium. For this purpose, the day before cell seeding, semi solid medium was thawed at room temperature. On the day of cell seeding the appropriate volume of semi solid medium was mixed with additional component such as L-Glutamine and antibiotics if required, as per supplier indications. In the case of GS system, the L-Glutamine was not added into the semi solid media for successful selection of transfectants. Cells were transferred into CHO Growth A medium (Molecular Devices) and mixed throughly to obtain an omogenous cell suspension. 300 cells were seeded for stable and robust pools, weather 1×10^3 cells were seeded in the case of fresh transfections. A total of 2mL of semi solid medium was then dispensed into each well of a 6 well plate. Demineralised water was added into the spaces between wells to prevent semi solid to dry during the incubation time. Semi solid plates were incubated at 37°C, 5% CO₂, 100% humidity for 10-12 days. Then, plates were inspected at inverted microscope and/or screened using Cytation 5 imaging system to evaluate colonies growth and shape. Thigh single cell colonies were picked from semi solid medium, under laminar flow using an inverted microscope and transferred in in 96-well plates 100 µL of fresh medium.

4.4.5 Flow cytometry and single cell-cloning

Cell fluorescence measurements were performed using a MACSQuant® Analyzer 16 flow cytometer (Miltenyi Biotec, 488 nm laser and 525/50 nm (B1) filter for EGFP detection and 579/34 nm (B2) filter for DsRed respectively. Empty CHO-S cells were used for setting morphological gates to distinguish between double negative, single positive (EGFP+ or DsRed+) or double positive cells (EGFP+ and DsRed+). Double positive cells were isolated and sorted utilizing a BD FACS Aria III (BD Biosciences, San Jose, CA) using 488 nm laser and 530/30 nm filter for EGFP detection, and 562 nm laser and 585/12 nm filter for DsRed detection. Data analyses were conducted in BD FACSDiva V8.0 software and FlowJo v10.6.2 software. Cells were sorted in 96 well plates (in 180 µL of CD CHO with 8 mM L-glutamine), after recovery they were expanded and maintained at 37°C, 10% CO₂.

4.5 Generation of host cell line containing 5' chicken lysozyme MAR-rich landing pads

For the generation of MHC lines, pLP_EGFP and pLP_DsRed were linearized using AflIII/BstZ17I and ApaLI/BstZ17I restriction enzymes, respectively. Plasmids were then purified by EtOH precipitation (paragraph X) and resuspended in nucleases-free water at a concentration of 2 µg/mL. Approximately 2×10^5 CHO-S cells were transfected with 2 µg of LP_DsRed using Neon electroporation system (1130 V, 20 ms, 3 pulses). After transfection, the cells were transferred in 12 well plates in 1 mL of CD CHO + 8 mM of L glutamine and incubated at 37°C, 10% CO₂, 120 rpm (25mm shaking diameter) and 85% relative humidity. Cells were transfected again as described above after 21 h after the first transfection and selected with G418 (added after 48 h from second transfection) at a concentration of 700 µg/mL for three weeks. After selection, the stable pool expressing DsRed was additionally transfected with 4 µg of LP_EGFP as previously described. 48 h after transfection, cells were transferred in semi-solid medium (supplemented with 700 µg/mL of G418). Single-cell derived colonies were picked from semi-solid medium after 2 weeks of incubation at 37°C, 10% CO₂, 85% humidity in static mode. Selected landing pad cell lines in 6 well plates over 90 generation without antibiotic selection at 37°C, 10% CO₂ at 120 rpm. Cells were passaged every 3-4 days and analyzed every two weeks by flow cytometry to test fluorescence intensity and percentage of EGFP+/DsRed+ cells.

4.6 Generation of control host cell line containing landing pads without MAR

For the generation of control MHC lines containing landing pads without MAR, pLP_EGFP-w/oMAR and pLP_DsRed-w/oMAR were linearized using AflIII/BstZ17I and ApaLI/BstZ17I restriction enzymes, respectively. Plasmids were then purified by EtOH precipitation (paragraph 4.2.3) and resuspended in nucleases-free water at a concentration of 2 µg/mL. Approximately 2×10^5 CHO-S cells were transfected with 2 µg of LP_DsRed using Neon electroporation system (1130 V, 20 ms, 3 pulses). After transfection, the cells were transferred in 12 well

plates in 1 mL of CD CHO + 8 mM of L glutamine and incubated at 37°C, 10% CO₂, 120 rpm (25mm shaking diameter) and 85% relative humidity. Cells were transfected again as described above after 21 h after the first transfection and selected with G418 (added after 48 h from second transfection) at a concentration of 700 µg/mL for three weeks. After selection, the stable pool expressing DsRed was additionally transfected with 4 µg of LP_EGFP as previously described. 48 h after transfection, cells were transferred in semi-solid medium (supplemented with 700 µg/mL of G418). Single-cell derived colonies were picked from semi-solid medium after 2 weeks of incubation at 37°C, 10% CO₂, 85% humidity in static mode. Selected landing pad cell lines in 6 well plates over 90 generation without antibiotic selection at 37°C, 10% CO₂ at 120 rpm. Cells were passaged every 3-4 days and analyzed every two weeks by flow cytometry to test fluorescence intensity and percentage of EGFP+/DsRed+ cells.

4.7 Generation of host cell line containing h1-68 MAR-rich landing pads

For the generation of control MHC lines containing h1-68-MAR rich landing pads, pLP_1-68MAR_EGFP and pLP_1-68MAR_DsRed were linearized using AflIII/BstZ17I and ApaLI/BstZ17I restriction enzymes, respectively. Plasmids were then purified by EtOH precipitation (paragraph X) and resuspended in nucleases-free water at a concentration of 2 µg/mL. Approximately 2×10^5 CHO-S cells were transfected with 4 µg of digested pLP_1-68MAR vector mix (1:6 ratio, pLP_1-68MAR_EGFP : pLP_1-68MAR_DsRed) using Neon electroporation system (1130 V, 20 ms, 3 pulses). After transfection, the cells were transferred in 12 well plates in 1 mL of CD CHO + 8 mM of L glutamine and incubated at 37°C, 10% CO₂, 120 rpm (25mm shaking diameter) and 85% relative humidity. Cells were transfected again as described above after 21 h after the first transfection and selected with G418 (added after 48 h from second transfection) at a concentration of 700 µg/mL for three weeks. After selection, the stable pool expressing DsRed was additionally transfected with 4 µg of LP_EGFP as previously described. 48 h after transfection, cells were transferred in semi-solid medium (supplemented with 700 µg/mL of G418). Single-cell derived colonies were picked from semi-solid medium after 2 weeks of incubation at 37°C, 10% CO₂, 85% humidity in static mode. Selected landing pad cell lines in 6 well plates over 90 generation without antibiotic selection at 37°C, 10% CO₂ at 120 rpm. Cells were passaged every 3-4 days and analyzed every two weeks by flow cytometry to test fluorescence intensity and percentage of EGFP+/DsRed+ cells.

4.8 Generation of stable msAb clones using the LP system

The monospecific antibody expressing stable cell lines were generated by transfecting stable LP clones with Donor_Light, Donor_Heavy and pCAG-NLS-HA-BxB1 (Addgene plasmid # 51271; <http://n2t.net/addgene:51271>; RRID:Addgene_51271) vectors. 2×10^5 cells were transfected with 500 ng BxB1 expression plasmid and 1.5 µg of donor vectors (ratio 1:1 between Donor_Light and Donor_Heavy), using the same parameters described above. After transfection, cells were transferred in 12 well plates in 1 mL of CD CHO supplemented with 8 mM

of L-glutamine and incubated at 37°C, 10% CO₂, 120 rpm. Three days after transfection, cells were subjected to double antibiotic selection with 20 µg/mL of puromycin and 600 µg/mL of hygromycin. Integration of both GOIs into the landing pad was monitored by following the loss of fluorescence. After two weeks of selection, clonal selection was carried out by plating cells in semi-solid medium. After 10 days, single colonies were picked from semi-solid medium and transferred in 96-well plates. Clones were screened for antibody production by dot-blot. MsAb producing clones were transferred and maintained in 6 well plates over 90 generation without antibiotic selection. Cells were passaged every 3-4 days and analysed every 20 generation for msAb production in 30mL fed-batch cultures.

4.9 Generation of stable msAb clones using the GS system

For the generation of stable msAb transfectant using the GS system, DGV vector was linearised using PvuI and AvII restriction enzymes. DNA was then purified by EtOH precipitation (paragraph X) and resuspended in nucleases-free water at a concentration of 2 µg/mL. On the day of transfection, approximately 2 x 10⁵ CHO-S cells were transfected with 4 µg of linearized DGV vector and then transferred in 12 well plates in 1 mL of fresh CD CHO medium without glutamine. 24h post-transfection selection was started by adding 50 µM of MSX. Cell viability was monitored from day 7 onwards and started to be subcultured once cells reached 0.6 x 10⁶ viable cells/mL. Stable pool was then subcultured four times before starting clonal selection. A total of 300 cells were seeded into semi solid media and after 10-14 days, single cell derived colonies were picked from semi-solid medium and transferred into 96-well plates. Once cells reached 70-90% of confluency, clones were screened by dot-blot using Anti-IgG (H+L) antibody.

4.10 Generation of stable bsAb clones using the LP system

BsAb-expressing stable cell lines were generated by transfecting LP stable clones with Donor_cLight, Donor_KHeavy, Donor_HHeavy and pCAG-NLS-HA-BxB1 vectors. For transfection, an equimolar mix of donor vectors was mixed with the BxB1 expression vector in a 1:3 ratio (recombinase:payloads) and 2x10⁵ cells were transfected with 4 µg of total DNA mixture, using the same parameters described above. After transfection, cells were transferred in 12 well plates in 1 mL of CD CHO supplemented with 8 mM of L-glutamine and incubated at 37°C, 10% CO₂, 120 rpm. After 3 days from transfection, cells were subjected to double antibiotic selection with 10 µg/mL of puromycin and 600 µg/mL of hygromycin. Clones were isolated from semi-solid medium and screened by dot blot using a mouse anti Strep-Tag Classic:HRP detection antibody for the detection of knob heavy chain, HRP-conjugated His-Tag monoclonal antibody for the detection of hole heavy chain and Peroxidase-AffiniPure Donkey Anti-Human IgG (H+L) for the detection of the whole antibody.

4.11 Generation of stable bsAb clones using the GS system

For the generation of stable bsAb transfectant using the GS system, TGV vector was linearised using PvuI and AvII restriction enzymes. DNA was then purified by EtOH precipitation (paragraph X) and resuspended in nucleases-free water at a concentration of 2 µg/mL. On the day of transfection, approximately 2×10^5 CHO-S cells were transfected with 4 µg of linearized TGV vector and then transferred in 12 well plates in 1 mL of fresh CD CHO medium without glutamine. 24h post-transfection selection was started by adding 50 µM of MSX. Cell viability was monitored from day 7 onwards and started to be subcultures, once cells reached 0.6×10^6 viable cells/mL. Stable pool was then subcultured four times before starting clonal selection. A total of 300 cells were seeded into semi solid media and after 10-14 days, single cell derived colonies were picked from semi-solid medium and transferred into 96-well plates. Once cells reached 70-90% of confluency, clones were screened by dot-blot using Anti-IgG (H+L) antibody.

4.12 Cell adaptation to different media

Clonal cell line expressing msAb and bsAb were adapted in Balan CD – CHO growth A, ActiPro and OptiCHO media following a sequential adaptation protocol. Clones were thawed as described in paragraph X and passed in CD CHO medium supplemented with 8 mM of L-glutamine for four passages. Then, at each subculturing step, cells were diluted at 1×10^5 cell/mL in a fresh medium composed by a mix of new medium and CD CHO. At each passages, the proportion between new medium and CD CHO was augmented (25%, 50%, 75%) until reaching 100%. Cell growth and viability was monitored daily to evaluate cell adaptation. If cells show a reduction in growth rate or in viability after subculturing in the new medium, several passages were repeated in the same medium until total adaptation. Cells were maintained for, at least, four passages in 100% new medium before banking.

4.13 Fed-batch cultures

Best performing clones expressing msAb (2B9, 2B12 and 3E2) and bsAb (D9 and D11) were tested in fed-batch cultures using different media and feed strategy. Cryovials of cells at the same generation number were thawed in fresh medium and passed four times before inoculating the fed batch culture. At day 0, cultures were inoculated from a middle exponential phase culture at a concentration of 2×10^5 cells/mL in 30 mL of fresh medium. From day three onwards, cultures were fed using the following combinations of feeds and medium (Table 1):

Table 1 medium and feed used in fed batch cultures

| Condition | Medium | Feeds |
|-----------|--|--|
| CD CHO 1 | CD CHO + 8 mM L-Glutamine | 1% HyClone Cell Boost 7a + 0.5% HyClone Cell Boost 7b |
| CD CHO 2 | CD CHO + 8 mM L-Glutamine | 2% HyClone Cell Boost 7a + 0.2% HyClone Cell Boost 7b |
| BalanCD | BalanCD – CHO Growth A + 8 mM L-Glutamine | 2% HyClone Cell Boost 7a + 0.2% HyClone Cell Boost 7b |
| ActiPro | HyClone ActiPro medium + 8 mM L-Glutamine | 2% HyClone Cell Boost 7a + 0.2% HyClone Cell Boost 7b |
| OptiCHO | CD OptiCHO + 8 mM L-Glutamine | 2% HyClone Cell Boost 7a + 0.2% HyClone Cell Boost 7b |

VCD and viability were tested daily by trypan blue exclusion using ViCell Blue system. From day 4 onwards, sampling and glucose evaluation were started. Glucose concentration was evaluated using GlucCell device. Glucose supplementation up to 5g/L was done when its concentration in the culture drop below 3g/L. When viability drop below 70%, cultures were stopped and supernatant was harvested. Cultures were transferred into a 50 mL falcon tube and centrifuged at 200 x g for 15 min. Then, supernatant was transferred into a new 50 mL falcon tube and centrifuged at maximum speed for 10 min. Clarified supernatant was sterile filtered using 0.22 µm syringe filter and stored at 4°C for short term storage or -20°C for long term storage.

4.14 Culture expansion for shake flask scale up and bioreactor inoculum

One vial of bsAb D7 cell line adapted in ActiPro medium was thawed and transferred in 125mL shake flask in 19 mL of fresh ActiPro medium supplemented with 8mM of L glutamine. Cells were maintained in culture and passaged two times before starting the expansion steps. Cells in mid-exponential phase were used to inoculate a 250mL shake flask (50 mL total volume) and a 500mL shake flask (100 mL total volume) at 1×10^5 cells/mL. After 3-4 days, when cells reached $3-4 \times 10^6$ cell/mL, the 50 mL culture was used to inoculate 500 mL shake flask with 140 mL working volume and 125 mL shake flask with 20 mL working volume at 2×10^5 cells/mL, both in triplicate. Fed batches in shake flask were run as described in paragraph 4.13, using the combination of ActiPro medium and 2% HyClone Cell Boost 7a + 0.2% HyClone Cell Boost 7b.

The 100 mL culture was further expanded in two 500 mL culture in 2L shake flask, by diluting cells at 2×10^5 cells/mL. After two-three days, when cell density reached $3-4 \times 10^6$ cell/mL, cultures were used to inoculate the BioFlo 320 (Eppendorf) with a working volume of 2.5L and the SB10-X single use bioreactor (Kuhner) with a working volume of 5L, at a concentration of 2×10^5 cells/mL.

4.15 SB 10-X bioreactor set-up and run

Before installing the single use bag, one of the silicon tubes on the upper part of the bag (tube 6, Figure 8 A and B) was modified adding a sterile “Y” extensor using the BioWelder system. This tube extension was needed for feed and glucose supplementation. The single use bag was carefully installed into the SB 10-X vessel module. The bag was fully inflated with air and then it was filled with 4.5 L of ActiPro medium supplemented with 8 mM of L-glutamine. To control the pH in the bioreactor, a bottle containing 1M of NaHCO_3 was connected to the bioreactor using the tube 6 (Figure 8 B and C) by sterile welding. DO and pH were calibrated as indicated in the SB 10-X manual, using the parameters indicated in the bag envelope. Process parameters and culture condition were set as shown in Figure 8 D, and a sterile run was performed for 12 hours.

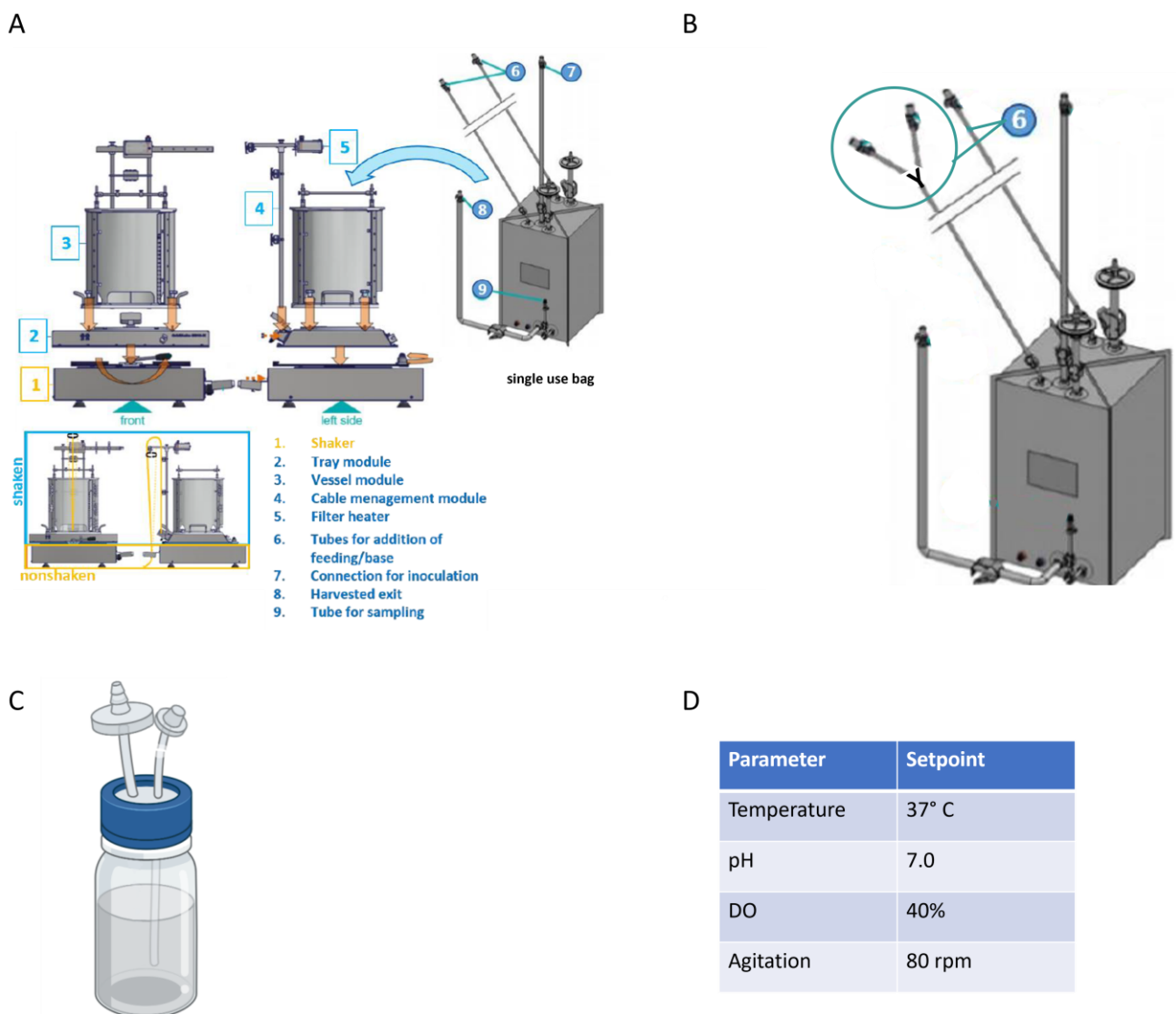


Figure 8 SB-10X bioreactor set-up. (A) SB-10X assembly and bioreactors parts. **(B)** Feeding tube set-up. **(C)** Bottle for bioreactor connection, feeding and supplementation. **(D)** Bioreactor parameters. Images A and B were modified from Kühner SB-10X bioreactor user manual.

On the day on the inoculum, viable cell density and viability of the preculture were evaluated and the appropriate amount of culture volume was estimated to inoculate the bioreactor at a final concentration of 2×10^5 cell/mL. Inoculum was realized using the tubing 7 (fig x) and sterile connecting the silicon tubing using the BioWelder system. Additional medium was added to the inoculum to reach the final volume of 5 L. Bottles for inoculum, base, feeds and glucose were prepared using screw cups with tubing connectors as shown in fig X, and autoclaved. Appropriate silicon tubing were prepared using TPE C-flex tubing suitable for welding, pharmed tubing suitable for peristalting pumping and appropriate plastic connectors. Inoculum, base, feed and glucose addition were realised using peristaltic pump system. From day 3 onwards, bioreactor was fed with 2% HyClone Cell Boost 7a + 0.2% HyClone Cell Boost 7b. Feeds were added using tubes 6 in figure X by connecting it to the feed containing bottles by sterile welding. A daily sampling (5 mL) was performed, using the sampling tubing and male luer lock syringe. The sample was used for VCD and viability testing, external pH evaluation. VCD and viability were tested daily by trypan blue exclusion using ViCell Blue system. After centrifugation and filtration, supernatant was tested for glucose concentration and then stored at 4°C for short term storage or -20°C for long term storage. Glucose concentration was evaluated using GlucCell device. Glucose supplementation up to 5g/L was done when its concentration in the culture drop below 3g/L, using a 30% sterile glucose solution. When viability drop below 70%, cultures were stopped and supernatant was harvested.

A total of 1L of culture was recovered from the bioreactor for harvest using the harvest exit (tube X fig X). Culture suspension was centrifuged using the 250mL bottles in a Sigma 4-5L centrifuge, at 200 x g for 1h. The supernatant was then further centrifuged at maximum speed for 15 minutes and filtered using 0.22 µm vacuum filter (Corning). Supernatant was stored at -20°C for long term storage.

4.16 BioFlo320 Eppendorf bioreactor set-up and run

A 3L autoclavable vessel has been prepared for installation by filling the water jacket with demineralized water using the appropriate water inlet, connecting pH and temperature probes, tubing and filters, pitched-blade impeller and a ring sparger and the exhaust condenser. After autoclaving, vessel and tubing were connected to the bioprocess control system. The vessel was filled with 2L of ActiPro medium with 8 mM of L-glutamine and the DO have been calibrated, and the base bottle was connected to the bioreactor before running a sterile run (12 hours). Process parameters and culture condition were set as shown in Table 2.

Table 2 BioFlo320 Eppendorf bioreactor parameters

| Parameter | Setpoint |
|---------------------------------|----------|
| Temperature | 37°C |
| pH | 7.0 |
| DO (ring sparger) | 40% |
| Stirring (pitch blade impeller) | 80 rpm |

On the day on the inoculum, viable cell density and viability of the preculture were evaluated and the appropriate amount of culture volume was estimated to inoculate the bioreactor at a final concentration of 2×10^5 cell/mL. Additional medium was added to reach the final volume of 2.5L. . Bottles for inoculum, base, feeds and glucose were prepared using screw cups with tubing connectors as shown in fig X, and autoclaved. Appropriate silicon tubing were prepared using TPE C-flex tubing suitable for welding, pharmed tubing suitable for peristalting pumping and appropriate plastic connectors. Inoculum, base, feed and glucose addition were realised using peristaltic pump system. A daily sampling (5 mL) was performed, using the sampling port and tubing and male luer lock syringe. The sample was used for VCD and viability testing, external pH evaluation. VCD and viability were tested daily by trypan blue exclusion using ViCell Blue system. After centrifugation and filtration, supernatant was tested for glucose concentration and then stored at 4°C for short term storage or -20°C for long term storage. Glucose concentration was evaluated using GlucCell device. Glucose supplementation up to 5g/L was done when its concentration in the culture drop below 3g/L, using a 30% sterile glucose solution. When viability drop below 70%, cultures were stopped and supernatant was harvested as described in paragraph 4.13.

4.17 Stability studies

Selected landing pad cell lines with and without MAR were maintained in 6 well plates (2mL of total volume) over 90 generation in CD CHO without antibiotic selection at 37°C, 10% CO₂ at 120 rpm. Cells were passaged every 3-4 days and analyzed every two weeks by flow cytometry to test fluorescence intensity and percentage of EGFP+/DsRed+ cells.

Selected msAb producing cells lines were continuously propagated over 90 generations in 6 well plates without antibiotic selection and subsequently used to inoculate 125 mL shake flask for fed-batch cultures in 30 mL CD CHO supplemented with 8 mM L-glutamine at 2×10^5 cells/mL. Fed-batches were repeated every 20 generation to test antibody titer, VCD and cell viability.

Selected bsAb clones were continuously propagated over 90 generations in 6 well plates (2mL of total volume) without antibiotic selection. Cells were subcultured every 3-4 days and diluted at 1×10^5 cells/mL in 2mL of fresh CD CHO medium supplemented with 8 mM of L-glutamine. At each subculturing steps, 1mL sampling was done to further analyse the sample for antibody concentration.

4.18 Transcript level analysis

RNA was isolated from stable msAb producing clones using the RNeasy mini kit (Qiagen) following the manufacturer's instruction. RT-qPCR was performed on the Rotor-Gene Q machine (Qiagen) using Rotor-Gene Multiplex Rt-PCR kit (Qiagen) in a triplex assay (two GOIs and one control). The thermal conditions were 15 min

at 50°C and 5 min at 95°C for reverse transcription step and PCR initial activation step followed by 45 cycles of 15 s at 95°C and 15 s at 60°C. Relative expression of HC and LC were calculated using delta Ct analysis method. The expression of eEF1 α 1 housekeeping gene was used as reference to normalize different RNA samples in each reaction. Each experiment included a “no template control” and each sample was tested in triplicate. Primers and probes are listed in Table S7 (Supporting Information).

4.19 Determination of gene copy number

DNA was isolated from stable clones using the DNeasy Blood & Tissue Kit (Qiagen) following the manufacturer’s instruction. 50 ng of genomic DNA were used to calculate the transgene copy number using QuantiTect Multiplex PCR Kit (Qiagen) and Rotor-Gene Q machine. Thermocycling condition were set up as suggested by the supplier and mRNA level were calculated using Rotor-Gene Q Series Software as described by Karlen et al.[42] Sequences of probes for GOIs and reference gene (Beta-2 microglobuline) as well as primers are listed in Table S7 (Supporting Information). Each experiment included a “no template control” and each sample was tested in triplicate.

4.20 Genomic PCR amplification of targeted regions

Targeted integration was verified by PCR on genomic DNA using primers binding outside the recombination site into the Landing Pad and primers specific for the gene of interest. PCR set up is shown on Figure S2 (Supporting Information) and primers are listed in Table S7 (Supporting Information). For the extraction of genomic DNA, cells were collected by centrifugation and the extraction was performed with DNeasy Blood & Tissue Kit (Qiagen). PCR was carried out using Q5 High-Fidelity 2X Master Mix and 250 ng of genomic DNA as template in a 25 μ L reaction. Thermocycling conditions: 98°C for 30 s; 30x: 98°C for 10 s, 72° for 1min and 20 s; 72°C for 2 min.

4.21 Fluorescence in situ hybridization analyses

FISH was performed using fluorescent probes generated by PCR using HighFidelity Fluorescein/Orange PCR Labeling kit. Probes were generated by PCR using pLP_EGFP, pLP_DsRed, pDonor_H and pDonor_L as template and probes listed in paragraph 3.4.4, following supplier instruction. Thermocycling conditions were: 95°C for 2min; 30x: 95°C for 20 sec, 58°C for 30 sec, 68°C for 60 sec; 68°C for 2min. After amplification, samples were loaded into 1% Agarose gel and resolved by electroporation at 120V for 50 min. Then fragments of interest were purified using QIAquick gel extraction kit following supplier indication.

Exponentially growing cell have been used to prepare metaphase chromosome spreading for fluorescent *in situ* hybridization as described by Girod et al.[21,43] Cells were treated with colcemide for 1 h at a concentration of

0.1 µg/mL and then pelleted at 200xg for 5 min. Supernatant was removed being attentive to leave approximately 0.5 mL in the tube and carefully resuspend the cells in this remaining volume. Cells were then subjected to hypotonic shock by gently adding 0.075 M of KCl solution for 20 min at 37°C. Subsequently, cells were pre-fixed by adding 50 µL of fixative solution (3:1 methanol/acetic acid solution), well mixed and centrifuged at 200xg for five min. Supernatant was discarded and 5 mL of ice-cold fixative solution were added drop by drop to the cells by continuously mixing the cell suspension. Cells were pelleted again at 200xg for 5 min and resuspended in 1-2 mL of ice-cold fixative solution. Few drops of cell suspension were drop onto an alcohol cleaned slide and let air-dry for minimum 1h. Slides were then denatured in 70% (v/v) formamide at 70°C for 2 min, dehydrated in ethanol solutions (70%, 80%, 100%) for 2min each and let air-dry. Probes were diluted in 10 µL of Formamide at a concentration of 5-25 ng/µL, denatured at 72°C for 5 min and incubated on ice. Hybridization buffer was mixed to the probes (10 µL), the mixture was added to the centre of the hybridization area on the dry slide and cover with a coverslip. Edges of coverslip were sealed with rubber cement and slides were incubated at 37°C for 16-24h. After hybridization, coverslip was disassembled, and slides were washed in 50% formamide in 2X SSC solution for 5min and in 0.05% Tween in 1X SSC for other 5 min. A counterstaining with DAPI was done by adding 10 µL of DAPI working solution in mounting medium (0.1 µg/mL) on the hybridization area. Chromosome were visualized using Cytation5 imager with DAPI, FITC and Texas Red filters and a 20X objective.

4.22 Analytical Methods

4.22.1 Protein purification and buffer exchange

Supernatant from cell culture was clarified before purification and additional analyses. For this purpose, cell suspension from last fed-batch cultivation day was recover and centrifuged at 200xg for 15 min in order to recover the supernatant. The latter was centrifuged at 2700xg for 30 min and then sterile filtered at 0.45 µm using top filters. Monospecific antibody was purified using NAb™ Protein A Plus Spin Columns (1mL). Approximately 1mL of clarified supernatant was loaded into the column and purified following supplier instruction. Bispecific antibody was purified using using NAb™ Protein A Plus Spin Columns in combination with Strep-tacting XT Spin Culumn and His60 Ni Gravity Columns. For Strep-tactin purification, 1mL of clarified supernatant was loaded into the column and the purification protocol was followed as per supplier indication. To increase the antibody yield, the flow-through was loaded a second time into the column. For the His-tag purification, supplier instruction were followed and 5 mL of clarified supernatant were loaded into the column and incubated for 1 hour at 4°C in a rotating incubator. Antibody were eluted using 10 column volumes of elution buffer and collecting 0.5 mL fractions.

Purified fraction containing the protein of interest were concentrated and transferred in PBS 1X using protein concentrator centrifugal devices and following supplier indications. Protein concentration was determined,

before and after buffer exchange, by absorbance at 280 nm using DeNovix DS-11 Nanodrop system. For monospecific antibody $E^{1\%}$ of 13.7 was used to calculate antibody concentration. For bispecific antibody, molar extinction factor of $226630 \text{ M}^{-1}\text{cm}^{-1}$ and molecular weight of 148128.54 Da were used to calculate antibody concentration.

4.22.2 SDS-PAGE and immunoblotting

SDS-PAGE was performed utilizing Mini-PROTEAN TGX precast gels. Samples were prepared by mixing them with Laemmli Sample Buffer 4x either with 10% of 2-mercaptoethanol (reducing) or without (non-reducing). Samples were incubated at 95°C for 5min and then loaded on the gel. Precision Plus Protein™ All Blue unstained standard was loaded on the gel as protein ladder. Electrophoresis was conducted at constant voltage of 180V for approximately 45 min, then protein separation was visualized at ChemiDoc imager using automatic exposition in stain-free gel set-up mode. Proteins were transferred to Trans-Blot Turbo Mini PVDF membranes using the Trans-Blot Turbo Transfer System. For dot-blot analysis, Amersham™ Protran® Western blotting membranes was used to assemble a dot blot manifold and 100 μL of culture supernatant were added in each well. The membrane was blocked using 5% NonFat Milk powder in TBS, then incubated with the primary detection antibody. After three washes in TTBS, bound detection antibody was visualized using Clarity Western ECL Substrate using Chemidoc gel imaging system. For msAb samples, Peroxidase-AffiniPure Donkey Anti-Human IgG (H+L) was used as detection antibody. For BsAb samples, three different immunoblot were prepared that were incubated with different detection antibodies: mouse anti Strep-Tag Classic:HRP detection antibody for the detection of the knob heavy chain, HRP-conjugated His-Tag monoclonal antibody for the detection of the hole heavy chain and Peroxidase-AffiniPure Donkey Anti-Human IgG (H+L) for the detection of the full-length antibody.

4.22.3 BLI antibody quantitation analysis

Antibody quantitation analyses were done using Octet K2 system using protein A biosensor. Standard curves (0, 0.125, 0.25, 0.5, 1.01, 2.01, 4.03, 8.06, 16.1, 32.3, 64.5, 129 $\mu\text{g}/\text{mL}$) were realized by serial (2X) dilution using purified msAb and bsAb in PBS to test antibody concentration in supernatant samples as well as in purified fractions. For measurement, 200 μL of samples and standard were added into plate wells. Each sample was diluted at least five times in PBS in order to reduce eventual matrix effect.

4.22.4 Size exclusion chromatography

Size exclusion chromatography was performed using Yarra SEC3000 column on HPLC system using 0.1 M NaH_2PO_4 as mobile phase. Clarified supernatant as well as purified samples were filtered at 0.45 μm using syringe filter before analysis. System and column were equilibrated in mobile phase before starting analyses. System parameters are reported in Table 3 .

Table 3 HPLC parameters for size exclusion chromatography using Yarra SEC-3000 column

| Parameter | Value |
|------------------|---|
| Injection volume | 10 µL |
| Flow rate | 1 ml/min |
| Analysis time | 15 min |
| Detector | DAD (Diode Array Detector), 210nm, 280 nm. |
| Buffer | 10 mM Phosphate, 15 mM NaCl (0.22 µm filtered). |

4.22.5 HPLC quantification of Glucose and Lactate in sample supernatant

Glucose and lactate concentration was evaluated by HPLC analysis using Aminex HPX-87H column (300x7.8mm). Standard curves for lactate and glucose were prepared by serial dilution (2x) to obtain a range of 10 – 0.19 g/L, starting from a stock solution 1% of sodium lactate and a stock solution of 1% of glucose. All the solutions and dilutions were prepared in demineralized water and filtered at 0.45 µm using syringe filter before analysis. Supernatant samples for analysis were obtained as described in paragraph 4.22.1. Supernatant and calibration samples were analysed using the following parameters :

Table 4 HPLC parameters for glucose and lactate quantification using Aminex HPX-87H column

| Parameter | Value |
|------------------|--|
| Injection volume | 10 µL |
| Flow rate | 0.6 ml/min |
| Analysis time | 30 min |
| Detector | RI |
| Temperature | 35°C |
| Eluent | H ₂ SO ₄ 5mM filtered at 0.45 µm |

HPLC system and columns were stabilized for 1h in the eluent before injecting the samples. Glucose and lactate concentration of supernatant samples was evaluated by interpolation using the linear fitting of calibration points. Elution peak for glucose and lactate were 8.9 min and 12.9 min respectively.

5 Results and discussion

5.1 Generation of host cell line containing landing pads

The use of site-specific recombinases for the integration of GOIs requires two fundamental steps: the generation of stable host cell lines containing the landing pads integrated into their genome followed by recombinase-mediated integration of GOIs into these landing pads. Our aim in this study was to develop a recombinase-mediated system for the integration and expression of monoclonal antibodies using two separate expression vectors for the heavy and light chain. To this end, we generated host cell lines containing multiple copies of two different MAR-rich landing pads for recombinase-mediated DNA integration of two donor vectors. The design of the landing pad vectors, described in the next section, facilitated host cell line selection and the monitoring of GOI integration during the generation step of the mAb-expressing cell line.

5.1.1 Generation of chicken 5' lysozyme MAR (cMAR)-rich landing pad clones

Landing pad vectors containing the full chicken 5' lysozyme MAR sequence were generated as described in paragraph 4.3.1 and sequences were verified by sequencing (Microsynth). These vectors contain the same MAR sequence (≈ 2.9 kb) followed by the CMV promoter, the recombination site for BxB1, a reporter gene, the bovine growth hormone polyadenylation signal (GH-Bt polyA) and a neomycin resistance cassette conferring geneticin (G418) resistance in eukaryote cells²²⁴.

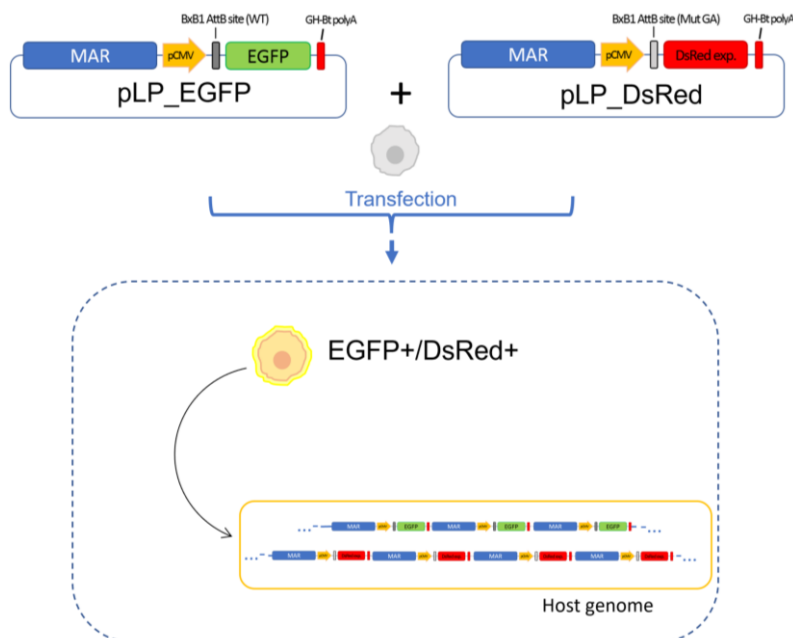


Figure 9 LP vectors and host cell line generation. Schematic representation of the generation of LPs-cMAR containing cells. Cells were transfected with the landing pad vectors harbouring the 5' chicken lysozyme MAR and then selected by G418 selection and/or by sorting double positive fluorescent cells. pLP_EGFP vector contains the chicken 5' lysozyme MAR, pCMV, AttB-WT site for BxB1 recombinase, EGFP reporter gene, and a ghb polyA tail. pLP_DsRed vector contains the chicken 5' lysozyme MAR, pCMV, AttB-GA (mutated) site for BxB1 recombinase, DsRed reporter gene, and a ghb polyA tail. In addition, both vectors contain the Neomycin resistance cassette (pSV40-NeoR-SV40polyA) for G418 antibiotic selection.

In addition, the bacterial cassette containing the pUC ori origin of replication and the ampicillin resistance cassette are also present in the vector for its replication in *E. coli*, which were already included in the pD603 (Atum) precursor vector²²⁴. The two different landing pad vectors (pLP_EGFP and pLP_DsRed) differ for the recombination site for BxB1 and for the reporter gene (AttB_WT – EGFP or AttP_GA – DsRed), (paragraph 3.3 and Figure 9). The presence of two different reporter genes (EGFP and DsRed) helps the selection of cells which integrated both landing pads which results in the expression of EGFP and DsRed. If both signals are merged, cells will appear yellow due to both fluorescence signals. The central dinucleotide mutation, from GT to GA, in BxB1 recombination site allows the use of the WT site in combination with the mutated form without the risks of cross-recombination, as already shown by Ghosh *et al.* and Inniss *et al.*^{202,215} In addition, recent comparative study of orthogonal Bxb1 recombination sites, generated by changing the central dinucleotide with alternative non-palindromic bases, identified the GA-mutant as the most efficient site-specific integrase system in mammalian cells²¹⁴.

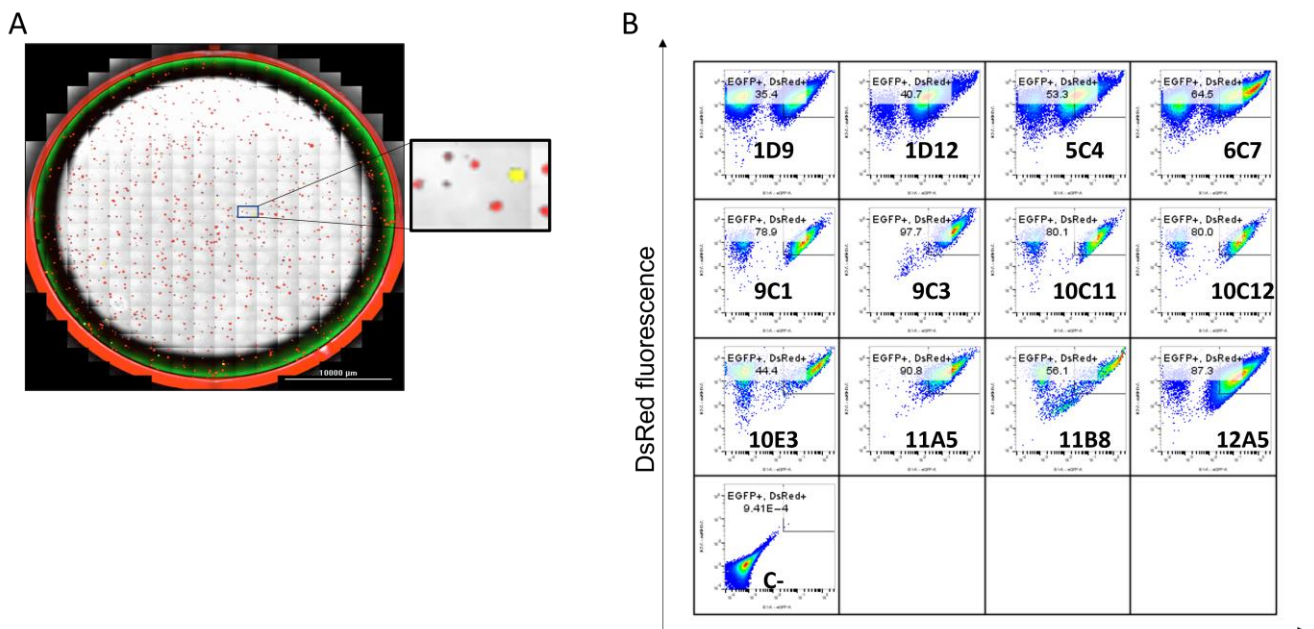


Figure 10 Results from semi-solid clone selection and FCM analysis of obtained clones. (A) Visualization of single-cell derived colonies in semi-solid medium 10 days after seeding. Yellow colonies derived from EGFP+/DsRed+ clones and were picked from semi-solid medium and transferred in 96 well plates. EGFP+/DsRed-, EGFP-/DsRed+ and EGFP-/DsRed- colonies were discarded during colony picking step. **(B)** Flow-cytometry results of clones selected during the first round of clonal selection. Clones were analysed using a 488 nm laser and 525/50 nm (B1) filter for EGFP detection and 579/34 nm (B2) filter for DsRed detection. Untransfected CHO-S cells were used as negative control.

To generate stable cell lines integrating both landing pads, CHO-S cells were co-transfected with linearized cMAR_pLP vectors (2 µg total DNA) using the Neon electroporation system as described in paragraph 4.4.3. However, despite cell recovery after transfection and selection, a rapid loss of expression of both reporter genes was registered. In particular, cells showed a loss in DsRed expression while retaining EGFP expression (data not shown). For this reason, based on the approach of Grandjean *et al.*¹⁷², CHO-S cells were transfected consecutively after 21h with 2 µg of linearized cMAR_pLP_DsRed vector, in order to increase the reporter gene

expression level facilitating a more reliable selection of a stable cell pool expressing DsRed. After two weeks of selection with 700 µg/mL G418, cells showed stable DsRed fluorescence. This stable LP_DsRed pool was transfected again with 4 µg of linearized cMAR_pLP_EGFP and transferred in semi-solid medium (supplemented with 700 µg/mL G418) after 48h post transfection. After 10-12 days in semi-solid medium, colonies were analysed with Cytation 5 imager (Figure 10 A) and the percentage of colonies showing double positive colonies was estimated by merging phase contrast, FITC and Texas Red channels. A total of 150 single-cell derived yellow colonies were picked from semi-solid medium, transferred in 96-well plate and then the most promising clones were expanded to 12- and 6- well plates. Flow cytometry analyses were done to evaluate the fluorescence level of the selected clones and eventual subpopulations (Figure 10 B).

Most of the selected clones showed clearly the presence of two populations, a double positive (DP) population EGFP+/DsRed+ and a single positive population EGFP-/DsRed+. The presence of these two distinguished populations could be due to a progressive loss of EGFP fluorescence, indicating an instability of EGFP expression for these clones. However, caused by difficulties during manual picking from semi-solid media, it could be possible that these populations were not derived from single-cell colonies and were not clonal. For these reasons, clones showing a DP population lower than 90% were excluded from following steps. Clones 9C3 and 11A5 showed the highest percentage for double positive cells population of 97.7% and 90.8%, respectively. Clone 9C3 was maintained in culture for further clonal selection step as described in paragraph 4.5. To ensure cell monoclonality, clone 9C3 was used for single cell sorting as described in 4.4.5. Approximately 1100 clones were sorted in 96-well plates and a total of 14 clones were expanded to 20 mL (125mL shake flask) and used for cell bank preparation.

Among them, the five best-performing clones in terms of mean fluorescence intensity and percentage of double fluorescence cells were maintained in culture for further analyses (Figure 11 A). Stability tests based on cell fluorescent were conducted to evaluate stable integration of both landing pad. Cells were kept in culture over 90 generations and cells were tested by flow cytometry every 20 generations. All five clones containing MAR-rich landing pads (LPs-cMAR) showed a homogeneous double-positive population ($\geq 96\%$ of the total cell population), which remained stable over the tested time period without any drop neither in median fluorescence intensity nor in percentage of double-positive cells (Figure 11 B). The use of the chicken lysozyme MAR should help the integration of the landing pad vector, into the host genome, at one or few chromosomal loci^{172,178} by promoting plasmid concatamerization in the cell nucleus and its integration in open chromatic regions of the genome. To assess the integration of the landing pad at one or few spot of host genome, we performed fluorescence in situ hybridization (FISH) analyses on metaphase chromosomes of two test clones (clone 1F8 and clone 6C1). Probes used for FISH analyses were prepared by PCR using fluorescence-labelled dUTP and using EGFP and DsRed gene sequences as template for landing pads hybridization.

Results indicate one random integration spot for LP_EGFP and one random integration spot for LP_DsRed, showing no multiple integration events in the genome of host cell lines (Figure 12 A).

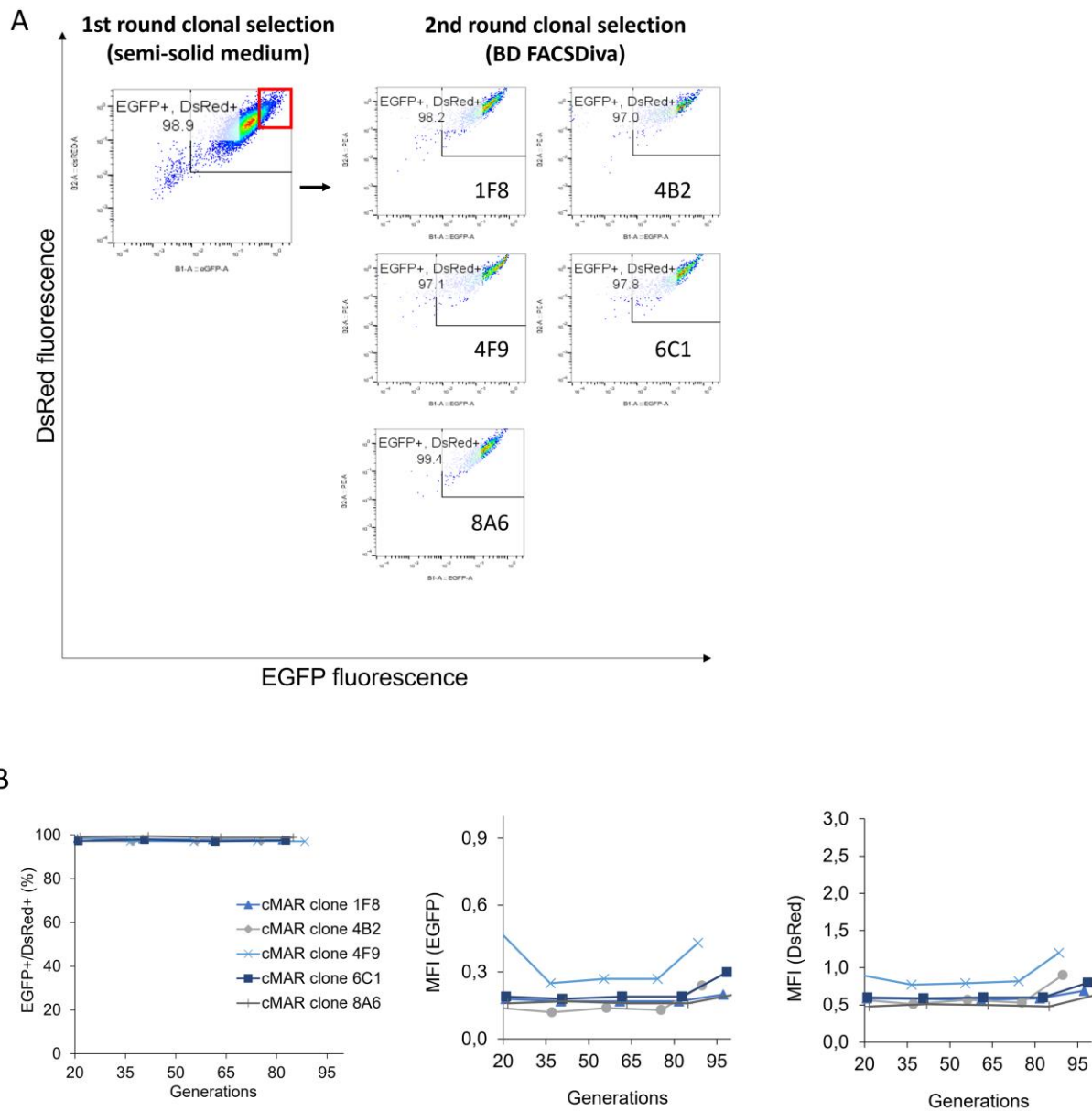


Figure 11 cMAR clones and stability test. (A) cMAR clone selected in semi-solid medium during the first round of clonal selection was used for a second round of clonal selection by fluorescence activated cell sorting (BD FACSDiva). In the panel on the right are shown the best performing clones in terms of fluorescence, stability and cell growth, selected through clonal screening and expansion steps. **(B)** Stability test representing the frequency of EGFP+/DsRed+ clones and median fluorescence intensity (MFI) of the LPs_cMAR clones for EGFP and DsRed.

Although the clones showed homogeneous EGFP and DsRed fluorescence and little variation in fluorescence intensity, gene copy number analyses revealed differences in pLPs copy number and pLPs ratio. All clones showed 1.4-7 times higher pLP_DsRed copy number than pLP_EGFP (Figure 12 B and Table S1). The highest ratio of pLP_DsRed compared to pLP_EGFP was recorded for 1F8 (pLP_DsRed/pLP_EGFP copy ratio of 7), while 4B2 showed only a 1.4-fold difference in GCN for pLP_DsRed compared to pLP_EGFP. Clones 4F9, 6C1 and 8A6

showed a similar pLP_DsRed/pLP_EGFP ratio of 5:1. This difference in copy number is probably due to the two consecutive transfections with pLP_DsRed. In fact, the effect of iterative transfection on transgene expression and gene integration combined with the inclusion of MAR element into the expression vector was already described by Grandjean et al.¹⁷² MAR element and iterative transfection seems to act synergistically by increasing the formation of vector concatamers into the cell nucleus and thus, further increasing the number of copies of the vector that can be integrated into the genome and being expressed. However, the fact that no particular differences in fluorescence intensity are observed for both reporter genes despite the differences in GCNs between clones, suggests that the different landing pads are expressed differently even if the MAR element has been included in the landing pad.

To assess whether differences in copy number could affect cell growth, clones were cultured in batch mode and daily tested for VCD and viability. Cultures were inoculated at 1×10^5 cells/mL in CD CHO supplemented with 8 mM of L-glutamine and harvested when the viability dropped below 70%. Clones showed similar growth curves besides the different LPs copies integrated into the genome. Most of the clones were maintained in culture for 10 days reaching a max. VCD between $6.5\text{-}10 \times 10^6$ cells/mL. Clone 4B2 showed a longer culture duration (12 days) and higher VCD.

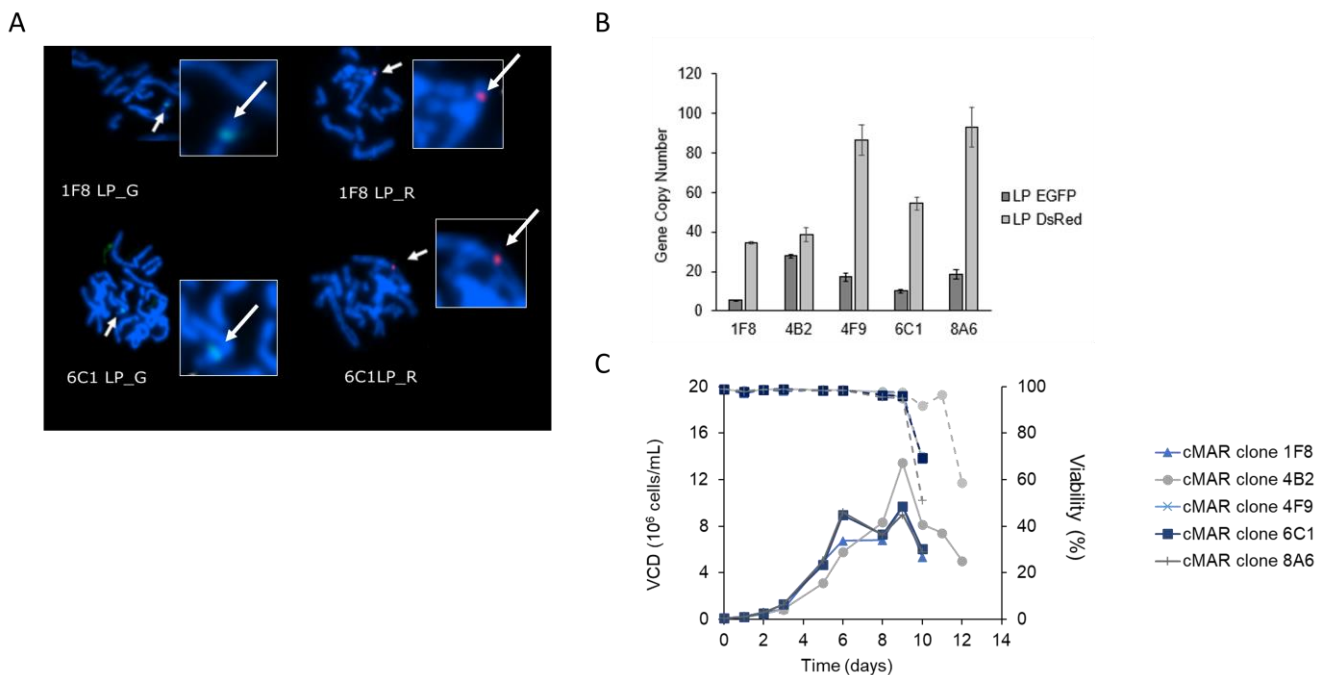


Figure 12 Characterization of selected cMAR clones. A) FISH analyses on metaphase chromosomes of clones 1F8 and 6C1. Chromosomes were hybridized with FITC-labelled probe against LP_EGFP and ATTO594-/AF594-/Texas Red-labelled probe against LP_DsRed. **B)** Gene copy number analysis of LP_EGFP and LP_DsRed for cMAR clones showing mean and standard deviation (SD) for technical replicates. GCN were calculated as described by Karlen et al. using Rotor-Gene Q Series Software.

5.1.1 Generation of human 1-68 MAR (h1-68_MAR)-rich landing pad clones

To test other MAR elements than the chicken 5' lysozyme MAR, two landing pad vectors, similar to those described in paragraph 5.1.1, were generated containing the sequence of human 1-68 MAR (GenBank EF694965.1)¹⁵⁸. This MAR element has been described as one of the most potent MAR elements within the human genome, able to increase transgene expression up to 4-fold compared to control systems as well as the occurrence of high expressing clones¹⁵⁸.

After 1-68MAR_pLP vectors generation, CHO-S cells were transfected as already described in paragraph 4.4.3. However, the cells did not survive the sequential transfection with 1-68MAR_pLP_DsRed. Therefore, different transfection conditions were tested to get a double positive transfectant pool. Only cells co-transfected with LP vectors at a ratio 1:6 (EGFP:DsRed) and 4 µg of total DNA recovered from transfection and selection. After transfection, cells were transferred in semi-solid medium and, after colony picking, only four clones were selected showing a double positive population higher than 60%. Among them, only one clone (showing 91.6% DP population) was used for a second round of clonal selection. Since cell sorting using BD FACS Aria III CS Aria was not successful (all the clones died after sorting), clones were selected in semi-solid medium as single cell-derived colonies. A total of 288 clones were isolated and the five best performing clones were expanded from 96-well plates to 12- and 6-well plates and maintained in culture for stability studies over 90 generations. Selected clones showed mainly double positive cells with a ratio of 89.8-99.6%. Clone 7 showed a homogeneous EGFP+/DsRed+ population whereas the other clones showed, since generation 20, a loss of fluorescence for EGFP as well as DsRed. This observation was confirmed for clones 8 and 10 which showed a rapid reduction of DP population (48% and 66% after 80 generations). Clone 20 showed a slight decrease in DP frequency after 60 generation, whereas the ratio for double positive cells for clones 4 and 7 was stable above 99% over 95 generations. Interestingly, despite the fact that h1-68MAR is reported to be able to increase the expression of a transgene up to 1.5 times compared to the chicken 5' lysozyme MAR²²⁵, mean fluorescence values for reporter genes were higher for cMAR_LP clones. However, this observation could be due to the different transfection strategy and selection method used to obtain the different clones.

In addition, despite previous study on h1-68MAR where it showed its ability to prevent heterochromatin silencing thus increasing clonal stability^{172,178}, in our study we did not observe an improvement in terms of stability compared to the clones harbouring the 5' chicken lysozyme MAR. Loss of fluorescence could be due to both gene silencing and loss of LP copies due to potential recombination mechanisms²²⁶. Further analysis such as LP copy number determination for 1-68MAR_LP clones and FISH analyses, should be conducted to discuss differences between selected clones. Preliminary tests using BxB1 site-specific integration system on 1-68MAR_LP_4 and 1-68MAR_LP_7 clones resulted in unsuccessful cell recovery and GOI integration. Therefore, these clones were not further characterized or used in this study.

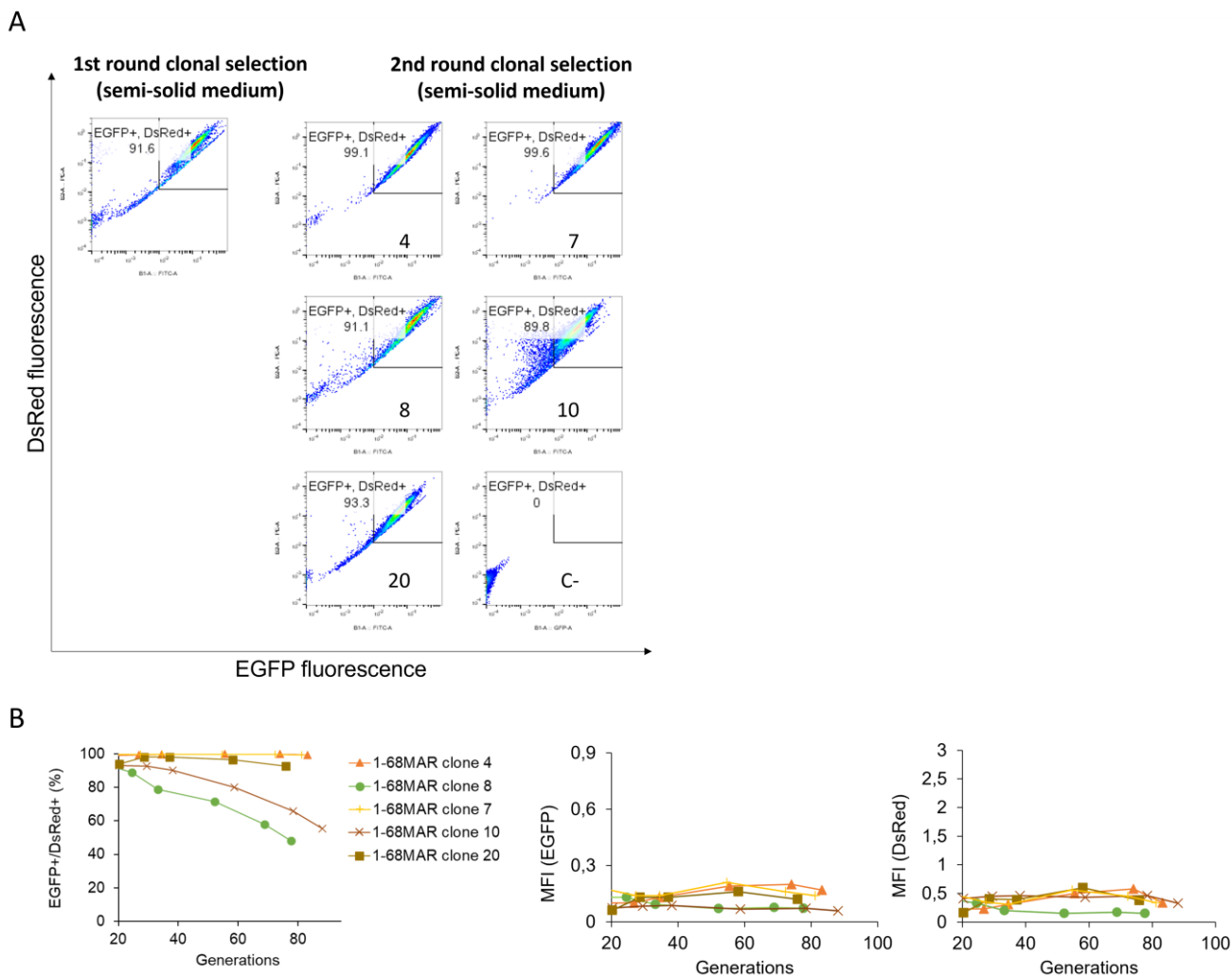


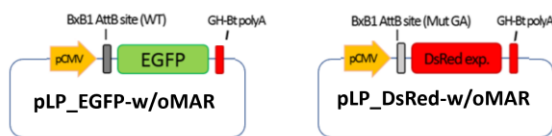
Figure 13 1-68MAR clones, FCM analyses and stability studies. A) 1-68MAR clone selected in semi-solid medium during the first round of clonal selection was used for a second round of clonal selection by fluorescence activated cell sorting (BD FACSDiv). In the panel on the right are shown the best performing clones in terms of fluorescence, stability and cell growth, selected through clonal screening and expansion steps. **(B)** Stability test representing the frequency of EGFP⁺/DsRed⁺ clones and median fluorescence intensity (MFI) of the 1-68MAR clones for EGFP and DsRed.

5.1.2 Generation of control (w/o_MAR) landing pad clones

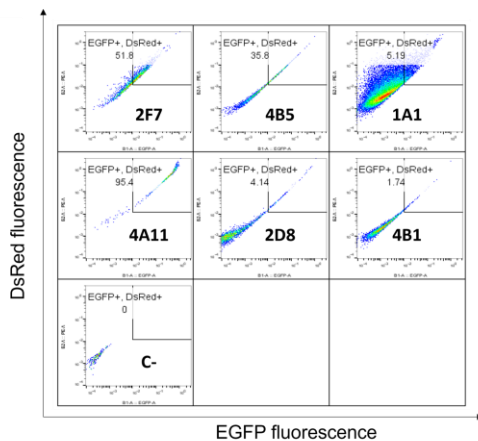
To assess the effect of incorporating a MAR sequence in the landing pad, control cells containing LPs without MAR were generated. For this purpose, pLP_w/o-MAR vectors were generated as discussed in paragraph 4.6 and CHO-S cells were transfected as previously described (paragraph 4.4.3). A first round of clonal selection was done in semi-solid medium. Approximately 200 single cell derived colonies were picked from semi-solid medium, and after the expansion and screening step, the six best performing clones were selected (Figure 14 A). The percentage of double positive cells resulted lower compared with clones harboring the MAR element, ranging from 95.4% (clone 4A11) to 1.7% (clone 4B1). However, clone 4A11 did not recover from the expansion steps.

Clones 1A1 and 2F7, were used for the second clonal selection round for which 500 clones were sorted. The previous applied gating strategy to isolate cMAR clones was utilized to sort EGFP+/DsRed+ clones (Figure 14 B, panel on the top, red square). Only clones derived from the 1A1 clonal population recovered from sorting and after screening and expansion, the five best clones in terms of fluorescence and growth properties were kept in culture and analyzed in stability studies (Figure 14 B). Clones showed a DP population of 15-80% and MFI values lower compared to clones with MAR (Figure 15 A) suggesting that MAR element could increase transgene expression and ratio of double positive clones. In addition, these stability tests revealed a significant drop in DP for all the tested clones. Clones 3B10 showed the strongest drop as early as after 40 generation (from 87% to 17% of DP frequency). At generation 90, all clones showed a 40% reduced fluorescence signal for both reporter proteins. Since all clones showed a gradual and continuous loss of reporter gene expression over 90 generations, they were considered not stable¹⁰⁵. These observations revealed the effect of the MAR element in clonal stability as already proven by Girod *et al.*, and Zhao *et al.*^{176,183}.

A



B



C

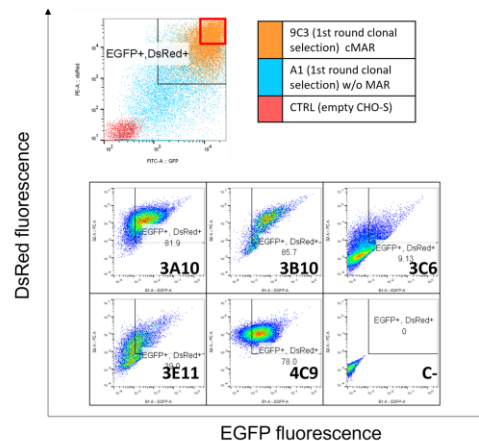


Figure 14 FCM analyses of w/o_MAR clones and stability tests. A) Vector construct of pLP_EGFP-w/oMAR and pLP_DsRed-w/oMAR. **B)** Flow cytometry analysis of w/o MAR clones selected by FACS during the second round of clonal selection. **C)** Stability tests representing the percentage of EGFP+/DsRed+ clones and median fluorescence intensity (MFI) of the 1-68MAR clones for EGFP and DsRed.

Due to their poor stability, selected o_MAR clones were not used for subsequent Site Specific Integration (SSI) experiment with BxB1. However, clones 3A10, 3B10 and 4C9 were further characterized to evaluate if the lower observed MFI level compared with the clones harboring the MAR was due to differences in LP copy numbers. GCN analyses were conducted at generation 40 only for clones 3A10, 3B10 and 4F9. These clones contain higher

LP_DsRed copies then LP_EGFP copies showing a ratio LP_DsRed/LP_EGFP ranging between 2:1 (clone 4F9) and 1:1 (clone 3B10) as reported in Table S1 (annex). However, the copy number for both landing pads was lower than previously reported for the cMAR-containing cells (ranging between 5-6 copies and 6-10 copies for LP_EGFP and LP_DsRed, respectively).

These differences in LP copy numbers could be the cause of the lower observed MFI for both reporter genes and could be explained by the ability of the chicken 5' lysozyme MAR to mediate plasmid integration into the genome as previously demonstrate by Girod et al. and Kostyrko et al.^{173,176}

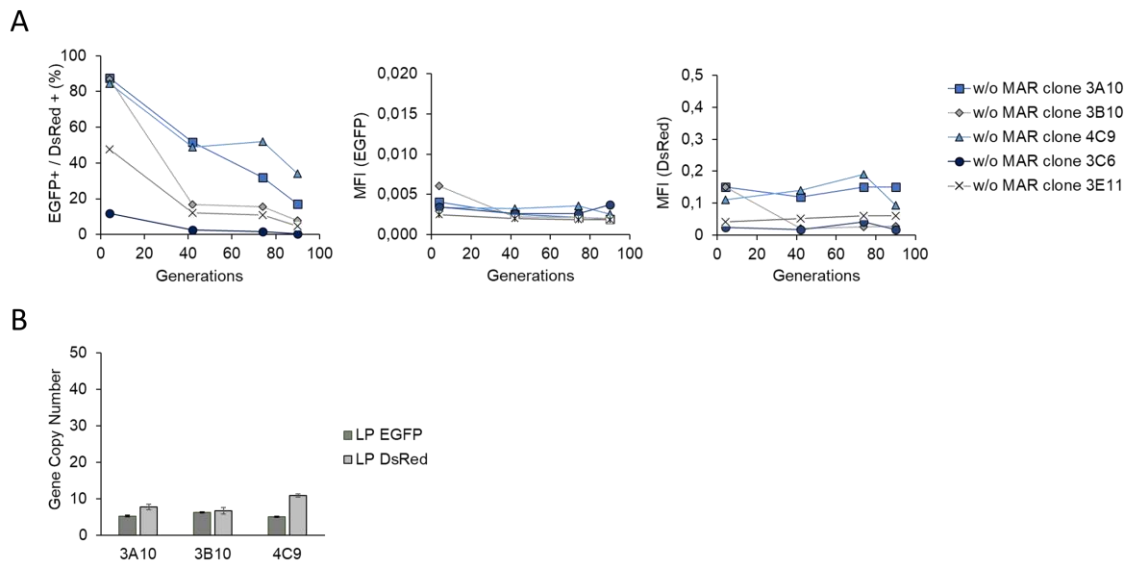


Figure 15 analyses of w/o MAR clones. (A) Stability test representing? the frequency of EGFP+/DsRed+ clones and median fluorescence intensity (MFI) of the w/o MAR clones for EGFP and DsRed. **(B)** Gene copy number analysis of LP_EGFP and LP_DsRed for w/o MAR clones showing mean and standard deviation (SD) for technical replicates. GCN were calculated as described by Karlen et al. using Rotor-Gene Q Series Software.

5.2 Generation, selection, and characterization of LP-derived anti-CCR9-expressing clones

To test the developed cMAR_LP cell lines for site-specific integration system using BxB1 recombinase we constructed two donor vectors for the expression of a monospecific antibody msAb-Fer, an anti-CCR9 human IgG1 (Ferring SA). Heavy and light chain sequences were codon optimized for CHO cells and were cloned into pD607_MCS and pD609_MCS respectively, as described in paragraph 4.3.4. The heavy chain (HC) gene was inserted into a modified pD607 vector containing the BxB1 AttP-WT recombination site followed by the promotor-less hygromycin selection marker (donor_heavy). The light chain (LC) gene was inserted into a modified pD609 vector containing the mutated BxB1 AttP-GA recombination site followed by the promotorless puromycin selection marker (donor_light) (Figure 16). The design of the donor vectors in combination with the design of the landing pads allowed the monitoring of GOIs genomic integration by recombinase-mediated integration. The entire vector containing the heavy chain cassette should be integrated into LP_EGFP site and

the entire vector containing the light chain cassette should be integrated into LP_DsRed site. This because the donor vector with the heavy chain contains the AttP WT which could recombine only with AttB WT in the LP_EGFP. On the other hand, the donor vector with the light chain contains the AttP GA could recombine only with AttB GA in LP_DsRed (Figure 16). Since multiple copies of LP_EGFP and LP_DsRed were integrated into the genome, several copies of the donor_heavy and donor_light can be integrated.

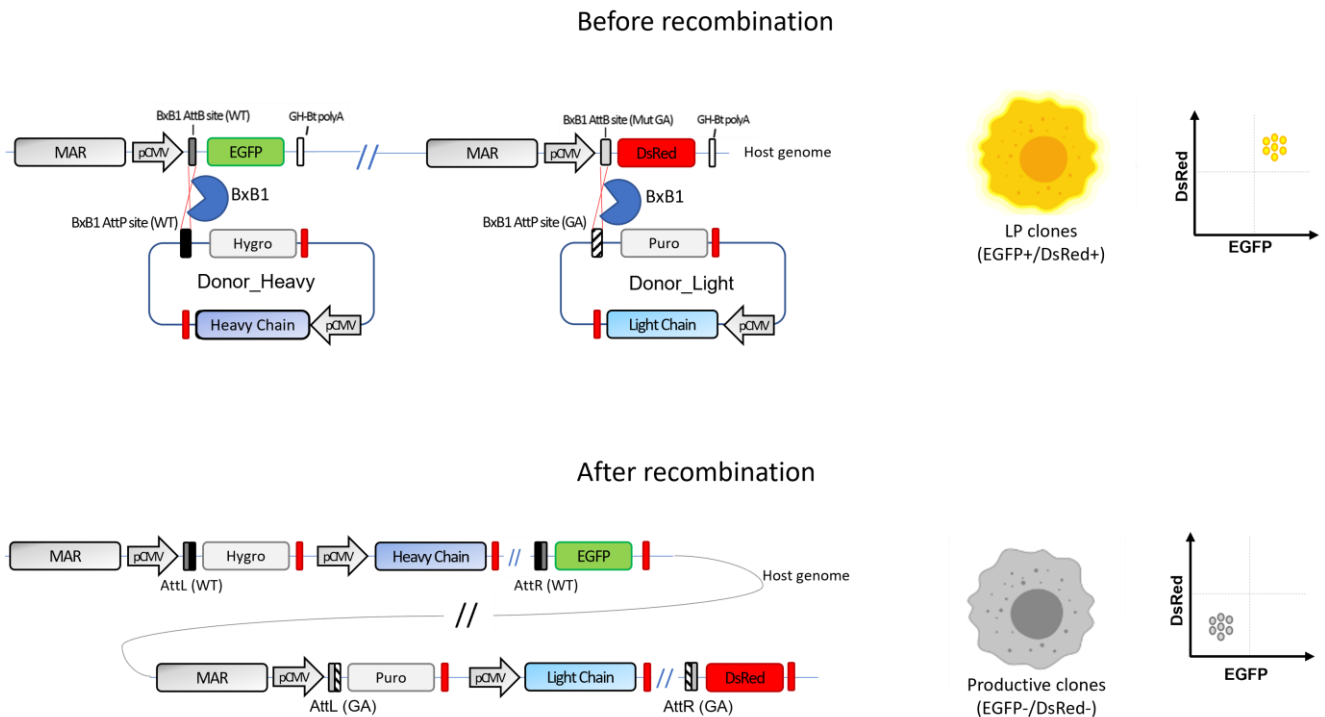


Figure 16 Schematic representation of the integration of the donor vectors containing HC and LC genes into LP_EGFP and LP_DsRed, respectively. After integration, the entire donor vector will be integrated into the landing pad. The selection genes will be then close to pCMV promoter and will be expressed. In addition, the fluorescence marker will be too far from the promoter to be expressed after recombination. After integration of GOIs, cells can be selected by double antibiotic selection and/or sorting EGFP-/DsRed-cells.

After recombination, the entire donor vectors will be integrated into the LPs and the reporter genes will be moved away from the recombination sites. Then, the loss of EGFP fluorescence will be caused by donor-heavy integration while the loss of DsRed fluorescence will be caused by donor-light integration. In addition, the donor vectors contain promoter-less selection markers (puromycin and hygromycin) which are placed immediately after the recombination site. Thus, after recombination, those selection markers will be placed close to the pCMV promoter in the LP, and they will be expressed. Consequently, cells which stably integrate both donor vectors can be selected by double-antibiotic selection and/or by sorting EGFP-/DsRed- cells. Similar approaches were described by Gaidukov et al. and Baser et al.^{204,205}. However, in the first case, heavy and light chain were located in the same donor vector making potentially necessary gene dosage adjustment between light and heavy chain difficult. Whereas, Baser et al. described a binary RMCE system for the co-expression of two different

target protein though not for antibody expression. LPs_cMAR clones 1F8, 4B2, 4F9, 6C1 and 8A6 were co-transfected with the two donor vectors and the helper vector for BxB1 expression pCAG-NLS-HA-BxB1. Donor vectors were mixed in a 1:1 molar ratio and combined with helper vector in a ratio of 3:1 payloads/recombinase vector for BxB1²¹⁵. Cells were transfected with 2 µg of vector mixture as described in paragraph 4.4.3. Stable pools were obtained after two weeks of double antibiotic selection (20 µg/mL of puromycin and 600 µg/mL of hygromycin). Figure 17 showed the loss of fluorescence of the pool generated from LPs_cMAR clone 8A6. After 4 days post transfection a shift from EGFP+/DsRed+ to EGFP-/DsRed- is already visible (Figure 17 A). These double negative cells could be sorted to select stable HC/LC integrants as soon as four days from transfection without the need of any antibiotic selection. After 13 days from transfection, the obtained pool exhibited a significant reduction of fluorescence for both reporter genes reaching 78% of EGFP-/DsRed- population (Figure 17 B).

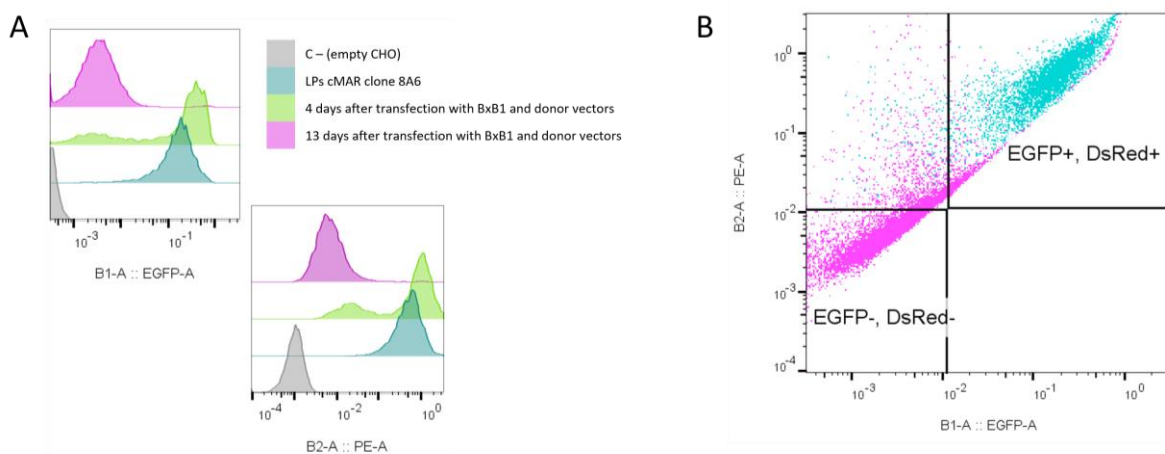


Figure 17 Fluorescence analysis of productive pool generated using bxb1 system (from clone 8A6). (A) Fluorescence analysis (histogram) of empty CHO cells (grey), untransfected 8A6 cMAR clone (dark green), 8A6 clone transfected with helper and donor vectors at 4 days post transfection (light green), 8A6 clone transfected with helper and donor vectors 13 days post transfection (purple). (B) Fluorescence analysis of untransfected 8A6 clone (dark green) and selected productive pool (purple).

Clonal selection was done by transferring the obtained stable pools in semi-solid medium and by picking double-negative single cell-derived colonies. A total of 94 single-cell derived colonies were picked from each stable pool and transferred in 96-well plates. When cells reached 70-90% confluency in 96-well plates, dot blot analysis was done to select positive clones (Figure S1) and 74-83% of the picked clones resulted positive to the analysis screening. These data from clonal screening revealed the high potentiality of our developed method, since it can be used in combination with high throughput systems, such as FACS or ClonePix, to efficiently screen a multitude of clones. On the other hand, it can be used with low-cost, non-high throughput methods, such as limiting dilution or manual picking from semi-solid medium, for the direct visualization of clones which stably integrates the GOIs. After screening, six clones were selected and maintained in culture for further analysis. Selected clones derived from 1F8 (productive clones 1C10 and 1E5), 8A6 (productive clones 2B9, 2B12 and 3E2), 6C1 (productive clone 5E2).

Other productive clones derived from other hosts were low producers (e.g., those derived from LPs_cMAR clone 4F9) or did not survive cell picking and/or expansion steps (e.g., those derived from LPs_cMAR clone 4B2). To test cell growth and final product titer, selected clones were tested in shake flasks cultivated in fed batch mode with a working volume of 30mL CD CHO supplemented with 8mM of L-glutamine. Cells were fed daily with 1% Hyclone Feed A and 0.5% Hyclone Feed B starting from day 3 and glucose was added to the culture when the glucose concentration dropped below 3 g/L to reach 5 g/L. Clones showed similar growth curves, reaching a maximum VCD between 14-19 x 10⁶ cells/mL and a culture duration of 10-12 days (Figure 18 A). Supernatant was analysed at Octet K2 to evaluate antibody titer. Clones 1C10, 1E5 and 5E2 showed low titer (2.7 µg/mL, 0.9 µg/mL and 1.04 µg/mL at day 10 respectively) and a slight increase of product titer between day 5 and day 11. Clones 2B9, 2B12 and 3E2 showed higher titers (6.3 µg/mL, 7.5 µg/mL and 2.9 µg/mL at day 10 respectively) and an increase of product titer between day 5 to day 12 (Figure 18 B). These results were confirmed by SDS PAGE and western blot analysis of supernatant samples from day 7 (Figure 18 C and D). No antibody was detected by SDS PAGE stained with comassie blue. However, western blot analyses of fed batch supernatants under reduced conditions showed two clear bands corresponding to the heavy chain (50 kDa) and the light chain (25 kDa) for

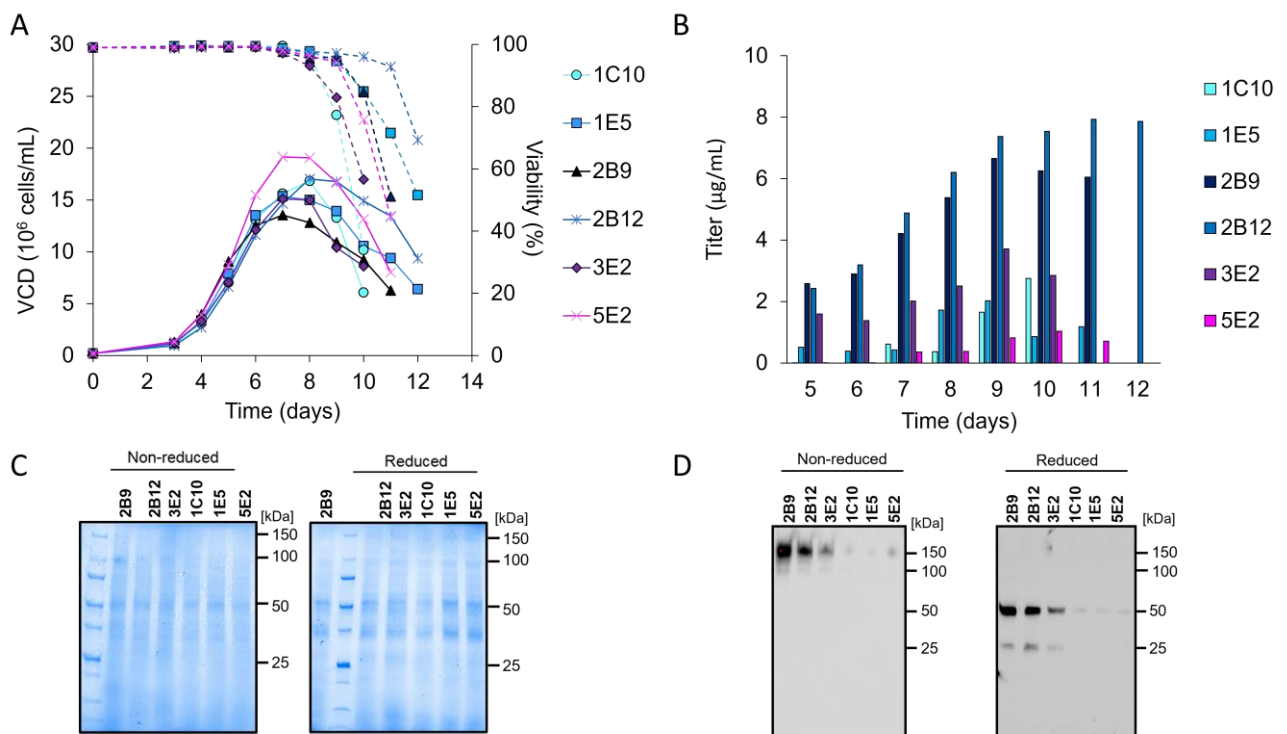


Figure 18 FB culture of msAb expressing clones. (A) Results of fed-batch cultures of msAb expressing clones in CD-CHO. Cells were fed with 1% Hyclone Feed 7a and 0.5% Hyclone Feed 7b, daily from day 3. Solid lines represent the viable cell density (VCD) (right y-axis); dotted lines represent the cell viability (right y-axis). **(B)** Quantification of antibody titer during fed batch culture. Bar charts represent antibody titer measurements performed with Protein A biosensors via BLI. **(C)** SDS-PAGE analyses (Coomassie blue staining) of fed batch supernatants for six cell lines under non-reduced (left) and reduced conditions(right). 10 µL of supernatant, collected on harvest day, were loaded in each lane. **(D)** Western Blot with anti-Human IgG (H+L) analyses of fed batch supernatants for six cell lines under non-reduced (left) and reduced conditions (right). 10 µL of supernatant, collected on harvest day, were loaded in each lane.

the samples derived of clones 2B9, 2B12 and 3E2. For the other samples, a weak band at 50 kDa is visible under reduced condition, whereas no signal at 25 kDa was detectable. Under non-reducing conditions, all the samples showed the 150 kDa band corresponding to the full-length antibody molecule. In addition, for sample 2B9, 2B12 and 3E2, a faint band at 100 kDa is also visible under non-reducing conditions, probably representing heavy chain dimers. To evaluate if the low antibody titer was caused by low landing pads availability, off-target integration of GOIs or potential transcriptional bottlenecks, clones were further characterized. Analyses of residual fluorescence by cytofluorimetry (Figure 19) revealed that most of the selected productive clones showed an EGFP-/DsRed- population of 94-99% with the exception of clone 2B9 and 3E2 (67.8% and 93.6% respectively).

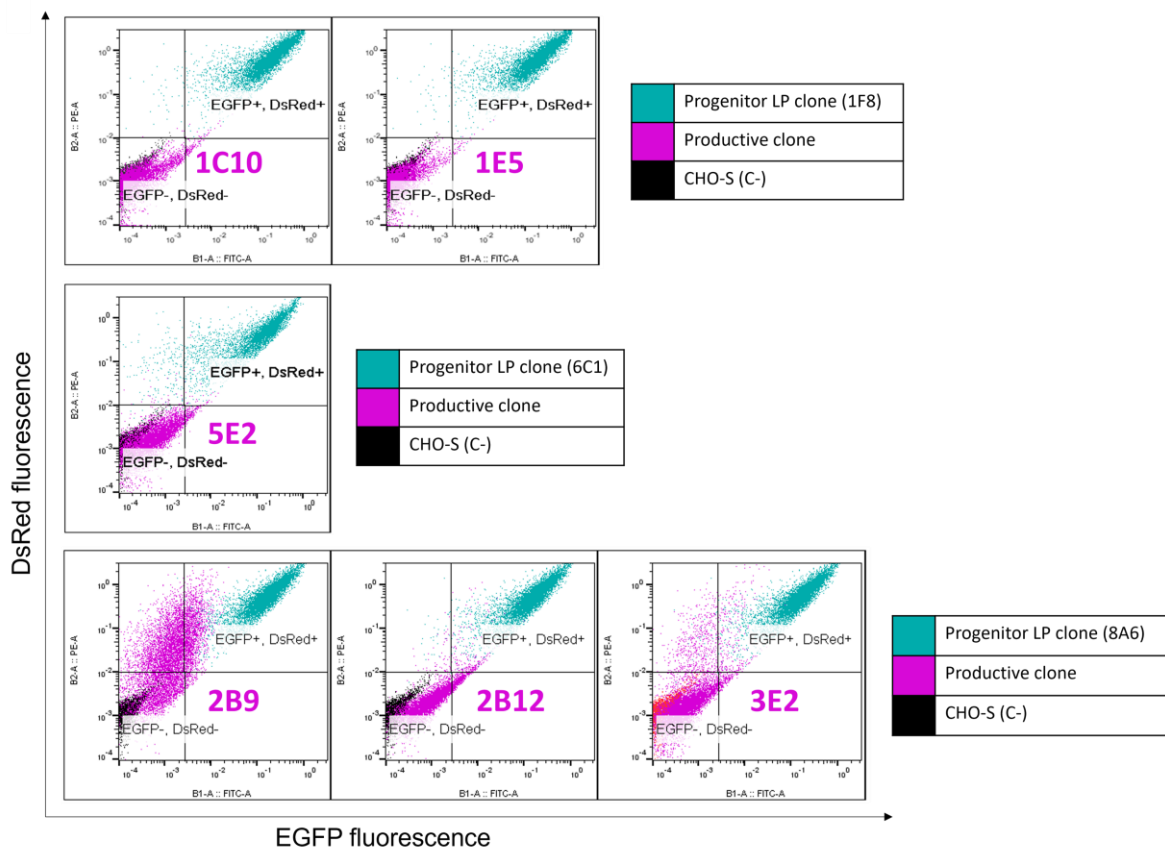


Figure 19 Evaluation of residual fluorescence in productive clones derived from cMAR-rich landing pad clones. Clones were analysed using a 488 nm laser and 525/50 nm (B1) filter for EGFP detection and 579/34 nm (B2) filter for DsRed detection. Productive clones (purple) were compared to progenitor cell line, the cMAR-rich landing pad progenitor clone (dark green), untransfected CHO-S cells were used as negative control (black).

Both clones exhibited a residual DsRed fluorescence resulting in EGFP-/DsRed+ population of 25% for clone 2B9 and 3.4% for clone 3E2. However, since clone 2B9 was one of the most productive among the selected clones, we conclude that the expression of residual DsRed did not impact the expression of the protein of interest. Gene copy number analyses, as well as genomic PCR analyses were conducted to assess whether the residual DsRed fluorescence was due to an incomplete occupancy of LP_DsRed landing pad from donor_light vector. LC copy number ranged from 1.7 for clone 1E5 to 8.9 copies for clone 2B12, resulting always below the number of

available LP_DsRed sites (Table S2). Clones 2B9 showed the lowest number of occupied LP_DsRed sites (2%), according to the FCM results, whereas clone 1C10 showed the highest one (13.1%). These findings are also supported by the genomic PCR results (Figure S2) which showed a clear band at 0.5 kb corresponding to the unoccupied LP_DsRed and an additional band at 1.5 kb corresponding to the integrated donor_light vector. Clone 1C10 showed the strongest signal at 1.5 kb and a weak band at 0.5kb whereas the opposite was observed for all other clones. Again, these findings were supported by the genomic PCR results which showed a strong band at 2 kb corresponding to the integrated donor_heavy and no signal for unoccupied LP_EGFP. However, qPCR results revealed the presence of unoccupied LP_EGFP sites ranging from 1.6% (for clone 2B12) to 65.7% (for clone 5E2) and HC copy number ranging from 1.9 (clone 1E5) to 18.2 (clone 2B12) copies (Figure 20 A). These differences between genomic PCR and qPCR could be due to potential genomic rearrangement leading to the loss of genetic elements in the LP itself (e.g., copies of the pCMV) which are needed either for the amplification in the genomic PCR or the EGFP expression. However, these hypotheses should be further investigated by analysing the organization of the landing pads into the host genome. In addition to the evaluation of LPs occupancy rate, qPCR analyses revealed clonal heterogeneity in terms of GOIs copy number and HC:LC ratio. Low-producer clones 5E2 (derived from LP clone 6C1), clone 1C10 and 1E5 (both derived from clone 1F8) showed a ratio HC:LC of 0.5, 0.8 and 1.1, respectively. Clones 2B9, 2B12 and 3E2, which derived from LP clone 8A6, showed a HC:LC ratio of 4.1, 2 and 1.5, respectively. Clones showing higher HC:LC ratio exhibit also higher msAb final titer in fed batch cultures, revealing a potential correlation between antibody titer and integrated HC cassettes. To assess whether the differences in GOI copy number were reflected on mRNA level and antibody production, qRT-PCR analyses were done to analyze HC and LC mRNA expression levels. mRNA of each clone was extracted from cell pellets on day 7 of fed batch cultures and qRT-PCR results were relativized to the expression levels of clone 1C10 and normalized to the housekeeping gene eEF1A1. All clones displayed a direct correlation between HC copy number and its mRNA level (Figure 20 A). However, the same correlation was not found for LC copy number and its transcript level. This observation suggested that msAb-Fer used in this study was a hard-to-express antibody²²⁷. For clones 2B9, 2B12 and 3E2, which reached the highest final titer in fed-batch culture and derived from the same MHC progenitor (clone 8A6), the final antibody titer correlated to the HC mRNA. Clones 1E5 and 5E2 showed lower HC/LC mRNA level resulting in lower antibody titers. Interestingly, mRNA levels of HC and LC for clone 3E2 were lower compared to clone 1C10. However, quantification revealed a 4-fold increased antibody titer for 3E2 suggesting potential clone-to-clone variation as well as additional post-

translational bottlenecks for Fer-9 human monoclonal antibody which can not be identified with the utilized analysis techniques.

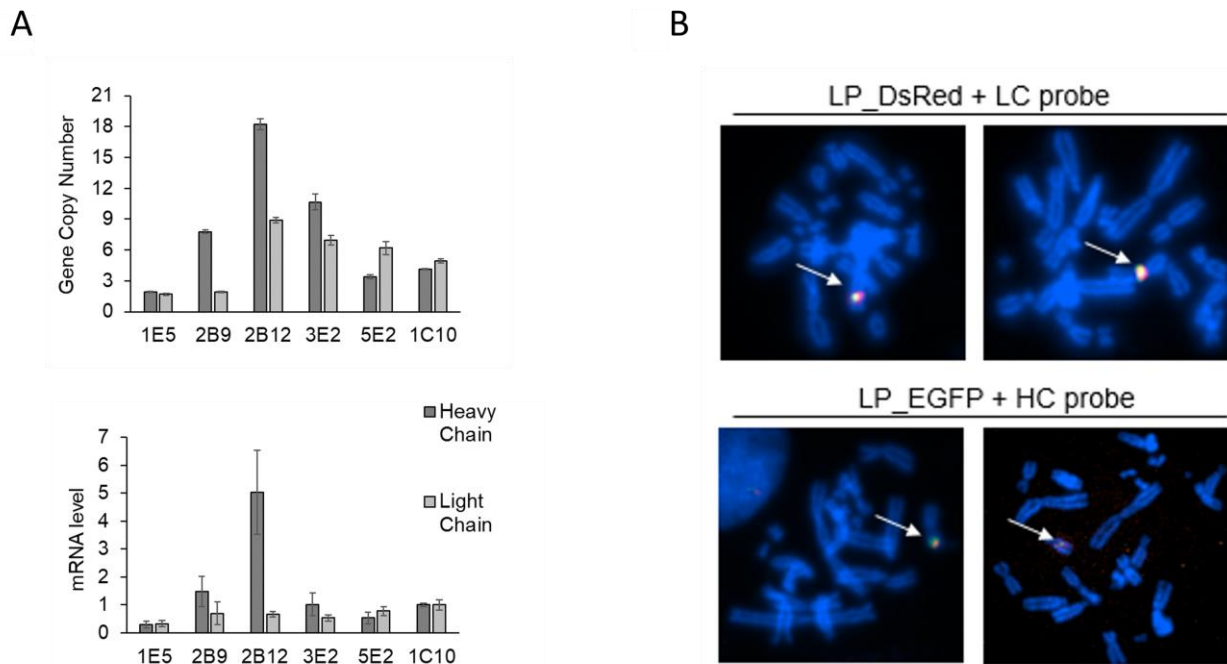


Figure 20 Evaluation of GCN, mRNA level and FISH analysis on selected clones. (A) GCN analysis (upper chart) and mRNA level (lower chart) for msAb expressing clones, showing the mean and the SD for technical replicates. Dark grey bars represent heavy chain copy number/mRNA level, light grey bars represent light chain copy number/mRNA level. Values are relative to the expression level of clone 1C10 and normalized to the housekeeping gene eEF1A1. **(B)** FISH analyses using probes against LP_DsRed and the light chain gene (upper panel) or LP_EGFP and the heavy chain gene (lower panel), respectively. Probes against LP_DsRed and the heavy chain gene were labelled with ATTO594-/AF594-/Texas Red-dUTP; Probes against LP_EGFP and the light chain gene were labelled with FITC-dUTP.

To evaluate if heavy and light chain genes integrated into LP_EGFP and LP_DsRed respectively, a FISH analysis was conducted by using two couples of labelled probes. Probes against LP_EGFP and LP_DsRed were labelled with Fluorescein-12-dUTP and AF594-/ATTO594-dUTP fluorescent nucleotides, respectively. Probes against HC and LC were labelled with AF594-/ATTO594-dUTP and Fluorescein-12-dUTP fluorescent nucleotides, respectively. Mixture of LP_EGFP/HC and LP_DsRed/LC probes were incubated with metaphase chromosomes for hybridization. Results showed colocalization of probes without visible off-target integration. Despite that, additional test should be done in the future to confirm these results since FISH analysis alone cannot totally exclude random integration events. Due to CHO genomic plasticity and potential genomic rearrangements, stable integration of GOIs into the LPs and their expression needed be tested in stability studies to exclude a drop in productivity over time. Stable productive cell line should retain at least 70% of volumetric productivity titer over 70 generations because the scale up from a master cell bank cryo vial to a production bioreactor run takes typically 60 generations¹⁰⁵. To test antibody production and stability, clones were routinely propagated over 85 generations and used to seed 20 mL cultures at 2×10^5 cells/mL cultured in fed-batch mode every 20-30

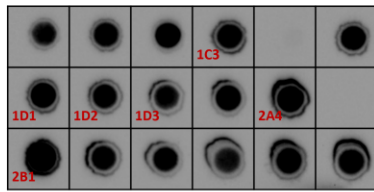
generations. None of the clones showed a drop in antibody titer or decreased growth rate (Figure S3), proving that BxB1 site-specific integration (SSI) system resulted in stable integration of GOIs over time and in stable expression from both LP sites of HC and LC.

5.3 Generation and selection of CHO-K1 SV GS⁻(Lonza)anti-CCR9-expressing clones

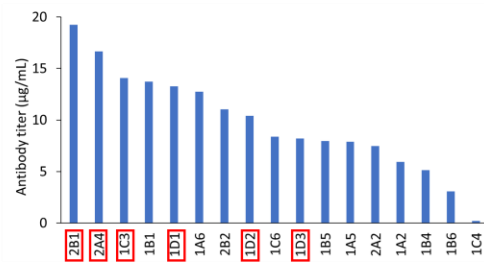
To evaluate if the msAb-Fer could be expressed in a commercial relevant cell line and to exclude that the low titer observed using the LP-derived anti-CCR9-expressing clones was due to the landing pad design, we expressed msAb-Fer using the GS Xceed[®] gene expression system and the CHO K1 SV GS KO⁻ cell line (Lonza). A *Double Gene Vector* (DGV) for the expression of msAb-Fer was generated by subcloning light chain and heavy chain into the pXC-17.4 and pXC-18.4 vectors, respectively. Then, DGV was constructed from the generated *Single Gene Vectors* (SGVs) as described in paragraph 4.3.5. The DGV final vector contains the GS gene cassette followed by the light chain cassette and the heavy chain cassette (paragraph 3.3).

CHO K1SV GS KO⁻ cells were transfected and selected as described in paragraph 4.9. After 26 days under MSX selection, the stable pool was transferred in semi-solid medium for clonal selection. After 10-14 days, a total of 42 single cell derived colonies were picked from semi-solid medium and transferred into 96-well plates. Once cells reached 70-90% of confluency, clones were screened by dot-blot using Anti-IgG (H+L) antibody (Figure 21 A). A total of 17 clones were selected based on dot blot results and expanded in 12-well plates. Among them, a total of six clones were selected based on BLI screening (Figure 21 B) and cell growth and maintained in culture for further studies. Clones showed similar growth curves (Figure 21 C) reaching a maximum VCD between 13.9 and 18.8 x 10⁶ viable cells/mL and fed batches were stopped once the viability dropped to 70% or below (on day 11 for clones 1C3 and 2B1 and on day 12 for the other clones). Compared with LP clones, Lonza clones reached a lower maximum VCD and comparable culture duration; however, antibody titer at harvest day were up to 56 times higher than LP clones (Figure 21 D). Clone 2B1 showed the highest antibody titer of 425 µg/mL on day 11, while clone 1D3 showed the lowest antibody harvest titer of 145 µg/mL. These differences in antibody titer could be due to differences in the HC/LC ratio in the LP system and indicate the need for an in-depth study on GCN and genomic integration of HC and LC sequences as well as an optimization in clone selection. The antibody titer obtained with the GS system was still far from the acclaimed titer of 6 g/L that can be obtained with this technology for antibody molecules²²⁸. This observation further strengthens the hypothesis that msAb-Fer is a hard-to-express antibody.

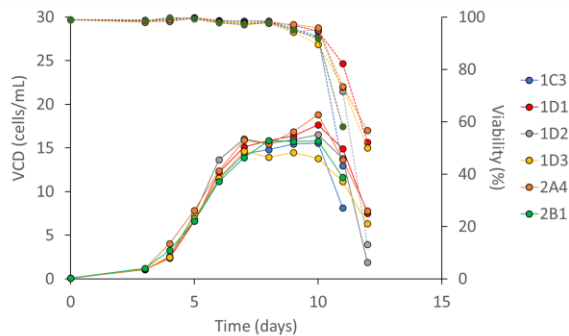
A



B



C



D

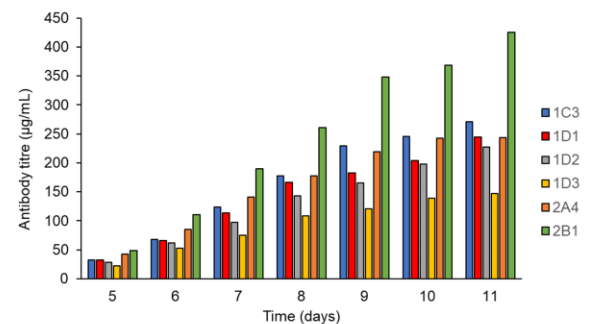


Figure 21 msAb-Fer expressing clones generated using Lonza GS system (A) Dot-Blot analysis of cell culture supernatants using anti-IgG (H+L) detection antibody; selected clones are highlighted in red. **(B)** Antibody titer measurement from clones expanded in 12-well plates. Bar charts represent antibody titer measurements performed with protein A biosensors using BLI. **(C)** Results of fed-batch cultures of msAb expressing clones in CD-CHO. Cells were fed with 1% Hyclone Feed A and 0.5% Hyclone Feed B, daily feeding from day 3. Solid lines represent the viable cell density (VCD; depicted on the left y-axis); dotted lines represent the cell viability (depicted on the right y-axis). **(D)** Quantification of antibody titer during fed batch culture. Bar charts represent antibody titer measurements performed with protein A biosensors using BLI.

5.4 Generation, selection and characterization of LP-derived bsAb-Fer-expressing clones

To test the feasibility of the developed TI approach for complex recombinant protein expression, LP-bearing host cell lines were tested for the production of a humanized chicken-derived bispecific antibody (bsAb-Fer). BsAb-Fer is composed of two identical common LCs and two different HCs, which have been engineered for knob-into-hole pairing to promote heterodimerization⁷⁶. In addition, knob and hole HCs (referred to as kHC and hHC) have been modified to contain a Twin-Strep-tag and His-tag, respectively, to facilitate purification and homo-/heterodimer identification. Three different donor vectors were generated using the three genes coding for the bsAb and the DNA sequences were codon optimized for CHO codon usage using GenSmart™ (Genscript) software. HC cassettes (hHC and kHC) were subcloned into the donor vector containing a hygromycin gene and a AttP-WT recombination site (paragraph 3.3 and 4.3.4). Therefore, both donor-kHC and donor-hHC targeted LP_EGFP and their integration could be monitored by the loss of EGFP fluorescence (Figure 22 A). The common

LC was subcloned into a donor vector containing puromycin and AttP-GA site and its integration into LP_DsRed could be monitored by loss of red fluorescence.

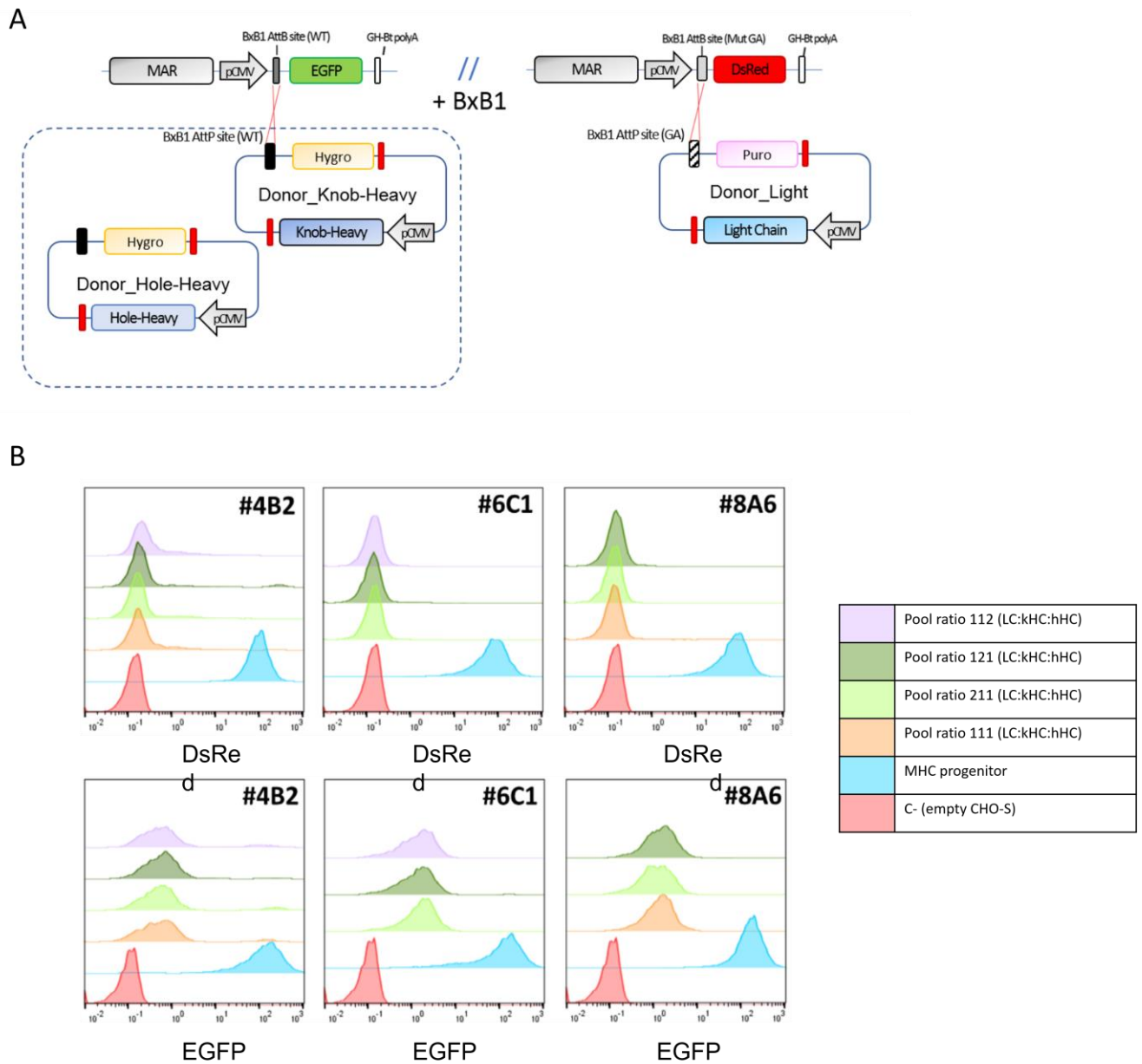


Figure 22 Generation of bsAb stable cell line using LP system and FCM analyses of stable pools. (A) Schematic overview of the integration of donor vectors containing kHC/hHC and cLC genes into LP_EGFP and LP_DsRed, respectively. Integration of Donor_Knob-Heavy and Donor_Hole-Heavy into LP_EGFP will induce EGFP fluorescence loss and the expression of hygromycin resistance. Integration of Donor_Light into LP_DsRed will induce DsRed fluorescence loss and the expression of puromycin resistance. **(B)** Fluorescence analyses of selected stable pools obtained after 20 days from transfection, using different ratio kHC-hHC-cLC. DsRed fluorescence is shown in the upper panels. EGFP fluorescence is shown in the lower panels. Selected pools were compared to the landing pad progenitor (MHC progenitor) and to the negative control (empty CHO-S).

Different ratios of donor vectors (kHC:hHC:LC) were tested for transfection into LP-bearing host cell lines 4B2, 6C1 and 8A6: 1:1:1, 1:1:2, 2:1:1, 1:2:1. Stable pools were selected using double antibiotic selection as described in paragraph 4.10. However, pool 6C1 1:1:1 and pool 8A6 1:1:2 did not recover from transfection and selection

with puromycin and hygromycin. Stable pools were transferred in semi-solid into 96-well plates. A total of 40 clones were picked for each pool (for a total of 400 clones) and once they reached 70-90% of confluency, they were screened by dot-blot using a Anti-IgG (H+L) detection antibody. Based on the dot-blot screening, we selected 13 clones from the 4B2 pool, 24 clones from the 6C1 pool and 107 clones from the 8A6 pool. These clones were expanded in 24-well plates and screened again by dot-blot using anti-strep and anti-his detection antibodies to detect both knob and hole heavy chains (Figure S4 A). 13 clones from 8A6, 3 clones from 6C1, and 6 clones from 4B2 pools showed a strong signal with both anti-IgG (H+L), anti-Strep and anti-His detection antibody in dot blot analyses (Figure S4 B). These clones were expanded and tested in fed batch culture. Clones derived from MHC 8A6 and 6C1 (Figure 23 A and B) reached the highest VCD (1.59×10^6 cells/mL and 1.44×10^6 cells/mL for clones 8A6 211 C6 and 6C1 121 B1, respectively).

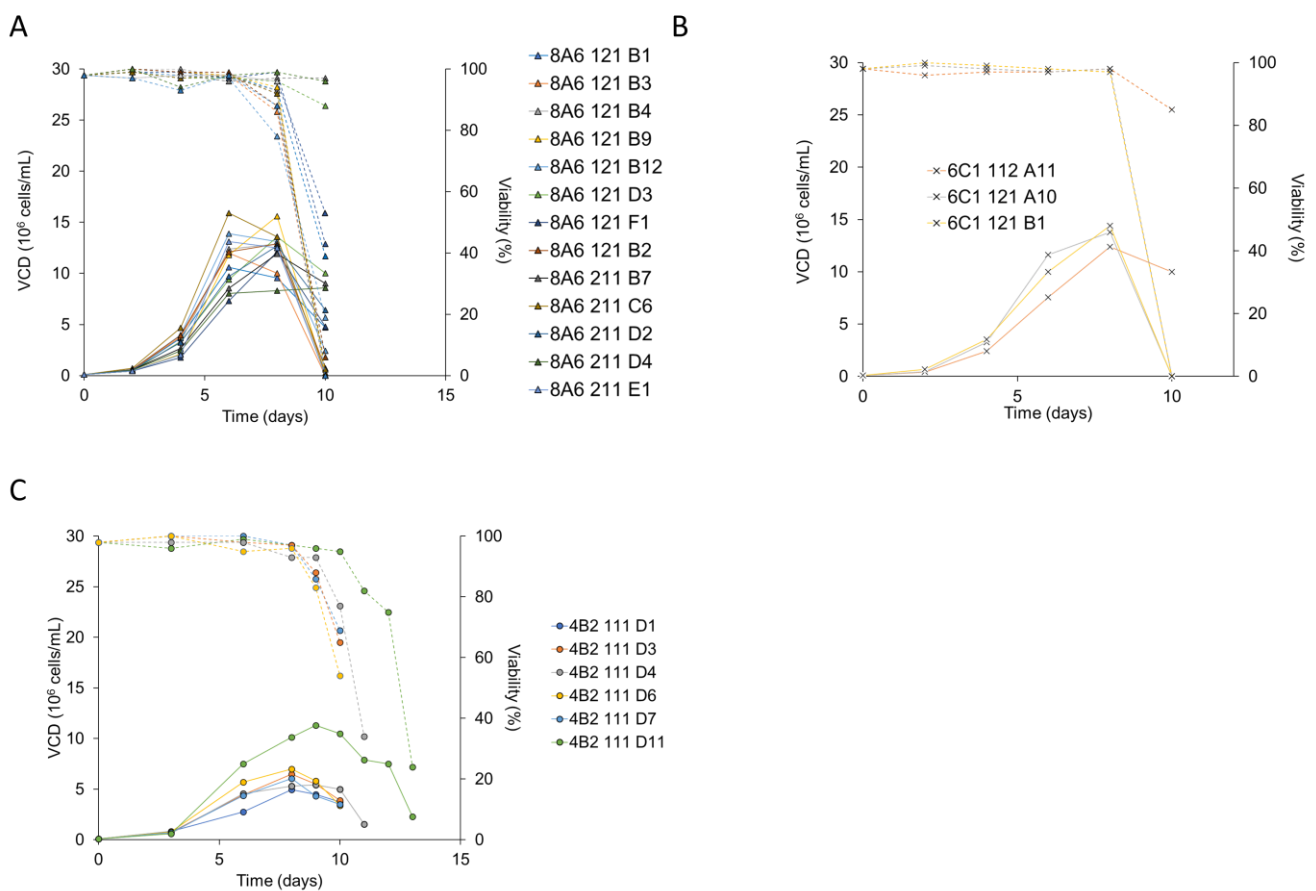


Figure 23 Fed batch cultures of bsAb-Fer expressing clones obtained using landing pad system. (A) Results of fed-batch cultures of bsAb expressing clones in CD-CHO. Selected clones derived from progenitor 8A6 cMAR-rich landing pad clone. Cells were fed with 1% Hyclone Feed A and 0.5% Hyclone Feed B, daily feeding from day 3. Solid lines represent the viable cell density (VCD; y-); dotted lines represent the cell viability (y-). **(B)** Results of fed-batch cultures of bsAb expressing clones in CD-CHO. Selected clones derived from progenitor 6C1 cMAR-rich landing pad clone. Cells were fed with 1% Hyclone Feed A and 0.5% Hyclone Feed B, daily feeding from day 3. Solid lines represent the viable cell density (VCD); dotted lines represent the cell viability. **(C)** Results of fed-batch cultures of bsAb expressing clones in CD-CHO. Selected clones derived from progenitor 4B2 cMAR-rich landing pad clone. Cells were fed with 1% Hyclone Feed A and 0.5% Hyclone Feed B, daily feeding from day 3. Solid lines represent the viable cell density (VCD); dotted lines represent the cell viability.

However, for most of these clones the viability dropped below 70% at day 10. Clones derived from MHC 4B2 (Figure 23 C) reached a VCD between $5.31\text{-}7 \times 10^6$ cells/mL and culture duration of 10 days, except clone 4B2 111 D11 which reached a higher VCD (11.31×10^6 cells/mL) and a culture duration of 12 days. The supernatant of all cultures was analysed by SDS-PAGE and western blot using both Anti IgG (H+L), anti-Strep and antiHis-Tag antibodies to evaluate the production of the bispecific antibody (Figure 24).

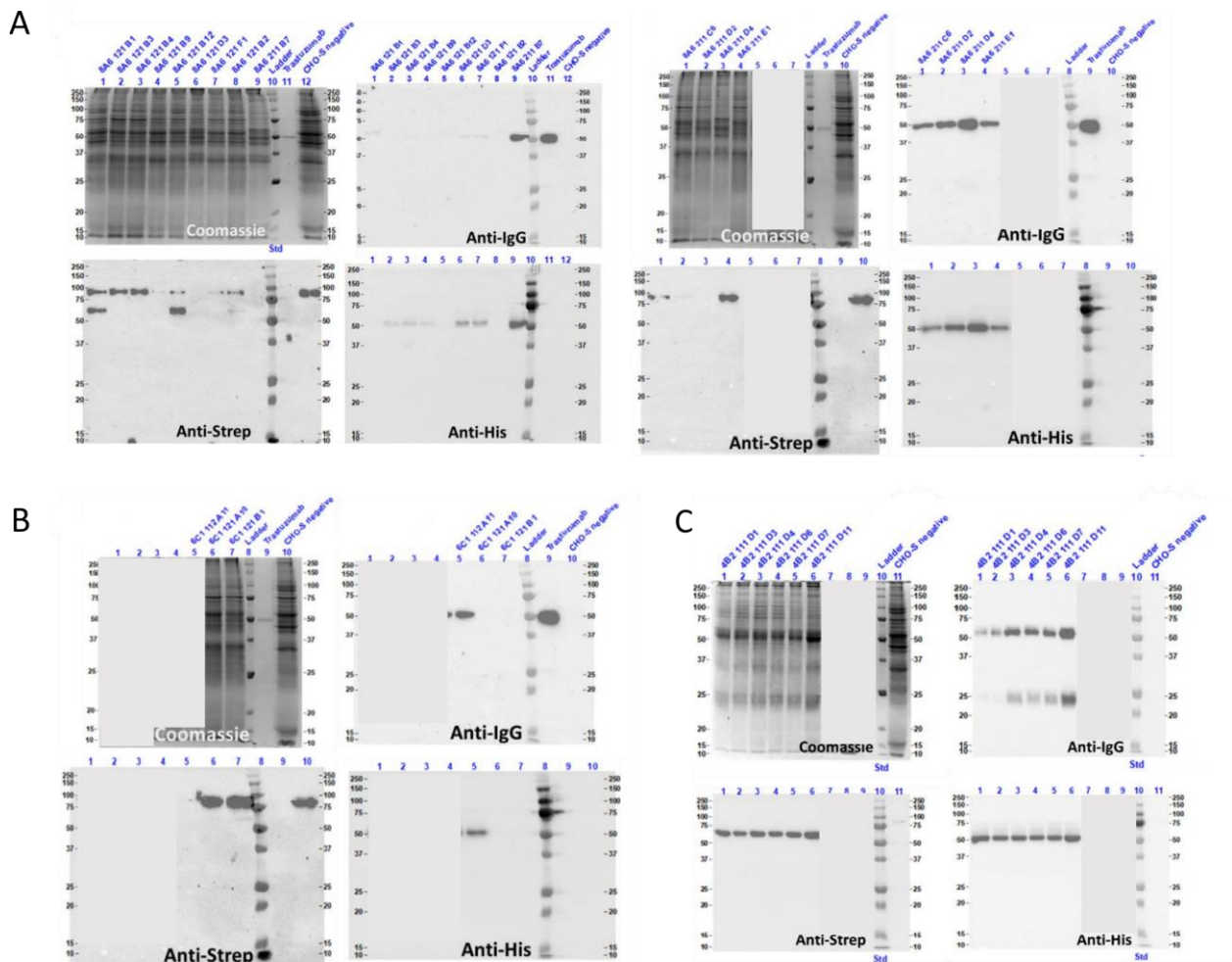


Figure 24 SDS-PAGE and western blot analyses of harvest supernatant from fed batch cultures of bsAb-Fer expressing clones. (A) Analyses of harvest supernatants from fed batches of clones derived from progenitor 8A6. Upper panel on the left: SDS PAGE (Coomassie Blue staining); upper panel on the right: western blot utilizing anti-IgG (H+L) detection antibody; lower panel on the left: western blot analysis using anti-Strep detection antibody (for the detection of knob-heavy chain); western blot analysis using anti-His detection antibody (for the detection of hole-heavy chain). **(B)** Analyses of harvest supernatants from fed batch of clones derived from progenitor 6C1. Upper panel on the left: SDS PAGE (Coomassie Blue staining); upper panel on the right: western blot using anti-IgG (H+L) detection antibody; lower panel on the left: western blot analysis using anti-Strep detection antibody (for the detection of knob-heavy chain); western blot analysis using anti-His detection antibody (for the detection of hole-heavy chain). **(C)** Analyses of harvest supernatants from fed batch of clones derived from progenitor 4B2. Upper panel on the left: SDS PAGE (Coomassie Blue staining); upper panel on the right: western blot using anti-IgG (H+L) detection antibody; lower panel on the left: western blot analysis using anti-Strep detection antibody (for the detection of knob-heavy chain); western blot analysis using anti-His detection antibody (for the detection of hole-heavy chain).

Surprisingly, clones derived from MHC 6C1 and 8A6 did not produce the entire bispecific antibody since the western blot showed bands just for one heavy chain (kHC or hHC, Figure 24 A and B). On the other hand, all the clones derived from MHC 4B2 showed bands corresponding to all three polypeptide chains of the bispecific molecule (cLC, hHC and kHC, Figure 24 C). Among them, clones D7 and D11 were maintained in culture for further studies. Analysis of gene copy number showed that the two selected clones, contained a similar copy number and ratio of kHC and hHC, which occupied >98% of LP_EGFP sites available in the progenitor genome (Table S3). However, the cLC gene copy number varied more, with clone D7 containing 3.8 times more LC gene copies than clone D11 and an occupancy rate of LP_DsRed of 67.4% (Figure 25 A, Table S3). Differences in gene copy number were reflected on mRNA level (Figure 25 B), with clone D7 showing 2.9fold increased mRNA levels in comparison with D11. In addition, these clones were tested in fed-batch cultures and further analyzed for bsAb production.

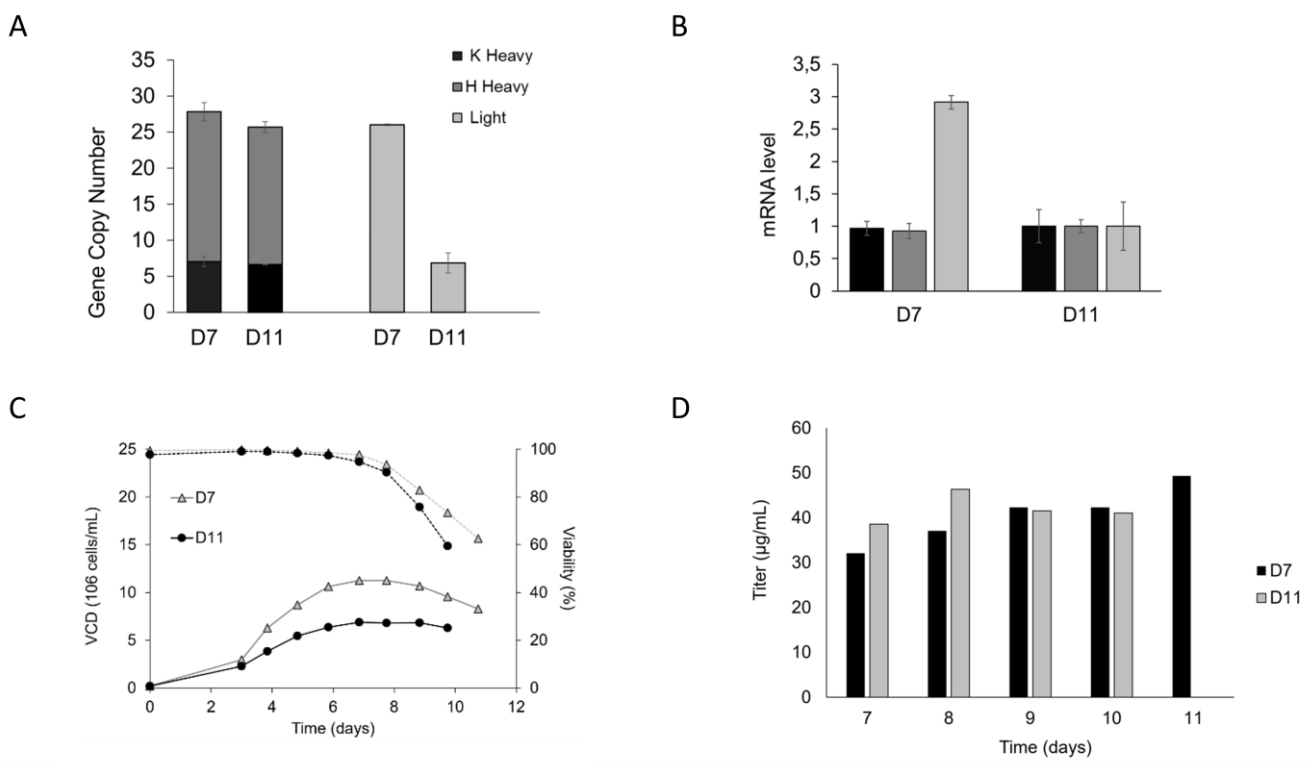


Figure 25 Characterization of selected bsAb-Fer expressing clones generated using the landing pad system. (A) Copy number analyses bsAb expressing clones showing the mean and the SD for three technical replicates. **(B)** mRNA level for bsAb expressing clones showing the mean and the SD for three technical replicates. **(C)** Results of fed-batch cultures of bsAb expressing clones in CD-CHO. Cells were fed with 1% Hyclone Feed A and 0.5% Hyclone Feed B, daily feeding starting on day 3. Solid lines represent viable cell density (VCD); dotted lines represent viability; D7 and D11 clones are indicated as triangle or solid circle points respectively. **(D)** Quantification of antibody titer during fed batch culture. Bar charts represent antibody titer measurements performed with protein A biosensors via BLI.

Both clones showed similar behavior in culture, with clone D7 reaching the higher VCD (1.6 times higher than clone D7, Figure 25 C) and a longer culture duration. Despite differences in LC expression and VCD, clones displayed similar final titers of ~40 µg/mL at day 10 (Figure 25 D). D7 and D11 supernatants were purified using a Strep-Tactin column which allows the purification of heterodimeric molecules as well as eventual knob-knob homodimer structures. The elutions of the Strep-Tactin purification were subsequently analysed by SDS-PAGE (Figure 26 A) to evaluate the presence of the two different heavy chains and the common light chain. Results

indicate the presence of two different bands at around 50 kDa which could correspond to the knob heavy chain (MW: 54 kDa) and the hole heavy chain (MW: 52 kDa) and a band at 25 kDa corresponding to the common light chain. The intensity of the two bands at 50 kDa was similar both D7 and D11 elution. D11 supernatant was further purified using a His60 column and analysed by SDS-PAGE, under denaturing and non-denaturing conditions, to compare the outcome of both purification methods (Figure 26 B). SDS-PAGE band patterns under denaturing conditions were similar for both Strep-Tactin and His60 elutions. Under non-denaturing condition, both elutions showed a band at 150 kDa corresponding to the full-length bispecific antibody comprising both LCs and a band at 100 kDa corresponding to the HC dimer. D11 His60 elution showed additional faint bands between 75 kDa and 50 kDa corresponding to other assembly intermediates (e.g. (HC)₂, (HC-LC)). Strep-tactin purified bispecific antibody produced by D11 was concentrated in PBS using Amicon 30 kDa centrifugal devices and analysed by Size Exclusion Chromatography (SEC).

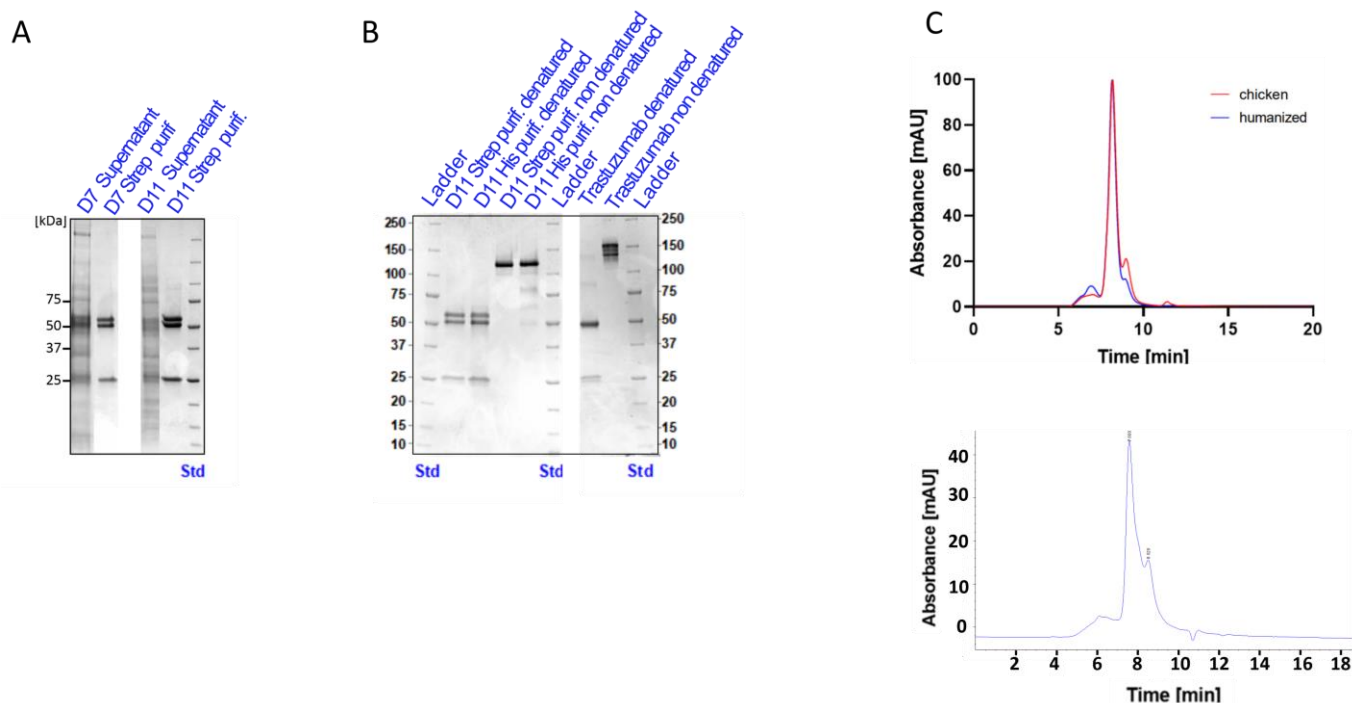


Figure 26 SDS PAGE and SEC analyses of purified bsAb-Fer . (A) SDS-PAGE (stain-free) analysis of unpurified supernatant (harvest day) and purified bsAb from clone D7 (lane 1 and 2), unpurified supernatant (harvest day) and purified bsAb from clone D11 (lane 3 and 4). **(B)** SDS-PAGE (stain-free) analysis of purified samples from clone D11. Lane 1: ladder; lane 2: strep-tactin purification of D11 supernatant (harvest day) under denatured condition; lane 3: his-tag purification of D11 supernatant (harvest day) under denatured condition; lane 4: strep-tactin purification of D11 supernatant (harvest day) under non-denatured condition; lane 5: his-tag purification of D11 supernatant (harvest day) under non-denatured condition; lane 6: Ladder; lane 7: commercial Trastuzumab under denatured condition; lane 8: commercial Trastuzumab under non-denatured condition; lane 8: ladder. **(C)** SEC analysis of bsAb-Fer produced in TU Darmstad during the antibody discovery campaign (upper panel) and the bsAb produced by clone D11 (lower panel). Red lines in the upper panel represent the chicken-derived antibody whereas the blue line represent the humanized one.

The bispecific antibody profile was compared to that one obtained for the same bispecific antibody produced in TU Darmstad (at Ferring Darmstadt Laboratory) during the antibody discovery campaign (Figure 26 C). Results showed a similar profile for both the humanized and chicken version of the antibody produced during this study

and in Darmstadt, respectively. The main peak showed a retention time of 7.6 min for both antibodies. Two shoulders were visible at a retention time of 6 min and 8.5 min. The latter could be caused by the presence of high and low molecular species additional to the monomer, however, no further analysis has been performed. These results indicate the feasibility of using a LP-bearing cell line generated in this study for simultaneous expression of more than two different genes and the development of stable recombinant cell lines able to produce intact complex molecules. Furthermore, the expression of other molecules than the msAb-Fer antibody initially used in this study demonstrates the versatility of this system.

The use of integrases on LP cell lines for stable transgene integration drastically reduced the generation time of stable cell clones from months to a few weeks or even days. This system could therefore find wide use not only in production but also during the development phases of new molecules since this system could be suitable for rapid construction of combinationatorial variants²⁰⁵.

5.5 Generation and selection of CHO-K1 SV GS⁻ (Lonza) bsAb-Fer-expressing clones

To set up a commercial baseline for bsAb-Fer production, single cell derived clones expressing the bispecific antibody were generated using the GS Exceed gene expression system. CHO K1 GS KO cells were transfected with 4 µg of bsAb-Fer_TGV vector generated as described in paragraph 4.11. A stable pool was generated using 50 µM of MSX as selection reagent as per supplier instructions. After 20 days from transfection, the cell pool recovered from selection and was transferred in semi-solid medium for clonal selection, without MSX. After 10 days, 380 colonies were picked from semi-solid medium and transferred in 96-well plates. Then, single cell derived colonies were screened by dot blot for bsAb production using an anti-IgG detection antibody. 185 colonies were positive to this first screening and a total of 16 clones showed a strong signal at dot blot analysis. Those clones were subsequently selected and transferred into 14-well plates for further studies. Among them, five clones (1B7, 1C8, 2E4, 2D6, 3H6) were positive at dot-blot screening for both heavy chains. These clones were then tested in 30 mL fed batch cultures to verify the observations. The clones showed a similar growth behavior with the exception of clone 3H6 that showed a much slower growth reaching a maximum VCD of 3×10^5 cells/mL (Figure 27 A). At day 14, the cultures were stopped and the supernatant was analyzed by SEC (Figure 27 B), SDS PAGE and western blot using anti-IgG (H+L), anti-Strep and anti-His detection antibodies (Figure 27 C). Same volume (15 µL) of cultures supernatant was loaded in each well for SDS-PAGE and WB. Results showed bands at 50 and 25 kDa for all the samples. In addition, western blot analyses revealed the presence of both heavy chains in the supernatant of all the selected clones. Clones 2D6 and 3H6 showed the strongest signal for the heavy and light chains indicating higher antibody production. These results were then confirmed by antibody quantification by SEC which showed an harvest titer of ≈ 1 mg/mL and 1.4 mg/mL for clone 2D6 and 3H6, respectively. These commercial cell lines showed titers that reached values easily 10-20 fold higher than the LP cell lines without any optimization. However, expression vector, transfection and MSX selection strategy used for the generation of TGV cell line have been extensively improved and optimized by the supplier.

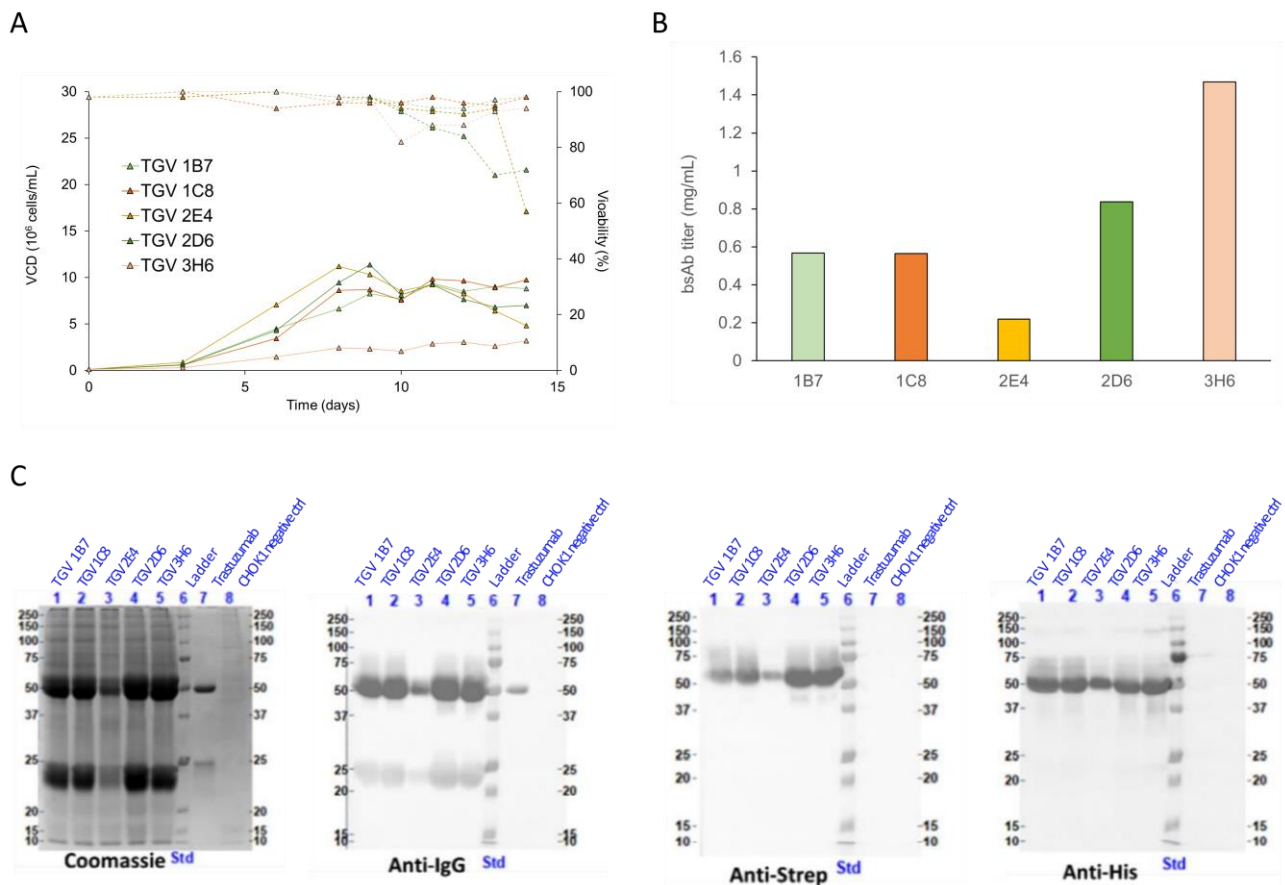


Figure 27- bsAb-Fer expressing clones generated by GS Exceed gene expression system (A) Results of fed-batch cultures of bsAb expressing clones in CD-CHO. Cells were fed with 1% Hyclone Feed A and 0.5% Hyclone Feed B, daily feeding starting on day 3. Solid lines represent viable cell density (VCD); dotted lines represent viability; Different line colours represent different clones. **(B)** Quantification of antibody titer during fed batch culture. Bar charts depict antibody titer measurements performed with protein A biosensors via BLI. **(C)** SDS-PAGE and Western Blot analyses of selected clones. From left to right: SDS-PAGE (Coomassie blue staining) of harvest supernatant; Western Blot analysis using Anti-IgG detection antibody of harvest supernatant; Western Blot analysis using Anti-Strep detection antibody of harvest supernatant; Western Blot analysis using Anti-His60 detection antibody of harvest supernatant. Different lines represent the harvest supernatant of different clones.

The SEC profile of culture supernatants showed a peak at 7.5 min corresponding to the whole bsAb molecule (Figure 28 A). The supernatant of the 2D6 culture was then purified using a Strep-tag column (strep-purified antibody) and a His-60 column (his-purified antibody) and analysed by SDS-PAGE under denaturing and non-denaturing conditions (Figure 28 B). Under denaturing condition, both strep-purified and his-purified antibody showed the two bands at 50 kDa and one band at 25 kDa, similar to what has been observed during the production of the bsAb utilizing the LP cell line. Heavy chain bands showed same intensity for both strep- and his- purified antibody. Under non-denaturing condition, his-purified bsAb antibody showed one intense band at ≈ 150 kDa corresponding to the whole IgG structure, and a fainter band at ≈ 100 kDa which could correspond to (HC)₂ species. Strep-purified antibody, under non-denaturing conditions, showed also additional bands at ≈ 75 kDa corresponding to other assembly intermediates. These results indicate the feasibility to express bsAb-Fer in

a commercial cell line and that the produced bispecific antibody showed similar characteristics at SDS-PAGE, WB and SEC analyses than the bsAb produced in LP cell line.

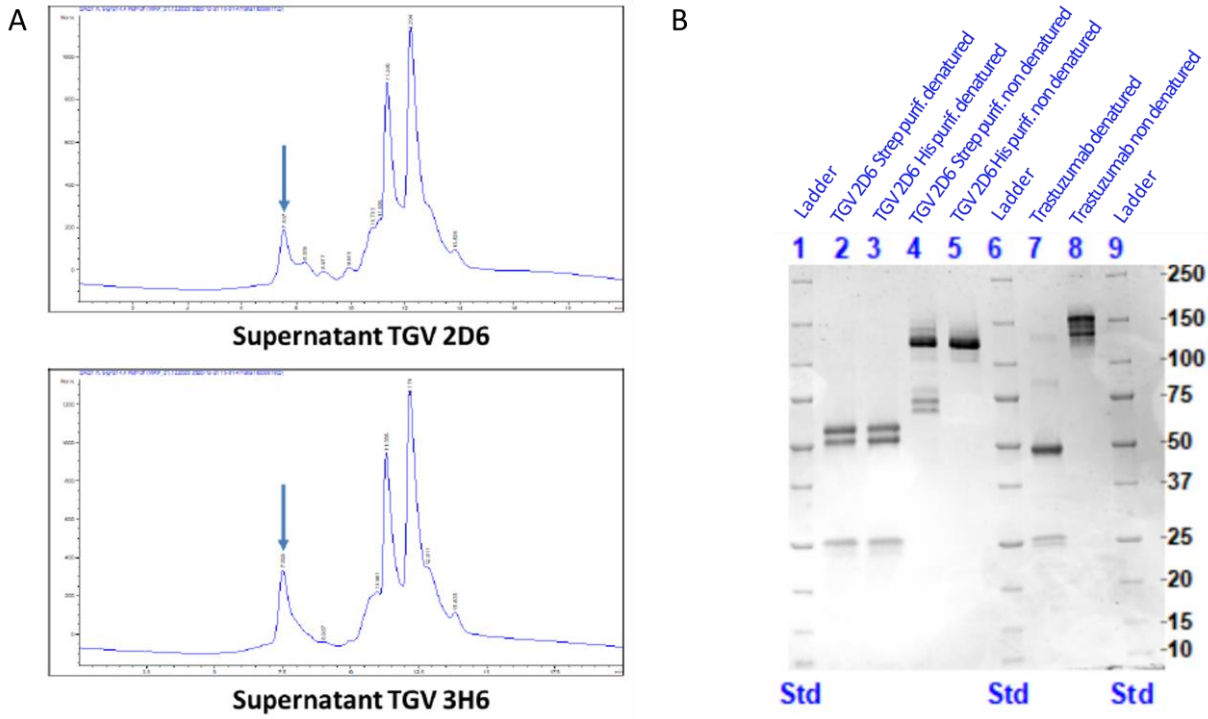


Figure 28 Analyses of produced baAb-Fer by selected clones (GS system). (A) SEC analysis of supernatant from clone TGV 2D6 and TGV 3H11. Arrows represent the peak corresponding to the bsAb. (B) SDS-PAGE (stain-free) of purified bsAb. Lane 1: ladder; lane 2: strep-tactin purification of 2D6 supernatant under denatured condition; lane 3: His60 purification of 2D6 supernatant under denatured condition; lane 4: strep-tactin purification of 2D6 supernatant under non-denatured condition; lane 5: His60 purification of 2D6 supernatant under non-denatured condition; lane 6: ladder; lane 7: commercial Trastuzumab under denatured condition; lane 8: commercial Trastuzumab under non-denatured condition.

5.6 Fed-batch cultures and media test for msAb and bsAb

Several studies reported the impact of culture media of cell growth, specific productivity, process duration and final titer^{102,229}. In order to improve the culture conditions for the developed recombinant cell lines, we tested four different commercial media (CD CHO, BalanCD, OptiCHO and ActiPro). The best-performing cell lines expressing Fer-msAb (2B9, 2B12 and 3E2) and Fer-bsAb (D7 and D11) were first adapted to the different new media. The transition from the CD CHO to the new media was realised via sequential adaptation. At each subculturing step, the cells were transferred into new medium using different dilutions of it (25%, 50%, 75%, 100% respectively). In the case of poor recovery or unstable cell doubling time after passage, the cells were kept for several passages in the diluted medium before moving on to the next medium dilution step. Then, the cells were passaged twice in 100% new medium before being considered fully adapted. After four passages in 100% new medium, cells were used to inoculate 30 mL cultures for fed-batch tests. Cells were fed with HyClone Feed 7a and HyClone Feed 7b (2% and 0.2%, respectively) daily from day 3. An additional feeding strategy was tested in CD CHO medium (condition CD CHO 1), by adding HyClone Feed 7a and HyClone Feed 7b daily from day 3 at different concentrations (1% and 0.5% respectively). The latter was the feeding strategy used during the previous fed-batch tests (Figure 18 A and Figure 25 C). For clones producing msAb-Fer, the tested conditions showed an increase in both culture duration and final harvest titer. BalanCD and OptiCHO, in combination with the aforementioned feeding strategy, supported an increase in culture duration up to four days compared CD CHO 1 condition, for a total of 13 days of culture. The highest VCD value was achieved in ActiPro medium, which resulted in a 1.7-, 1.5- and 1.4-fold increase compared to the CD CHO 1 condition, for clone 2B9, 2B12 and 3E2 respectively (Figure 29 A, B and C). The ActiPro medium also supported the highest final harvest titer, reaching

15.8 $\mu\text{g/mL}$, 18.3 $\mu\text{g/mL}$ and 8.2 $\mu\text{g/mL}$ for clone 2B9, 2B12 and 3E2 respectively, which resulted in a maximum increase in the harvest titer of 5.4-fold, compared to the CD CHO 1 condition, for clone 2B12.

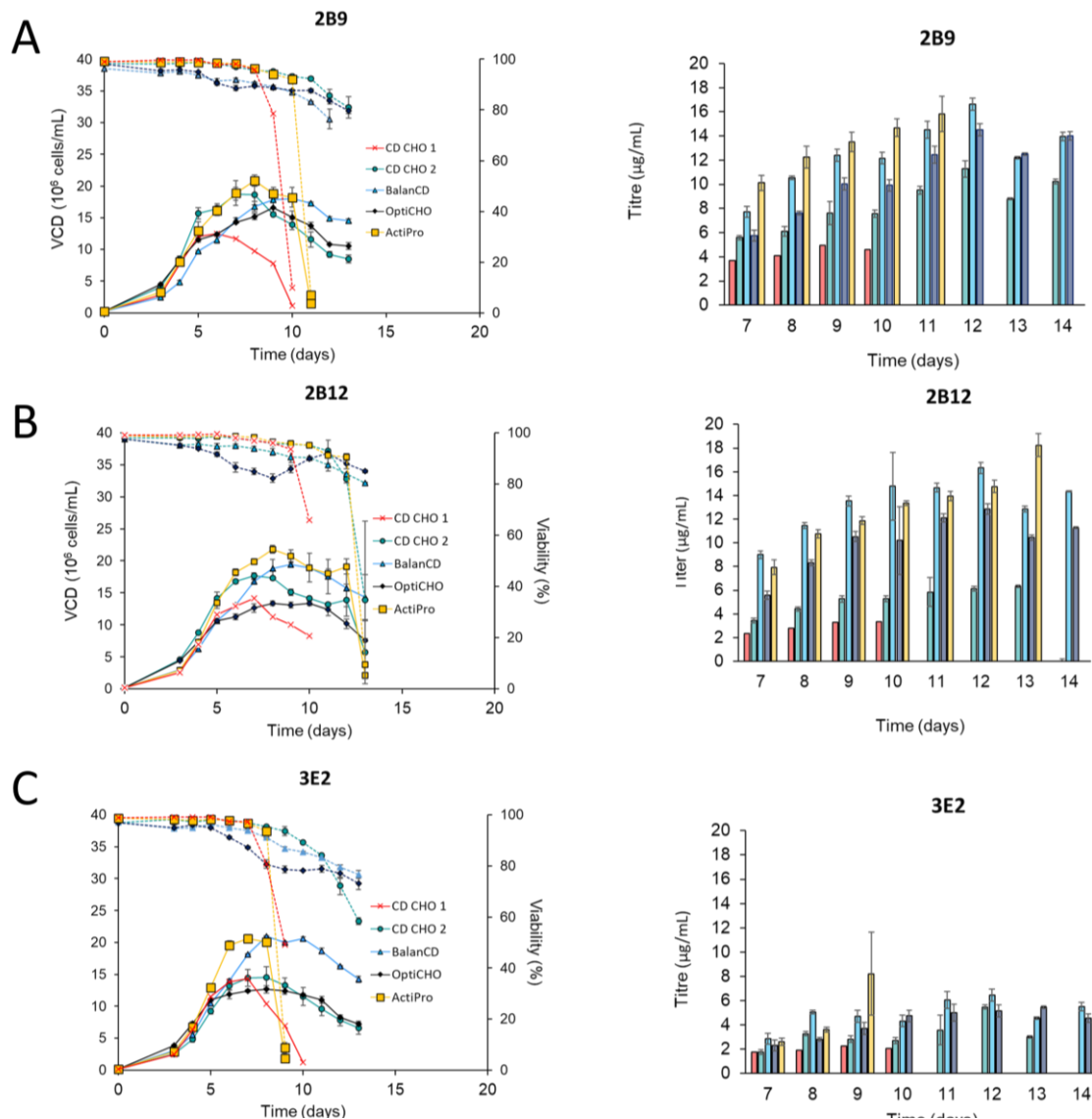
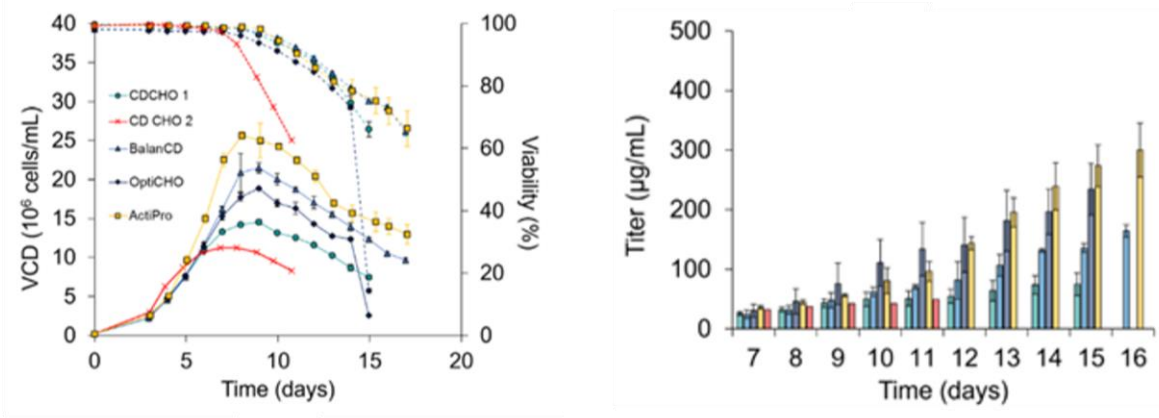


Figure 29 Fed-batch cultures with msAb-Fer (LP system) producing clones. (A) Results of fed-batch cultures of bsAb expressing clones 2B9. Panel on the left represent viable cell density (VCD, solid line) and viability (dotted line); Different line colours represent different medium and feed strategy. Panel on the right shows antibody titer during fed batch culture. Bar charts represent antibody titer measurements performed with protein A biosensors via BLI. **(B)** Results of fed-batch cultures of bsAb expressing clones 2B12. Panel on the left represent viable cell density (VCD, solid line) and viability (dotted line); Different line colours represent different medium and feed strategy. Panel on the right shows antibody titer during fed batch culture. Bar charts represent antibody titer measurements performed with protein A biosensors via BLI. **(C)** Results of fed-batch cultures of bsAb expressing clones 3E2. Panel on the left represent viable cell density (VCD, solid line) and viability (dotted line); Different line colours represent different medium and feed strategy. Panel on the right shows antibody titer during fed batch culture. Bar charts represent antibody titer measurements performed with protein A biosensors via BLI.

Red line – cross marker: cells are adapted in CD CHO and fed with HyClone Feed 7a and HyClone Feed 7b (1% and 0.5%, respectively) daily from day 3. Green line – circle marker: cells are adapted in CD CHO and fed with HyClone Feed 7a and HyClone Feed 7b (2% and 0.2%, respectively) daily from day 3. Light blue line - triangle: cells are adapted in BalanCD and fed with HyClone Feed 7a and HyClone Feed 7b (2% and 0.2%, respectively) daily from day 3. Dark blue line – rhombus marker: cells are adapted in OptiCHO and fed with HyClone Feed 7a and HyClone Feed 7b (2% and 0.2%, respectively) daily from day 3. Yellow line – square marker: cells are adapted in CD CHO and fed with HyClone Feed 7a and HyClone Feed 7b (2% and 0.2%, respectively) daily from day 3

A



B

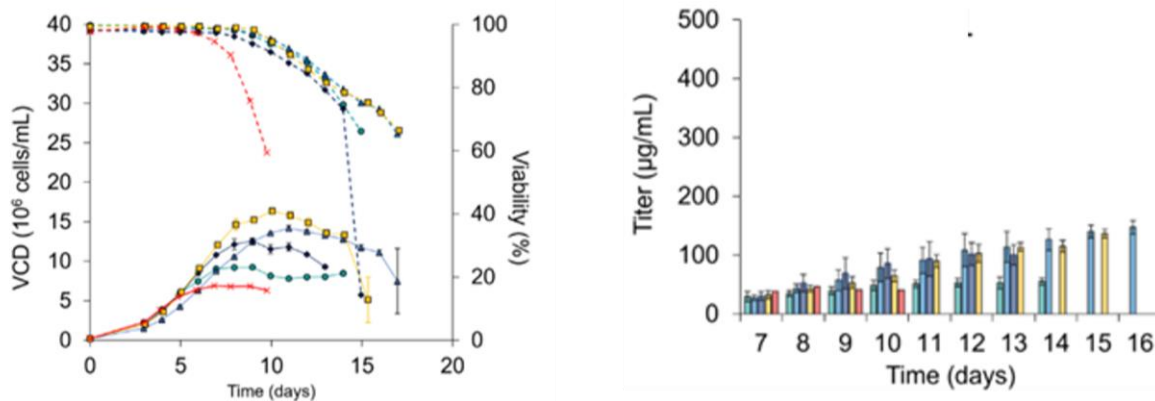


Figure 30 Fed-batch cultures with bsAb-Fer (LP system) producing clones (A) Results of fed-batch cultures of bsAb expressing clones 2B9. Panel on the left represent viable cell density (VCD, solid line) and viability (dotted line); Different line colours represent different medium and feed strategy. Panel on the right shows antibody titer during fed batch culture. Bar charts represent antibody titer measurements performed with protein A biosensors via BLI. **(B)** Results of fed-batch cultures of bsAb expressing clones 2B12. Panel on the left represent viable cell density (VCD, solid line) and viability (dotted line); Different line colours represent different medium and feed strategy. Panel on the right shows antibody titer during fed batch culture. Bar charts represent antibody titer measurements performed with protein A biosensors via BLI.

Red line – cross marker: cells are adapted in CD CHO and fed with HyClone Feed 7a and HyClone Feed 7b (1% and 0.5%, respectively) daily from day 3. Green line – circle marker: cells are adapted in CD CHO and fed with HyClone Feed 7a and HyClone Feed 7b (2% and 0.2%, respectively) daily from day 3. Light blue line - triangle: cells are adapted in BalanCD and fed with HyClone Feed 7a and HyClone Feed 7b (2% and 0.2%, respectively) daily from day 3. Dark blue line – rhombus marker: cells are adapted in OptiCHO and fed with HyClone Feed 7a and HyClone Feed 7b (2% and 0.2%, respectively) daily from day 3. Yellow line – square marker: cells are adapted in CD CHO and fed with HyClone Feed 7a and HyClone Feed 7b (2% and 0.2%, respectively) daily from day 3

Similar improvements were achieved with the bispecific cell lines by adopting the same feeding strategy described above, after cell sequential adaptation in the new medium. Culture duration was improved up to 6 days and bsAb final titer was increased up to 7-fold compared to CD CHO 1 condition (Figure 30 A and B)).

The highest VCD was achieved in Balan-CD and ActiPro media, which also supported the highest harvest titer. Results showed an increase in final titer for both recombinant cell lines expressing monospecific and bispecific

antibodies attributable to an improvement in culture conditions compared to the initial fed-batch strategy, which increased culture duration and maximum VCD suggesting that further culture optimization might enable maximizing the antibody titer and specific productivity.

5.7 System scale-up to 5L using LP-derived bsAb-expressing clone

To evaluate the scalability of the generated cell lines, after testing the clones generated during this study in fed batch cultures in shake flask up to a volume of 30 mL, the same should be scaled up to higher volumes and in bioreactors. To this end, the D7 clone expressing the bsAb antibody was used for a scale up from shake flask (20 mL and 140 mL as total volume) to bioreactors of 2.5 and 5 L (Figure 31 A). Both tests in shake flask were conducted in triplicate whereas the bioreactors were run in simplicate. Clone D7 was thawed and expanded as described in paragraph 4.14 in order to inoculate the flasks and the bioreactor at the same cell generation number. Two different bioreactors were tested during the scale up, a stirred tank bioreactor, the BioFlo 320 system (Eppendorf) equipped with an autoclavable glass vessel, a pitch blade impeller and ring sparger; and an orbital shaker bioreactor, SB 10-X (Kühner) equipped with a 10 L disposable bag. The fed batch strategy for shake flasks and bioreactors remained unchanged and was described in paragraph 4.14, 4.15 and 4.16, respectively. Up to day 6 all systems show similar cell growth, with the exception of the Kühner system (WV 5 L) which shows a longer lag phase (Figure 31 B). The 140 mL shake flask shows a delay in growth after day 6 compared to the other systems. It reached a maximum VCD of 16.7×10^6 cells/mL and then it showed a stationary phase of about 7 days (day 6 to day 13); on day 14 the viability dropped below 60% and therefore the culture was stopped. The bsAb titre at harvest day was about 85 µg/mL and showed an increase of 2.4-fold from day 7 to day 14., The 5L Kühner bioreactor reached a maximum VCD at day 10 of about 20.83×10^6 cells/mL and showed a stationary phase from day 10 to day 18, with a gradual reduction in viability from day 12 onwards. The culture was stopped on day 19 and the antibody titer on harvest day was about 260 µg/mL. It is interesting to note that from day 12 onwards there is an approximately 1.3-fold daily increase in antibody titer in the supernatant without reaching a plateau.

The growth curve for the system in the shake flask with 20 mL and the stirred tank bioreactor with 2.5 L (Eppendorf) was very similar. In both cases the culture reached a similar max. VCD at day 8 (25.71×10^6 and 26.6×10^6 cells/mL for the system in 20 mL and the 2.5 L bioreactor respectively). The stationary phase lasted about 7 days (day 9 to day 16) and the culture was stopped on day 17 when the viability dropped to 66% on average (in one of the triplicates the viability had dropped below 55% so it was decided to stop all flasks). In contrast, the 2.5L bioreactor showed a stationary phase of only two days and a rapid reduction in viability after day 9, which led to the stop of the culture on day 12. This different behaviour compared to the other systems and volumes tested could be attributable to an oxygen shortage of about 12h that occurred between day 9 and 10 for the 2.5L bioreactor and between day 10 and 11 for the 5L bioreactor due to a technical error.

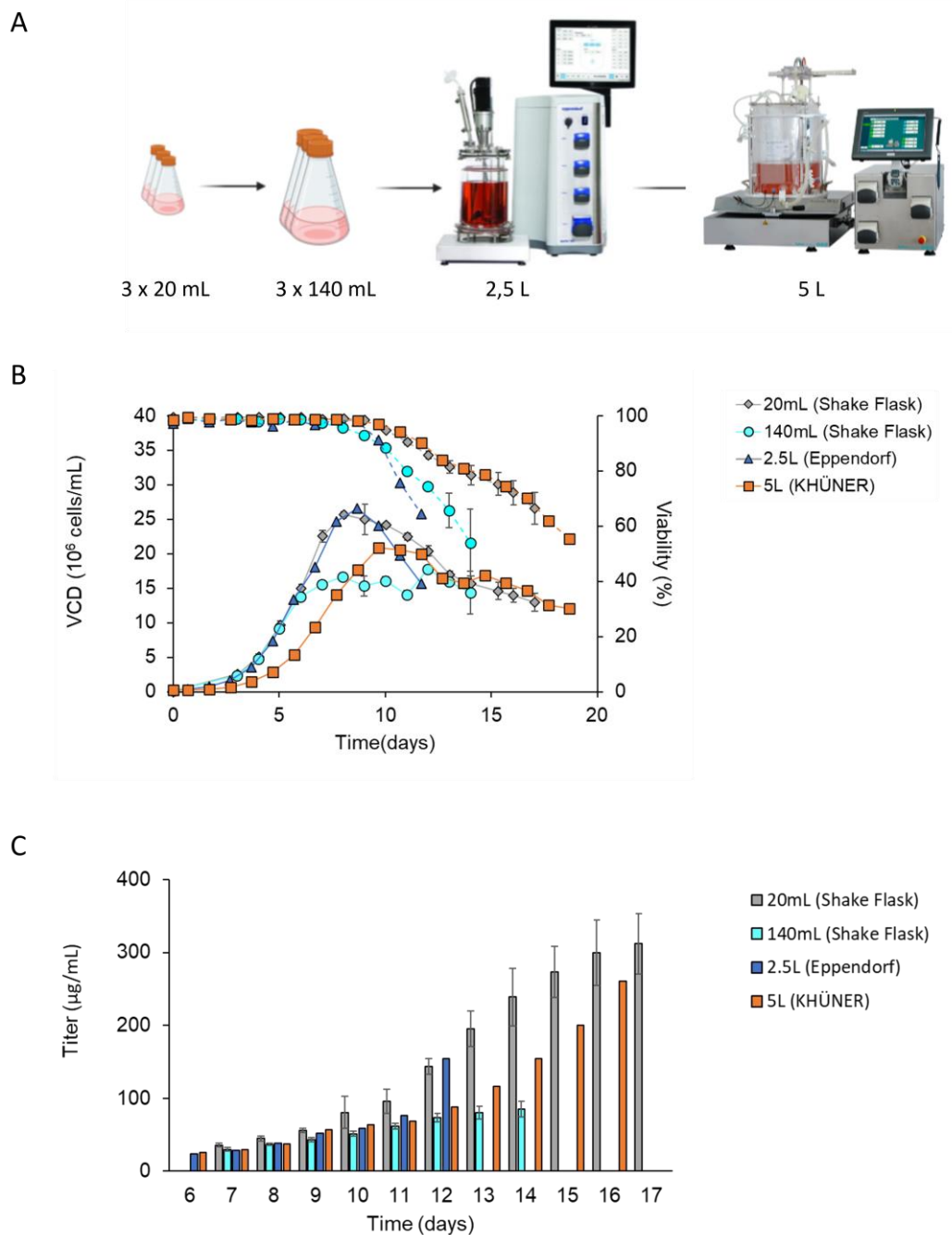


Figure 31 Scale-up of D7 bsAb-Fer expressing clone (A) Scale-up scheme. From the left to the right: 125 mL shake flask for 20 mL total culture volume (in triplicate); : 500 mL shake flask for 140 mL total culture volume (in triplicate); BioFlo 320 system (Eppendorf) equipped with an autoclavable glass vessel, a pitch blade impeller and ring sparger, for 2.5L total culture volume; SB 10-X (Kuhner) equipped with a 10 L disposable bag for 5L total culture volume. **(B)** Scale-up results for bsAb expressing clone D7. Cells were adapted in ActiPro medium and fed with 2% Hyclone Feed 7a and 0.2% Hyclone feed 7B, daily feeding starting on day 3. Solid lines represent viable cell density (VCD); dotted lines represent viability; Different line colours represent different culture volume. **(C)** Quantification of antibody titer during culture. Bar charts represent antibody titer measurements performed with protein A biosensors via BLI. Different bar colours represent different culture volume.

To assess whether this oxygen deficiency had an impact on the metabolic level, glucose and lactate levels were evaluated for the two bioreactors via a liquid chromatography system (HPLC, Figure 32). In both systems, the

glucose concentration was assessed daily using the GlucCell system. When the glucose concentration dropped below 2 g/L, a glucose feed was performed using a 30% glucose solution to a concentration of 5 g/L. In both systems, an early phase, corresponding to the early and mid exponential phase (from day 0 to day 4-5), is observed in which glucose levels were always above 2 g/L. By day 4 for the 2.5L Eppendorf and day 6 for the 5 L Kühner system, high glucose consumption is observed and maintained throughout the stationary phase of growth. It should be noted that the measurements shown in Figure 32 A are made via HPLC on the daily supernatant obtained before glucose feeding. Thus, it can be observed that between day 8 and 17 in the case of the 5 L system and between day 8 and 10 for the 2.5 L system, a drop in glucose concentration close to 0 is observed despite daily feeding. From day 10 onwards for the 2.5L system and from day 17 onwards for the 5L system, a stop in glucose consumption and its slight accumulation is observed corresponding to a reduction in cell growth and viability. Regarding lactate consumption/accumulation, the trend is similar in both systems. From day 3 onwards for the 2.5 L system, and from day 4 onwards for the 5L system, an initial accumulation of lactate is observed. In the 2.5 L system, the lactate concentration reaches 3.5 g/L on day 6 and then a consumption phase begins corresponding to the late exponential and stationary phase of growth. From day 9 onward, a subsequent increase in lactate concentration is observed until it reaches 5.5 g/L on day 12. In the 5L system, the lactate concentration reaches 3.2 g/L on day 8. Then, corresponding to the stationary phase of growth, there is a first phase of lactate consumption (from day 8 to day 10) followed by a second peak of lactate accumulation at day 11 (4.6 g/L) and consumption until day 13. From day 14 onward, a steady increase in lactate is observed until it reaches 8.7 g/L on day 19.

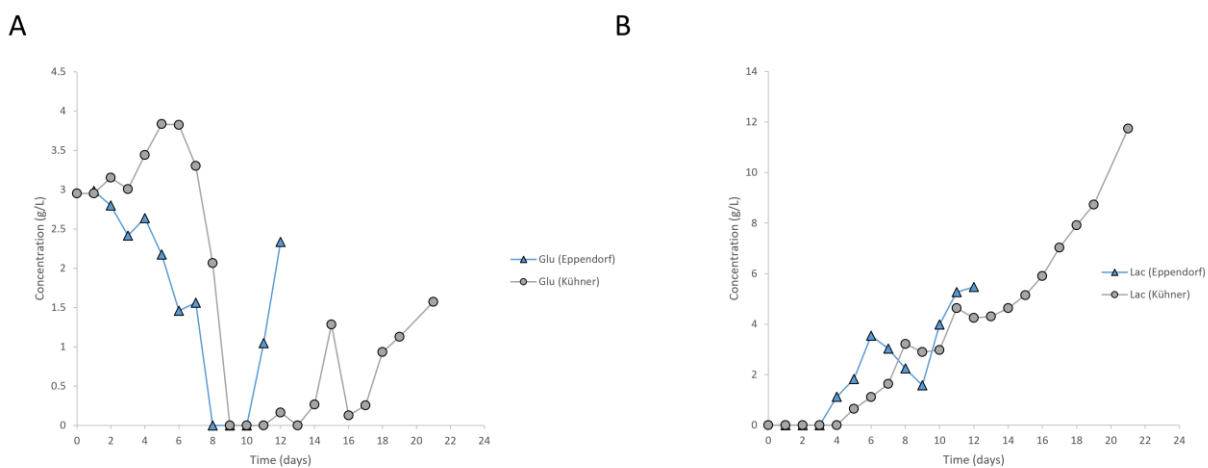


Figure 32 Glucose and Lactate concentration in Eppendorf and Kuhner system **(A)** Evaluation of glucose concentration during the culture in the 2.5 L Eppendorf bioreactor (blue line) and in the 5L Kühner bioreactor (grey line). **(B)** Evaluation of lactate concentration during the culture in the 2.5 L Eppendorf bioreactor (blue line) and in the 5L Kühner bioreactor (grey line).

This behaviour involving a lactate production phase followed by a consumption phase is quite common as the majority of CHO cells in a production system are glycolytic and will therefore produce lactate from the glucose

in the system²³⁰. During a production run, a key event is the so-called 'metabolic switch' which sees a change from a lactate-producing culture to a lactate-consuming one. This metabolic switch is a desired feature during production as it has been associated with improved metabolic efficiency and high productivity^{231–233}. In both production runs of 2.5 and 5 L, a metabolic shift towards lactate consumption is observed in correspondence with a reduction in glucose levels. This corresponds, in both cases, to the late-exponential phase of the growth curve and the transition into the stationary phase, as previously observed in the literature^{234–236}. In both systems, the O₂ shortage does not seem to have had an impact on glucose and lactate metabolism probably due to the fact that DO levels did not change much in either system). However, the O₂ shortage may have caused the rapid reduction in viability after day 10 in the Eppendorf system. The 5 L kuhner system based on orbital shaking technology seems to support a prolonged culture by being able to reproduce the same antibody titer as obtained in shake flask, demonstrating efficient scale up. To further verify this, it would also be necessary to assess the quality of the antibody produced, to evaluate a scale-up to higher volumes and by optimising the different parameters for the production run.

6 Conclusion and Outlook

Due to the continuous expansion of the commercial market for therapeutic proteins in recent years, there is a growing interest in the development of production systems with improved efficiency in focusing on productivity, product quality, and high genetic stability²³⁷. Recent progress in genome engineering technologies resulted in methods that allowed a targeted integration (TI) of a GOI into a specific site of the host genome. These techniques are either based on the use of site-specific recombinases (integrases such as BxB1, Flp, PhiC31, and CRE) or nucleases (such as zinc finger nucleases, TALE nucleases, or the CRISPR–Cas system)^{220,238–241}. Nucleases help the integration of transgenes into a specific genomic locus by inducing DNA double-strand breaks and promoting the self-repair mechanism of the cells²⁴². Known drawbacks are the challenging enzyme engineering, off-target effects and long-term stability after integration of the GOI^{243–245}. Site specific integrases recognize and bind defined recombination sites and catalyse DNA breaks, strand inversion and re-ligation. To exploit this mechanism for transgene integration, a host cell line harboring a specific recombination site in the host cell genome (referred to as landing pad) needs to be generated. Subsequently, the corresponding integrase can be used to integrate the transgene into the landing pad. Integrase-based TI resulted in high stability, showed low off-target effects and low limitation in terms of length of DNA payload^{189,215}. In recent years, numerous landing pad harboring cell lines have been developed utilizing different combinations of recombination sites and integrases. Most of the developed systems have been examined by integrating msAb sequences into the landing pad to generate a production platform^{187,205,215}. However, these TI-generated cell lines resulted in cell-specific productivities ranging between 1-20 pg/cell/day, hence not meeting the criteria for large industrial scale productions for which stable cell lines, generated by random integration, reaching commonly productivities well above 20 pg/cell/day^{101,219,240,246,247}. To increase the productivity of TI-based cell lines, commonly used strategies are the inclusion of the landing pad itself into genomic regions which promote a high and stable transcription rate (referred to as “genomic hot-spot”) and the use of multi-copy expression vectors for transgene integration (donor vector) to increase GOIs copies that can be integrated into the host cell^{107,122,205,219,246,248}. The process of hot-spot screening remains laborious and time-consuming, and the use of large donor vectors carrying multiple copies of the GOI reduces the efficiency of integration into the LP^{219,249}. A recent study reported the integration of multiple landing pads in pre-screened CHO genomic hot spots that were investigated by lentiviral integration and sequencing. However, the number of integrated landing pads remained limited to three. To increase the number of GOI copies, the authors utilized multi-gene vectors expressing up to three msAb copies. This approach resulted in a reduction of integration efficiency and difficulties in clone characterization and validation^{205,219}. In research of a novel approach for the generation of stable cell lines using a TI system in the scope of this doctoral research, we developed a dual landing pad system combined with a strong epigenetic element, a MAR sequence. This novel approach was developed in order to facilitate the integration of multiple copies of LPs into the host genome without the use of hard-to-engineering genomic tools or the time-consuming research of genomic hot

spots . The MAR element, included in both landing pad vectors, should help the generation of a genomic “artificial hot-spot” harboring several copies of the expression vector, each flanked by the MAR sequence, creating *de novo* a protected, independent chromatin environment for the landing pads.

During this study, we tested two different MAR sequences associated with the landing pads, the chicken lysozyme 5' MAR and the human 1-68 MAR. The chicken lysozyme 5' MAR has been proven to be a potent epigenetic element by reducing variegation effects on integrated transgene(s), enhancing gene expression and increasing transgene copy numbers co-integrated at unique chromosomal loci^{174–176}. The human 1-68 MAR is a MAR sequence found in the human genome in Chromosome 1 through genome-wide screening based on major structural features of these elements and appears to be one of the strongest epigenetic elements in the literature¹⁵⁸. This element significantly enhances and stabilizes gene expression and also suppresses variegation and gene silencing²⁵⁰. To obtain host cell lines based on MAR-rich landing pads and evaluate its characteristics, a total of five LP_cMAR clones (containing the 5' chicken lysozyme MAR), five 1-68_MAR (clones containing the human 1-68 MAR) and 5 clones (containing human 1-68 MAR) and five w/o_MAR clones (containing landing pads without MAR) were selected during this study. The latter exhibited lower fluorescence intensities for both EGFP and DsRed than clones with MAR sequences in the landing pad. Moreover, these selected clones are unstable with respect to reporter gene expression, as there is a reduction in the EGFP+/DsRed+ population by more than 40 percent in 40 generations since clonal selection. Interestingly, contrary to what has been observed in the literature, it appears that the h1-68 MAR does not have a strong impact on the expression of reporter genes and stability of selected clones in comparison with the chicken 5' lysozyme MAR (Figure 11 and Figure 13). These effects on reporter gene expression could have been due to the integration of several copies of LPs in the LP_cMAR clones compared to 1-68 MAR clones. However, this will not explain the poor clone stability observed for these clones. It cannot be excluded, that the observed events result from a combined effect due to other elements in the expression vector (such as the promoter) that might interfere differently depending on the MAR sequence used^{140,251–253}.

The selected LP_cMAR clones were further characterized in terms of gene copy number and FISH analysis to support the relevance of the chicken 5' lysozyme MAR inclusion in the landing pad. The differences in copy number between landing pads for each clone (Figure 12 B) are attributable to the consecutive transfections with LP_DsRed, which increased cellular DNA uptake and enhanced the probability of transgene integration as shown in previous studies in CHO cells using a MAR element¹⁷². FISH analyses showed single integration spots for each landing pad (Figure 12 A), supporting the hypothesis that the inclusion of cMAR helped the formation of concatemers and integration of LP copies at one or few chromosomal loci, even in the context of consecutive transfections, according to Grandjean et al. In addition, analyses of gene copy numbers revealed a higher number of LP copies clones containing the chicken 5' lysozyme MAR compared to clones which did not contain the MAR sequence as well as stronger and stable fluorescence expression for each reporter gene, indicating stable integration of both LPs. All these data suggest that the cMAR not only helps the integration of LP into the

genome, increasing the number of copies of LP per cell compared to the control, but it also improves the cells' long-term genetic stability, as previously proven in other studies. These positive effects of the MAR element, reasonably due to its role as an epigenetic element acting as a boundary element and its ability to mediate transgene integration into permissive and active sites of the genome, prevents the elaborate work of identifying genomic hot spots prior to integration^{254,255}. However, it will be interesting to have data on LP integration sites by analysing many more clones to determine if there are some preferential genomic insertion sites. In addition, it seems that the combination of different MARs in the same expression vector¹⁸³ or the presence of this sequence in different positions (5' or 3') in the vector may increase the effect of this epigenetic element^{256,257}. Testing different combinations of MARs in LP vectors as well as using a different design of the LP vector itself could lead to optimization of host clone generation.

In the next step, we tested whether the generated LP_cMAR cell lines could be used to integrate light and heavy chain genes for antibody expression. The LP system with its orthogonal BxB1 recombination sites (attP/attB wild type and with GA central mutation) ensured efficient integration of the donor vectors and avoided off-target integration events due to the very limited crosstalk between the utilized recombination sites. The use of these recombination sites has been tested in previous studies which demonstrated the high and precise integration ability of Bxb1 recombinase in the presence of orthogonal sites^{205,258}.

In addition, the promoter-trap strategy using donor vectors containing promoter-less selection markers further reduced the risks of off-target integration and allowed clone selection by loss of fluorescence and two orthogonal antibiotics, reducing time and resources needed for screening of productive cell lines. Heavy and light chain genes were successfully integrated into LP_EGFP and LP_DsRed, respectively. Generated cell lines showed a partial occupancy of LP_DsRed and LP_EGFP sites (Figure 19, Figure 20 A and Table S3), despite the fact that most of the clones analyzed showed an EGFP-/DsRed- population greater than 94%. This might indicate the presence of some genetic rearrangements at the landing pad level that make GOI integration difficult at all present sites. In other studies²⁰⁵, the approach to integrate multiple copies of a gene of interest using a landing pad system required the integration of a limited number of landing pad copies (up to 3) and the use of much larger donor vectors containing multiple copies of HC and LC. This approach, on the one hand it promotes the full occupancy of landing pad sites and verification of integration events, but at the same time, integration of large donor vectors is much more difficult and rare^{205,219}. The use of small donor vectors such as those used during this study facilitate integration, however, the presence of multiple landing pad sites certainly requires further optimization of transfection and donor vector integration conditions.

The developed msAb cell lines reached the maximum harvest titer in BalanCD and ActiPro (16-18 µg/mL), which is comparable to titers obtained in previous studies using BxB1 recombinase²⁰⁵. The obtained results and low titers for the msAb-expressing clones might be caused by translational and post-translational bottlenecks caused by the sequence among other potential causes.

To confirm this hypothesis, an msAb with a known expression profile should be tested. In addition, gene copy number analysis as well as the mRNA level analysis for the msAb cell lines showed inconsistent outcomes since the high copy number of the light chain gene did not translate to high mRNA levels. This transcriptional limitation has already been observed in similar studies²¹⁹ and could be due to many potential causes, including the hard-to-express antibody sequence, recombination or silencing of repetitive elements in the genome, or transcriptional interference between tandemly assembled gene copies^{241,259,260}. However, the presence of the MAR element in the landing pad should limit the latter mentioned effects. In support of this thesis and that msAb-Fer is a hard-to-express sequence/protein, the latter was used in the commercial GS system for the generation of new clones expressing the monospecific antibody. Although a higher antibody titer was obtained with these clones during fed-batch cultures, the obtained titers were still far from the results normally achieved in the literature with the Lonza GS system. This was further supported by the generation of cell lines expressing the humanized chicken bispecific antibody bsAb-Fer, using the LP system. The bsAb cell lines reached a maximum harvest titer in ActiPro medium (312 µg/mL) comparable to data previously reviewed by Wang et al. Gene copy number for hHC, kHC and cLC correlated with the mRNA level and antibody titer indicating no translational or post-translational bottleneck. The same bsAb-Fer sequence was used to generate stable clones with the Lonza GS system. Clones obtained with the GS system showed 5-10 times higher antibody titers than clones obtained with the LP system. This obviously indicates the possibility to improve the system developed during this study as well as optimizing the monoclonal antibody sequences used. Several points can be addressed to improve the system such as transfection conditions in order to find the best DNA amount and ratios for landing pad total occupancy, use most efficient clonal selection system such as FACS, convert TI to recombinase-mediated cassette exchange (RMCE) to avoid integration of additional DNA sequences (e.g. ampicillin resistance cassette) and also further optimize culture condition in fed-batch mode using a Design of Experiment (DOE) approach. Finally, we demonstrated the feasibility of using the generated LP clone expressing bsAb-Fer for a scale up from a 20 mL shake flask culture to a 5 L bioreactor. In addition, two different bioreactor geometries were tested, a classic stirred bioreactor (BioFlo 320 Eppendorf, 2.5 L working volume) and an orbital shaken bioreactor (SB-10X Kuhner, 5 L working volume). The culture behavior appears to be similar between the shake flasks and bioreactors, showing the typical stages of glucose and lactate metabolism observed in other CHO cell cultures in production²⁶¹. The results obtained in terms of growth curves and final antibody titer looked promising and open the possibility of testing larger volumes closer to production standards. Culture conditions and scale-up processes will need to be optimized for future applications of the developed system, however.

In summary, in this work, we developed a multi-copy MAR-rich landing pad system for the orthogonal, simultaneous integration of several copies of up to three GOIs. Generated LP-bearing host cell lines showed high stability and could be considered suitable for GOIs integration and expression. Presence of a MAR element helped the integration of several copies of both landing pads and increased system stability compared to a non-MAR comprising control cell line. The designed system allowed the monitoring of integration of up to two

different genes by the loss of fluorescence of reporter genes (EGFP and DsRed) and double antibiotic selection. However, integration of more than two genes is also possible as demonstrated by the expression of a bispecific antibody. The developed system helped the selection of stable integrant clones which produced the protein of interest, using low-cost easy to handle selection methods such as single cell derived colony picking from semi-solid medium. Having at disposition high throughput system (e.g., Beacon[®] , ClonePix[®]) or a FACS for single cell sorting, after TI, timelines for cell line development could be further optimized. In addition, the use of these aforementioned systems for future improvement would increase the possibility of screening a much larger number of clones and consequently the probability of selecting highly productive and stable clones. Despite the benefits, the lack of correlation between GOIs copy number and mRNA level should be further investigated and additional optimization is needed to improve the integration of the GOIs into the landing pads and its expression. However, the developed system resulted in a significant reduction of time and resources for cell line generation for both monospecific and more complex antibody formats and it represents a further step towards a more efficient and more rapid cell line development process.

7 Literature

1. Quianzon, C. C. & Cheikh, I. History of insulin. **1**, 1–3 (2012).
2. Behera, B. K., Prasad, R. & Behera, S. Biopharmaceuticals: New Frontier. 157–183 (2020) doi:10.1007/978-981-15-7590-7_5.
3. Fischbach, M. A., Bluestone, J. A. & Lim, W. A. Cell-Based Therapeutics: The Next Pillar of Medicine. *Sci. Transl. Med.* **5**, (2013).
4. Stryjewska, A., Kiepusa, K., Librowski, T. & Lochyński, S. Biotechnology and genetic engineering in the new drug development. Part I. DNA technology and recombinant proteins. *Pharmacol. Rep.* **65**, 1075–1085 (2013).
5. What Are ‘Biologics’ Questions and Answers | FDA. <https://www.fda.gov/about-fda/center-biologics-evaluation-and-research-cber/what-are-biologics-questions-and-answers>.
6. Makurvet, F. D. Biologics vs. small molecules: Drug costs and patient access. *Med. Drug Discov.* **9**, 100075 (2021).
7. Biosimilar medicines: Overview | European Medicines Agency. <https://www.ema.europa.eu/en/human-regulatory/overview/biosimilar-medicines-overview>.
8. Globerman, S. Intellectual Property Rights and the Promotion of Biologics, Medical Devices and Trade in Pharmaceuticals.
9. Patel, P. K., King, C. R. & Feldman, S. R. Biologics and biosimilars. *J. Dermatolog. Treat.* **26**, 299–302 (2015).
10. Butreddy, A., Janga, K. Y., Ajjarapu, S., Sarabu, S. & Dudhipala, N. Instability of therapeutic proteins — An overview of stresses, stabilization mechanisms and analytical techniques involved in lyophilized proteins. *Int. J. Biol. Macromol.* **167**, 309–325 (2021).
11. Song, J. G., Lee, S. H. & Han, H. K. The stabilization of biopharmaceuticals: current understanding and future perspectives. *J. Pharm. Investig. 2017 476* **47**, 475–496 (2017).
12. Pilely, K. *et al.* Monitoring process-related impurities in biologics–host cell protein analysis. *Anal. Bioanal. Chem.* 1–12 (2021) doi:10.1007/S00216-021-03648-2/FIGURES/3.
13. Oshinbolu, S., Wilson, L. J., Lewis, W., Shah, R. & Bracewell, D. G. Measurement of impurities to support process development and manufacture of biopharmaceuticals. *TrAC Trends Anal. Chem.* **101**, 120–128 (2018).
14. Doneva, N., Doytchinova, I. & Dimitrov, I. Predicting immunogenicity risk in biopharmaceuticals. *Symmetry (Basel)*. **13**, 1–15 (2021).
15. Tourdot, S. *et al.* European immunogenicity platform open symposium on immunogenicity of biopharmaceuticals. (2020) doi:10.1080/19420862.2020.1725369.
16. Lamanna, W. C. *et al.* Maintaining consistent quality and clinical performance of biopharmaceuticals.

-
- Expert Opin. Biol. Ther.* **18**, 369–379 (2018).
17. Biologic Therapeutic Drugs Market Size & Growth Analysis Report.
<https://www.bccresearch.com/market-research/biotechnology/biologic-therapeutic-drugs-technologies-markets-report.html>.
 18. Walsh, G. Biopharmaceutical benchmarks 2018. *Nat. Biotechnol.* **36**, 1136–1145 (2018).
 19. Hodgson, J. Refreshing the biologic pipeline 2020. *Nat. Biotechnol.* doi:10.1038/s41587-021-00814-w.
 20. Grilo, A. L. & Mantalaris, A. The Increasingly Human and Profitable Monoclonal Antibody Market. *Trends Biotechnol.* **37**, 9–16 (2019).
 21. Lu, R.-M. *et al.* Development of therapeutic antibodies for the treatment of diseases. doi:10.1186/s12929-019-0592-z.
 22. Kenneth M. Murphy. *Janeway's Immunobiology, 8th Edition*.
 23. Andrew, S. M. & Titus, J. A. Fragmentation of Immunoglobulin G. *Curr. Protoc. Immunol.* **21**, 2.8.1-2.8.10 (1997).
 24. Collins, A. M. & Watson, C. T. Immunoglobulin light chain gene rearrangements, receptor editing and the development of a self-tolerant antibody repertoire. *Front. Immunol.* **9**, 2249 (2018).
 25. Stavnezer, J. & Schrader, C. E. Ig heavy chain class switch recombination: mechanism and regulation. *J. Immunol.* **193**, 5370 (2014).
 26. Watson, C. T. & Breden, F. The immunoglobulin heavy chain locus: genetic variation, missing data, and implications for human disease. *Genes Immun.* **2012 135 13**, 363–373 (2012).
 27. Sheikh, B. A. *et al.* Immunoglobulin. *Basics Fundam. Immunol.* 139–174 (2021) doi:10.5581/1516-8484.20110102.
 28. Brezski, R. J. & Georgiou, G. Immunoglobulin isotype knowledge and application to Fc engineering. *Curr. Opin. Immunol.* **40**, 62–69 (2016).
 29. Vidarsson, G., Dekkers, G., Rispen, T. & Klinman, D. IgG subclasses and allotypes: from structure to effector functions. (2014) doi:10.3389/fimmu.2014.00520.
 30. Noviski, M. *et al.* IgM and IgD B cell receptors differentially respond to endogenous antigens and control B cell fate. *Elife* **7**, (2018).
 31. Geisberger, R., Lamers, M. & Achatz, G. The riddle of the dual expression of IgM and IgD. *Immunology* **118**, 429 (2006).
 32. Chen, K. & Cerutti, A. The function and regulation of immunoglobulin D. *Curr. Opin. Immunol.* **23**, 345–352 (2011).
 33. Woof, J. M. & Ken, M. A. The function of immunoglobulin A in immunity. *J. Pathol.* **208**, 270–282 (2006).
 34. Schroeder, H. W. & Cavacini, L. Structure and Function of Immunoglobulins. *J. Allergy Clin. Immunol.* **125**, S41 (2010).

-
35. Cymer, F., Beck, H., Rohde, A. & Reusch, D. Therapeutic monoclonal antibody N-glycosylation – Structure, function and therapeutic potential. *Biologicals* **52**, 1–11 (2018).
 36. Maureen Spearman, Ben Dionne, and M. B. & Abstract. The Role of Glycosylation in Therapeutic Antibodies. in *Antibody Expression and Production, Cell Engineering* vol. 7 25–52 (2011).
 37. Van Erp, E. A., Luytjes, W., Ferwerda, G. & Van Kasteren, P. B. Fc-mediated antibody effector functions during respiratory syncytial virus infection and disease. *Front. Immunol.* **10**, 548 (2019).
 38. Igietseme, J. U., Zhu, X. & Black, C. M. Fc Receptor-Dependent Immunity. *Antib. Fc Link. Adapt. Innate Immun.* 269–281 (2014) doi:10.1016/B978-0-12-394802-1.00015-7.
 39. Daëron, M., Malbec, O., Uénard, H., Bruhns, P. & Fridman, W. H. Immunoreceptor Tyrosine-based Inhibition Motif-dependent Negative Regulation of Mast Cell Activation and Proliferation. *Mast Cells Basophils* 185–193 (2000) doi:10.1016/B978-012473335-0/50014-3.
 40. Desjarlais, J. R. & Lazar, G. A. Modulation of antibody effector function. *Exp. Cell Res.* **317**, 1278–1285 (2011).
 41. Dunkelberger, J. R. & Song, W. C. Complement and its role in innate and adaptive immune responses. *Cell Res. 2010 201* **20**, 34–50 (2009).
 42. Pyzik, M. *et al.* The neonatal Fc Receptor (FcRn): A misnomer? *Front. Immunol.* **10**, 1540 (2019).
 43. Roopenian, D. C. & Akilesh, S. FcRn: the neonatal Fc receptor comes of age. *Nat. Rev. Immunol.* **2007 79** **7**, 715–725 (2007).
 44. Lu, L. L., Suscovich, T. J., Fortune, S. M. & Alter, G. Beyond binding: antibody effector functions in infectious diseases. (2017) doi:10.1038/nri.2017.106.
 45. Todd, P. A. *et al.* *Drug Evaluation Muromonab CD3 A Review of its Pharmacology and Therapeutic Potential.*
 46. Leavy, O. The birth of monoclonal antibodies. *Nat. Immunol.* **2016 171** **17**, S13–S13 (2016).
 47. Köhler G. Milstein C. Continuous cultures of fused cells secreting antibody of predefined specificity. *Nature* **256**, 495–497 (1975).
 48. Sgro, C. Side-effects of a monoclonal antibody, muromonab CD3/orthoclone OKT3: bibliographic review. *Toxicology* **105**, 23–29 (1995).
 49. Morrison, S. L., Johnson, M. J., Herzenberg, L. A. & Oi, V. T. Chimeric human antibody molecules: Mouse antigen-binding domains with human constant region domains (transfection/protoplast fusion/calcium phosphate transfection/intronic controlling elements/transfectoma). *Proc. Natl. Acad. Sci. USA* **81**, 6851–6855 (1984).
 50. Ibbotson, T., McGavin, J. K. & Goa, K. L. Abciximab: an updated review of its therapeutic use in patients with ischaemic heart disease undergoing percutaneous coronary revascularisation. *Drugs* **63**, 1121–1163 (2003).
 51. Plosker, G. L. & Figgitt, D. P. Rituximab: A review of its use in non-Hodgkin's lymphoma and chronic

-
- lymphocytic leukaemia. *Drugs* **63**, 803–843 (2003).
52. Jones, P. T., Dear, P. H., Foote, J., Neuberger, M. S. & Winter, G. Replacing the complementarity-determining regions in a human antibody with those from a mouse. *Nature* **321**, 522–525 (1986).
53. Williams, D. G., Matthews, D. J. & Jones, T. Humanising Antibodies by CDR Grafting. *Antib. Eng.* 319–339 (2010) doi:10.1007/978-3-642-01144-3_21.
54. Waldmann, T. A. Anti-Tac (daclizumab, Zenapax) in the treatment of leukemia, autoimmune diseases, and in the prevention of allograft rejection: a 25-year personal odyssey. *J. Clin. Immunol.* **27**, 1–18 (2007).
55. Krishan Maggon. Monoclonal Antibody ‘Gold Rush’. *Curr. Med. Chem.* **14**, 1978–1987 (2007).
56. Safdari, Y., Farajnia, S., Asgharzadeh, M. & Khalili, M. Antibody humanization methods – a review and update. <http://dx.doi.org/10.1080/02648725.2013.801235> **29**, 175–186 (2013).
57. Frenzel, A., Schirrmann, T. & Hust, M. Phage display-derived human antibodies in clinical development and therapy. *MAbs* **8**, 1177–1194 (2016).
58. Smith, G. P. Filamentous fusion phage: novel expression vectors that display cloned antigens on the virion surface. *Science* **228**, 1315–1317 (1985).
59. McCafferty, J., Griffiths, A. D., Winter, G. & Chiswell, D. J. Phage antibodies: filamentous phage displaying antibody variable domains. *Nat.* 1990 3486301 **348**, 552–554 (1990).
60. • Top pharmaceutical drugs by projected 2021 global sales | Statista. <https://www.statista.com/statistics/973523/top-drugs-by-year-on-year-sales-increase/>.
61. Valldorf, B. *et al.* Antibody display technologies: Selecting the cream of the crop. *Biol. Chem.* (2021) doi:10.1515/HSZ-2020-0377/ASSET/GRAPHIC/J_HSZ-2020-0377_FIG_005.JPG.
62. Lonberg, N. *et al.* Antigen-specific human antibodies from mice comprising four distinct genetic modifications. *Nature* **368**, 856–859 (1994).
63. Brüggemann, M. *et al.* Human antibody production in transgenic animals. *Arch. Immunol. Ther. Exp. (Warsz.)* **63**, 101–108 (2015).
64. Jakobovits, A. Production of fully human antibodies by transgenic mice. *Curr. Opin. Biotechnol.* **6**, 561–566 (1995).
65. Wu, M., Rivkin, A. & Pham, T. Panitumumab: human monoclonal antibody against epidermal growth factor receptors for the treatment of metastatic colorectal cancer. *Clin. Ther.* **30**, 14–30 (2008).
66. Top 10 Blockbuster Drugs In 2021 | Nasdaq. <https://www.nasdaq.com/articles/top-10-blockbuster-drugs-in-2021>.
67. Gao, Y., Huang, X., Zhu, Y. & Lv, Z. A brief review of monoclonal antibody technology and its representative applications in immunoassays. *J. Immunoassay Immunochem.* **39**, 351–364 (2018).
68. Brinkmann, U. *et al.* The making of bispecific antibodies The making of bispecific antibodies. *MAbs* **9**, 182–212 (2017).

-
69. Huang, S., van Duijnhoven, S. M. J., Sijts, A. J. A. M. & van Elsas, A. Bispecific antibodies targeting dual tumor-associated antigens in cancer therapy. *J. Cancer Res. Clin. Oncol.* **146**, 3111 (2020).
 70. Chiu, M. L., Goulet, D. R., Teplyakov, A. & Gilliland, G. L. Antibody Structure and Function: The Basis for Engineering Therapeutics. doi:10.3390/antib8040055.
 71. Ma, J. *et al.* Bispecific Antibodies: From Research to Clinical Application. *Front. Immunol.* **12**, (2021).
 72. Wang, Q. *et al.* Design and Production of Bispecific Antibodies. *Antibodies* **8**, 43 (2019).
 73. Schaefer, W. *et al.* Heavy and light chain pairing of bivalent quadroma and knobs-into-holes antibodies analyzed by UHR-ESI-QTOF mass spectrometry. *MAbs* **8**, 49 (2016).
 74. Milstein, C. & Cuello, A. C. Hybrid hybridomas and their use in immunohistochemistry. *Nat.* **1983** 3055934 **305**, 537–540 (1983).
 75. Shatz, W. *et al.* An efficient route to bispecific antibody production using single-reactor mammalian co-culture. *MAbs* **8**, 1487 (2016).
 76. Krah, S. *et al.* Engineering bispecific antibodies with defined chain pairing. *N. Biotechnol.* **39**, 167–173 (2017).
 77. Ridgway, J. B. B., Presta, L. G. & Carter, P. ‘Knobs-into-holes’ engineering of antibody C H 3 domains for heavy chain heterodimerization. *Protein Eng.* **9**, 617–621 (1996).
 78. Xu, Y. *et al.* Production of bispecific antibodies in ‘knobs-into-holes’ using a cell-free expression system. *MAbs* **7**, 231–242 (2015).
 79. Muda, M. *et al.* Therapeutic assessment of SEED: A new engineered antibody platform designed to generate mono- and bispecific antibodies. *Protein Eng. Des. Sel.* **24**, 447–454 (2011).
 80. Krah, S., Kolmar, H., Becker, S. & Zielonka, S. Engineering IgG-Like Bispecific Antibodies—An Overview. *Antibodies* **7**, 28 (2018).
 81. Klein, C. *et al.* Engineering therapeutic bispecific antibodies using CrossMab technology. *Methods* **154**, 21–31 (2019).
 82. Wu, X. *et al.* Protein design of IgG/TCR chimeras for the co-expression of Fab-like moieties within bispecific antibodies. *MAbs* **7**, 364–376 (2015).
 83. Lewis, S. M. *et al.* Generation of bispecific IgG antibodies by structure-based design of an orthogonal Fab interface. *Nat. Biotechnol.* **32**, 191–198 (2014).
 84. Fischer, N. *et al.* Exploiting light chains for the scalable generation and platform purification of native human bispecific IgG. *Nat. Commun.* **2015** 61 **6**, 1–12 (2015).
 85. Spiess, C., Zhai, Q. & Carter, P. J. Alternative molecular formats and therapeutic applications for bispecific antibodies. *Mol. Immunol.* **67**, 95–106 (2015).
 86. Blair, H. A. Emicizumab: A Review in Haemophilia A. *Drugs* **79**, 1697–1707 (2019).
 87. Lee, D.-Y. *et al.* Recent Developments in Bioprocessing of Recombinant Proteins: Expression Hosts and Process Development. *Front. Bioeng. Biotechnol.* | www.frontiersin.org **7**, 420 (2019).

-
88. Gronemeyer, P., Ditz, R. & Strube, J. Trends in upstream and downstream process development for antibody manufacturing. *Bioengineering* **1**, 188–212 (2014).
 89. Abu-Absi, S. F. *et al.* Defining process design space for monoclonal antibody cell culture. *Biotechnol. Bioeng.* **106**, 894–905 (2010).
 90. Yang, S.-T. & Liu, X. Cell culture processes for biologics manufacturing: recent developments and trends. *Pharm. Bioprocess.* **1**, 133–136 (2013).
 91. Bielser, J. M., Wolf, M., Souquet, J., Broly, H. & Morbidelli, M. Perfusion mammalian cell culture for recombinant protein manufacturing – A critical review. *Biotechnol. Adv.* **36**, 1328–1340 (2018).
 92. Gagliardi, T. M., Chelikani, R., Yang, Y., Tuozzolo, G. & Yuan, H. Development of a novel, high-throughput screening tool for efficient perfusion-based cell culture process development. *Biotechnol. Prog.* **35**, e2811 (2019).
 93. O’Flaherty, R. *et al.* Mammalian cell culture for production of recombinant proteins: A review of the critical steps in their biomanufacturing. *Biotechnol. Adv.* **43**, 107552 (2020).
 94. Yusibov, V., Kushnir, N. & Streatfield, S. J. Antibody Production in Plants and Green Algae. (2016) doi:10.1146/annurev-arplant-043015-111812.
 95. Lalonde, M. E. & Durocher, Y. Therapeutic glycoprotein production in mammalian cells. *J. Biotechnol.* **251**, 128–140 (2017).
 96. Graumann, K. & Premstaller, A. Manufacturing of recombinant therapeutic proteins in microbial systems. *Biotechnol. J.* **1**, 164–186 (2006).
 97. Overton, T. W. Recombinant protein production in bacterial hosts. *Drug Discov. Today* **19**, 590–601 (2014).
 98. Ghaderi, D., Zhang, M., Hurtado-Ziola, N. & Varki, A. Biotechnology and Genetic Engineering Reviews Production platforms for biotherapeutic glycoproteins. Occurrence, impact, and challenges of non-human sialylation. doi:10.5661/bger-28-147.
 99. Hunter, M., Yuan, P., Vavilala, D. & Fox, M. Optimization of Protein Expression in Mammalian Cells. *Curr. Protoc. Protein Sci.* **95**, 1–28 (2019).
 100. Dhara, V. G., Naik, H. M., Majewska, N. I. & Betenbaugh, M. J. Recombinant Antibody Production in CHO and NS0 Cells: Differences and Similarities. *BioDrugs* **32**, 571–584 (2018).
 101. Kunert, R. & Reinhart, D. Advances in recombinant antibody manufacturing. *Appl. Microbiol. Biotechnol.* **100**, 3451–3461 (2016).
 102. Ritacco, F. V., Wu, Y. & Khetan, A. Cell culture media for recombinant protein expression in Chinese hamster ovary (CHO) cells: History, key components, and optimization strategies. *Biotechnol. Prog.* **34**, 1407–1426 (2018).
 103. Reinhart, D. *et al.* Bioprocessing of Recombinant CHO-K1, CHO-DG44, and CHO-S: CHO Expression Hosts Favor Either mAb Production or Biomass Synthesis. *Biotechnol. J.* **14**, 1–11 (2019).

-
104. Kim, J. Y., Kim, Y. G. & Lee, G. M. CHO cells in biotechnology for production of recombinant proteins: Current state and further potential. *Appl. Microbiol. Biotechnol.* **93**, 917–930 (2012).
 105. Dahodwala, H. & Lee, K. H. The fickle CHO: a review of the causes, implications, and potential alleviation of the CHO cell line instability problem. *Curr. Opin. Biotechnol.* **60**, 128–137 (2019).
 106. Zhang, H.-Y., Fan, Z.-L. & Wang, T.-Y. Advances of Glycometabolism Engineering in Chinese Hamster Ovary Cells. *Front. Bioeng. Biotechnol.* **9**, (2021).
 107. Lai, T., Yang, Y. & Ng, S. K. Advances in mammalian cell line development technologies for recombinant protein production. *Pharmaceuticals* **6**, 579–603 (2013).
 108. Kelley, B. mAbs Industrialization of mAb production technology: The bioprocessing industry at a crossroads. (2009) doi:10.4161/mabs.1.5.9448.
 109. Noh, S. M., Sathyamurthy, M. & Lee, G. M. Development of recombinant Chinese hamster ovary cell lines for therapeutic protein production. *Curr. Opin. Chem. Eng.* **2**, 391–397 (2013).
 110. Omasa, T., Onitsuka, M. & Kim, W.-D. Cell Engineering and Cultivation of Chinese Hamster Ovary (CHO) Cells. *Curr. Pharm. Biotechnol.* **11**, 233–240 (2010).
 111. Wurm, F. M. & Wurm, M. J. Cloning of CHO Cells, productivity and genetic stability—a discussion. *Processes* **5**, (2017).
 112. Wurm, F. M. & Hacker, D. First CHO genome. *Nat. Biotechnol.* **2011 298 29**, 718–720 (2011).
 113. Wurm, M. J. & Wurm, F. M. Naming CHO cells for bio-manufacturing: Genome plasticity and variant phenotypes of cell populations in bioreactors question the relevance of old names. *Biotechnol. J.* **16**, 2100165 (2021).
 114. Urlaub, G. & Chasin, L. A. *Isolation of Chinese hamster cell mutants deficient in dihydrofolate reductase activity.* *Genetics* vol. 77 (1980).
 115. Kaas, C. S., Kristensen, C., Betenbaugh, M. J. & Andersen, M. R. Sequencing the CHO DXB11 genome reveals regional variations in genomic stability and haploidy. *BMC Genomics* **16**, 1–9 (2015).
 116. Urlaub, G., Käs, E., Carothers, A. M. & Chasin, L. A. Deletion of the diploid dihydrofolate reductase locus from cultured mammalian cells. *Cell* **33**, 405–412 (1983).
 117. Thompson, L. H. & Baker, R. M. Isolation of mutants of cultured mammalian cells. *Methods Cell Biol.* **6**, 209–281 (1973).
 118. Wurm, F. M. CHO Quasispecies—Implications for Manufacturing Processes. *Process. 2013, Vol. 1, Pages 296-311* **1**, 296–311 (2013).
 119. Xu, X. *et al.* The genomic sequence of the Chinese hamster ovary (CHO)-K1 cell line. *Nat. Biotechnol.* **2011 298 29**, 735–741 (2011).
 120. Gutiérrez-Granados, S., Cervera, L., Kamen, A. A. & Gòdia, F. Advancements in mammalian cell transient gene expression (TGE) technology for accelerated production of biologics. *Crit. Rev. Biotechnol.* **38**, 918–940 (2018).

-
121. Nallet, S. *et al.* Glycan variability on a recombinant IgG antibody transiently produced in HEK-293E cells. *N. Biotechnol.* **29**, 471–476 (2012).
 122. Hamaker, N. K. & Lee, K. H. Site-specific integration ushers in a new era of precise CHO cell line engineering. *Curr. Opin. Chem. Eng.* **22**, 152–160 (2018).
 123. Xu, Z. J. *et al.* Effect of promoter, promoter mutation and enhancer on transgene expression mediated by episomal vectors in transfected HEK293, Chang liver and primary cells. *Bioengineered* **10**, 548–560 (2019).
 124. Romanova, N. & Noll, T. Engineered and Natural Promoters and Chromatin-Modifying Elements for Recombinant Protein Expression in CHO Cells. *Biotechnol. J.* **13**, 1–13 (2018).
 125. Zboray, K. *et al.* Heterologous protein production using euchromatin-containing expression vectors in mammalian cells. *Nucleic Acids Res.* **43**, 1–14 (2015).
 126. Rita Costa, A., Elisa Rodrigues, M., Henriques, M., Azeredo, J. & Oliveira, R. Guidelines to cell engineering for monoclonal antibody production. *Eur. J. Pharm. Biopharm.* **74**, 127–138 (2010).
 127. Dangi, A. K., Sinha, R., Dwivedi, S., Gupta, S. K. & Shukla, P. Cell line techniques and gene editing tools for antibody production: A review. *Front. Pharmacol.* **9**, 1–12 (2018).
 128. Tejwani, V., Chaudhari, M., Rai, T. & Sharfstein, S. T. High-throughput and automation advances for accelerating single-cell cloning, monoclonality and early phase clone screening steps in mammalian cell line development for biologics production. *Biotechnol. Prog.* **37**, e3208 (2021).
 129. Lilly, E. *et al.* Industry view on the relative importance of “clonality” of biopharmaceutical-producing cell lines Biologicals Industry view on the relative importance of “clonality” of biopharmaceutical-producing cell lines. *Biologicals* **44**, 117–122 (2018).
 130. Chusainow, J. *et al.* A study of monoclonal antibody-producing CHO cell lines: What makes a stable high producer? *Biotechnol. Bioeng.* **102**, 1182–1196 (2009).
 131. Feary, M., Moffat, M. A., Casperson, G. F., Allen, M. J. & Young, R. J. CHOK1SV GS-KO SSI expression system: A combination of the Fer1L4 locus and glutamine synthetase selection. *Biotechnol. Prog.* 1–12 (2021) doi:10.1002/btpr.3137.
 132. Noh, S. M., Shin, S. & Lee, G. M. Comprehensive characterization of glutamine synthetase-mediated selection for the establishment of recombinant CHO cells producing monoclonal antibodies. *Sci. Rep.* **8**, 1–11 (2018).
 133. Jun, S. C., Kim, M. S., Hong, H. J. & Lee, G. M. Limitations to the development of humanized antibody producing chinese hamster ovary cells using glutamine synthetase-mediated gene amplification. *Biotechnol. Prog.* **22**, 770–780 (2006).
 134. Noh, S. M., Shin, S. & Lee, G. M. Cell Line Development for Therapeutic Protein Production. *Cell Cult. Eng.* 23–47 (2019) doi:10.1002/9783527811410.ch2.
 135. Yeo, J. H. M. *et al.* Optimized Selection Marker and CHO Host Cell Combinations for Generating High

-
- Monoclonal Antibody Producing Cell Lines. *Biotechnol. J.* **12**, 1700175 (2017).
136. Caron, A. W. *et al.* Fluorescent labeling in semi-solid medium for selection of mammalian cells secreting high-levels of recombinant proteins. *BMC Biotechnol.* **9**, 1–11 (2009).
 137. Hacker, D. L. & Balasubramanian, S. Recombinant protein production from stable mammalian cell lines and pools. *Curr. Opin. Struct. Biol.* **38**, 129–136 (2016).
 138. Hong, J. K., Lakshmanan, M., Goudar, C. & Lee, D. Y. Towards next generation CHO cell line development and engineering by systems approaches. *Curr. Opin. Chem. Eng.* **22**, 1–10 (2018).
 139. Le, H., Vishwanathan, N., Jacob, N. M., Gadgil, M. & Hu, W. S. Cell line development for biomanufacturing processes: recent advances and an outlook. *Biotechnol. Lett.* **37**, 1553–1564 (2015).
 140. Harraghy, N. *et al.* Epigenetic regulatory elements: Recent advances in understanding their mode of action and use for recombinant protein production in mammalian cells. *Biotechnol. J.* **10**, 967–978 (2015).
 141. Oberbek, A., Matasci, M., Hacker, D. L. & Wurm, F. M. Generation of stable, high-producing cho cell lines by lentiviral vector-mediated gene transfer in serum-free suspension culture. *Biotechnol. Bioeng.* **108**, 600–610 (2011).
 142. Izsvák, Z. & Ivics, Z. Sleeping Beauty transposition: Biology and applications for molecular therapy. *Mol. Ther.* **9**, 147–156 (2004).
 143. Balasubramanian, S. *et al.* Rapid recombinant protein production from piggyBac transposon-mediated stable CHO cell pools. *J. Biotechnol.* **200**, 61–69 (2015).
 144. Chi, X., Zheng, Q., Jiang, R., Chen-Tsai, R. Y. & Kong, L. J. A system for site-specific integration of transgenes in mammalian cells. *PLoS One* **14**, 1–14 (2019).
 145. Ea, V., Baudement, M.-O., Lesne, A. & Forné, T. Contribution of Topological Domains and Loop Formation to 3D Chromatin Organization. *Genes (Basel)*. **6**, 734–750 (2015).
 146. Mirkovitch, J., Mirault, M. E. & Laemmli, U. K. Organization of the higher-order chromatin loop: specific DNA attachment sites on nuclear scaffold. *Cell* **39**, 223–232 (1984).
 147. Boulikas, T. Chromatin Domains and Prediction of MAR Sequences. *Int. Rev. Cytol.* **162**, 279–388 (1996).
 148. Heng, H. H. Q. *et al.* Chromatin loops are selectively anchored using scaffold/matrix-attachment regions. *J. Cell Sci.* **117**, 999–1008 (2004).
 149. Majocchi, S., Aritonovska, E. & Mermod, N. Epigenetic regulatory elements associate with specific histone modifications to prevent silencing of telomeric genes. *Nucleic Acids Res.* **42**, 193–204 (2014).
 150. Bode, J. *et al.* Scaffold/matrix-attached regions: structural properties creating transcriptionally active loci. *Int. Rev. Cytol.* **162A**, 389–454 (1995).
 151. Loc, P. V. & Strätling, W. H. The matrix attachment regions of the chicken lysozyme gene co-map with the boundaries of the chromatin domain. *EMBO J.* **7**, 655–664 (1988).
 152. A P jarman & D R Higgs. Sites of attachment to the nuclear scaffold in the human alpha and beta globin

-
- gene complexes - PubMed. *Prog Clin Biol Res* . **316 B**, 33–35 (1989).
153. Petrov, A. *et al.* Chromatin loop domain organization within the 4q35 locus in facioscapulohumeral dystrophy patients versus normal human myoblasts. (2006).
 154. Braem, C. *et al.* Genomic Matrix Attachment Region and Chromosome Conformation Capture Quantitative Real Time PCR Assays Identify Novel Putative Regulatory Elements at the Imprinted Dlk1/Gtl2 Locus * □ S. (2008) doi:10.1074/jbc.M801883200.
 155. Holmes-Davis, R. & Comai, L. Nuclear matrix attachment regions and plant gene expression. *Trends Plant Sci*. **3**, 91–97 (1998).
 156. Izaurrealde, E., Mirkovitch, J. & Laemmli, U. K. Interaction of DNA with nuclear scaffolds in vitro. *J. Mol. Biol.* **200**, 111–125 (1988).
 157. Namciu, S. J. & Fournier, R. E. K. Human Matrix Attachment Regions Are Necessary for the Establishment but Not the Maintenance of Transgene Insulation in *Drosophila melanogaster*. *Mol. Cell. Biol.* **24**, 10236 (2004).
 158. Girod, P. A. *et al.* Genome-wide prediction of matrix attachment regions that increase gene expression in mammalian cells. *Nat. Methods* **4**, 747–753 (2007).
 159. Chavali, P. L. & Chavali, S. Nuclear Architecture and Transcriptional Regulation of MicroRNAs. *MicroRNA Regen. Med.* 1129–1158 (2015) doi:10.1016/B978-0-12-405544-5.00043-5.
 160. Bode, J. *et al.* Biological Significance of Unwinding Capability of Nuclear Matrix-Associating DNAs. *Science (80-)*. **255**, 195–197 (1992).
 161. Fiorini, A., Gouveia, F. D. S. & Fernandez, M. A. Scaffold/Matrix Attachment Regions and intrinsic DNA curvature. *Biochemistry. (Mosc)*. **71**, 481–488 (2006).
 162. Yamasaki, K., Akiba, T., Yamasaki, T. & Harata, K. Structural basis for recognition of the matrix attachment region of DNA by transcription factor SATB1. *Nucleic Acids Res.* **35**, 5073–5084 (2007).
 163. Boulikas, T. Transcription factor binding sites in the matrix attachment region (MAR) of the chicken α -globin gene. *J. Cell. Biochem.* **55**, 513–529 (1994).
 164. Britanova, O., Akopov, S., Lukyanov, S., Gruss, P. & Tarabykin, V. Novel transcription factor Satb2 interacts with matrix attachment region DNA elements in a tissue-specific manner and demonstrates cell-type-dependent expression in the developing mouse CNS. *Eur. J. Neurosci.* **21**, 658–668 (2005).
 165. Razin, S. V., Vassetzky, Y. S. & Hancock, R. Nuclear matrix attachment regions and topoisomerase II binding and reaction sites in the vicinity of a chicken DNA replication origin. *Biochem. Biophys. Res. Commun.* **177**, 265–270 (1991).
 166. Fernández, L. A., Winkler, M. & Grosschedl, R. Matrix attachment region-dependent function of the immunoglobulin mu enhancer involves histone acetylation at a distance without changes in enhancer occupancy. *Mol. Cell. Biol.* **21**, 196–208 (2001).
 167. Forrester, W. C., Fernandez, L. A. & Grosschedl, R. Nuclear matrix attachment regions antagonize

-
- methylation-dependent repression of long-range enhancer–promoter interactions. *Genes Dev.* **13**, 3003 (1999).
168. Gombert, W. M. *et al.* The c-myc Insulator Element and Matrix Attachment Regions Define the c-myc Chromosomal Domain. *Mol. Cell. Biol.* **23**, 9338–9348 (2003).
 169. Galbete, J. J., Bucetaz, M. & Mermod, N. MAR elements regulate the probability of epigenetic switching between active and inactive gene expression. doi:10.1039/b813657b.
 170. Kwaks, T. H. J. & Otte, A. P. Employing epigenetics to augment the expression of therapeutic proteins in mammalian cells. *Trends Biotechnol.* **24**, 137–142 (2006).
 171. Saunders, F., Sweeney, B., Antoniou, M. N., Stephens, P. & Cain, K. Chromatin function modifying elements in an industrial antibody production platform - Comparison of UCOE, MAR, STAR and cHS4 elements. *PLoS One* **10**, 1–20 (2015).
 172. Grandjean, M. *et al.* High-level transgene expression by homologous recombination-mediated gene transfer. *Nucleic Acids Res.* **39**, (2011).
 173. Kostyrko, K. *et al.* MAR-Mediated transgene integration into permissive chromatin and increased expression by recombination pathway engineering. *Biotechnol. Bioeng.* **114**, 384–396 (2017).
 174. Zahn-Zabal, M. *et al.* Development of stable cell lines for production or regulated expression using matrix attachment regions. *J. Biotechnol.* **87**, 29–42 (2001).
 175. Phi-Van, L. & Strätling, W. H. Dissection of the ability of the chicken lysozyme gene 5' matrix attachment region to stimulate transgene expression and to dampen position effects. *Biochemistry* **35**, 10735–10742 (1996).
 176. Girod, P. A., Zahn-Zabal, M. & Mermod, N. Use of the chicken lysozyme 5' matrix attachment region to generate high producer CHO cell lines. *Biotechnol. Bioeng.* **91**, 1–11 (2005).
 177. Sun, Q. L., Zhao, C. P., Chen, S. N., Wang, L. & Wang, T. Y. Molecular characterization of a human matrix attachment region that improves transgene expression in CHO cells. *Gene* **582**, 168–172 (2016).
 178. Arope, S., Harraghy, N., Pjanic, M. & Mermod, N. Molecular characterization of a human matrix attachment region epigenetic regulator. *PLoS One* **8**, (2013).
 179. WO2008023247A3 - Matrix attachment regions (mars) for increasing transcription and uses thereof - Google Patents. <https://patents.google.com/patent/WO2008023247A3>.
 180. US7129062B2 - Matrix attachment regions and methods for use thereof - Google Patents. <https://patents.google.com/patent/US7129062B2/en>.
 181. Wang, X. *et al.* Impact of Different Promoters on Episomal Vectors Harboring Characteristic Motifs of Matrix Attachment Regions. *Nat. Publ. Gr.* 1–10 (2016) doi:10.1038/srep26446.
 182. Zhang, J. H. *et al.* Distance effect of matrix attachment regions on transgene expression in stably transfected Chinese hamster ovary cells. *Biotechnol. Lett.* **36**, 1937–1943 (2014).
 183. Zhao, C. P. *et al.* Matrix attachment region combinations increase transgene expression in transfected

-
- Chinese hamster ovary cells. *Sci. Rep.* **7**, 1–7 (2017).
184. Ho, S. C. L., Mariati, Yeo, J. H. M., Fang, S. G. & Yang, Y. Impact of Using Different Promoters and Matrix Attachment Regions on Recombinant Protein Expression Level and Stability in Stably Transfected CHO Cells. *Mol. Biotechnol.* **57**, 138–144 (2014).
185. Grindley, N. D. F., Whiteson, K. L. & Rice, P. A. Mechanisms of Site-Specific Recombination. (2006) doi:10.1146/annurev.biochem.73.011303.073908.
186. Turan, S., Zehe, C., Kuehle, J., Qiao, J. & Bode, J. Recombinase-mediated cassette exchange (RMCE) - A rapidly-expanding toolbox for targeted genomic modifications. *Gene* **515**, 1–27 (2013).
187. Srirangan, K., Loignon, M. & Durocher, Y. The use of site-specific recombination and cassette exchange technologies for monoclonal antibody production in Chinese Hamster ovary cells: retrospective analysis and future directions. *Crit. Rev. Biotechnol.* **0**, 1–19 (2020).
188. Guye, P., Li, Y., Wroblewska, L., Duportet, X. & Weiss, R. Rapid, modular and reliable construction of complex mammalian gene circuits. *Nucleic Acids Res.* **41**, (2013).
189. Duportet, X. *et al.* A platform for rapid prototyping of synthetic gene networks in mammalian cells. *Nucleic Acids Res.* **42**, 13440–13451 (2014).
190. Landy, A. The λ Integrase Site-specific Recombination Pathway. doi:10.1128/microbiolspec.MDNA3-0051-2014.
191. Turan, S. *et al.* Recombinase-mediated cassette exchange (RMCE): Traditional concepts and current challenges. *J. Mol. Biol.* **407**, 193–221 (2011).
192. Groth, A. C. & Calos, M. P. Phage integrases: biology and applications. *J. Mol. Biol.* **335**, 667–678 (2004).
193. Sauer, B. Site-specific recombination: developments and applications. *Curr. Opin. Biotechnol.* **5**, 521–527 (1994).
194. Olorunniji, F. J., Rosser, S. J. & Stark, W. M. Site-specific recombinases: molecular machines for the Genetic Revolution. *Biochem. J.* **473**, 673–684 (2016).
195. Rajeev, L., Malanowska, K. & Gardner, J. F. Challenging a Paradigm: the Role of DNA Homology in Tyrosine Recombinase Reactions. *Microbiol. Mol. Biol. Rev.* **73**, 300–309 (2009).
196. Hirano, N., Muroi, T., Takahashi, H. & Haruki, M. Site-specific recombinases as tools for heterologous gene integration. *Appl Microbiol Biotechnol.* 227–239 (2011) doi:10.1007/s00253-011-3519-5.
197. Tian, X. & Zhou, B. Strategies for site-specific recombination with high efficiency and precise spatiotemporal resolution. *J. Biol. Chem.* **296**, 100509 (2021).
198. Rice, P. A. Serine Resolvases. *Microbiol. Spectr.* **3**, (2015).
199. Smith, M. C. M., Brown, W. R. A., McEwan, A. R. & Rowley, P. A. Site-specific recombination by ϕ C31 integrase and other large serine recombinases. *Biochem. Soc. Trans.* **38**, 388–394 (2010).
200. O’Gorman, S., Fox, D. T. & Wahl, G. M. Recombinase-Mediated Gene Activation and Site-Specific Integration in Mammalian Cells. *Science (80-)*. **251**, 1351–1355 (1991).

-
201. Kawabe, Y. *et al.* Repeated integration of antibody genes into a pre-selected chromosomal locus of CHO cells using an accumulative site-specific gene integration system. *Cytotechnology* **64**, 267–279 (2012).
 202. Ghosh, P., Kim, A. I. & Hatfull, G. F. The orientation of mycobacteriophage Bxb1 integration is solely dependent on the central dinucleotide of attP and attB. *Mol. Cell* **12**, 1101–1111 (2003).
 203. Snoeck, N. *et al.* Serine integrase recombinational engineering (SIRE): A versatile toolbox for genome editing. *Biotechnol. Bioeng.* **116**, 364–374 (2019).
 204. Baser, B., Spehr, J., Büssow, K. & van den Heuvel, J. A method for specifically targeting two independent genomic integration sites for co-expression of genes in CHO cells. *Methods* **95**, 3–12 (2016).
 205. Gaidukov, L. *et al.* A multi-landing pad DNA integration platform for mammalian cell engineering. *Nucleic Acids Res.* **46**, 4072–4086 (2018).
 206. Koduri, R. K., Miller, J. T. & Thammana, P. An efficient homologous recombination vector pTV(I) contains a hot spot for increased recombinant protein expression in Chinese hamster ovary cells. *Gene* **280**, 87–95 (2001).
 207. Baumann, M. *et al.* Preselection of recombinant gene integration sites enabling high transcription rates in CHO cells using alternate start codons and recombinase mediated cassette exchange. *Biotechnol. Bioeng.* **114**, 2616–2627 (2017).
 208. Shin, S. *et al.* Comprehensive Analysis of Genomic Safe Harbors as Target Sites for Stable Expression of the Heterologous Gene in HEK293 Cells. *ACS Synth. Biol.* **9**, 1263–1269 (2020).
 209. Mayrhofer, P. *et al.* Accurate comparison of antibody expression levels by reproducible transgene targeting in engineered recombination-competent CHO cells. *Appl. Microbiol. Biotechnol.* **98**, 9723–9733 (2014).
 210. Baer, A. & Bode, J. Coping with kinetic and thermodynamic barriers: RMCE, an efficient strategy for the targeted integration of transgenes. *Curr. Opin. Biotechnol.* **12**, 473–480 (2001).
 211. Qiao, J., Oumard, A., Wegloehner, W. & Bode, J. Novel Tag-and-Exchange (RMCE) Strategies Generate Master Cell Clones with Predictable and Stable Transgene Expression Properties. *J. Mol. Biol.* **390**, 579–594 (2009).
 212. Kameyama, Y., Kawabe, Y., Ito, A. & Kamihira, M. An accumulative site-specific gene integration system using Cre recombinase-mediated cassette exchange. *Biotechnol. Bioeng.* **105**, 1106–1114 (2010).
 213. Pristovšek, N. *et al.* Systematic Evaluation of Site-Specific Recombinant Gene Expression for Programmable Mammalian Cell Engineering. *ACS Synth. Biol.* **8**, 757–774 (2019).
 214. Jusiak, B. *et al.* Comparison of Integrases Identifies Bxb1-GA Mutant as the Most Efficient Site-Specific Integrase System in Mammalian Cells. *ACS Synth. Biol.* **8**, 16–24 (2019).
 215. Inniss, M. C. *et al.* A novel Bxb1 integrase RMCE system for high fidelity site-specific integration of mAb expression cassette in CHO Cells. *Biotechnol. Bioeng.* **114**, 1837–1846 (2017).
 216. Xu, Z. *et al.* Accuracy and efficiency define Bxb1 integrase as the best of fifteen candidate serine

-
- recombinases for the integration of DNA into the human genome. *BMC Biotechnol.* **13**, 1–17 (2013).
217. Scarcelli, J. J., Shang, T. Q., Iskra, T., Allen, M. J. & Zhang, L. Strategic deployment of CHO expression platforms to deliver Pfizer’s Monoclonal Antibody Portfolio. *Biotechnol. Prog.* **33**, 1463–1467 (2017).
218. Rose, T. *et al.* A robust RMCE system based on a CHO-DG44 platform enables efficient evaluation of complex biological drug candidates. *BMC Proc.* **2013 76 7**, 1–3 (2013).
219. Sergeeva, D., Lee, G. M., Nielsen, L. K. & Grav, L. M. Multi-copy targeted integration for accelerated development of high-producing CHO cells Multi-copy targeted integration for accelerated development of high- producing CHO cells. *ACS Synth. Biol.* (2020) doi:10.1021/acssynbio.0c00322.
220. Ng, D. *et al.* Development of a targeted integration Chinese hamster ovary host directly targeting either one or two vectors simultaneously to a single locus using the Cre/Lox recombinase-mediated cassette exchange system. *Biotechnol. Prog.* 1–3 (2021) doi:10.1002/btpr.3140.
221. Whittle, N. *et al.* Expression in COS cells of a mouse—human chimaeric B72.3 antibody. *Protein Eng. Des. Sel.* **1**, 499–505 (1987).
222. United States Patent US007129062B2.
223. pDsRed-Express-1 Sequence and Map. https://www.snapgene.com/resources/plasmid-files/?set=fluorescent_protein_genes_and_plasmids&plasmid=pDsRed-Express-1.
224. Mammalian Expression Vectors.
225. Girod, P.-A., Zahn-Zabal, M. M. & Mermod, N. Mar Elements as Tools to Increase Protein Production by CHO Cells. *Anim. Cell Technol. Meets Genomics* 411–415 (2005) doi:10.1007/1-4020-3103-3_81.
226. Kim, M., O’Callaghan, P. M., Droms, K. A. & James, D. C. A mechanistic understanding of production instability in CHO cell lines expressing recombinant monoclonal antibodies. *Biotechnol. Bioeng.* **108**, 2434–2446 (2011).
227. Tihanyi, B. & Nyitray, L. Recent advances in CHO cell line development for recombinant protein production. *Drug Discov. Today Technol.* **38**, 25–34 (2020).
228. Lonza. A Fully Integrated Toolbox for Therapeutic Protein Expression The GS Xceed[®] Gene Expression System Enabling a healthier world.
229. Reinhart, D., Damjanovic, L., Kaisermayer, C. & Kunert, R. Benchmarking of commercially available CHO cell culture media for antibody production. *Appl. Microbiol. Biotechnol.* **99**, 4645–4657 (2015).
230. Young, J. D. Metabolic flux rewiring in mammalian cell cultures. *Curr. Opin. Biotechnol.* **24**, 1108–1115 (2013).
231. Templeton, N., Dean, J., Reddy, P. & Young, J. D. Peak antibody production is associated with increased oxidative metabolism in an industrially relevant fed-batch CHO cell culture. *Biotechnol. Bioeng.* **110**, 2013–2024 (2013).
232. Charaniya, S. *et al.* Mining manufacturing data for discovery of high productivity process characteristics. *J. Biotechnol.* **147**, 186–197 (2010).

-
233. Mulukutla, B. C., Khan, S., Lange, A. & Hu, W. S. Glucose metabolism in mammalian cell culture: New insights for tweaking vintage pathways. *Trends Biotechnol.* **28**, 476–484 (2010).
234. Altamirano, C., Cairó, J. J. & Gòdia, F. Decoupling cell growth and product formation in Chinese hamster ovary cells through metabolic control. *Biotechnol. Bioeng.* **76**, 351–360 (2001).
235. Martínez, V. S. *et al.* Flux balance analysis of CHO cells before and after a metabolic switch from lactate production to consumption. *Biotechnol. Bioeng.* **110**, 660–666 (2013).
236. Ma, N. *et al.* A single nutrient feed supports both chemically defined NS0 and CHO fed-batch processes: Improved productivity and lactate metabolism. *Biotechnol. Prog.* **25**, 1353–1363 (2009).
237. Barnes, L. M. & Dickson, A. J. Mammalian cell factories for efficient and stable protein expression. *Curr. Opin. Biotechnol.* **17**, 381–386 (2006).
238. Schulze, S. & Lammers, M. The development of genome editing tools as powerful techniques with versatile applications in biotechnology and medicine: CRISPR/Cas9, ZnF and TALE nucleases, RNA interference, and Cre/loxP. *ChemTexts* **7**, 1–18 (2021).
239. Gupta, S. K. & Shukla, P. Gene editing for cell engineering: trends and applications. *Crit. Rev. Biotechnol.* **37**, 672–684 (2017).
240. Crawford, Y. *et al.* Fast identification of reliable hosts for targeted cell line development from a limited-genome screening using combined ϕ C31 integrase and CRE-Lox technologies. *Biotechnol. Prog.* **29**, 1307–1315 (2013).
241. Wang, X. *et al.* Accumulative scFv-Fc antibody gene integration into the hprt chromosomal locus of Chinese hamster ovary cells. *J. Biosci. Bioeng.* **124**, 583–590 (2017).
242. Gaj, T., Gersbach, C. A. & Barbas, C. F. ZFN, TALEN, and CRISPR/Cas-based methods for genome engineering. *Trends Biotechnol.* **31**, 397–405 (2013).
243. Phan, Q. V., Contzen, J., Seemann, P. & Gossen, M. Site-specific chromosomal gene insertion: FLP recombinase versus Cas9 nuclease. *Sci. Rep.* **7**, 1–12 (2017).
244. Lee, J. S., Grav, L. M., Lewis, N. E. & Kildegaard, H. F. CRISPR/Cas9-mediated genome engineering of CHO cell factories: Application and perspectives. *Biotechnol. J.* **10**, 979–994 (2015).
245. Zhang, H. X., Zhang, Y. & Yin, H. Genome Editing with mRNA Encoding ZFN, TALEN, and Cas9. *Mol. Ther.* **27**, 735–746 (2019).
246. Zhang, L. *et al.* Recombinase-mediated cassette exchange (RMCE) for monoclonal antibody expression in the commercially relevant CHOK1SV cell line. *Biotechnol. Prog.* **31**, 1645–1656 (2015).
247. Tevelev, B. *et al.* Genetic rearrangement during site specific integration event facilitates cell line development of a bispecific molecule. *Biotechnol. Prog.* 1–15 (2021) doi:10.1002/btpr.3158.
248. Nehlsen, K. *et al.* Recombinant protein expression by targeting pre-selected chromosomal loci. *BMC Biotechnol.* **9**, 1–12 (2009).
249. Zhou, S., Chen, Y., Gong, X., Jin, J. & Li, H. Site-specific integration of light chain and heavy chain genes

-
- of antibody into CHO-K1 stable hot spot and detection of antibody and fusion protein expression level. *Prep. Biochem. Biotechnol.* **49**, 384–390 (2019).
250. Harraghy, N., Gaussin, A. & Mermoud, N. Sustained Transgene Expression Using MAR Elements. *Curr. Gene Ther.* **8**, 353–366 (2008).
251. Goetze, S. *et al.* Performance of Genomic Bordering Elements at Predefined Genomic Loci. *Mol. Cell. Biol.* **25**, 2260–2272 (2005).
252. Šenigl, F., Plachý, J. & Hejnar, J. The core element of a CpG island protects avian sarcoma and leukosis virus-derived vectors from transcriptional silencing. *J. Virol.* **82**, 7818–7827 (2008).
253. Ho, S. C. L., Mariati, Yeo, J. H. M., Fang, S. G. & Yang, Y. Impact of Using Different Promoters and Matrix Attachment Regions on Recombinant Protein Expression Level and Stability in Stably Transfected CHO Cells. *Mol. Biotechnol.* **57**, 138–144 (2014).
254. Gaidukov, L. *et al.* A multi-landing pad DNA integration platform for mammalian cell engineering. *Nucleic Acids Res.* **46**, 4072–4086 (2018).
255. Hilliard, W. & Lee, K. H. Systematic identification of safe harbor regions in the CHO genome through a comprehensive epigenome analysis. *Biotechnol. Bioeng.* **118**, 659–675 (2021).
256. Jia, Y. L., Guo, X., Wang, X. C. & Wang, T. Y. Human genome-derived TOP1 matrix attachment region enhances transgene expression in the transfected CHO cells. *Biotechnol. Lett.* **41**, 701–709 (2019).
257. Ley, D. *et al.* MAR Elements and Transposons for Improved Transgene Integration and Expression. *PLoS One* **8**, (2013).
258. Jusiak, B. *et al.* Comparison of Integrases Identifies Bxb1-GA Mutant as the Most Efficient Site-Specific Integrase System in Mammalian Cells. *ACS Synth. Biol.* **8**, 16–24 (2019).
259. Shearwin, K. E., Callen, B. P. & Egan, J. B. Transcriptional interference—a crash course. *Trends Genet* **21**, 339–345 (2005).
260. Garrick, D., Fiering, S., Martin, D. I. K. & Whitelaw, E. Repeat-induced gene silencing in mammals. *Nat. Genet.* **18**, 56–59 (1998).
261. Coulet, M., Kepp, O., Kroemer, G. & Basmaciogullari, S. Metabolic Profiling of CHO Cells during the Production of Biotherapeutics. *Cells* **11**, 1–21 (2022).

8 Appendix

8.1 Supplementary figures

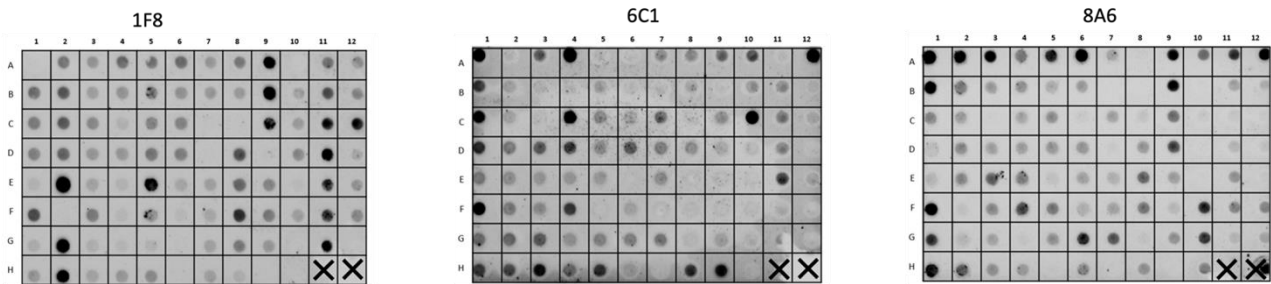


Figure S1 Dot-blot analyses for msAb screening using anti-IgG (H+L) detection antibody.

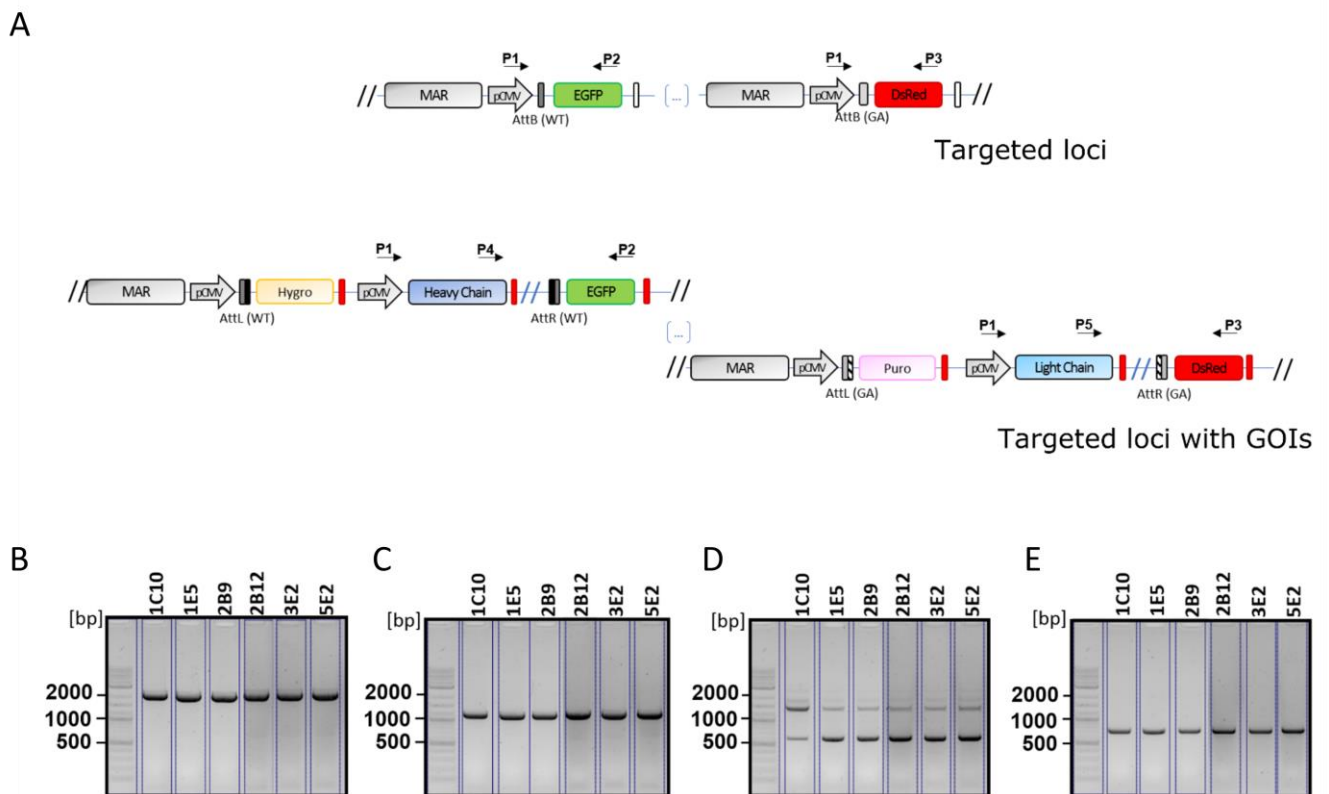
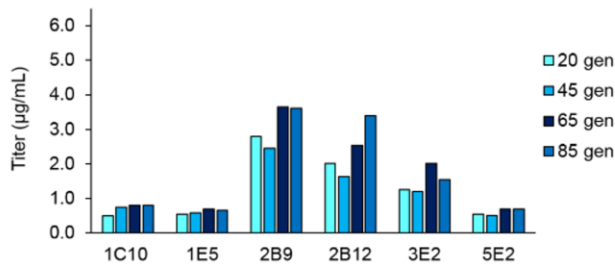


Figure S2 Characterization of msAb expressing clones and stability tests. A) Set up of genomic PCR for evaluation of SSI on DNA extracted by msAb expressing clones. B) Results of genomic PCR using primers P1-P2 (expected amplicon size for integrated HC: 2 kb; expected amplicon size for unoccupied LP_EGFP: 0.5 kb). C) Results of genomic PCR using primers P4-P2 (expected amplicon size for integrated HC: 1.2 kb). D) Results of genomic PCR using primers P1-P3 (expected amplicon size for integrated LC: 1.5kb; expected amplicon size for unoccupied LP_EGFP: 0.6kb). E) Results of genomic PCR using primers P5-P3 (expected amplicon size for integrated LC: 0.8kb).

A



B

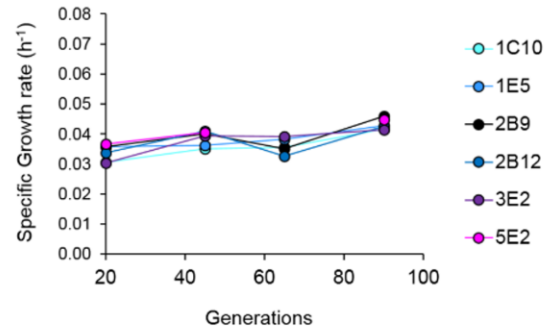
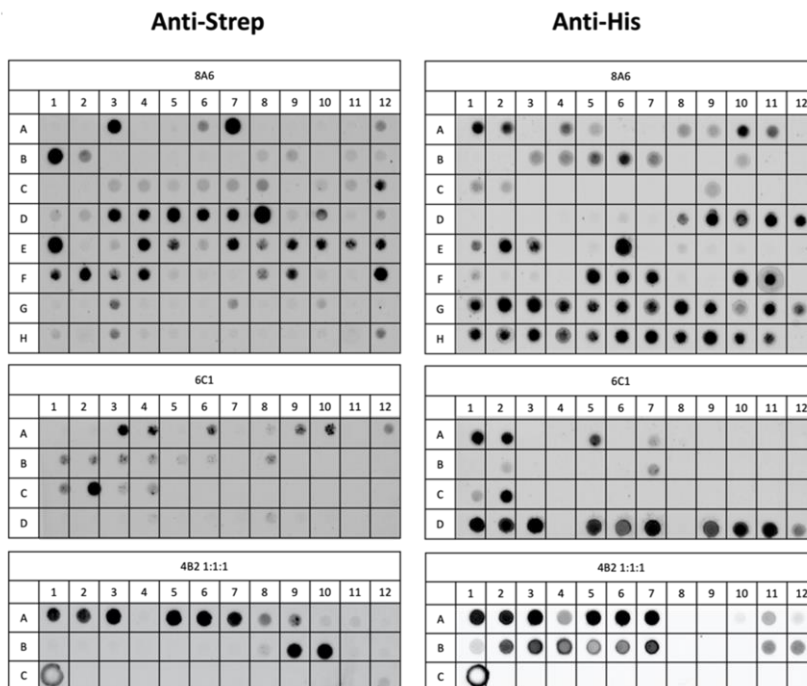


Figure S3 Stability test for mAb expressing clones over 85 generations. Clones were tested for antibody titer (A) and growth(B). Bars represent antibody titer evaluated on day 7 of fed batch cultures.

A



B

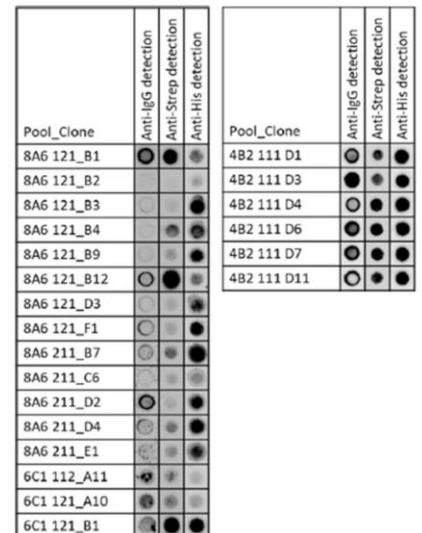


Figure S4 Dot-blot analyses for bsAb screening. A) dot-blot analyses of picked colonies using Anti-Strep and Anti-His detection antibodies. B) dot-blot analyses of productive clones using Anti-Strep, Anti-His, anti IgG (H+L) detection antibodies.

8.2 Supplementary tables

Table S1. Data summary for LPs copy number for clones with and without MAR

| Clone | LP_EGFP copy number | LP_DsRed copy number | Ratio LP_DsRed/LP_EGFP |
|-------------------|---------------------|----------------------|------------------------|
| 1F8 cMAR clone | 5.2 | 36.6 | 7.0 |
| 4B2 cMAR clone | 27.8 | 38.6 | 1.4 |
| 4F9 cMAR clone | 17.2 | 86.5 | 5.0 |
| 6C1 cMAR clone | 9.9 | 54.5 | 5.5 |
| 8A6 cMAR clone | 18.5 | 92.8 | 5 |
| 3A10 w/oMAR clone | 5.3 | 7.8 | 1.5 |
| 3B10 w/oMAR clone | 6.3 | 6.8 | 1.1 |
| 4C9 w/oMAR clone | 5.1 | 10.9 | 2.1 |

Table S2. Data summary for GOI copy numbers for msAb expressing clones

| Clone | HC copy number | LC copy number | Ratio HC:LC | % occupied LP_EGFP | % occupied LP_DsRed |
|-------|----------------|----------------|-------------|--------------------|---------------------|
| 1C10 | 4.1 | 4.8 | 0.8 | 78.8% | 13.1% |
| 1E5 | 1.9 | 1.7 | 1.1 | 36.5% | 4.6% |
| 2B9 | 7.8 | 1.9 | 4.1 | 42.2% | 2% |
| 2B12 | 18.2 | 8.9 | 2 | 98.4% | 9.6% |
| 3E2 | 10.6 | 6.9 | 1.5 | 57.3% | 7.4% |
| 5E2 | 3.4 | 6.2 | 0.5 | 34.3% | 11.4% |

Table S3. Data summary for GOI copy numbers for bsAb expressing clones. Individual gene copy numbers for knob heavy chain (kHC), hole heavy chain (hHC) and common light chain gene (cLC)

| Clone | kHC copy number | hHC copy number | cLC copy number | % occupied LP_EGFP | % occupied LP_DsRed |
|-------|-----------------|-----------------|-----------------|--------------------|---------------------|
| D7 | 20.8 | 7.05 | 26.03 | 100% | 67.4% |
| D11 | 19.05 | 6.64 | 6.84 | 92.4% | 17.7% |

8.3 Protein sequence

EGFP:

MVSKGEELFTGVVPILVELDGDVNGHKFSVSGEGEGDATYGKLT LKFICTTGKLPVPWPTLVTTLTLYGVQCFSRYPDHMKQHD
FFKSAMPEGYVQERTIFFKDDGNYKTRAEVKFEGDTLVNRIELKGI DFKEDGNILGHKLEYNNSHNVIYIMADKQKNGIKVNFKI
RHNIEDGSVQLADHYQNTPIGDGPVLLPDNHYLSTQSALS KDPNEKRDHMLLEFVTAAGITLGMDELYK

DsRed express 1:

MASSEDVKEFMRFKVRMEGSVNGHEFEIEGEGEGRYPYEGTQTAKLKVTKGGPLPFAWDILSPQFQYGSKVYV KHPADIPDYK
KLSFPEGFKWERVMNFEDGGVVTQDSSLQDGSFIYKVKFIGVNFPSDGPVMQKKTMGWEASTERLYPRDGV LKGEIHKAL
KLKDGGHYLVFESYIMAKKPVQLPGYYYYVDSKLDITSHNEDYTIVEQYERAEGRHHLFL

MsAb-Fer light chain:

LPVLTQPHSVSESPGKTVTISCTRSSGSIASNYVQWYQQRPGSAPTTVIYEDNQRPSGVPDRFSGSIDSSNSASLTISGLKTEDE
ADYYCQSYDSSNPVVFVGGGKTLTVLGQPKAAPSVTLPFSSSEELQANKATLVCLISDFYPGAVTVAWKADSSPVKAGVETTPS
KQSNNKYAASSYLSLTPEQWKSHRSYSCQVTHEGSTVEKTVAPTECS

MsAb-Fer heavy chain:

QVQLVESGGGVVQPGRSLRLSCAASGFTFSSYAMSWVRQAPGKGLEWVSAISGSGGSTYYADSVKGRFTISRDN SKNTLYLQ
MNSLRAEDTAVYYCTTGGYWGQGT LTVSSASTKGPSVFPLAPSSKSTSGGTAALGCLVKDYFPEPVTVSWNSGALTSGVHTF
PAVLQSSGLYSLSSVTVPSSSLGTQTYICNVNHKPSNTKVDKKVEPKSCDKTHTCPPCPAPELLGGPSVFLFPPKPKDTLMISRT
PEVTCVVVDVSHEDPEVKFNWYVDGVEVHNAKTKPREEQYNSTYRVVSVLTVLHQD WLNGKEYKCKVSNKALPAPIEKTISKA
KGQPREPQVYTLPPSRDELTKNQVSLTCLVKGFYPSDIAVEWESNGQPENNYKTTTPVLDSDGSFFLYSKLTVDKSRWQQGNV
FSCSVMHEALHNHYTQKLSLSPGK

BsAb-Fer common light chain:

SYELMQPPSVSVSPGQTARITCSGGYDGSYYYGWYQQKPGQAPVTVIYDNTNRPSGIPERFSGSNSGNTITLTISGVQAEDEA
DYICGGYDRSGGIFGGGKTLTVLGQPKANPTVTLFPPSSEELQANKATLVCLISDFYPGAVTVAWKADGSPVKAGVETTKPSKQ
SNNKYAASSYLSLTPEQWKSHRSYSCQVTHEGSTVEKTVAPTECS

BsAb-Fer knob heavy chain:

EVQLLESQGGGLVQPGGSLRLSCAASGFTFSSHGMLWVRQAPGKGLEWVGGISTDGSSTSYGAPVKGRFTISRDN SKNTVYLQ
MNSLRAEDTAVYYCAKDAYRCRNCAEDIDAWGQGT LTVSSASTKGPSVFPLAPSSKSTSGGTAALGCLVKDYFPEPVTVSWN
SGALTSGVHTFPAVLQSSGLYSLSSVTVPSSSLGTQTYICNVNHKPSNTKVDKRV EPKSCDKTHTCPPCPAPEAAGGPSVFLFP
PKPKDTLMISRTPEVTCVVVDVSHEDPEVKFNWYVDGVEVHNAKTKPREEQYNSTYRVVSVLTVLHQD WLNGKEYKCKVSNK
ALPAPIEKTISKAKGQPREPQVYTLPPSREEMTKNQVSLWCLVKGFYPSDIAVEWESNGQPENNYKTTTPVLDSDGSFFLYSKLT
VDKSRWQQGNV FSCSVMHEALHNHYTQKLSLSPGGGWSHPQFEKGGGSGGGGSAWVSHHPQFEK

Bsab-Fer hole heavy chain:

EVQLLESQGGGLVQPGGSLRLSCAASGFTFSSYNMGWVRQAPGKGLEFVASIDDDGSFTHYGA AVKGRVTISRDN SKNTLYLQ
MNSLRAEDTAVYYCAKSSINGYRCSGGLCVPIYITGNIDAWGQGT LTVSSASTKGPSVFPLAPSSKSTSGGTAALGCLVKDYFPE
PVTVSWNSGALTSGVHTFPAVLQSSGLYSLSSVTVPSSSLGTQTYICNVNHKPSNTKVDKRV EPKSCDKTHTCPPCPAPEAAG
GPSVFLFPPKPKDTLMISRTPEVTCVVVDVSHEDPEVKFNWYVDGVEVHNAKTKPREEQYNSTYRVVSVLTVLHQD WLNGKE
YKCKVSNKALPAPIEKTISKAKGQPREPQVYTLPPSREEMTKNQVSLSCAVKGFYPSDIAVEWESNGQPENNYKTTTPVLDSDG
SFFLVSKLTVDKSRWQQGNV FSCSVMHEALHNRFQKLSLSPGGGSHHHHHH

8.4 MAR sequences

Chicken 5' lysozyme MAR:

TCTACAAAACAATATATTTCCAAATGAAAAAAAAAATCTGATAAAAAGTTGACTTTAAAAAAGTATCAATAAATGTATGCAT
TTCTACTAGCCTTAACTCTGCATGAAGTGTTTGATGAGCAGATGAAGACAACATCATTCTAGTTTCAGAAATAATAAC
AGCATCAAACCCGAGCTGTAECTCACTGAGCTCACGTTAAGTTTTGATGTGTGAATATCTGACAGAAGTACATAATGA
GCACTGCAAGGAAATCAGACAAGTCAAATGAAGACAGACAAAAGTATTTTTAATAAAAAATGGTCTTTATTTCTTCAA
TACAAGGTAACTACTATTGCAGTTTAAAGACCAACACAAAAGTTGGACAGCAAATTGCTTAACAGTCTCCTAAAGGCTGA
AAAAAAGGAACCCATGAAAGCTAAAAGTTATGCAGTATTTCAAGTATAACATCTAAAAATGATGAAACGATCCCTAAAGG
TAGAGATTAECTAAGTACTTCTGCTGAAAATGTATTAATAATCCGCGAGTTGCTAGGATACCATCTTACCTGTTGAGAAATA
CAGGTCTCCGGCAACGCAACATTCAGCAGACTCTTTGGCCTGCTGGAATCAGGAACTGCTTACTATATACACATATAAAT
CCTTTGGAGTTGGGCATTCTGAGAGACATCCATTTCTGACATTTTGCAGTGCAACTCTGCATTCCAACCTCAGACAAGCTCC
CATGCTGTATTTCAAAGCCATTTCTTGAATAGTTTACCCAGACATCCTTGTGCAAATTTGGGAATGAGGAAATGCAATGGTA
CAGGAAGACAATACAGCCTTATGTTTAGAAAGTCAGCAGCGCTGGTAATCTTCATAAAAAATGTAAGTGTTCCTTCAAATAGG
AATGTATTTCACTTGTAACACCTGGTCTTTTTATATTACTTTTTTTTTTTTTAAGGACACCTGCACTAATTTGCAATCAC
TTGTATTTATAAAGCACACGCACTCCTCATTTTCTTACATTTGAAGATCAGCAGAATGTCTCTTTCATAATGTAATAATCTT
ATGCACAGTTTAAAATATTTTCTATTACAAAATACAGTACACAAGAGGGTGAGGCCAAAGTCTATTACTTGAATATATTCC
AAAGTGTGAGCACTGGGGGTGTAATAATTACATTACATGGTATGAATAGGCGCAATCTTTTACAACCTGAAATGCTCGATT
CATTGGGATCAAAGGTAAGTACTGTTTACTATCTTCAAGAGACTTCAATCAAGTCGGTGTATTTCCAAAGTAGCTTAAAAG
ATTGAAGCACAGACACAGGCCACACCAGAGCCTACACCTGCTGCAATAAGTGGTGTATAGAAAGGATTGAGGAACTAA
CAAGTGCATAATTTACAAATAGAGATGCTTTATCATACTTTGCCAACATGGGAAAAAAGACATCCCATGAGAATATCCAA
CTGAGGAACCTTCTGTTTCATAGTAACTCATCTACTACTGCTAAGATGGTTTAAAAGTACCCAGCAGGTGAGATATGTT
CGGGAGGTGGCTGTGTGGCAGCGTGTCCCAACACGACACAAAGCACCCACCCCTATCTGCAATGCTCACTGCAAGGCA
GTGCCGTAACAGCTGCAACAGGCATCACTTCTGCATAAATGCTGTGACTCGTTAGCATGCTGCAACTGTGTTTAAAACCT
ATGCACTCCGTTACCAAATAATTTAAGTCCAAATAAATCCATGCAGCTTGCTTCTATGCCAACATATTTTAGAAAGTAT
TCATTCTTTTAAAGAATATGCACGTGGATCTACACTTCTGGGATCTGAAGCGATTTATACCTCAGTTGCAGAAGCAGTTT
AGTGTCTGGATCTGGGAAGGCAGCAGCAAACGTGCCGTTTTACATTTGAACCCATGTGACAACCCGCCTTACTGAGCA
TCGCTCTAGGAAATTTAAGGCTGTATCCTTACAACACAAGAACCAACGACAGACTGCATATAAAAATCTATAAATAAAAAAT
AGGAGTGAAGTCTGTTTGACCTGTACACACAGAGCATAGAGATAAAAAAAAAAAGGAAATCAGGAATTACGTATTTCTATA
AATGCCATATATTTTACTAGAAACACAGATGACAAGTATATAACAACATGTAATCCGAAGTTATCAACATGTTAACTAGG
AAAACATTTACAAGCATTGGGTATGCAACTAGATCATCAGGTAATAAATCCCATTAGAAAAATCTAAGCCTCGCCAGTTT
CAAAGGAAAAAACAGAGAACGCTCACTACTTCAAAGGAAAAAATAAAGCATCAAGCTGGCCTAACTTAATAAGG
TATCTCATGTAACAACAGCTATCCTAGCTTTCAAGCCACACTATAAATAAAAACCTCAAGTTCGGATCAACGTTTTCCATAA
TGCAATCAGAACCAAAGGCATTGGCACAGAAAGCAAAAAGGGAATGAAAGAAAAGGGCTGTACAGTTTCCAAAAGGTTT
TTCTTTTGAAGAAATGTTTCTGACCTGTCAAACATAACAGTCCAGTAGAAATTTTACTAAGAAAAAAGAACACCTTACTTAA
AAAAAACAACAAAAAACAGGCAAAAAACCTCTCCTGTCACTGAGCTGCCACCACCAACCACCTGCTGTG
GGCTTTGTCTCCAAGACAAAGGACACACAGCCTTATCCAATATTCAACATTACTTATAAAAAACGCTGATCAGAAGAAATA
CCAAGTATTTCTCAGAGACTGTTATATCCTTTTATCGGCAACAAGAGATGAAATACAACAGAGTGAATATCAAAGAAGG
CGGCAGGAGCCACCGTGGCACCATCACCAGGCGAGTGCAGTGCCCAACTGCCGTTTTCTGAGCACGCATAGGAAGCCGTC
AGTCACATGTAATAAACCAAACCTGGTACAGTTATATTATCGATCC

Human 1-68 MAR:

TCGACTCTAGATTATACCAACCTCATAAATAAGAGCATATATAAAGCAAATGCTCTTATCTTGCAGATCCCTGAACTGA
GGAGGCAAGATCAGTTTGGCAGTTGAAGCAGCTGGAATCTGCAATTCAGAGAATCTAAGAAAAGACAACCCTGAAGAGA
GAGACCCAGAAACCTAGCAGGAGTTTCTCAAACATTCAAGGCTGAGGGATAAATGTTACATGCACAGGGTGAGCCTCC
AGAGGCTTGTCCATTAGCAACTGCTACAGTTTTCATTATCTCAGGGATCACAGATTGTGCTACCTATTGCCTACCATCTGAAA
ACAGTTGCTTCTATATTTTATCCAGTTTAAATATTTTAAACCAAGAAGGTTAATCTGGCACCAGCTATCCGTTGTGAG
TGGATGTGAAAGTACCAATTCATTCTGTTTTACTATTAATCTTCTTGCCTAATATGTATCAGTAGGTGGCTTGTGCTA
GGAAATATTAATGAATGGCATGTTTTCATAGGTTGTGTTTAAAGTTGTTTTTGGAGTTAAATCTTTCTTAAATAACTTTCT
GATGTCAAACACTTAGAAGTCATGGTGTGAAACATCTATATAGGGTTGGATCTAAAATAGCTTCTTAACTTTCTAAC
CACTGTTTTTGTGTTGTTTTTAACTAAGCATCCAGTTTGGGAAATCTGAATTAGGGGAATCATAAAGGTTTTCATTTT
AGCTGGGCCACATAAGGAAAGTAAGAaATCAAATGTAAAAATCGTTAAGAAGTCTATCCCATCTGAAGTGTGGGTTAG

GTGCCTCTTCTCTGTGCTCCCTAACATCCTATTTTATCTGTATATATATATATTCTTCAAATATCCATGGGAAAAAATC
TGATCATAAAAAATTTTAGGCTGGGAGTGGTGGCTCACGCCTGTAATCCCAGCACTTTGGGAGGCTGAGGTGGGCGGA
TCATGAGGTCAAGAGATCGAGACCATCCTGACCAATATGGTGAACCCCATCTCTACTAAAGATACAAAATATTAGCTG
GACGTGGTGGCACGTGCCTGTAGTCCCAGCTACTCGGGAGGCTGAGGCAGGAGAACGGCTTGAACCCAGGAGGTGGAG
GTTGCAGTGAGCTGAGATCGCGCCACTGCACTCCAGCCTGGGCGACAGAGCGAGACTCTGTCTCAAAAAAAAAATATATA
TATATATATATACACATATATATATAAAATATATATATATACACACATATATATATAAAATATATATATACACACATAT
ATATAAAATATATATATATACACACATATATATAAAATATATATATATACACACATATATATAAAATATATATATACACACATAT
ATATAAAATATATATATATACACACATATATATAAAATATATATATATACACACATATATATAAAATATATATATACACACATATAT
ATAAAATATATATATATACACACATATATATAAAATATATATATATACACACATATATATAAAATATATATATATACACACATATATAT
AAAATATATATATACACACATATATATAAAATATATATATATACACACATATATAAAATATATATATATACACACATATATAAAAT
ATATATATACACATATATATAAAATATATATATATACACATATATATAAAATATATATATACACACATATATATAAAATATATATAT
ACACACATATATATAAAATATATATATATACACATATATATAAAATATATATATATACACATATATATAAAATATATATATATACAC
ATATATATAAAATATATATACACACATATATATAAAATATATATATATACACACATATATATAAAATATATATATATACACATATAT
ATAAAATATATATATACACATATATATAAAATATATATATACACATATATATAAAATATATATATATATATATATATATATATATAT
CCAATTGCTCACTTTGTGGATGAGAAAAAGAAGTAGTTAGAGGTCAAGTAACTTGGCCTACATCTTTTCTCAAGATTGTA
AACTCCTAGTGAGCAATAACCACATCTTCATTTTCTTTGTATAAAACAAGAAAGTTAGCATGAAAAAGGTAAGTCAATTAC
AAATGTGTTGGATTGAATTGAAGACCCTTGAAGGGGATTTGTACCTGAGGATCTCTTTCTTTTGGCCATATTGTTCAAT
GGACAAAATTTAGCCTTGAAGGCAGGCCGATTTGAGGTTAATACTACCTTTACCACTTGATAGCTATGTGACCTTGGCCA
TGTGGTTTCAACAGTCTGAACCTCATTTTCTCTGTGTATGTGTGGTCTCCTTACAAGTTTGTGAAAAATGTGAAGTCTTA
GCCATGATAGCCCAATATAACAGGCTAAATGATAATAGGTTTATGTTCTTTTCTTTTATATTCTCAGATAAGCACTGTCCAA
GTTTGAAGTGTGTTGAGGTCTCGCCTGATTTGGATTGTTTGAAGTTTATGCTATTCTTTGAATTCTTTGAGCTGTTCTGAAGC
AGTGTATCATGAACAAAAACATCCCCAGTTCAGTCCAAACCCTGGTTACATATCATTCTTATGCCATGTTATAACCAGTTT
GAGAGTGTCCCTCTGTTATTGCATTTAAGTTTCAGCCTCACACAGAAATTCAGCAGCCAATTTCTAAGCCCTAAGCATAAAA
ATCTGGGGTGGGGGGGGGGGATGGCCTGAAGAGCAGCATTATGAATAGCACCATTATAATTAATGATCTCTCAGGAAGA
TTTACAATCACAGGTAGCAGATAAAAACAAATAGTACTGCTTCTGCACTTCCCCTCTTTTATTGCTATGAAATTTTATGGG
AAATCAGTCCAGTGAAAAATGTAAGCTCTTAATCTTTCCAGAAATCCTACCTCATTTGATGAATACTTTGAGGGAATGAA
TTAGAGCATTTTTTTCTTTTATAGTCTACTTCGCATTTACGAAGTGAGGACGGTAGCTTAGGCTGCCTGGCCAAGTATGA
GAAGGTCAGAGGCATTTTATAGAGACCTCTGTTGTCTTTTATTGTTTCCACAAGGCAAGTAATTTCCAACAAATC
AGTGTCTTCATTAGTAATAAGATTATTAACAACAATAATAGTCATAGTAACTATTGAGTCCATTATATATCAGGC
ATTCTACAAGTACTTTATATACATCTGAGTAAACCTCACACAATTCTACAGGGAGGATTTCTATCCCATTAAACAATA
AGGAAACGAAGTCCAAGTAAATTAACCTGCCCCAAGGTCACACAGATAGTACCTGGCAGAACAGGAATTTAAACCTAAAT
TGCCAACTCCAAAAGCAGCCTTCTATTTGTTATAAATGCTGCCTCTCATTATCACATATTTTATTATTAACAACAACAACA
TACCAATTAGCaTAAGATACAATAACAACCAGATAATCATGATGACAACAGTAATTGTTATACTATTATAATAAAATAGATG
TTTTGTATGTTACTATAATCTTGAATTTGAATAGAAATTTGCATTTCTGAAAGCATGTTCTGTCTAATATGATTCTGTA
TCTATTAATAAGTACTACATCTAGAG

8.5 List of figures

| | |
|--|-----|
| Figure 1. Antibody structure and immunoglobulin classes. | 6 |
| Figure 2 From murine to fully human antibodies..... | 8 |
| Figure 3 Overview of bispecific format..... | 10 |
| Figure 4 Optimization areas and parameters in upstream processing | 12 |
| Figure 5 Cell line development scheme. | 15 |
| Figure 6 Site-specific recombinases. | 19 |
| Figure 7 Landing pad-based cell line development..... | 22 |
| Figure 8 SB-10X bioreactor set-up..... | 50 |
| Figure 9 LP vectors and host cell line generation..... | 57 |
| Figure 10 Results from semi-solid clone selection and FCM analysis of obtained clones. | 58 |
| Figure 11 cMAR clones and stability test | 60 |
| Figure 12 Characterization of selected cMAR clones | 61 |
| Figure 13 1-68MAR clones, FCM analyses and stability studies..... | 63 |
| Figure 14 FCM analyses of w/o_MAR clones and stability tests | 64 |
| Figure 15 analyses of w/o MAR clones..... | 65 |
| Figure 16 Schematic representation of the integration of the donor vectors containing HC and LC genes into LP_EGFP and LP_DsRed, respectively..... | 66 |
| Figure 17 Fluorescence analysis of productive pool generated using bxb1 system (from clone 8A6). | 67 |
| Figure 18 FB culture of msAb expressing clones. | 68 |
| Figure 19 Evaluation of residual fluorescence in productive clones derived from cMAR-rich landing pad clones. | 69 |
| Figure 20 Evaluation of GCN, mRNA level and FISH analysis on selected clones..... | 71 |
| Figure 21 msAb-Fer expressing clones generated using Lonza GS system | 73 |
| Figure 22 Generation of bsAb stable cell line using LP system and FCM analyses of stable pools..... | 74 |
| Figure 23 Fed batch cultures of bsAb-Fer expressing clones obtained using landing pad system. | 75 |
| Figure 24 SDS-PAGE and western blot analyses of harvest supernatant from fed batch cultures of bsAb-Fer expressing clones..... | 76 |
| Figure 25 Characterization of selected bsAb-Fer expressing clones generated using the landing pad system.... | 77 |
| Figure 26 SDS PAGE and SEC analyses of purified bsAb-Fer . | 78 |
| Figure 27- bsAb-Fer expressing clones generated by GS Exceed gene expression system for a commercial baseline..... | 81 |
| Figure 28 Analyses of produced baAb-Fer by selected clones (GS system).. | 82 |
| Figure 29 Fed-batch cultures with msAb-Fer (LP system) producing clones. | 84 |
| Figure 30 Fed-batch cultures with bsAb-Fer (LP system) producing clones..... | 85 |
| Figure 31 Scale-up of D7 bsAb-Fer expressing clone | 87 |
| Figure 32 Glucose and Lactate concentration in Eppendorf and Kuhner system)..... | 88 |
| | |
| Figure S1 Dot-blot analyses for msAb screening using anti-IgG (H+L) detection antibody..... | 111 |
| Figure S2 Characterization of msAb expressing clones and stability tests..... | 111 |
| Figure S3 Stability test for mAb expressing clones over 85 generations.. | 112 |
| Figure S4 Dot-blot analyses for bsAb screening..... | 112 |

8.6 List of tables

| | |
|---|-----|
| Table 1 | 56 |
| Table 2 | 56 |
| Table S1. Data summary for LPs copy number for clones with and without MAR 113 | |
| Table S2. Data summary for GOI copy numbers for msAb expressing clones | 113 |
| Table S3. Data summary for GOI copy numbers for bsAb expressing clones. Individual gene copy numbers for knob heavy chain (kHC), hole heavy chain (hHC) and common light chain gene (cLC) | 113 |

8.7 Acknowledgments

So many people have been with me during this journey as a Ph.D. student, which has been not just a work path but a real journey of personal growth.

The first person I would like to thank is Prof. Dr. Gerrit Hagens who from my first arrival in Switzerland believed in me and supported me so much. Every discussion and meeting from the most heated to the quiet ones allowed me to get where I am today and improve so much professionally and personally. More than a professor he became a mentor and a friend, a solid pillar who taught me so much and there are no words that can describe how grateful I am to him.

My thanks go to Prof. Dr. Harald Kolmar who has been my thesis godfather at TU Darmstadt during this long journey and has helped and supported me with valuable advice during our meetings, publication writing and thesis correction.

I definitely must thank Dr. Björn Hock and Dr. Henri Kornmann (Ferring) who enabled this thesis work by approving and supporting the research project. It was very formative to have the opportunity to do a PhD in collaboration with a company like Ferring and to be able to have an insight into industrial dynamics that are very different from the academia. Without them this whole project would not have been possible.

My thanks go to Prof. Dr. Giulio Gherzi of the University of Palermo for his long-distance support and for always being ready to accompany me even on the last step of this journey as a PhD examiner.

I would also like to thank Prof. Dr. Tobias Meckel who quickly and kindly responded to my request to be my examiner.

Special thanks go to Dr. Steffen C. Hinz, who came in the middle of my doctoral project at one of the most difficult times, always supporting and helping me. In these years of working together I have found a friend, and I am extremely grateful to him for all the help and support he has given me. He taught me how to deal with the difficulties of the doctoral program and how to get back up in the difficult moments of this journey. Without him finishing this path would have been very difficult and I will always remember with happiness our coffee breaks with the German class.

Another essential person of this PhD path is Luc Malbois, who from my first day in the lab taught me so much but especially how to approach problems in the lab with inventiveness and creativity allowing me to develop my

"problem-solving" side. Without his guidance and help working in the lab would have been much more difficult but also much less fun.

I would then like to express my gratitude for all the people I have worked with during these three years, even if for short periods or even and only for a quick exchange of ideas, all of them have left me something and allowed me to grow so much. Alexandre, Anne, Gordana, Loïc, all the students I supervised and who worked in the lab with us over these three long years, the list would be too long to mention them all but I am truly grateful.

I would also like to thank Dr. Julius Grzeschik for his help and cooperation in writing the second publication and for advice on the doctoral journey.

Special thanks go to all my friends, from the most distant ones who supported me even and only with a phone call, to the closest ones like Michele with whom I shared this journey from Palermo to Switzerland. A special thanks definitely goes to Francesco, who has always supported me even in many complicated moments and always believing in me.

To make a list of all the friends I have and who support me every day would not be enough a whole thesis, I am a lucky person surrounded by wonderful friends.

Finally, a more than special thanks goes to my family, my father Agostino, my brother Fabrizio, Elisabetta, Beatrice, Rosa Maria, Isaia and Alessandra, their support has been crucial and without them all this would not have been possible. A special thought goes to my mom Giovanna, who was not able to see the end of this thesis but would have been happy and proud.

8.8 Affirmations

Erklärungen

(declarations are to be given in German and included in the dissertation)



TECHNISCHE
UNIVERSITÄT
DARMSTADT

§8 Abs. 1 lit. c der Promotionsordnung der TU Darmstadt

Ich versichere hiermit, dass die elektronische Version meiner Dissertation mit der schriftlichen Version übereinstimmt und für die Durchführung des Promotionsverfahrens vorliegt.

§8 Abs. 1 lit. d der Promotionsordnung der TU Darmstadt

Ich versichere hiermit, dass zu einem vorherigen Zeitpunkt noch keine Promotion versucht wurde und zu keinem früheren Zeitpunkt an einer in- oder ausländischen Hochschule eingereicht wurde. In diesem Fall sind nähere Angaben über Zeitpunkt, Hochschule, Dissertationsthema und Ergebnis dieses Versuchs mitzuteilen.

§9 Abs. 1 der Promotionsordnung der TU Darmstadt

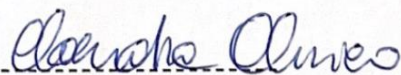
Ich versichere hiermit, dass die vorliegende Dissertation selbstständig und nur unter Verwendung der angegebenen Quellen verfasst wurde.

§9 Abs. 2 der Promotionsordnung der TU Darmstadt

Die Arbeit hat bisher noch nicht zu Prüfungszwecken gedient.

Darmstadt, den

CLAUDIA OLIVIERO



(name and signature)